REFERENCE ONLY

# UNIVERSITY OF LONDON THESIS

Degree PhD Year 2003 Name of Author HICKMAN, D.J.


## COPYRIGHT

This is a thesis accepted for a Higher Degree of the University of London. It is an unpublished typescript and the copyright is held by the author. All persons consulting the thesis must read and abide by the Copyright Declaration below.

## COPYRIGHT DECLARATION

I recognise that the copyright of the above-described thesis rests with the author and that no quotation from it or information derived from it may be published without the prior written consent of the author.

## LOANS

Theses may not be lent to individuals, but the Senate House Library may lend a copy to approved libraries within the United Kingdom, for consultation solely on the premises of those libraries. Application should be made to: Inter-Library Loans, Senate House Library, Senate House, Malet Street, London WC1E 7HU.

## REPRODUCTION

University of London theses may not be reproduced without explicit written permission from the Senate House Library. Enquiries should be addressed to the Theses Section of the Library. Regulations concerning reproduction vary according to the date of acceptance of the thesis and are listed below as guidelines.

A. Before 1962. Permission granted only upon the prior written consent of the author. (The Senate House Library will provide addresses where possible).

B. 1962 - 1974. In many cases the author has agreed to permit copying upon completion of a Copyright Declaration.

C. 1975 - 1988. Most theses may be copied upon completion of a Copyright Declaration.

D. 1989 onwards. Most theses may be copied.

***This thesis comes within category D.***

☑ This copy has been deposited in the Library of UCL

☐ This copy has been deposited in the Senate House Library, Senate House, Malet Street, London WC1E 7HU.

# Membrane currents evoked by vasoactive compounds in vascular endothelial cells: contributions of small and intermediate conductance calcium-activated potassium channels

**David James Hillman**

**2005**

A thesis submitted for the degree of Doctor of Philosophy

Department of Pharmacology
University College London

UMI Number: U592902

All rights reserved

INFORMATION TO ALL USERS
The quality of this reproduction is dependent upon the quality of the copy submitted.

In the unlikely event that the author did not send a complete manuscript
and there are missing pages, these will be noted. Also, if material had to be removed,
a note will indicate the deletion.


UMI U592902
Published by ProQuest LLC 2013. Copyright in the Dissertation held by the Author.
Microform Edition © ProQuest LLC.
All rights reserved. This work is protected against
unauthorized copying under Title 17, United States Code.


ProQuest LLC
789 East Eisenhower Parkway
P.O. Box 1346
Ann Arbor, MI 48106-1346

# Abstract

The contribution of different calcium-activated potassium channel subtypes to agonist-evoked whole-cell currents was studied in cultured pig coronary artery endothelial cells.

From a resting membrane potential of -5.9±0.5mV (n=102), 1-10μM ATP, 1-10nM substance P and 1-100nM bradykinin hyperpolarised cell rafts to -50.7±1.6mV (n=76), -45.7±4.7mV (n=19) and -59.1±3.5mV (n=16), respectively.

In small clusters of cells, 10μM ATP evoked outward currents which reversed close to $E_K$ and were sensitive to both the $SK_{Ca}$ channel blocker UCL 1848 ($IC_{50}$ 1.2nM; ~65% maximal block) and the $IK_{Ca}$/$BK_{Ca}$ channel blocker charybdotoxin (~85% block at 30-100nM). Surprisingly 10μM clotrimazole, a non-selective blocker of $IK_{Ca}$ channels, abolished ATP-evoked currents in a total of three out of five cells. This requires further study.

1mM 1-EBIO, which increases the calcium sensitivity of $SK_{Ca}$ and $IK_{Ca}$ channels, activated currents which were sensitive to 100nM UCL 1848 and 1μM clotrimazole (blocked by 57.0±15.1% (n=3) and 89.0±1.6% (n=4), respectively). When applied in combination, these two blockers essentially abolished 1-EBIO evoked currents.

Buffering intracellular calcium to 1.5μM activated outward currents which were sensitive to 100nM UCL 1848, 100nM charybdotoxin and 1μM clotrimazole (blocked by 28.3±5.4% (n=27), 101.2±0.5% (n=3), and 82.6±3.7% (n=22), respectively.

Plasma membrane delimited expression of the SK3 channel protein was detected using fluorescence immunohistochemistry.

In many vessels endothelium-derived hyperpolarising factor (EDHF)-mediated vasodilation is abolished by a *combination* of $SK_{Ca}$ and $IK_{Ca}$ channel blockers, which are frequently ineffective when applied alone. This has led some to suggest the existence of a novel channel with unusual pharmacology. The present study demonstrates, however, that separate $SK_{Ca}$ and $IK_{Ca}$ channels contribute to endothelial cell currents underlying the EDHF pathway. Based on protein expression and UCL 1848-sensitivity it is further proposed that the contributing $SK_{Ca}$ channels are formed of SK3 subunits.

# Acknowledgements

I would like to express deep gratitude to my supervisor, Dennis Haylett, for his invaluable teaching and endless patience over the past four years.

For being the lab electrophys guru, all-round genius and a great laugh, I am also indebted to David Benton.

My thanks to Tom Carter for his advice on endothelial cells, and to Don Jenkinson for his kind words of encouragement during testing times. I am grateful also to Guy Moss and Richard Burt for many useful discussions.

I would like to extend my thanks to all those in the Department who have helped me during my PhD. In particular, Tina Bashford for looking after us Postgrads, Tracy Boot for her help with printing, and Roger Allman for processing piles of my macabre expenses claims.

For help on scores of trips into the Essex countryside, my thanks to Matt, Tony, Jackie and colleagues at Cheale Meats; also to John, Rob and the other guys at Abby cars.

I have some great friends without whom the past few years would have been much less fun. In particular: Parmvir, Nick, Tom, Luciana, Kim and the Biochemists, Liz, Johnny, Gideon, Virginia, Justin, Erica, Pete and the boyz, and the Kings' Pharmers. Em, you're a star for being such a great support during my write-up.

Finally, I would like to thank my entire family for their love, support and encouragement; especially Mum - thanks for being my one-in-a-million 'Ma', Dad - thanks for saying the right things at the right time, and Jon - thanks for making me laugh. Most of all, I would like to thank my Grandfather and Grandmother who provided the bedrock for my education. You have both keenly followed the development of this project, and through difficult months your encouragement alone kept me going. I dedicate this thesis to both of you.

DJH

October 2005

# Contents

*Page*

**Chapter 2: Methods & Materials**

**Chapter 3: Endothelial cell culture**



**Chapter 4: Rat explant cell electrophysiology**



**Chapter 5: Pig endothelial cell electrophysiology**

**Chapter 7: Discussion**



**Appendices**

# Figures

*Page*

# Tables

*Page*

# Acronyms & Abbreviations

| | |
|---|---|
| 1-EBIO | 1-ethyl-2-benzimidazolinone |
| 4-AP | 4-aminopyridine |
| 5-HT | 5-hydroxytryptamine *synonym: serotonin* |
| ABB | antibody blocking buffer |
| ACh | acetylcholine |
| AHP | after-hyperpolarisation |
| aLDL | acetylated low density lipoprotein |
| ATP | adenosine 5′-triphosphate |
| BK | $BK_{Ca}$ channel protein *synonym: Slo1* |
| $BK_{Ca}$ | large-conductance calcium-activated potassium (channel) *synonym: MaxiK* |
| CaCC | see $Cl_{Ca}$ |
| cAMP | adenosine 3′,5′-cyclic monophosphate |
| CB1 | cannabinoid receptor (subtype-1) |
| CB2 | cannabinoid receptor (subtype-2) |
| CC | current-clamp recording |
| CCE | capacitative calcium entry |
| cGMP | guanosine 3′,5′-cyclic monophosphate |
| CGRP | calcitonin gene related peptide |
| ChTx | charybdotoxin |
| cir | circumflex coronary artery |
| CLCA | see $Cl_{Ca}$ |
| $Cl_{Ca}$ | calcium-activated chloride (channel) |
| CNP | C-type natriuretic peptide |
| COX | cyclooxygenase |
| cP450 | cytochrome P-450 |
| C terminus | carboxyl terminus |
| CTZ | clotrimazole |
| CVR | current-voltage relationship |

DAG diacylglycerol

| | |
|---|---|
| Cx | connexin |
| DCEBIO | 5,6-Dichloro-1-ethyl-1,3-dihydro-2H-benzimidazole-2-one |
| DHS-I | dehydrosoysaponin I |
| DMEM | Dulbecco's modified Eagle's medium |
| DMSO | dimethyl sulphoxide |
| DPBS | Dulbecco's phosphate buffered saline |
| *Drosophila* | *Drosophila melanogaster* |
| E | endothelium |
| $EC_{50}$ | concentration evoking 50% maximal excitation |
| ECGS | endothelial cell growth supplement |
| $E_{Cl}$ | chloride equilibrium potential |
| EDHF | endothelium-derived hyperpolarising factor |
| EET | epoxyeicosatrienoic acid |
| $E_K$ | potassium equilibrium potential |
| $E_m$ | resting membrane potential |
| eNOS | endothelial nitric oxide |
| epi | epicardial coronary artery |
| ER | endoplasmic reticulum |
| $E_{rev}$ | reversal potential |
| ES | extracellular solution |
| F | Faraday's constant |
| FBS | foetal bovine serum |
| GA | glycyrrhetinic acid |
| GFP | green fluorescent protein |
| gl | glucose |
| gx | Glutamax |
| HBSS | Hank's buffered salt solution |
| HEK | human embryonic kidney cell line 293 |
| hIK1 | human orthologue of IK1 *synonym: hSK4* |
| HPASM | human pulmonary artery smooth muscle cell |
| h*slo* | human homologue of *slo* |
| hSK1 | human orthologue of SK1 |

| | |
|---|---|
| hSK2 | human orthologue of SK2 |
| hSK3 | human orthologue of SK3 |
| hSK4 | see *hIK1* |
| HUVEC | human umbilical vein endothelial cell |
| I | blocker (inhibitor) |
| IbTx | iberiotoxin |
| Ic | intracellular electrode recording |
| $IC_{50}$ | concentration at which inhibition is 50% |
| IgG | Immunoglobulin type-G |
| $I_h$ | hyperpolarisation-activated current |
| IK1 | $IK_{Ca}$ channel $\alpha$-subunit channel protein *synonym: SK4* |
| $IK_{Ca}$ | intermediate-conductance calcium-activated potassium (channel) |
| inh. | inhibition |
| $IP_3$ | inositol 1,4,5-triphosphate |
| IS | intracellular solution |
| $K_{ATP}$ | ATP-sensitive potassium (channel) |
| $K_{Ca}$ | calcium-activated potassium (channel) |
| $K_{IR}$ | inwardly-rectifying potassium (channel) |
| $K_V$ | voltage-dependent potassium (channel) |
| LAD | left anterior descending |
| lg | L-glutamine |
| L-NOARG | L-NG-nitro arginine |
| MAP kinase | mitogen activated protein kinase |
| MaxiK | see $BK_{Ca}$ |
| MEM | modified Eagle's medium |
| mRNA | messenger ribonucleic acid |
| n | sample size |
| $x^n$ | (n signifies the Hill coefficient) |
| Na/K-ATPase | sodium-potassium pump |
| NCX | sodium-calcium exchanger |
| NO | nitric oxide |
| NOS | nitric oxide synthase |

| | |
|---|---|
| NPPB | 5-Nitro-2-(3-phenylpropylamino)benzoic acid |
| NPR-B | natriuretic peptide receptor (subtype B) |
| NPR-C | natriuretic peptide receptor (subtype C) |
| NSC | non-selective cation channel |
| $NSC_{Ca}$ | calcium-activated non-selective cation (channel) |
| N terminus | amino terminus |
| P2X | purinoceptor (subtype 2,X) |
| P2Y | purinoceptor (subtype 2,Y) |
| $P_{Cl}$ | chloride permeability constant |
| PGI2 | prostacyclin |
| PBS | phosphate buffered saline |
| PE | patch electrode |
| $P_K$ | potassium permeability constant |
| PKA | protein kinase A |
| PKB | protein kinase B |
| PKG | protein kinase G |
| PLC | phospholipase C |
| P-loop | pore-forming loop |
| $P_{Na}$ | sodium permeability constant |
| P/S | penicillin / streptomycin mix |
| py | pyruvate |
| R | right |
| R | universal gas constant |
| rSK2 | rat orthologue of SK2 |
| rSK3 | rat orthologue of SK3 |
| RT-PCR | real-time polymerase chain reaction |
| S*(0-10)* | trans-membrane domain *(0-10)* |
| SCG | superior cervical ganglion |
| SK1 | $SK_{Ca}$ $\alpha$-subunit channel protein (subtype 1) |
| SK2 | $SK_{Ca}$ $\alpha$-subunit channel protein (subtype 2) |
| SK3 | $SK_{Ca}$ $\alpha$-subunit channel protein (subtype 3) |
| SK4 | see *IK1* |

| | |
|---|---|
| $SK_{Ca}$ | small-conductance calcium-activated potassium (channel) |
| *Slo*1 | *Slopoke* protein (subtype 1) *synonym: BK* |
| SM | smooth muscle |
| SNP | sodium nitroprusside |
| SOC | store-operated channel |
| SOD | superoxide dismutase |
| SR | sarcoplasmic reticulum |
| STOC | spontaneous transient outward current |
| supp. | supplement |
| T | temperature (°K) |
| TBA | tetrabutylammonium |
| TEA | tetraethylammonium |
| TRPC | transient receptor potential (canonical) protein |
| TRPV1 | transient receptor potential (vanilloid) protein (subtype 1) *formerly VR1* |
| VR1 | see *TRPV1* |
| VRAC | volume-regulated anion channel |
| vWF | von Willebrand factor |
| *Xenopus* | *Xenopus tropicalis* |
| z | valency |

# Chapter 1: Introduction

## 1.1.) Introduction

Calcium-activated potassium ($K_{Ca}$) channels provide a mechanism through which changes in cytosolic calcium ion concentration can influence membrane potential. In excitable cells, the hyperpolarising current carried by these channels can reduce action potential firing rate by causing the closure of voltage-dependent channels. In non-excitable cells, hyperpolarisation may provide a membrane potential particularly suited to sustained calcium influx and thus support calcium-dependent processes.

$K_{Ca}$ channels have recently been implicated in arterial dilation attributed to a putative 'endothelium-derived hyperpolarising factor' (EDHF). This thesis explores the role of these channels within the context of EDHF-mediated vasodilation.

By way of introduction, the basic anatomy of blood vessels including the function of the principal cell phenotypes is briefly described. $K_{Ca}$ channels are then introduced, and their expression within the vessel wall is considered.

Since $K_{Ca}$ channels involved in EDHF-mediated vasodilation appear to be located in the endothelium, the electrophysiological properties of endothelial cells, including responses to physiological stimuli, are also discussed.

Finally, current understanding of EDHF-mediated vasodilation is briefly reviewed.

## 1.2) Blood vessel anatomy

Blood vessels contain two distinct major cell types relevant to this thesis, the endothelium and smooth muscle.

Endothelial cells form a continuous monolayer lining the innermost surface of the vessel, also known as the *tunica intima* (*figure 1.1*). The middle portion of the vessel wall, the *tunica media*, contains multiple layers of circular smooth muscle cells which are aligned perpendicularly to the flow of blood. Arterioles may contain only a couple of layers of smooth muscle, whilst large human conduit arteries can have several tens of layers. Veins generally contain less smooth muscle and have less vascular tone than arteries.

The outermost portion of the vessel wall, the *tunica adventitia*, consists mainly of structural and connective elements such as collagen and elastin fibres, and also other cell types such as fibroblasts. Also present are nerves and microvessels, the *nervi vasorum* and *vasa vasorum*, respectively. These serve the adventitial and medial layers of the vessel wall.

Once thought to provide merely a semi-permeable barrier to nutrients, the endothelium is now regarded as having a wide range of functions. These include regulation of angiogenesis, involvement in immune responses, involvement in blood clotting and fibrinolysis, and regulation of vascular tone, in addition to regulating the exchange of molecules between blood and tissues (Michiels, 2003). Endothelial cells respond not only to chemical stimulation through the action of neurotransmitters, endocrine- and paracrine-factors, but also to physical forces such as shear-stress.

Intercellular coupling between endothelial cells occurs via gap junctions which coordinate electrical responses, enabling regions of the monolayer to function as a syncytium. Gap junctions are also permeable to a number of intracellular mediators (see *section 1.5.4.7*).

Endothelial cells interact with neighbouring smooth muscle cells and also circulating cells of differing phenotypes. This occurs through physical contact such as adhesion or gap junction formation, or via the release and reception of chemical mediators.

Vascular smooth muscle cells are spindle-like in shape and contain an arrangement of contractile elements including actin, myosin, desmin and vimentin.

The contractile apparatus shortens the cells along their longitudinal axes in response to raised cytosolic calcium. Simultaneous contraction of circular smooth muscle cells in the *tunica media* results in vessel constriction. Unlike endothelial cells, smooth muscle cells contain voltage-dependent calcium channels which can give rise to propagation of action potentials and so lead to contraction. Calcium release from the sarcoplasmic reticulum also occurs through the activation of $G_q$ protein-linked receptors. Like endothelial cells, smooth muscle cells are coupled by gap junctions allowing fast propagation of electrical responses and exchange of intracellular mediators.

At the contiguous border between the *tunica intima* (endothelium) and the *tunica media* (smooth muscle) lies the internal elastic lamina. The region between and around this matrix of elastic fibres is referred to as the myoendothelial space, through which substances diffuse between the two cell types. In both endothelial and smooth muscle cells, the membrane at the myoendothelial space is convoluted, forming invaginations termed caveolae. These greatly increase the membrane surface area and form microdomains in which functionally related membrane proteins are co-localised. In endothelial cells this includes G-proteins and $IP_3$ receptors.

In some vessels, gap junctions directly connect endothelial cells to adjacent smooth muscle, bridging the myoendothelial space. This allows direct electrical coupling and/or mediator transfer between the different cell types (see *section 1.5.4.7.*).

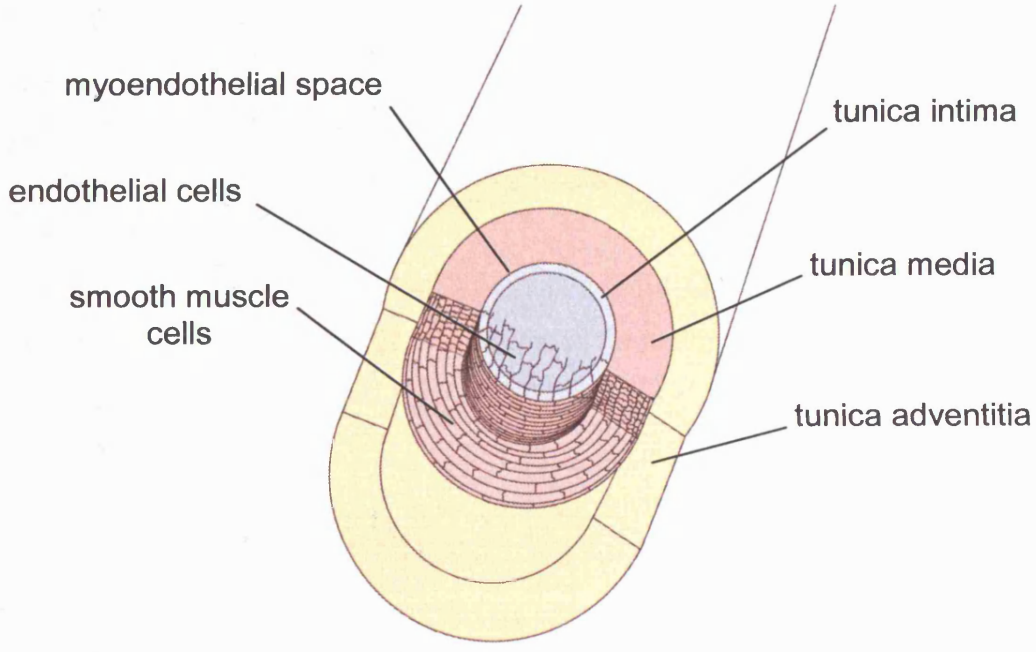


**Figure 1.1)** A schematic representation of an artery.

## 1.3) Calcium-activated potassium channels

### 1.3.1) Introduction

Calcium-activated potassium ($K_{Ca}$) channels belong to the same structurally-related family of proteins as voltage-dependent potassium ($K_V$) channels. Channels of both types are formed by proteins containing six transmembrane domains with a pore-forming re-entrant P-loop between domains five (S5) and six (S6) (*figure 1.2a*). N and C termini are both intracellular. Those family members which exhibit voltage-sensitivity contain a highly conserved motif of negatively charged residues at the fourth transmembrane domain (S4). Both $K_{Ca}$ and $K_V$ channels are highly potassium-selective and blocked by tetraethylammonium ions (TEA) at both cytoplasmic and external sites.

Despite similarity in structure, the primary amino acid sequences of $K_V$ and $K_{Ca}$ channel alpha-subunit proteins are distinct with the exception of conserved regions encoding the pore and potassium selectivity filter.

$K_{Ca}$ channels exist as members of three subfamilies distinguished by different conductances under symmetrical high potassium conditions: small ($SK_{Ca}$); 2-18pS, intermediate ($IK_{Ca}$); 18-80pS and large ($BK_{Ca}$); 150-300pS. The three subtypes are also pharmacologically distinct; $SK_{Ca}$ channels are selectively blocked by apamin, $IK_{Ca}$ by TRAM-34 and $BK_{Ca}$ by iberiotoxin.

$BK_{Ca}$ are dissimilar to $SK_{Ca}$ and $IK_{Ca}$ channels in that they are gated by voltage as well as by cytosolic calcium. The $BK_{Ca}$ channel alpha subunit is also considerably larger than that of its counterparts with a further five hydrophobic domains (*figure 1.2b*).

Each of the channel subtypes has a distinct pattern of expression within mammalian tissues and will be considered throughout the following sections.

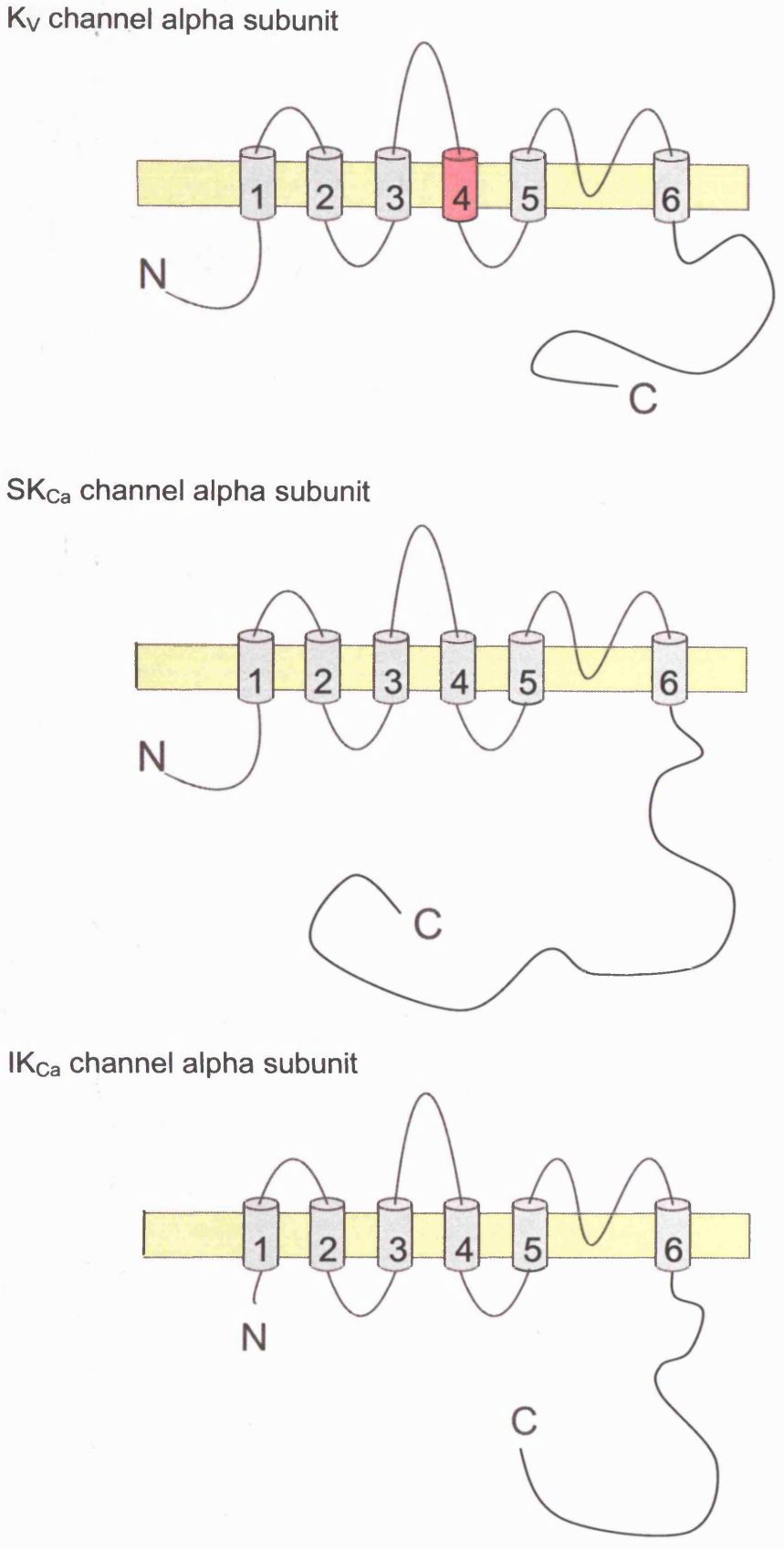


**Figure 1.2a)** Protein structure of six-transmembrane-domain potassium channel alpha subunits. N and C represent amino and carboxy termini, respectively. The $K_V$ channel voltage sensor is highlighted in pink. Numeric labels indicate segment (S) number. All C-termini are intracellular.

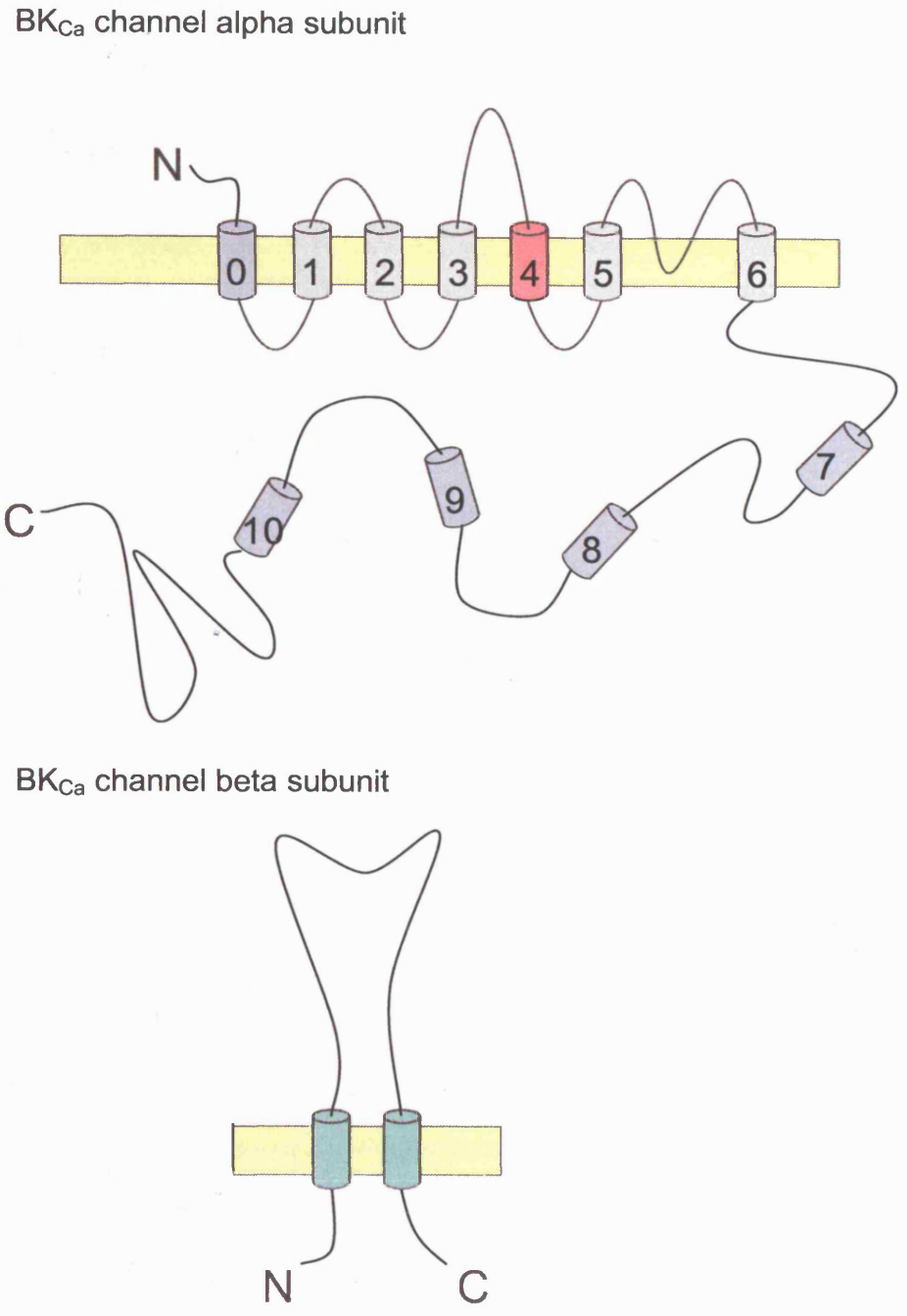


**Figure 1.2b)** Protein structure of $BK_{Ca}$ channel alpha and beta subunits. N and C represent amino and carboxy termini, respectively. The S4 voltage sensor is highlighted in pink. Hydrophobic segments additional to the six-transmembrane-domain template are highlighted in blue. Numeric labels indicate segment (S) number. All C-termini are intracellular.

| Channel subtype | Channel protein(s) | Encoding gene |
|---|---|---|
| SK1 | KCa2.1 | KCNN1 |
| SK2 | KCa2.2 | KCNN2 |
| SK3 | KCa2.3 | KCNN3 |
| IK1 (SK4) | KCa3.1 | KCNN4 |
| BK (alpha) | KCa1.1 (Slo1) | KCNMA1 |
| BK (beta 1) | Slo-beta-1 | KCNMB1 |
| BK (beta 2) | Slo-beta-2 | KCNMB2 |
| BK (beta 3) | Slo-beta-3 | KCNMB3 |
| BK (beta 4) | Slo-beta-4 | KCNMB4 |

**Table 1.1)** Nomenclature of $K_{Ca}$ channel proteins and encoding genes.

## 1.3.2) $SK_{Ca}$ channels

### 1.3.2.1) Introduction

The potassium-conductance blocking activity of apamin was first described by Banks *et al.* (1979) following reports that this peptide prevented neurotransmitter-evoked hyperpolarisation in a number of tissues. In the years that followed, the target channel was discovered to be gated by intracellular calcium and named the small-conductance calcium-activated potassium ($SK_{Ca}$) channel on account of its relatively small single channel conductance compared with other calcium-activated potassium channels (Blatz & Magleby, 1986).

$SK_{Ca}$ channels are widely expressed in both excitable and non-excitable cells including smooth muscle, liver cells and lymphocytes. In particular, they have been intensively studied regarding their role in dampening the excitability of neurones. The phenomenon of the after-hyperpolarisation (AHP), which follows bursts of firing in some neurones, is partly attributable to $SK_{Ca}$ channel activity and is thought to prevent excitotoxicity and facilitate spike-frequency adaptation (Sah & Faber, 2002).

Upon cloning in 1996, three $SK_{Ca}$ channel protein orthologues were identified, each from the KCNN gene family (*table 1.1*) (Kohler *et al.*, 1996). SK1, SK2 and SK3 proteins have since been identified in many cell types where native $SK_{Ca}$ channels are present.

Co-expression studies reveal that cloned $SK_{Ca}$ channel subunits can form heteromultimers (Ishii *et al.*, 1997a; Benton *et al.*, 2003; Monaghan *et al.*, 2004) although it is unclear whether such channels exist *in vivo*. Recently, novel isoforms of SK2 (Strassmaier *et al.*, 2005) and SK3 (Wittekindt *et al.*, 2004a; Kolski-Andreaco *et al.*, 2004) together with splice variants of SK1 (Zhang *et al.*, 2001) and SK3 (Wittekindt *et al.*, 2004b) have also been shown to occur. These have yet to be fully studied.

The biophysical properties of cloned $SK_{Ca}$ channels studied in various expression systems concur with observations on the equivalent native channels. Single channel conductances recorded under conditions of high symmetrical potassium are approximately 10pS (Kohler *et al.*, 1996). Currents are potassium selective and weakly inwardly rectifying, a property attributed to voltage-dependent block by intracellular divalent cations, including calcium. Channels open in response to intracellular calcium with reported $EC_{50}$ values of 300-800nM and Hill coefficients of 2-4, consistent with there being a calcium binding site on each of the four subunits required for a functional channel. Unlike large-conductance calcium-activated potassium ($BK_{Ca}$) channels and voltage-gated potassium ($K_V$) channels, $SK_{Ca}$ channels are not gated by changes in membrane potential. This is consistent with the absence of the 'voltage sensor' motif at the fourth transmembrane domain (S4).

Amongst the transmembrane regions, the three SK proteins are 80-90% identical, although distinct N and C termini reduce this to 60% for the entire sequences (Kohler *et al.*, 1996). Functionally, $SK_{Ca}$ channel subtypes are distinguishable by their relative sensitivity to apamin; SK2>SK3>SK1, with approximate $IC_{50}$ values of 100pM, 1.5nM (Hosseini *et al.*, 2001) and 8nM (Shah & Haylett, 2000), respectively. Apamin-insensitive $SK_{Ca}$-like conductances have been described, and an isoform of human SK3 with this property has recently been identified (hSK3_ex4) (Wittekindt *et al.*, 2004b).

In addition to apamin, $SK_{Ca}$ channels are selectively and potently blocked by a number of other agents including the peptide scyllatoxin (Auguste *et al.*, 1992) and

UCL 1848 (Chen *et al.*, 2000). NS309 (Strobaek *et al.*, 2004), 1-EBIO, chlorzoxazone and zoxazolamine activate $SK_{Ca}$ channels (Syme *et al.*, 2000).

There is no calcium-binding region of SK alpha sub-unit proteins, calcium-sensitivity coming instead from the calcium-binding protein calmodulin. This is itself constitutively bound to an area of the C-terminal region of the SK protein, adjacent to the S6 domain. Upon binding calcium, calmodulin cross-links adjacent sub-units effecting conformational change and opening of the channel (Schumacher *et al.*, 2001).

Modulation of channel activity is possible through a number of determined phosphorylation sites, and an interaction with putative unidentified regulatory subunits should not be ruled out. Studies using amino acid substitution suggest that selective $SK_{Ca}$ channel blockers apamin and scyllatoxin bind to the same sites on either side of the P-loop (Auguste *et al.*, 1992). Appropriate mutations have also been shown to make channels sensitive to the intermediate- ($IK_{Ca}$) and large-conductance calcium activated potassium ($BK_{Ca}$) channel blocker, charybdotoxin (Jager & Grissmer, 2004).

This topic has been reviewed by Maylie *et al.* (2004) and Stocker (2004).

### 1.3.2.2) $SK_{Ca}$ channels in vascular endothelium

It is well established that calcium-activated potassium channels underlie the phenomenon of agonist-evoked endothelial cell hyperpolarisation, although the subtype(s) of channels involved has only recently been studied.

An endothelial cell potassium channel with a single channel conductance of 9pS was first identified in a study of rabbit aorta (Sakai, 1990). The channel could be activated either by the whole-cell response to acetylcholine or by direct application of calcium to the inner face of the membrane. A further study identified a channel of similar conductance and calcium-sensitivity in primary cultures of pig aortic endothelial cells. The channel which activated upon cell stimulation by bradykinin was voltage-independent and blocked by tetrabutylammonium (TBA) (Groschner *et al.*, 1992).

Apamin sensitivity of a 9.1pS calcium-activated potassium channel recorded under conditions of symmetrical high potassium was demonstrated in excised

endothelial cell membrane patches of intact rat aortae (Marchenko & Sage, 1996). The conductance was voltage-insensitive, weakly inwardly rectifying and became active at cytosolic calcium concentrations greater than 500nM. The channel was insensitive to the $IK_{Ca}$, $BK_{Ca}$ and $K_V$ channel blocker, charybdotoxin, but sensitive to d-tubocurarine, another $SK_{Ca}$ channel blocker.

Two $SK_{Ca}$ channels have been described in freshly isolated endothelial cells from pig coronary artery (Burnham *et al.*, 2002). A channel with a single channel conductance of 10.1pS under conditions of symmetrical high potassium, showed similar pharmacological properties to that described in rat aorta, although with a higher sensitivity to calcium and no obvious rectification. Unlike the 10.1pS channel which had a conductance of 6.8pS in quasi-physiological solutions, a less frequently observed channel exhibited a 2.7pS conductance under these conditions. This channel also exhibited $SK_{Ca}$ channel pharmacology and voltage-insensitivity, though its identity remains unresolved.

Whole-cell currents consistent with the activation of $SK_{Ca}$ channels have also been studied in endothelial cells from rat carotid artery (Kohler *et al.*, 2001), mouse mesenteric artery (Taylor *et al.*, 2003) and human umbilical vein (Muraki *et al.*, 1997).

RT-PCR and Western blotting have revealed expression of SK3 mRNA and protein in endothelial cells from porcine coronary (Burnham *et al.*, 2002), mouse mesenteric (Taylor *et al.*, 2003) and rat carotid arteries (Kohler *et al.*, 2001), and from human saphenous vein (Sultan *et al.*, 2004). SK2 protein has also been detected in the endothelium of porcine coronary artery and human saphenous vein, although expression appears lower than for SK3 (Burnham *et al.*, 2002). Unlike SK3 which appears to be located at the periphery, SK2 seems to be to be located in the peri-nuclear region of pig coronary artery endothelial cells. SK2 has been demonstrated to be up-regulated to similar levels to SK3 in endothelial cells from human saphenous vein exposed for several hours to conditions simulating shear stress (Taylor *et al.*, 2003). SK1 protein appears to be absent from the endothelium of rat carotid- (Kohler *et al.*, 2001) and pig coronary-arteries (Burnham *et al.*, 2002).

1.3.2.3) $SK_{Ca}$ channels in vascular smooth muscle

Despite much electrophysiological study of smooth muscle originating from a wide range of vascular beds, there is little evidence to suggest a physiological role for smooth muscle $SK_{Ca}$ channels. A number of recent studies have suggested that these channels may in fact be present in some vascular smooth muscle although their function remains unclear.

Apamin-sensitive $SK_{Ca}$ channels with a single channel conductance of ~24pS have been described in freshly isolated rabbit aortic smooth muscle cells under conditions of symmetrical high potassium (Gauthier *et al.*, 2004).

Dioclein, a flavanoid, has been shown to relax pre-constricted endothelium-denuded smooth muscle in an apamin-sensitive manner (Cortes *et al.*, 2001). It should be noted, however, that apamin was applied at a very high concentration (1μM), far greater than the low nM concentrations required for effective $SK_{Ca}$ channel block. Furthermore, the effect of dioclein was also inhibited by $BK_{Ca}$ and $K_V$ channel blockers, inconsistent with $SK_{Ca}$ channel pharmacology.

An earlier study of cultured rat aortic smooth muscle cells described a 'small-conductance' calcium-activated potassium channel with a single channel conductance of 38pS in symmetrical high potassium (Van Renterghem & Lazdunski, 1992). However, apamin-insensitivity and charybdotoxin-sensitivity suggest that this conductance is perhaps better described as $IK_{Ca}$-like. Unlike either $SK_{Ca}$ or $IK_{Ca}$, the channel showed no sign of rectification.

Apamin-sensitive whole-cell currents have been described in guinea pig carotid arteries, indicating a presence of $SK_{Ca}$ channels (Quignard *et al.*, 2000).

Recently, mRNA encoding SK2 and SK3 channel proteins has been detected in the smooth muscle of human pulmonary artery (Platoshyn *et al.*, 2004). In porcine coronary artery smooth muscle, mRNA for SK2 has been detected, although this appears confined to a peri-nuclear location (Burnham *et al.*, 2002). In smooth muscle of rat carotid artery, mRNA encoding SK proteins could not be detected (Kohler *et al.*, 2003).

## 1.3.3) $IK_{Ca}$ Channels

### 1.3.3.1) Introduction

The calcium-dependent conductance now attributed to the intermediate-conductance calcium-activated potassium ($IK_{Ca}$) channel was first described in erythrocytes (Gardos, 1958). For many years, the attribution of this conductance to the activity of an ion channel was controversial until the matter was finally resolved following the advent of single channel recording (Hamill, 1981).

$IK_{Ca}$ channels are highly expressed in epithelia, endothelia and blood cells. Until recently, it was generally considered that these channels were only expressed in non-excitable cells, although recently $IK_{Ca}$ channels have been shown to be present in rat sensory neurones (Mongan *et al.*, 2005), and enteric neurones of several species (Furness *et al.*, 2003; Furness *et al.*, 2004; Neylon *et al.*, 2004b). In guinea pig enteric neurones, channels with some of the characteristics of $IK_{Ca}$ contribute to the phenomenon of afterhyperpolarisation (AHP) (Vogalis *et al.*, 2002; Vogalis *et al.*, 2003). Transient expression of $IK_{Ca}$ channels in other cells may relate to specific stages of cell development. In particular, blockade of $IK_{Ca}$ channels appears to suppress proliferation of a range of tumour cells *in vitro* (Parihar *et al.*, 2003; Jager *et al.*, 2004; Ouadid-Ahidouch *et al.*, 2004).

The only $IK_{Ca}$ channel alpha-subunit protein cloned to date was identified in 1997 by several groups and named both SK4 (Joiner *et al.*, 1997) and IK1 (Ishii *et al.*, 1997b; Logsdon *et al.*, 1997) (*table 1.1*). Similarly to the respective $SK_{Ca}$ channel proteins, the IK1 orthologue is a product of the KCNN gene family. Since the primary amino acid sequence is only 40-42% identical to those of the SK proteins, IK1 is the sole-member of a distinct sub-family.

It is not yet known whether splice variants of the IK1 protein exist.

The biophysical properties of IK1 expressed in various expression systems are similar to those of the original 'Gardos channel' and other native $IK_{Ca}$ currents; potassium selective, weakly inwardly rectifying, and with a single channel conductance of 30-40pS for inward currents in conditions of high symmetrical potassium. The channels are activated by calcium, with reported $EC_{50}$s ranging from

100-700nM and Hill coefficients between 1.7 and 3.2. Similarly to $SK_{Ca}$, $IK_{Ca}$ channels are not gated by changes in membrane potential.

$IK_{Ca}$ are pharmacologically distinguished from $SK_{Ca}$ channels by their insensitivity to apamin. The clotrimazole-based compounds TRAM-34 and TRAM-39 (Wulff *et al.*, 2000), and the peptide maurotoxin (Castle *et al.*, 2003) are considered the most selective $IK_{Ca}$ channel blockers, whilst charybdotoxin also provides potent block (Castle & Strong, 1986). Although charybdotoxin also blocks $BK_{Ca}$ and some $K_V$ channels, $IK_{Ca}$ channels are insensitive to the selective $BK_{Ca}$ blocker, iberiotoxin, and a number of selective $K_V$ channel blockers. As with $SK_{Ca}$, $IK_{Ca}$ channels are activated by NS109 (Strobaek *et al.*, 2004), 1-EBIO, chlorzoxazone and zoxazolamine (Syme *et al.*, 2000), although an $IK_{Ca}$-specific analogue of 1-EBIO, DCEBIO, has been described (Singh *et al.*, 2001).

Despite sharing only 40-42% primary sequence identity with the SK proteins, $IK_{Ca}$ channels are structurally very similar, albeit with significantly shorter N- and longer C- termini. As with $SK_{Ca}$ channels, it is widely assumed that $IK_{Ca}$ form as tetramers. Calcium sensing is believed to occur via constitutively bound calmodulin at the same region and in the same manner as $SK_{Ca}$ channels. As with the SK proteins, IK1 has no inherent calcium-sensing domain.

IK1 has several putative modulation sites, an N-linked glycosylation site, one recognition site for protein kinase A (PKA) and two for protein kinase B (PKB). Protein kinase A has been reported in different studies to have both inhibitory (Neylon *et al.*, 2004a) and facilitatory (Gerlach *et al.*, 2000) influences on $IK_{Ca}$ channel conductances, the latter triggered through ATP binding at the cytoplasmic face of the channel.

This topic has been reviewed by Jensen *et al.* (2001).

### 1.3.3.2) $IK_{Ca}$ channels in vascular endothelium

Endothelial cell calcium-activated potassium channels of similar conductance to the 'Gardos' channel were first reported in cells cultured from bovine aorta (Sauve *et al.*, 1988). Although its pharmacology was not established, this potassium channel was calcium-activated, inwardly rectifying and had a single channel conductance of 40pS under conditions of 200mM symmetrical potassium. Charybdotoxin-

sensitivity, together with iberiotoxin-insensitivity of this channel were shown a number of years later (Cai *et al.*, 1998).

In primary cultures of pig coronary artery endothelial cells, voltage-independent, inwardly rectifying, calcium-activated potassium channels had a single channel conductance of 25pS (200mM potassium at the channel outer face, 150mM at the cytoplasmic face) (Sharma & Davis, 1994). Calcium activated the channel with an $EC_{50}$ of ~300nM. A subsequent study of cultured cells from the same vascular bed reported a single channel conductance of 30pS under conditions of high symmetrical potassium although with a higher $EC_{50}$ of ~800nM for calcium activation (Sollini *et al.*, 2002). In this later study, charybdotoxin sensitivity and apamin-insensitivity was established, together with channel activation by 1-EBIO. Similar findings have since been reported in a study of freshly isolated endothelial cells from the same vascular bed; single channel conductances of ~17pS in quasi-physiological solutions (Bychkov *et al.*, 2002).

An $IK_{Ca}$ channel in microvascular endothelial cells cultured from rat brain has been reported to have a single-channel conductance of 40pS in symmetrical high potassium solutions (Van Renterghem *et al.*, 1995). The biophysical and pharmacological properties of this channel are consistent with those previously described in other endothelial cells. $IK_{Ca}$ channel activity recorded under similar conditions in endothelial cell patches from rat aorta (Marchenko & Sage, 1996) and cultured mouse aorta (Ahn *et al.*, 2004) have revealed single channel conductances of ~18pS. A contribution of $IK_{Ca}$ channels to whole-cell currents has also been demonstrated in freshly isolated endothelial cells of human mesenteric- (Kohler *et al.*, 2000), rat mesenteric- (Walker *et al.*, 2001) and rat carotid- (Eichler *et al.*, 2003) arteries.

Expression of mRNA encoding the $IK_{Ca}$ channel protein in the endothelium was first established in cells freshly isolated from human mesenteric arteries (Kohler *et al.*, 2000). Similar expression has also been reported in freshly isolated endothelium from pig coronary arteries (Bychkov *et al.*, 2002) and cultured endothelial cells from both human umbilical vein (Brakemeier *et al.*, 2003b) and mouse aorta (Ahn *et al.*, 2004).

1.3.3.3) $IK_{Ca}$ channels in vascular smooth muscle

Until recently it was believed that $IK_{Ca}$ channels were not expressed in vascular smooth muscle cells. However, it has now become apparent that whilst mature, contractile smooth muscle does not usually express $IK_{Ca}$ channels, immature (proliferating) smooth muscle cells do.

A calcium-activated potassium channel with a single channel conductance of 32pS in symmetrical high potassium solutions has been identified in immature smooth muscle cells cultured from rat aorta (Neylon *et al.*, 1999). The conductance was sensitive to charybdotoxin and insensitive to iberiotoxin. mRNA encoding IK1 was isolated from these cells and reversed transcribed into DNA whereupon cloning and expression in *Xenopus* oocytes allowed electrophysiological characterisation. In addition to the aforementioned properties, conductances were inwardly rectifying and voltage-independent. Calcium activated the channel with an $EC_{50}$ of ~100nM and with a Hill coefficient of 2.9. The channel was absent from mature smooth muscle cells cultured from the same vascular bed.

mRNA encoding IK1 has been identified in immature but not mature smooth muscle cells of rat carotid artery (Kohler *et al.*, 2003). The pharmacology of whole-cell currents from these cells is consistent with the presence and absence of functional $IK_{Ca}$ channels in the immature and mature phenotype, respectively. This study further demonstrated that triggering proliferation of cells from the smooth muscle cell line, A7r5, resulted in a similar appearance of previously absent functional $IK_{Ca}$ channels. mRNA encoding the $IK_{Ca}$ channel protein has also been isolated from mature smooth muscle from human pulmonary artery (Platoshyn *et al.*, 2004), rat pulmonary artery and rat aorta (Saito *et al.*, 2002). However, functional expression of $IK_{Ca}$ channels has yet to be demonstrated in these cells.

## 1.3.4) $BK_{Ca}$ channels

### 1.3.4.1) Introduction

Large conductance calcium-activated potassium ($BK_{Ca}$) channels, also referred to as MaxiK, have intrigued electrophysiologists since their discovery. This section provides only a brief overview of $BK_{Ca}$ channels, however a comprehensive general review is given by Vergara *et al.* (1998).

Immediately conspicuous by their large single channel conductance of 100-300pS, $BK_{Ca}$ channels have been extensively studied in a number of cell types. They were originally described in chromaffin cells (Marty, 1981), but have since been shown to perform key functions in smooth muscle, where they regulate contraction, and neurones, where they modulate excitability and action potential duration.

Although in the same family of channels as $SK_{Ca}$ and $IK_{Ca}$, $BK_{Ca}$ channels are distinct in a number of ways, in particular their voltage-sensitivity. $BK_{Ca}$ channels are gated by both intracellular calcium and cell depolarisation in a co-dependent manner. Under conditions of high intracellular calcium, the voltage-activation curve for the channel is shifted considerably in the hyperpolarised direction. In some studies, extreme depolarisation has been demonstrated to activate the channel in the complete absence of intracellular calcium, however, others report the channel failing to open in the absence of calcium.

The pore-forming alpha protein subunit of the $BK_{Ca}$ channel is encoded by the *Slo*1 gene, first cloned from *Drosophila* (Atkinson *et al.*, 1991) (*table 1.1*). Although containing the familiar six transmembrane region of $SK_{Ca}$, $IK_{Ca}$ and $K_V$ channel proteins, the $BK_{Ca}$ alpha subunit is much larger with an additional transmembrane domain, S0, between S1 and the N-terminus, and a large C-terminus containing four additional hydrophobic regions, S7-S10. The S0 domain results in an extracellular N terminus, and the S7-S10 domains are predicted to reside within the cytosol despite their hydrophobic nature. So large is the intracellular region from S6 to the C terminus, that it accounts for two thirds of the entire channel protein.

As with other six trans-membrane domain potassium channels, $BK_{Ca}$ are predicted to form as alpha-subunit tetramers. They also contain the familiar pore forming 'P-loop' between domains S5 and S6, encoding the highly potassium-

selective pore region. As with $K_V$ channels, key positive residues implicated in voltage sensing are conserved at the S4 domain. Calcium-binding appears to be dissimilar to that in $SK_{Ca}$ and $IK_{Ca}$ channels, indeed many $BK_{Ca}$ channels are noticeably less sensitive to calcium ($EC_{50}$ >5$\mu$M at 0mV). A high-affinity calcium binding domain, the 'calcium bowl', has been identified between S9 and S10 on the intracellular C-terminal 'tail', although a number of further lower affinity calcium binding sites have also been proposed. The interdependence of channel gating on voltage and calcium is still incompletely understood; a simple model in which calcium binding is dependent on voltage has been ruled out. Current theories on $BK_{Ca}$ channel gating are critically appraised in a review by Magleby (2003).

Although there are considerable differences in the pharmacology and biophysics of different native $BK_{Ca}$ channels, no further genes encoding alpha subunits have been identified. Other members of the *Slo* gene family have been described, but these encode channels which are biophysically distinct from $BK_{Ca}$ channels. Diversity of $BK_{Ca}$ channel activity appears to be entirely due to interaction with optional beta subunits, splice-variation and phosphorylation.

Four beta subunits have been identified, all of which significantly influence the biophysical and/or pharmacological properties of $BK_{Ca}$ channels. Beta subunits are not essential for channel function, and many native $BK_{Ca}$ channel assemblies do not include these proteins. Each beta subunit comprises two transmembrane domains with an extracellular loop and cytoplasmic N&C termini. One beta binds at the external region of the S0 domain of each alpha subunit resulting in a channel comprising four alpha and four beta proteins. $\beta_1$ was initially identified in smooth muscle, and forms channels which are more sensitive to depolarisation and cytosolic calcium, and more sensitive to charybdotoxin. $\beta_2$ is expressed in chromaffin cells and the brain, and forms channels which rapidly inactivate. Like channels that incorporate $\beta_1$, those that include $\beta_2$ are more sensitive to cytosolic calcium and depolarisation, however, their charybdotoxin sensitivity is lower compared to channels that lack beta subunits. $\beta_3$ which has been identified in testis, pancreas and spleen, has three functional splice variants which confer different degrees of inactivation on $BK_{Ca}$ channels. $\beta_4$ is found in the brain and is unlike the other accessory subunits since it decreases sensitivity to calcium. Similarly to $\beta_2$, $\beta_4$ reduces channel sensitivity to charybdotoxin. The role of $BK_{Ca}$ channel $\beta$-subunits is detailed in a review by Orio *et al.* (2002).

Facilitation of gating by cyclic nucleotides such as cAMP and cGMP, and other endogenous ligands, occurs with some native $BK_{Ca}$ channels. Functional changes in response to these molecules are conferred through the activation of phosphorylation 'switches'.

$BK_{Ca}$ channels can be potently blocked by a number of peptides including iberiotoxin and limbatoxin, and charybdotoxin which also blocks $IK_{Ca}$ channels. Each of these structurally related peptides binds to the outer pore of the channel, physically occluding the ion pathway. Non-peptide selective inhibitors include paxilline, penitrem-A and tetrandrine. Some $BK_{Ca}$ channels may also be sensitive to the $IK_{Ca}$ channel blocker clotrimazole (Rittenhouse *et al.*, 1997; Wu *et al.*, 1999b), although this does not appear to be the case for all $BK_{Ca}$ channels since some physiological responses which show sensitivity to iberiotoxin are insensitive to clotrimazole (Fernandez-Fernandez *et al.*, 2002; Sobey *et al.*, 1998).

A number of $BK_{Ca}$ channel activators have been identified including benzimidazoline derivatives NS1619 and NS004, structurally related NS1608 and chlorzoxazone (Liu *et al.*, 2003b). DHS-I is a further example of a $BK_{Ca}$ channel opener, although it acts only on channels containing beta subunits.

This topic has been reviewed by Vergara *et al.* (1998), Calderone (2002), Orio *et al.* (2002) and Magleby (2003)

### 1.3.4.2) $BK_{Ca}$ channels in vascular endothelium

The first evidence of large conductance calcium-activated potassium channels in endothelium was presented in a study of cells cultured from bovine aorta (Fichtner *et al.*, 1987). Activated jointly by calcium and voltage, with a single channel conductance of ~150pS in symmetrical high potassium solutions, the channel was selective for potassium ions and non-rectifying.

$BK_{Ca}$ channels have subsequently been observed in cultures of porcine aortic (Graier *et al.*, 1993) and coronary (Baron *et al.*, 1996) endothelial cells, human coronary endothelial cells (Liu *et al.*, 2003a) and both primary cultures (Kestler *et al.*, 1998) and cell lines (Wu *et al.*, 1999a; Haburcak *et al.*, 1997) derived from human umbilical vein endothelium. Cultures of human capillary endothelial cells

have also been shown to exhibit whole-cell currents with an iberiotoxin-sensitive voltage-dependent component (Jow *et al.*, 1999).

It has been suggested that $BK_{Ca}$ channels are not present in freshly isolated endothelium, and that channel expression occurs during culture (Gauthier *et al.*, 2002b). In some instances this may be true since, in cultures of endothelium from human umbilical vein (Kestler *et al.*, 1998) and human coronary artery (Liu *et al.*, 2003a; Zunkler *et al.*, 1995), cells from early passages do not express functional $BK_{Ca}$ channels. Altering culture conditions also appears to influence expression of $BK_{Ca}$ channels in human capillary and bovine aortic endothelial cells (Jow *et al.*, 1999; Fichtner *et al.*, 1987). However, $BK_{Ca}$ channel activity has been recorded in both freshly isolated endothelium and patches from the endothelium of intact vessels, including rabbit aorta (Rusko *et al.*, 1992), rat aorta (Hoyer *et al.*, 1996) and porcine renal artery (Brakemeier *et al.*, 2003a).

In a study of human mesenteric arteries, endothelial cell patches of vessels from patients with colonic adrenocarcinoma contained iberiotoxin-sensitive $BK_{Ca}$ channels with a conductance of ~210pS (Kohler *et al.*, 2000). Interestingly, these channels were not present in the endothelium of subjects without this condition. mRNA encoding h*slo* was detected in cells from adrenocarcinoma patients, but not those originating from the control population.

The occurrence of $BK_{Ca}$ channel beta subunits has not been widely studied in endothelial cells, however $BK_{Ca}$ channels observed in pig aortic endothelium are reported to be insensitive to DHS-I, suggesting an absence of beta subunits (Papassotiriou *et al.*, 2000). Accordingly, cells from this study were found to express mRNA encoding the *Slo*1 alpha, but not the $\beta_1$ subunit. Expression of *Slo*1 has also been determined in cultured bovine aortic endothelial cells, using PCR and Western blotting (Wang *et al.*, 2005).

The negative range of endothelial cell membrane potentials may not appear suited to the activation of $BK_{Ca}$ channels, however, raised intracellular calcium may be sufficient to enable activation at these potentials. Also, since in some vessels electrical events originating from the smooth muscle can be recorded in the endothelium (Coleman *et al.*, 2001b), endothelial cells may at times become considerably depolarised.

A further aid to activation of endothelial $BK_{Ca}$ channels may be through gating modulation by endogenous substances. Nitric oxide has been demonstrated to

directly facilitate activation of $BK_{Ca}$ channels in some vascular smooth muscle, and a similar effect has been reported in patches of intact porcine renal artery endothelium (Brakemeier *et al.*, 2003a), although not in EA.hy926 cells (Haburcak *et al.*, 1997). Epoxyeicosatrienoic acids (EETs), which are synthesised by and stored in the endothelium, have also been shown to facilitate $BK_{Ca}$ channel opening in inside-out patches of cultured porcine coronary endothelial cells (Baron *et al.*, 1997). Intracellular cAMP (Graier *et al.*, 1993) and cGMP (Begg *et al.*, 2003) also activate $BK_{Ca}$ channels in endothelial cells.

Because, in some vascular beds at least, $BK_{Ca}$ channels appear to be expressed in both the endothelium and smooth muscle, care should be taken when interpreting effects of $BK_{Ca}$ channel blockers on functionally intact vessels. Bradykinin-evoked iberiotoxin-sensitive currents were recently recorded from the endothelium of intact vessels, but since these were absent following inhibition of gap junctions, it was concluded that the channels in question were located in the smooth muscle (Weston *et al.*, 2005).

1.3.4.3) $BK_{Ca}$ channels in vascular smooth muscle

The occurrence of $BK_{Ca}$ channels in vascular smooth muscle is well documented, with expression occurring in practically all vascular beds (Nelson, 1993). In addition to extensive single-channel studies, a physiological role for $BK_{Ca}$ channels in vascular smooth muscle has also been identified.

Under resting conditions, vascular smooth muscle generates 'spontaneous transient outward currents' (STOCs) due to bursts of $BK_{Ca}$ channel activity. STOCs occur in response to 'calcium sparks' which are caused by calcium entering the cytosol from the sarcoplasmic reticulum (SR) or through L-type voltage-dependent calcium channels. Co-localisation of $BK_{Ca}$ channels, L-type calcium channels and/or SR ryanodine receptors enables rapid coupling between calcium sparks and STOCs.

STOCs serve to dampen electrical excitability by hyperpolarising smooth muscle cells and thus reducing the open probability of voltage-dependent calcium channels. As a result, STOCs help maintain a relaxed resting muscle tone (Nelson *et al.*, 1995). $BK_{Ca}$ channels in vascular smooth muscle consist of both $\alpha$- and $\beta_1$-subunits, so are more sensitive to calcium than those found in the endothelium.

Accordingly, mice lacking $\beta_1$, have been shown to suffer hypertension due to vessel constriction (Brenner *et al.*, 2000). Close examination of vessels from these animals revealed that smooth muscle calcium sparks failed to efficiently trigger STOCs.

Various agonists act on vascular smooth muscle to cause a rise in cytosolic calcium and thus trigger contraction. This calcium rise occurs predominantly through calcium release from the SR with subsequent capacitative calcium entry (see *section 1.4.3*), or through the opening of voltage-gated- or receptor-operated- calcium channels. However, vasoconstriction by angiotensin II, 5-HT or phenylephrine is also attributable to G-protein-mediated inhibition of $BK_{Ca}$ channels and hence inhibition of STOCs (Alioua *et al.*, 2002).

The first $BK_{Ca}$ channels to be detected in vascular smooth muscle were TEA and quinine-sensitive potassium channels, with a unitary conductance of 100-150pS. These original recordings were made from rabbit portal vein smooth muscle cells (Beech & Bolton, 1987).

$BK_{Ca}$ channels with a single channel conductance of ~210 pS in high symmetrical potassium have been described in freshly isolated rat mesenteric artery smooth muscle cells (Mistry & Garland, 1998). These channels were voltage-dependent, activated by calcium and blocked by iberiotoxin. $BK_{Ca}$ channels from pig coronary artery smooth muscle have been studied in lipid bilayers. The channels had single channel conductances of 250-300pS under conditions of high symmetrical potassium, were activated by membrane depolarisation or intracellular calcium and were sensitive to nanomolar concentrations of charybdotoxin (Toro *et al.*, 1991).

Expression of *Slo1* or beta subunits in smooth muscle of rat mesenteric artery or pig coronary artery has not been studied. However, mRNA encoding $\beta_1$ has been detected in smooth muscle of rat aorta (Tsang *et al.*, 2004), and $BK_{Ca}$ channels in human coronary artery smooth muscle are sensitive to the channel opener DHS-I, also indicating the presence of beta-subunits (Tanaka *et al.*, 1997).

This topic has been reviewed by Tanaka *et al.* (2004) and Nelson & Quayle (1995).

## 1.4) Electrophysiological properties of endothelial cells

### 1.4.1) Introduction

Endothelial cells perform a wide range of functions in response to chemical stimuli by neuroendocrine factors, or to mechanical stimuli such as shear-stress. These include secretion of vasodilators including nitric oxide and prostacyclin, release of 'endothelium-derived contracting factor', and exocytosis of the platelet adhesion molecule von Willebrand factor.

Many of these responses involve a rise in cytosolic calcium which occurs through the release of calcium ions from the endoplasmic reticulum and/or opening of calcium-permeable channels in the plasmalemma. Since endothelial cells also contain calcium-activated potassium ($K_{Ca}$) channels, such stimuli also cause cell hyperpolarisation. This may serve a number of purposes including the creation of a more favourable driving force for sustained calcium influx.

The nature of endothelial cell responses are determined by factors including: resting conductances; origin, maintenance and localisation of raised cytosolic calcium; $K_{Ca}$ channel subtype(s) activated; and electrical coupling, both within the endothelium, and between endothelial- and smooth muscle-cells. Each of these will be discussed throughout the following sections.

### 1.4.2) The endothelium under resting conditions

Endothelial cells are described as non-excitable, reflecting a lack of voltage-dependent ion channels.

Few membrane ion channels are open when endothelial cells are unstimulated, resulting in a high input resistance. Under these conditions, the opening or closing of only a few channels will have a relatively large impact on the determined resting membrane potential. This, along with differential channel expression, explains why such a large range of resting membrane potentials (-80 to 0mV) have been described in endothelial cells from different vascular beds.

The measurement of resting membrane potential ($E_m$) will also be influenced by the nature of the recording method. Damage to the cell membrane caused by introduction of an intracellular electrode may allow entry of extracellular calcium and therefore activate calcium-dependent ion channels and processes. For similar reasons, the free-calcium concentration of 'patch' electrode filling solutions is also critical when measuring membrane potential through current-clamp. Also, in intact vessels, coupling of smooth muscle cells to the endothelium is known to influence endothelial cell $E_m$, whilst the culture of isolated cells can cause alteration of ion channel expression, again affecting recorded values.

In many endothelial cells, $E_m$ is dominated by an inwardly rectifying potassium conductance ($K_{IR}$). The greater the dominance, the closer $E_m$ is to the reversal potential for potassium ions ($E_K$), typically between -80 and -90mV. Expression of $K_{IR}2.1$, $K_{IR}2.2$ and $K_{IR}2.4$ channel subunits have been identified in some endothelial cells (Forsyth *et al.*, 1997; Fang *et al.*, 2005).

$K_{IR}$ channels are not dominant or necessarily present in all endothelial cells. The less negative membrane potential of such cells is influenced by chloride channels and/or by non-selective cation (NSC) channels. These conduct currents which reverse at potentials closer to zero mV depending on precise properties of the channel. Examples of such channels active in non-stimulated endothelial cells include the volume-regulated anion channel (VRAC), and the NSC hyperpolarisation-activated current ($I_h$).

Electrogenic activity of the sodium-potassium pump has been demonstrated under resting conditions in some endothelial cells, since ouabain-block or removal of extracellular potassium results in cell depolarisation. Usually, the pump extrudes three sodium- in exchange for two potassium- ions, and thus causes a net build-up of negative charge within the cell.

This topic has been reviewed by Adams & Hill (2004) and Nilius & Droogmans (2001).

## 1.4.3) Effects of vasoactive substances on cytosolic calcium

A number of vasoactive agents including ATP, bradykinin and substance-P (*table 1.2*) trigger a rise in endothelial cell cytosolic calcium which occurs as a rapid peak followed by a lower plateau. Provided that the resting membrane potential is not already close to $E_K$, this causes hyperpolarisation through the activation of calcium-activated potassium channels. In some cells, the hyperpolarisation is biphasic, apparently following the rise and fall in cytosolic calcium (Schilling, 1989).

For agonists acting via a $G_q$-coupled receptor, the initial phase of calcium increase is both rapid and transient, and can occur in the absence of extracellular calcium. It is mediated by the release of calcium from the endoplasmic reticulum in response to $IP_3$ generated through activation of phospholipase C (PLC). The second phase consists of a low plateau and is entirely dependent on extracellular calcium. This is due to influx of calcium through putative 'store operated channels' (SOC) that remain open until calcium stores are replenished. Such 'capacitative calcium entry' (CCE) was first described in Jurkat cells and is well established in endothelium (Himmel *et al.*, 1993).

Upon store release, a signal is established between the endoplasmic reticulum (ER) and SOC, causing them to open. Despite much study, the nature of this signal has yet to be elucidated. Also unclear is the identity of the SOC, a family of channels which vary in selectivity for calcium ions (Nilius *et al.*, 2003). It is believed that SOC subunits may belong to the 'canonical transient receptor potential' (TRPC) family of channel proteins, of which endothelial cells variously express six of the seven currently identified isoforms.

Endothelial CCE can be disrupted either through inhibition of the ER refilling pump by thapsigargin, or via a number of non-specific SOC blockers including lanthanum, econazole and 5-Nitro-2-(3-phenylpropylamino)benzoic acid (NPPB). The gating signal for the channels appears to involve MAP kinase and can be inhibited by PKG or calmodulin.

In addition to store depletion through $IP_3$ - operated channels, ER ryanodine receptor-operated calcium channels provide a further calcium-release pathway. These provide a positive feedback for store depletion by opening in response to

raised intracellular calcium, and can also be activated by sub-micromolar concentrations of ryanodine (a non-endogenous alkaloid).

In response to the aforementioned agonists of $G_q$-linked receptors, endothelial cells also release stored vasoactive substances including ATP and acetylcholine. ATP not only acts through P2Y receptors to trigger calcium store depletion and CCE, but may also directly trigger calcium entry via P2X channels. Non-selective calcium-permeable cation channels which open in response to cyclic nucleotides have also been described in endothelial cells.

This topic has been reviewed by Nilius & Droogmans (2001) and Adams & Hill (2004).

| Ligand | Receptor | G-protein | Second-messengers | References |
|---|---|---|---|---|
| acetylcholine | *muscarinic* | | | |
| | **$M_1$, $M_3$**, $M_5$ | $G_q$ | $IP_3$ / DAG | i |
| | $M_2$ | $G_i$ | reduces cAMP | |
| | | | | |
| | *nicotinic* | | | |
| | *α3, α5, α7, β2, β4* | - | - | ii |
| | | | | |
| ATP | **$P2Y_1$, $P2Y_2$**, $P2Y_6$ | $G_q$ | $IP_3$ / DAG | iii |
| | | | | |
| | $P2X_1$, $P2X_2$, $P2X_3$, **$P2X_4$**, $P2X_5$, $P2X_6$, $P2X_7$ | - | - | iv |
| | | | | |
| bradykinin | **$B_1$, $B_2$** | $G_q$ | $IP_3$ / DAG | v, vi |
| | | | | |
| histamine | **$H_1$** | $G_q$ | $IP_3$ / DAG | vii |
| | $H_2$ | $G_s$ | increases cAMP | |
| | $H_3$ | $G_i$ | reduces cAMP | viii |
| | | | | |
| substance-P | $NK_1$ | $G_q$ | $IP_3$ / DAG | ix |

**Table 1.2)** Some substances which evoke a rise in endothelial cell cytosolic calcium (column 1) together with their relevant endothelial cell receptors (column 2) and second messenger pathways (column 3-4). Bold print indicates the predominantly expressed receptor(s). Expression of receptors varies between vascular beds. References: i(Walch *et al.*, 2001), ii(Sharma & Vijayaraghavan, 2002), iii(Guns *et al.*, 2005), iv(Pulvirenti *et al.*, 2000), v(McLean *et al.*, 2000), vi(Mombouli *et al.*, 1992), vii(Schaefer *et al.*, 2003), viii(Ea Kim *et al.*, 1992), ix(Quartara & Maggi, 1998).

## 1.4.4) Effects of raised cytosolic calcium

Calcium-activated potassium ($K_{Ca}$) channels are the dominant endothelial channels which open in response to an agonist-mediated rise in cytosolic calcium. Endothelium from different vascular beds differentially express the three $K_{Ca}$ channel subtypes: $SK_{Ca}$, $IK_{Ca}$ and $BK_{Ca}$ (see *sections 1.3.2* to *1.3.4*).

In some endothelial cells, hyperpolarisation evoked by vasoactive substances (*table 1.2*) is abolished by blocking $SK_{Ca}$ channels, whilst in other cells, $IK_{Ca}$ channels are implicated. In many cells, only a combination of apamin and charybdotoxin, but not apamin and iberiotoxin, is sufficient to abolish hyperpolarisation indicating that both $SK_{Ca}$ and $IK_{Ca}$ channels are active. This topic has been reviewed by Coleman *et al.* (2004).

Sensitivity of agonist-evoked endothelial hyperpolarisation to the selective $BK_{Ca}$ channel blocker iberiotoxin is apparent in only a few vessels, indicating that in the majority of vessels these channels play only a minor role or remain inactive. This may in part be due to the lower sensitivity of $BK_{Ca}$ channels to calcium compared with $IK_{Ca}$ and $SK_{Ca}$ channels. Activation of endothelial $BK_{Ca}$ channels may require additional factors.

It has been demonstrated that in cultured pig coronary artery endothelium, substance P activates $SK_{Ca}$ but not $BK_{Ca}$ channels, whilst the converse is true of bradykinin (Frieden *et al.*, 1999). This suggests subtle differences in intracellular signalling between these agonists which have yet to be elucidated. Both agonists activate $IK_{Ca}$ channels in these cells (Sollini *et al.*, 2002).

Both calcium-permeable (Baron *et al.*, 1996) and calcium-impermeable (Suh *et al.*, 2002) calcium-activated non-selective cation ($NSC_{Ca}$) channels have been identified in endothelial cells. The activity of either would be expected to counteract membrane hyperpolarisation although paradoxically, calcium-permeable $NSC_{Ca}$ channels would also provide an additional calcium-entry route and thus support hyperpolarising $K_{Ca}$ currents.

Sodium entry via $NSC_{Ca}$ channels is believed to trigger a reversal of the sodium-calcium transporter (NCX), resulting in a further mechanism for calcium-influx and generation of a hyperpolarising current. Blockade of the reversed mode of

NCX can inhibit the plateau phase of rat aortic endothelial cell hyperpolarisation in response to acetylcholine (Bondarenko, 2004).

Calcium-activated chloride ($Cl_{Ca}$) (also CaCC or CLCA) channels with differing properties have been described in vascular endothelial cells. These channels require intracellular ATP to activate and carry a current which, under physiological chloride conditions, would reverse at a membrane potential positive to that of potassium. This would have the effect of limiting the magnitude of hyperpolarisation.

This topic has been reviewed by Nilius & Droogmans (2001).

## 1.4.5) Effects of mechanical stimuli

Mechanosensitive ion channels, which open in response to physical forces acting on the cell membrane, have been described in endothelial cells. These include potassium channels, chloride channels and non-selective cation channels. The identity of many of these conductances has yet to be determined, and it is unclear whether they represent previously identified channels which open in response to other stimuli, or are distinct channels opened only through exposure to mechanical forces. Also to be determined is which of these channels have intrinsic mechanosensing properties and which are functionally coupled to other elements which respond to physical forces, such as the endoplasmic reticulum (ER).

*In vivo*, endothelial cells are exposed to two different physical stimuli: shear stress caused by the movement of blood over the cell surface and biaxial tensile stress caused by blood pressure and vessel stretching. Whilst chronic alteration to the levels of these stimuli results in altered gene transcription and protein phosphorylation, acute effects on ion channels and ER calcium handling also occur.

Release of calcium from the endoplasmic reticulum without the involvement of $IP_3$ has been reported in endothelium exposed to simulated mechanical stress. Such conditions also cause the opening of some calcium-permeable non-selective cation channels.

Secondary to rises in cytosolic calcium are the activation of calcium-activated conductances (see *section 1.4.4*), some of which themselves exhibit altered

behaviour in response to mechanical stress. Endothelial $BK_{Ca}$ channels, for example, become more sensitive to calcium when the plasmalemma is exposed to mechanical forces.

*In vivo*, the result of these continual mechanical stimuli, particularly shear stress, is vasodilation through endothelial release of nitric oxide, prostacyclin and activation of the EDHF-pathway. Such vasodilation is proportional to the degree of stress exerted on the endothelium.

This topic has been reviewed by Nilius & Droogmans (2001).

### 1.4.6) Additional ion conductances

Endothelial cells are coupled by gap junctions both to one another and, in a number of vessels, to vascular smooth muscle. Such is the extent of myoendothelial coupling in some vessels that electrical events originating at the smooth muscle can be recorded in the endothelium. Gap junctions are also permeable to other molecules including second messengers, so it is likely that in such vessels, smooth muscle will influence endothelial cell ion conductances in a number of ways. Gap junctions are described further in *section 1.5.4.7.*

*Section 1.4* has discussed a variety of ion conductances likely to bear relevance to endothelium-dependent vasodilation. Information about endothelial ion channels not discussed here can be found in reviews by Nilius & Droogmans (2001) and Adams & Hill (2004).

## 1.5) EDHF-mediated vasodilation

### 1.5.1) Endothelium-dependent regulation of vascular tone

Dilation of constricted vessels by a number of agents including acetylcholine, substance-P and bradykinin (*table 1.2*), occurs in an endothelium-dependent manner

(Furchgott & Zawadzki, 1980). This occurs via three established mechanisms each of which ultimately effect a lowering of smooth muscle cytosolic calcium and thus inhibit contraction; a calcium-dependent process.

1.) Nitric oxide produced by and released from the endothelium activates smooth muscle soluble guanylate cyclase. The resulting increase in cGMP causes both lowering of cytosolic calcium and reduction in the sensitivity of contractile elements to calcium.

2.) Prostacyclin release from the endothelium activates smooth muscle adenylyl cyclase and G-proteins. Increased levels of cAMP cause the opening of ATP-dependent potassium channels and large conductance calcium-activated potassium channels which results in smooth muscle hyperpolarisation. Subsequent closure of voltage-dependent calcium channels, hence lowering of cytosolic calcium, is accompanied by a reduction in the sensitivity of contractile elements to calcium.

3.) 'EDHF-type' vasodilation occurs independently of both nitric oxide and prostacyclin, and relaxes smooth muscle via hyperpolarisation. EDHF responses are also insensitive to inhibition of guanylate cyclase, and are absent when vessels are pre-constricted using raised extracellular potassium. Initially, it was postulated that a soluble endothelium-derived hyperpolarising factor (EDHF) caused the opening of smooth muscle potassium channels and thus led to hyperpolarisation.

There continues to be considerable disagreement surrounding the components and order of events that occur during the EDHF phenomenon. These will be considered throughout the following sections.

The nitric oxide, prostacyclin and EDHF pathways occur to varying degrees in different vascular beds. Endothelium-dependent dilation of small resistance vessels is generally mediated via 'EDHF' whilst in large conduit vessels, nitric oxide is the predominant factor. In many arteries, the three mediators play more equal roles, the triggering of either able to cause full dilation. *In vivo*, there is evidence for 'cross-talk' between different pathways, including suppression of 'EDHF' by nitric oxide.

In addition to relaxing factors, the endothelium also releases agents which contract smooth muscle. Vasoconstrictors such as angiotensin II cause endothelial production and release of endothelin which binds to smooth muscle receptors. This triggers both calcium release from the sarcoplasmic reticulum and the opening of non-selective cation channels which increase levels of smooth muscle cytosolic calcium, leading to contraction. *In vivo*, endothelin release is largely suppressed by nitric oxide, further demonstrating crosstalk between the various factors which influence vascular tone. Thromboxane $A_2$ and endoperoxidases have also been described as endothelium-derived contracting factors.

A complex equilibrium between vaso -constrictor and -dilator pathways serves to regulate vascular tone in response to both chemical and mechanical stimuli. These act alongside further mechanisms which alter vascular tone independently of the endothelium.

## 1.5.2) Introduction to 'EDHF'

Simultaneous hyperpolarisation and relaxation of contracted vascular smooth muscle was first established in carbachol-stimulated guinea pig mesenteric arteries (Bolton *et al.*, 1984). Both responses were determined as being endothelium-dependent, and it was postulated that hyperpolarisation may support smooth muscle relaxation by instigating the closure of voltage-dependent calcium channels. At the time, intertwining pathways involving prostacyclin and the yet elucidated nitric oxide (NO) had yet to be separated.

Following identification of agents which blocked the NO pathway, these were used in combination with cyclooxygenase (COX) inhibitors, to establish residual vascular responses to vasodilator agonists. The first such study was carried out in rat aorta and pulmonary artery *in vitro*, and revealed that endothelium-dependent smooth muscle hyperpolarisation was insensitive to both agents (Chen *et al.*, 1988). It was suggested that the remaining response could be explained by release of a putative endothelium-derived hyperpolarising factor (EDHF) which triggers activation of smooth muscle potassium channels. Although in this initial study vasodilation in response to 'EDHF' was small, further studies revealed that in

other vascular beds, 'EDHF' provided full reversal of smooth muscle contraction. As already mentioned, it is now recognised that with few exceptions, 'EDHF' is more prominent in resistance vessels (Shimokawa *et al.*, 1996), whereas NO is the main endogenous vasodilator in conduit vessels. In a significant number of vessels, NO and 'EDHF' are both able to provide full vasodilation, with NO acting as principal dilator, and 'EDHF' as a reserve. In some of these arteries, agonist-evoked relaxation is also partly mediated through release of endothelium-derived prostacyclin.

Distinguishing between the three pathways is important from an experimental standpoint since both NO and prostacyclin have also been demonstrated to cause smooth muscle hyperpolarisation through activation of $BK_{Ca}$ and $K_{ATP}$ channels, respectively. EDHF-mediated vasodilation is commonly defined as that which remains following inhibition of COX and endothelial nitric oxide synthase (eNOS). Some studies also include inhibitors of cGMP, further blocking the pathway through which NO predominantly acts. Recent studies have suggested that in some vessels, other precautions should be taken to ensure complete isolation of the EDHF response. These include application of nitric oxide chelators such as oxyhaemoglobin, to prevent the action of NO released from putative NO stores (Chauhan *et al.*, 2003a; Stoen *et al.*, 2003), and depletion of nerve terminals with capsaicin to prevent agonist-evoked release of relaxing factors from the *nervi vasorum* (Högestätt *et al.*, 2000).

The initial focus of studies aimed at characterising the 'EDHF' pathway was to identify the putative soluble factor and the smooth muscle potassium channels on which it was believed to act. At that time, the electrical involvement of the endothelium was overlooked, despite the description elsewhere in the literature of agonist-evoked endothelial hyperpolarisation. The discovery that EDHF-responses are potently inhibited by a combination of $SK_{Ca}$ and $IK_{Ca}$ channel blockers was a factor behind a rethink of the mechanism of the EDHF-pathway (Edwards & Weston, 1998). $SK_{Ca}$ and $IK_{Ca}$ channels were known not to be prominently expressed in smooth muscle, but had been identified in endothelial cells. Additionally, no soluble candidate for EDHF had received wide acceptance.

Revision of the EDHF model to include hyperpolarisation of the endothelium opened up more mechanistic opportunities for the pathway. This includes the possibility that myoendothelial gap junctions may convey hyperpolarisation directly to the muscle and thus circumvent the requirement of a soluble EDHF. For those

models which still propose a soluble factor, the question of smooth muscle potassium conductances is still relevant and, despite some strong candidates, remains an incompletely resolved issue. The following sections will consider the sensitivity of the EDHF-pathway to blockers of potassium conductances, and then discuss a number of proposed candidates suggested as the 'link' between the endothelium and smooth muscle.

## 1.5.3) Involvement of potassium conductances in the EDHF pathway

Early studies into EDHF suggested that potassium channels underlay the hyperpolarisation, as judged by rubidium efflux studies and electrophysiology (Chen *et al.*, 1988). According to the original model of the EDHF pathway, the relevant channels were presumed to be located on the smooth muscle.

An insensitivity of the EDHF response to agents which selectively block ATP-sensitive and voltage-gated potassium channels was established early on (Bray & Quast, 1991; Zygmunt & Högestätt, 1996; Zygmunt *et al.*, 1997a; Petersson *et al.*, 1997). However, less selective potassium channel blockers such as TEA, TBA and 4-AP were shown to attenuate hyperpolarisation and relaxation in some vessels (Hasunuma *et al.*, 1991; Hecker *et al.*, 1994; Kitagawa *et al.*, 1994).

The first examples of selective potassium channel blockers inhibiting the EDHF response were that of apamin in the rat mesenteric vascular bed (Adeagbo & Triggle, 1993) and charybdotoxin in rabbit aorta and carotid artery (Cowan *et al.*, 1993). In a number of other vascular beds however, neither apamin nor charybdotoxin produced substantial inhibition of the EDHF response. Interestingly, it was discovered that in these vessels effective block could be achieved by co-application of the two toxins (Waldron & Garland, 1994; Zygmunt & Högestätt, 1996; Coats *et al.*, 2001). Sensitivity of vascular smooth muscle hyperpolarisation and relaxation to a combination of apamin and charybdotoxin remains one of the hallmarks of the EDHF pathway.

Apamin is believed to block only $SK_{Ca}$ channels, and the concentrations used in these studies were consistent with selective block of this channel. Since charybdotoxin blocks both $IK_{Ca}$ and $BK_{Ca}$ channels, an important consideration was

which channel subtype(s) are involved. Since, in the presence of apamin, the selective $BK_{Ca}$ channel blocker iberiotoxin is an inadequate substitute for charybdotoxin, it was concluded that $IK_{Ca}$ and not $BK_{Ca}$ channels are involved in the EDHF response (Zygmunt & Högestätt, 1996). Recent studies have shown that TRAM-34 or TRAM-39, novel $IK_{Ca}$ channel blockers with very little $BK_{Ca}$ channel blocking activity, can abolish the EDHF response in combination with apamin (Eichler *et al.*, 2003; Hinton & Langton, 2003).

In a few vascular beds such as the rabbit renal (Kwon, 2001) or canine coronary arteries (Nishikawa *et al.*, 1999), EDHF responses are significantly attenuated by iberiotoxin suggesting a role for $BK_{Ca}$ channels in these vessels.

A number of studies have since demonstrated that both $SK_{Ca}$ (Burnham *et al.*, 2002; Frieden *et al.*, 1999) and $IK_{Ca}$ channels (Kohler *et al.*, 2000; Bychkov *et al.*, 2002; Sollini *et al.*, 2002) are located on the endothelium (see *sections 1.3.2.2 & 1.3.3.2*). It has also been demonstrated that a combination of apamin and charybdotoxin is effective when selectively applied to the intimal, but not the adventitial surface of blood vessels (Doughty *et al.*, 1999).

There are few reports of these channels also being located on the smooth muscle (see *sections 1.3.2.3 & 1.3.3.3*).

In many vessels, EDHF responses are also sensitive to ouabain or a combination of ouabain and barium (Edwards *et al.*, 1998). At sub-micromolar concentrations, ouabain is believed to be selective for $\alpha 2$ and $\alpha 3$ isoforms of the sodium-potassium pump (Na/K-ATPase) which are expressed in vascular smooth muscle (Weston *et al.*, 2002). $\alpha 2$ and $\alpha 3$ are inducible isoforms whereas $\alpha 1$, the housekeeping isoform is believed to be constitutively active and is less sensitive to ouabain. Although initially demonstrated to block EDHF responses at 1mM, ouabain was subsequently shown to be equally effective at sub-micromolar concentrations (Edwards *et al.*, 1999b). This is particularly important since ouabain is shown to have non-selective effects at high micromolar concentrations, including block of gap junctions (Weingart, 1977) and inhibition of sodium nitroprusside (SNP) -mediated dilation (Sathishkumar *et al.*, 2005). Despite this, many researchers studying 'EDHF' have continued to use ouabain at non-selective concentrations.

In some vessels, a sub-micromolar concentration of ouabain is effective in abolishing the EDHF response alone (Beny & Schaad, 2000).

At a concentration of 30$\mu$M, barium ions are considered to selectively block inwardly rectifying potassium ($K_{IR}$) channels. Although barium is frequently reported to have little or no effect on the EDHF response when applied alone, it can be additive to the blocking actions of ouabain (Edwards *et al.*, 1998).

Both Na/K-ATPase and $K_{IR}$ channels are known to be expressed in both endothelial cells and smooth muscle. However, since in some endothelium-denuded vessels, EDHF-mimicking actions of potassium ions are blocked by a combination of ouabain and barium, it has been suggested that the relevant proteins are located on the smooth muscle (Edwards *et al.*, 1998).

In a substantial number of studies, a combination of sub-micromolar ouabain and 30μM barium is unable to significantly block EDHF-mediated smooth muscle hyperpolarisation and relaxation (Coleman *et al.*, 2001a; Buus *et al.*, 2000; McIntyre *et al.*, 2001). This may reflect an involvement of other smooth muscle potassium channels such as those sensitive to 4-aminopyridine (Quignard *et al.*, 2000).

This topic has been reviewed by Coleman *et al.* (2004) and Busse *et al.* (2002).

## 1.5.4) EDHF candidates

### 1.5.4.1) Criteria

In order to be considered an endogenous EDHF, candidates should fulfil the following criteria:

In the case of soluble EDHF candidates:

- The Candidate should be able to both hyperpolarise and relax vascular smooth muscle in the absence of a functional endothelium. The response evoked by the Candidate should not be sensitive to any agent to which the native EDHF response is insensitive

- The Candidate should be synthesised at or stored in the endothelium and released upon application of agonists known to evoke EDHF responses. Release should be at a concentration sufficient to cause hyperpolarisation and relaxation comparable to the native EDHF response

- A combination of apamin and charybdotoxin should prevent release of the Candidate from the endothelium in response to agonists known to evoke EDHF responses, but not inhibit the actions of the Candidate when applied exogenously to endothelium-denuded smooth muscle

- In an intact vessel, prevention of synthesis, or chelation of the Candidate should abolish the native EDHF response

A role for myoendothelial gap junctions:

- The native EDHF response should be sensitive to gap junction uncouplers. If available, agents should be used which are believed to preferentially uncouple myoendothelial gap junctions over homocellular gap junctions

- The uncoupling agent should not affect the native NO or $PGI_2$ –mediated dilator responses of the vessel in question. Neither should it affect native EDHF attributed responses in vessels where it is believed that myoendothelial gap junctions play no role

- For a given vessel, the presence of myoendothelial gap junctions should be established using electron microscopy

- Electrophysiology should be used to determine similarity of endothelial and smooth muscle responses. It may also be possible to record smooth muscle electrical events (e.g. spontaneous transient outward currents) at the endothelium.

The following sections will briefly discuss some of the candidates which have been proposed to account for the 'endothelium-to-smooth muscle signal' in the EDHF pathway.

1.5.4.2) Anandamide

The endogenous cannabinoid, anandamide, was first proposed as an EDHF following the observation that EDHF responses of rat mesenteric arteries were sensitive to the selective CB1 receptor antagonist, SR141716A (Randall *et al.*, 1996). Furthermore, anandamide was demonstrated to be released from blood vessels stimulated with carbachol, and exogenous application of the cannabinoid caused vasodilation sensitive to raised external potassium. Subsequently it was confirmed that anandamide is able to elicit smooth muscle hyperpolarisation in an endothelium-independent manner (Plane *et al.*, 1997; White & Hiley, 1997). Smooth muscle responses to anandamide have been deemed sensitive to a number of different agents including potassium channel blockers TBA (Randall & Kendall, 1997), TEA and barium, and the $G_i$ protein inhibitor, pertussis toxin (White & Hiley, 1997).

The vasodilatory action of anandamide has proven to be highly varied. Across different vessels, exogenous application of anandamide not only appears to mimic EDHF responses but can also trigger endothelium-*dependent* smooth muscle hyperpolarisation (Zygmunt *et al.*, 1997b), cyclooxygenase-dependent endothelium-*independent* smooth muscle hyperpolarisation (Fleming *et al.*, 1999) and smooth muscle relaxation in the absence of hyperpolarisation (Zygmunt *et al.*, 2000).

Native EDHF responses are frequently described as insensitive or poorly sensitive to concentrations of ~~SR171614A~~ SR141716A considered selective for CB1 receptors (Plane *et al.*, 1997; Zygmunt *et al.*, 1997b; Vanheel & Van de Voorde, 2001). Selective CB2 receptor antagonists do not affect EDHF-responses (Harris *et al.*, 1999).

Smooth muscle responses to anandamide show sensitivity to ~~SR171614A~~ SR141716A in some studies (Zygmunt *et al.*, 1997b; O'Sullivan *et al.*, 2004), but not in others (Plane *et al.*, 1997; Vanheel & Van de Voorde, 2001). Structurally-unrelated CB1 agonists appear unable to mimic the effects of anandamide in these vessels (Plane *et al.*, 1997; Vanheel & Van de Voorde, 2001).

Further inconsistencies between native EDHF responses and those to exogenous anandamide include the difference in the time course of smooth muscle hyperpolarisation (Vanheel & Van de Voorde, 2001), and the sensitivity of anandamide- but not EDHF-mediated smooth muscle responses to ouabain and cooling (Zygmunt *et al.*, 2000).

Anandamide has been demonstrated to exert effects on vascular smooth muscle by acting on vanilloid receptors located on the *nervi vasorum* (Zygmunt *et al.*, 1999). This appears to be mediated through release of calcitonin gene related peptide (CGRP) since pre-treatment with capsaicin or antagonists of the TRPV1 vanilloid receptor prevent the actions of anandamide on endothelium-denuded vessels. Further vasodilator effects of anandamide may be mediated via endothelial cells (O'Sullivan *et al.*, 2004).

Paradoxically, anandamide and other CB1 receptor agonists have also been shown to block the native EDHF response in a number of different arteries (Fleming *et al.*, 1999). This appears to be due to an inhibitory effect on gap junction communication (Brandes *et al.*, 2002).

This topic has been reviewed by Randall *et al.* (2004) and McGuire *et al.* (2001).

### 1.5.4.3) C-type natriuretic peptide

C-type natriuretic peptide (CNP) is a paracrine factor which mediates endothelium-dependent vasodilation independently of cyclooxygenase and nitric oxide. In some large conduit vessels, CNP relaxes smooth muscle by binding to natriuretic peptide receptor (subtype B) (NPR-B) receptors and triggering a cGMP-dependent pathway. In smaller vessels, CNP has been shown to cause smooth muscle hyperpolarisation and relaxation through binding to the NPR-C receptor (Chauhan *et al.*, 2003b). Until recently, the NPR-C receptor was believed only to serve as a 'clearance receptor' involved in the binding and degradation of CNP.

CNP is formed upon conversion of its pro-hormone which is expressed in the endothelium and catabolised to the active form during cell stimulation by cytokines and 'EDHF agonists' such as ACh and bradykinin. Once released, CNP activates

smooth muscle NPR-B and NPR-C receptors and is degraded by endopeptidases or through the clearance activity of NPR-C.

Consistent with EDHF pharmacology of denuded vessels, smooth muscle hyperpolarisation and relaxation to CNP is sensitive to TEA or a combination of barium and ouabain, but not apamin and charybdotoxin (Honing *et al.*, 2001; Chauhan *et al.*, 2003b). Activation of NPR-C by CNP or $cANF^{4-23}$, a selective agonist of NPR-C, has been demonstrated to trigger opening of putative G-protein linked inwardly-rectifying potassium channels (GIRK) as defined by pharmacological sensitivity to tertiapin, a GIRK-specific inhibitor, and pertussis toxin, the classic $G_i$ protein inhibitor (Chauhan *et al.*, 2003b). Responses to exogenous CNP are blocked by the selective NPR-C antagonist M372049 (Hobbs *et al.*, 2004). Furthermore, native EDHF responses but not those mediated by NO have been demonstrated as sensitive to these inhibitors.

In small rat mesenteric arteries, blockade of NPR-B receptors by HS-142-1 has a negligible effect on responses to CNP or ACh-evoked EDHF, suggesting that CNP effects are mediated purely through NPR-C (Chauhan *et al.*, 2003b).

'EDHF-like' responses to CNP have been demonstrated as being abolished by the gap junction uncoupler 18α-GA (Chauhan *et al.*, 2003b), a finding which has been interpreted by some as a reason for discounting CNP as an EDHF candidate. It is possible, however that sensitivity to this agent reflects blockade of homocellular gap junctions at the endothelium or smooth muscle which are likely to play a role in propagating the EDHF response within the vessel wall. Determining the sensitivity of CNP responses to other gap junction uncoupling agents may help clarify this.

This topic has been reviewed by Chauhan *et al.* (2004).

### 1.5.4.4) Epoxyeicosatrienoic acids

Arachidonic acid can be metabolised into various vasoactive substances via three groups of enzymes: cyclooxygenases, lipoxygenases and cytochrome P-450 epoxygenases (cP450). The last is responsible for the formation of epoxyeicosatrienoic acids (EETs) which have been implicated as putative EDHFs. These molecules are variously produced and released by endothelial and smooth muscle cells, and mediate a range of functions.

EETs were the earliest of the proposed EDHF candidates, and though their identity was not formally established until 1996, the sensitivity of EDHF responses to inhibitors of cP450 had been previously described (Singer *et al.*, 1984; Hecker *et al.*, 1994; Campbell *et al.*, 1996). Although the enzyme inhibitors used in these early studies were largely non-selective, the findings are supported by more recent studies using such approaches as the selective 'inhibition' of specific EETs and antisense targeting of specific cP450 isoforms (Fisslthaler *et al.*, 1999; Gauthier *et al.*, 2002a).

Evidence for endothelial release of a cP450-related EDHF has also been provided via 'sandwich' bioassays where, in an organ bath preparation, an endothelium-denuded vessel is placed in close proximity to an intact vessel. If the endothelium-denuded tissue is able to respond to 'EDHF agonists' in the presence of an intact tissue, this is assumed to be via the release of a soluble factor(s) from the endothelium of the intact vessel (Feletou & Vanhoutte, 1988).

In some vessels, direct application of specific EET isoforms including 11,12-EET and 14,15-EET can be shown to hyperpolarise and relax endothelium-denuded smooth muscle (Campbell *et al.*, 1996; Pratt *et al.*, 2001).

Despite evidence for EETs as EDHFs in some vessels, in others blockade of cP450 or EET action does not affect the native EDHF response. Further still, where exogenously applied EETs are shown to mimic EDHF in denuded vessels, these responses are often sensitive to iberiotoxin or glibenclamide, blockers of $BK_{Ca}$ and $K_{ATP}$ channels respectively (Eckman *et al.*, 1998; Fukao *et al.*, 1997). This is inconsistent with the native EDHF responses from the vessels in question.

EETs have also been implicated in endothelium intracellular calcium signalling and gap junction function (Graier *et al.*, 1995; Popp *et al.*, 2002). Such mediatory roles are likely to account for the sensitivity of native EDHF to blockade of EET formation or function in some vessels.

Whilst EETs are unlikely to account for EDHF in most vessels, in some they may provide an intracellular signalling function within the endothelium, critical to the generation and/or transmission of endothelial hyperpolarisation.

This topic has been reviewed by Fleming (2004).

1.5.4.5) Hydrogen peroxide

Activity of enzymes in the endothelium including nitric oxide synthase (eNOS), cyclooxygenase and lipoxygenase results in the production of superoxide which subsequently degrades into hydrogen peroxide. In the case of eNOS, generation of superoxide may continue even during inhibition of NO production by the stable L-arginine analogue L-NOARG (Stroes *et al.*, 1998).

During agonist stimulation (Matoba *et al.*, 2000; Hatoum *et al.*, 2005) or in response to shear-stress (Miura *et al.*, 2003), enzyme activity, and hence hydrogen peroxide release from the endothelium, is increased. Direct application of physiological concentrations of hydrogen peroxide has been demonstrated to hyperpolarise and relax endothelium-denuded vascular smooth muscle (Matoba *et al.*, 2000; Matoba *et al.*, 2002). In the same vessels, EDHF-mediated hyperpolarisation and relaxation is sensitive to the hydrogen peroxide catabolic enzyme, catalase (Pomposiello *et al.*, 1999; Matoba *et al.*, 2000). Catalase is without effect on non-EDHF vasodilatory responses.

Superoxide dismutase (SOD) catabolises superoxide into hydrogen peroxide. Tiron, a membrane-permeable agent which mimics the actions of SOD, has been shown to enhance native EDHF responses in some studies (Matoba *et al.*, 2003; Fujiki *et al.*, 2005).

Reduced EDHF responses of mesenteric arteries from eNOS knockout- compared to control-mice suggest that eNOS activity accounts for the major source of endothelial hydrogen peroxide (Matoba *et al.*, 2000).

Further to the direct effects of hydrogen peroxide on smooth muscle, an autocrine effect at the endothelium cannot be ruled out. Application of exogenous hydrogen peroxide has been demonstrated to cause endothelium-*dependent* dilation in human sub-mucosal arteries (Hatoum *et al.*, 2005), and be sensitive to blockade by a combination of apamin & charybdotoxin in human coronary arteries (Miura *et al.*, 2003). The latter observation could alternatively be due to the blockade of smooth muscle $BK_{Ca}$ channels by charybdotoxin, since the blockers were not studied in isolation.

The manner in which hydrogen peroxide triggers smooth muscle hyperpolarisation has yet to be fully studied, although it has been demonstrated that catalase-sensitive dilations are sensitive to ouabain at a concentration believed to be

selective for inducible isoforms of the sodium-potassium pump (Pomposiello *et al.*, 1999).

It should also be noted that in some relaxed vessels, hydrogen peroxide causes vasoconstriction via a number of mechanisms (Gao *et al.*, 2003).

This topic has been reviewed by Shimokawa & Matoba (2004).

1.5.4.6) Potassium ions

Endothelium-independent vessel dilation in response to raised extracellular potassium has been described in numerous vascular beds throughout the past 70 years. Barium and/or ouabain are able to abolish these responses at concentrations which selectively block inwardly rectifying potassium channels and the $\alpha 2$ or $\alpha 3$ isoforms of the sodium-potassium pump respectively (Chen *et al.*, 1972; McCarron & Halpern, 1990; Edwards *et al.*, 1999b).

In conditions of raised extracellular potassium, inwardly rectifying potassium ($K_{IR}$) channels open at more depolarised potentials, which may result in a hyperpolarising current. Increased external potassium also activates sodium-potassium pumps (Na/K-ATPases) causing a net outward current via exchange of ions at a 3:2 ratio (sodium out, potassium in). In some vessels, block of the Na/K-ATPases alone may depolarise the membrane potential enough to prevent outward potassium flux via $K_{IR}$ channels.

Edwards *et al.* (1998) were the first to provide evidence for potassium-evoked smooth muscle hyperpolarisation in EDHF vasodilation. Opening of apamin and charybdotoxin sensitive channels located on the endothelium was proposed to release sufficient potassium into the myoendothelial space to trigger smooth muscle hyperpolarisation.

Agonist-evoked EDHF responses in rat hepatic and mesenteric arteries were shown to be abolished by a combination of ouabain and barium, as were identical responses of endothelium-denuded vessels to exogenous potassium (Edwards *et al.*, 1998; Coleman *et al.*, 2001b; Buus *et al.*, 2000). Later studies also demonstrated the ability of an externally applied 'potassium-chelator' to reversibly inhibit agonist-evoked EDHF responses in other vessels (Beny & Schaad, 2000; Bussemaker *et al.*, 2002).

Where potassium-induced dilation has been described, increasing extracellular potassium to <15mM causes smooth muscle hyperpolarisation and vasodilation, whereas higher concentrations cause depolarisation and constriction.

In order for potassium to qualify as an EDHF, agonist-evoked dilations should be sensitive to inhibition of the smooth muscle potassium 'sensors' (Na/K-ATPase and $K_{IR}$ channels). Furthermore, exogenously applied potassium should hyperpolarise and relax smooth muscle in the absence of a functional endothelium.

Numerous studies have been unable to reproduce endothelium-independent vasodilations in response to raised extracellular potassium, or block agonist-evoked EDHF responses with barium and/or ouabain. Many laboratories have produced conflicting results despite adopting a similar experimental design. Potassium-evoked phenomena often occur in only a proportion of tissues (Andersson *et al.*, 2000; Doughty *et al.*, 2000), or more commonly are small (Lacy *et al.*, 2000), transient, absent or inverted (depolarisation with constriction) (Vanheel & Van de Voorde, 1999).

In some of these studies, inconsistencies may relate to the necessity of pre-constricting vessels with phenylephrine or similar agents which depolarise smooth muscle and raise cytosolic calcium (Dora & Garland, 2001). Under these conditions, a build-up of external potassium caused by efflux via $BK_{Ca}$ channels may prevent $K_{IR}$ channel conduction and saturate Na/K-ATPases, rendering the smooth muscle 'potassium sensor' ineffective (Richards *et al.*, 2001; Dora *et al.*, 2002).

However, constrictor agents were not present in all studies in which vessels failed to respond to raised potassium, and in some vessels, barium and/or ouabain are without effect (Andersson *et al.*, 2000) or only partially reduce agonist-evoked EDHF responses (Vanheel & Van de Voorde, 1999). Other study design factors such as the manner of potassium administration (Beny & Schaad, 2000; Nelli *et al.*, 2003) and the temperature at which studies are performed (Zygmunt *et al.*, 2000) may be key factors in these further inconsistencies, although it is likely that potassium does not act as an EDHF in some vessels. For example, since agonist-evoked EDHF responses in guinea-pig sub-mucosal arterioles (Coleman *et al.*, 2001a) and human sub-cutaneous vessels (Buus *et al.*, 2000; McIntyre *et al.*, 2001) are insensitive to combinations of barium and ouabain, and as raised extracellular potassium neither hyperpolarises nor dilates these arteries following denudation, it is assumed that potassium is not an EDHF in these vessels.

Despite the simplistic appeal of potassium as an EDHF, a potential obstacle is the relative robustness of agonist-induced responses. Whereas dilations to potassium are highly sensitive to the presence of vasoconstrictors, agonist responses are clearly not. It may well be relevant that external application of potassium ions will lead to a global increase in myoendothelial potassium concentration whereas agonists may cause highly localised potassium increases in putative myoendothelial microdomains.

The ability of a monolayer of endothelial cells to provide the required concentration of potassium to sustain minutes of hyperpolarisation of multiple layers of smooth muscle may also be questioned. With limited capacity, endothelial cells would be expected to become depleted of potassium within a short period of time.

This topic has been reviewed by Busse *et al.* (2002) and Edwards & Weston (2004).

### 1.5.4.7) Myoendothelial gap junctions

Gap junctions provide aqueous pores linking the cytosol of adjacent cells, allowing the controlled exchange of various ions and molecules of up to ~1kDa in size. Such connections can be homo- or hetero-cellular in nature, forming between cells of the same or differing phenotype respectively. Within some tissues, gap junctions form hexagonal clusters conferring dense regions of intercellular communication.

A gap junction is formed by the docking of a pair of protruding connexons situated on adjacent cells. These in turn consist of six subunits termed connexins. Gap junctions can be homo- or hetero-typic, hence comprise of identical or non-identical connexons respectively. Connexons themselves are either homo- or hetero-meric, formed from identical or non-identical connexins.

The biophysical properties of gap junctions are dependent on their precise connexin make-up and regulation through phosphorylation. Expression studies in cell lines reveal single channel conductances of 30-300pS for channels formed from connexins found in vascular endothelial and smooth muscle cells. Gating can occur via a number of mechanisms including intracellular pH or calcium, or voltage-

sensing. The channels variously exhibit co-selectivity for a range of ions and second messengers including $Ca^{2+}$, cAMP and $IP_3$.

Homocellular endothelial gap junctions are large and abundant, whilst those which occur between smooth muscle cells or between the endothelium and smooth muscle (myoendothelial) are relatively small and sparse. Both cell types variously express connexins Cx37, Cx40, Cx43 and Cx45. Of the agents which block gap junction communication, so called 'uncouplers', the 'Gap' connexin-mimetic peptides and 18α-glycyrrhetinic are considered to have the fewest non-specific effects (*table 1.3*).

Prior to 1998, only a few studies had explored the effect of non-specific gap junction uncoupling agents on EDHF responses, with varied results. Following revision of the location of apamin- and charybdotoxin- sensitive channels to the endothelium however, the contribution of putative myoendothelial gap junctions to EDHF-mediated vasodilation became of great interest.

Sensitivity of agonist-evoked EDHF responses to selective gap junction uncouplers or connexin antisense has since been demonstrated in many vascular beds (Taylor *et al.*, 1998; Yamamoto *et al.*, 1999; Edwards *et al.*, 1999a; Hill *et al.*, 2000; De Vriese *et al.*, 2002; Luksha *et al.*, 2004). EDHF phenomena in some vessels are only partially sensitive to gap junction interruption whilst in others, responses are completely abolished.

Electron micrographs of vessels in which EDHF occurs reveal structures identified as myoendothelial gap junctions in addition to the homocellular variety amongst endothelial and smooth muscle cells (Sandow & Hill, 2000; Sandow *et al.*, 2003).

Loss of EDHF responses in arteries from ovariectomised rats is shown to correlate with reduced connexin expression (Liu *et al.*, 2002). Developmental changes in connexin expression (Sandow *et al.*, 2004) together with varied expression patterns within the rat mesenteric vascular tree (Sandow & Hill, 2000) may also explain why laboratories report differing EDHF responses in this and other vascular beds.

In intact vessels, endothelial and smooth muscle hyperpolarisation has been shown to occur almost simultaneously and with the same waveform; cells in the vessel wall appearing to act as a single syncytium (Emerson & Segal, 2000). Furthermore, smooth muscle action potentials can be recorded in the non-excitable

endothelium (von der Weid & Beny, 1993). These findings suggest a high degree of electrical coupling across the myoendothelial space, consistent with gap junction activity.

In addition to directly conveying hyperpolarisation, gap junctions could alternatively transfer a soluble intracellular EDHF from the endothelium to the smooth muscle. In several vascular beds, increases in smooth muscle cAMP which occur during the EDHF response are dependent on gap junction activity (Griffith & Taylor, 1999). Furthermore, cAMP has been shown to facilitate gap junction communication and could therefore provide a vital regulatory function rather than act as an EDHF *per se* (Griffith *et al.*, 2002). Inhibition of adenylate cyclase or prevention of cAMP hydrolysis have been shown to attenuate or prolong agonist-evoked EDHF phenomena respectively (Taylor *et al.*, 2001; Chaytor *et al.*, 2001). Increased cAMP-specific phosphodiesterase activity has also been linked to reduced EDHF responses in a rat model of diabetes (Matsumoto *et al.*, 2003).

In considering the findings of studies in which gap junction inhibitors attenuate the EDHF response, it is important to consider the effects of these agents on homocellular gap junctions. Since gap junction inhibitors are not selective for hetero- over homo-cellular connections, data are open to misinterpretation since blockade of the EDHF response may reflect a reduced spread of hyperpolarisation within the smooth muscle or endothelium (Tare *et al.*, 2002).

A further consideration is whether a monolayer of endothelial cells can provide sufficient current to hyperpolarise a considerably larger volume of smooth muscle. If myoendothelial gap junctions do account for EDHF then this may explain why this dilatory pathway is more prevalent in small vessels which have a lower ratio of smooth muscle to endothelium than their larger counterparts. Interestingly, and relevant to this study, the pig coronary artery is reported to comprise of between 15 and 20 smooth muscle layers, yet still exhibits EDHF-mediated vasodilation. However, EDHF-phenomena in these vessels have been deemed insensitive to gap junction inhibitors in some studies. Accordingly, in such large vessels such as this the EDHF-pathway may not involve myoendothelial gap junctions.

Reviewed by Griffith (2004), Griffith *et al.* (2004), Sandow (2004) and Moreno (2004).

| | |
|---|---|
| **Long ~~Chain~~ alcohols**<br>Octanol<br>Heptanol | non-selective |
| **Halothane** | non-selective |
| **Palmitoleic acid** | non-selective |
| **Glycyrrhetinic acid (GA) derivatives**<br>18$\alpha$ GA<br>18$\beta$ GA*<br>Carbenoxolone (a salt of 18$\alpha$GA)* | *~~Inhibit~~ smooth muscle contraction and depolarises endothelium (Chaytor *et al.*, 2000; Coleman *et al.*, 2001b) |
| **~~Connexon~~ mimetic peptides**<br>$^{37,43}$Gap27<br>$^{40}$Gap27<br>$^{43}$Gap26 | $^{X}$GapY where *X* denotes connexin specificity and *Y* denotes binding domain |

**Table 1.3)** Gap junction uncoupling agents.

1.5.5.) Summary

EDHF-mediated vasodilation is initiated by agonists or mechanical stimuli which trigger a rise in endothelial cytosolic calcium. This is accompanied by hyperpolarisation of endothelial cells in response to opening of calcium-activated potassium channels.

Communication between the endothelium and smooth muscle may occur via a number of different mechanisms:

- Release of soluble factors such as C-type natriuretic peptide, hydrogen peroxide, or, where the EDHF response is sensitive to iberiotoxin, EETs. As with nitric oxide, these factors may be released in a calcium-dependent manner and then directly or indirectly affect the activity of smooth muscle potassium conductances, leading to hyperpolarisation.

- The opening of endothelial calcium-activated potassium channels will raise the potassium concentration in the myoendothelial space. This may affect the activity of smooth muscle potassium conductances, triggering hyperpolarisation.

- Myoendothelial gap junctions could directly convey endothelial cell hyperpolarisation to the smooth muscle.

It seems unlikely that a single identity for EDHF will emerge owing to the considerable differences in pharmacology of the pathway between different vascular beds. Individual studies each involving a number of different arteries are particularly useful in highlighting this since they circumvent concerns about differing experimental conditions between laboratories (Dong *et al.*, 2000; Coleman *et al.*, 2001b; McNeish *et al.*, 2003). In some arteries, it appears that responses may be due to the simultaneous activity of a number of EDHF candidates (*table 1.4*).

The EDHF pathway in general appears to play a more prominent role in the microvasculature and may therefore provide an additional useful therapeutic target.

Alterations in the contribution of 'EDHF' to vascular tone have been determined in vessels affected by a number of pathophysiological conditions. These include hypertension (Coleman *et al.*, 2004), diabetes (Triggle *et al.*, 2004) and pre-eclampsia (Gillham *et al.*, 2003). Pharmacological targeting of the EDHF pathway may prove therapeutically beneficial in these and other conditions.

| Vascular bed / vessel | Anandamide | C-type natriuretic peptide | C-P450 metabolites | Hydrogen peroxide | Potassium ions | Myo-endothelial gap junctions |
|---|---|---|---|---|---|---|
| Pig coronary (arterial) | - | - | (Fisslthaler *et al.*, 2000) (Edwards *et al.*, 2001) | (Matoba *et al.*, 2003) | (Beny & Schaad, 2000) (Quignard *et al.*, 1999) | (Edwards *et al.*, 2001) (Beny & Schaad, 2000) |
| Rat mesenteric (arterial) | (Randall *et al.*, 1997) (Vanheel & Van de Voorde, 1999) | (Chauhan *et al.*, 2003b) | (Adeagbo, 1997) (Fukao *et al.*, 1997) | - | (Edwards *et al.*, 1998) (Doughty *et al.*, 2000) | (Hill *et al.*, 2000) |
| Human subcutaneous resistance (arterial) | - | - | (Coats *et al.*, 2001) (Luksha *et al.*, 2004) | (Luksha *et al.*, 2004) | (Coleman *et al.*, 2001b) | (Luksha *et al.*, 2004) |
| Guinea pig carotid artery | - | - | (Chataigneau *et al.*, 1998) | - | (Quignard *et al.*, 1999) | (Edwards *et al.*, 1999a) |
| Rabbit renal (arterial) | - | - | (Wang *et al.*, 2003) (Kagota *et al.*, 1999) | - | - | (Kagota *et al.*, 1999) |

**Table 1.4)** Evidence in support of (green) and in opposition to (red) various EDHF candidates in different vascular beds.

## 1.6) Aims and Objectives

In many vessels, EDHF-mediated vasodilation can be blocked by a combination of apamin and charybdotoxin but not apamin and iberiotoxin. This pharmacology implicates a role for $SK_{Ca}$ and $IK_{Ca}$, but not $BK_{Ca}$ channels. However, application of either apamin or charybdotoxin *alone* is sometimes entirely without effect on the smooth muscle relaxation. That these toxins are effective only when applied in combination implies a synergistic activity. The reason for this is undetermined and could relate either to redundancy amongst separate populations of channels, or the presence of hitherto uncharacterised channels.

The majority of studies regarding the role of $K_{Ca}$ channels in EDHF-mediated vasodilation have explored the effect of channel blockers on smooth muscle hyperpolarisation and/or relaxation in intact vessels. Since it is now widely accepted that the channels in question are situated on the endothelium, such studies may not be best suited to determining the relative contribution that different channel subtypes make to the EDHF phenomenon.

For studies of ion channels, voltage-clamp techniques offer the most effective way to determine the behaviour of cell currents since they allow control over cell membrane potential. Furthermore, measurement of current gives an accurate representation of channel activity whereas measurement of membrane potential does not. This is because, using potassium channels as an example, when channels open/close, the corresponding absolute increase/decrease in membrane potential will vary according to the initial distance from $E_K$.

Voltage-clamp is only effective, however, in single cells or 2-3 electrically coupled cells. This is an important limitation in relation to the study of endothelial cells which form vast electrical syncytia when *in situ*.

Several subtypes of $K_{Ca}$ channels have recently been identified in endothelial cells using a combination of single channel electrophysiology, and identification of expressed channel subunit proteins or encoding mRNA. In order to study the relative contribution that these channels make to agonist-evoked currents, it is necessary to measure the response of the entire cell(s). This is best achieved through the whole-cell voltage-clamp configuration of the patch-clamp technique.

The main objective of this study, therefore, was to investigate the pharmacology of agonist-evoked whole-cell currents in endothelial cells from vessels where the EDHF pathway is present. It was intended that this would help determine whether $SK_{Ca}$, $IK_{Ca}$ and/or channels of novel pharmacology contribute to EDHF responses.

The aims of this study were as follows:

- To isolate, from vessels in which EDHF-responses have been documented, vascular endothelial cells which could be used in the following experiments

- To study changes in membrane potential in response to agonists known to cause EDHF-mediated vasodilation

- To study, in response to EDHF-agonists, changes in whole-cell currents, and to investigate sensitivity of these to blockers of $K_{Ca}$ channels

- To determine whether currents similar to those evoked by EDHF-agonists could be activated by dialysing cells with micromolar intracellular calcium, or by applying pharmacological $K_{Ca}$ channel 'openers'

- To identify the presence of $K_{Ca}$ channel subunits using immunohistochemistry and/or biochemical techniques

Previous to this study, our laboratory had no experience of working with vascular endothelium, and it became clear from the outset that the above objectives would not be easy to achieve. In particular, endothelial cells can be difficult to isolate, are liable to alter rapidly during culture, and are very flat; making electrophysiological study particularly arduous. Nevertheless, this investigation seemed worthwhile even if the intrinsic technical difficulty was to ultimately limit what could be achieved in the available time.

# Chapter 2: Methods & Materials

## 2.1) Cell culture

### 2.1.1) Tissue harvesting

#### 2.1.1.1) Rat vessels

Sprague Dawley rats of either sex and weighing approximately 250g were sacrificed either by exposure to a rising concentration of carbon dioxide, or by concussion with immediate cervical dislocation. These procedures were carried out in accordance with the UK 'Animals (Scientific Procedures) Act, 1986'.

A cotton ligature was secured around the superior mesenteric artery where it branches from the abdominal aorta. Both aorta and intestines were then excised, and the mesentery separated by blunt dissection. Isolated mesentery was spread over the base of a Sylgard-lined Petri dish and covered with sterile Hanks balanced salt solution (HBSS). The superior mesenteric artery was relocated by gently pulling a loose end of the ligature, and a section of vessel (~20mm) was removed.

Mesenteric artery, together with sections of abdominal aorta and carotid arteries were rinsed in sterile HBSS. Connective tissue was then carefully removed using sharp dissection.

#### 2.1.1.2) Pig vessels

Hearts from domestic pigs (*Sus scrofa*) of either sex were obtained from and dissected at an abattoir. Sections of both left anterior descending and right coronary arteries were excised and submerged in ice cold Krebs solution for transport to the laboratory. Principles of aseptic technique were followed as much as possible, and care was taken to ensure that no air remained in the vessels. The time between slaughter and immersion in Krebs is estimated at 30 minutes.

## 2.1.2) Endothelial cell isolation

### 2.1.2.1) Enzymatic digestion

A number of similar protocols were followed in attempts to release endothelial cells from vessels using proteolytic enzymes. In some of these protocols, vessels were dissected into small segments and placed into enzyme solutions. In other protocols, intact vessels were luminally perfused with enzyme-containing solutions.

Enzymes: collagenase class II (1mg/ml), collagenase type 1a (1 mg/ml), protease (0.2 mg/ml) and papain/dithiothreitol (0.8 and 0.9 mg/ml, respectively) were dissolved in sterile HBSS and applied to vessels in various combinations. Tissues were incubated with enzymes over a range of durations (10-60mins) either at room temperature (~23°C), or 37°C. Some tissues were pre-exposed to neuraminidase type-V (0.1 U/ml) to increase sensitivity to collagenase. In some preparations, tissues were exposed to gentle shaking throughout incubation whilst in others, tissue was triturated using a wide-bore polished Pasteur pipette.

Enzyme activity was quenched by dilution with complete medium 'A' (see section 2.1.3.4). Vessel fragments were removed and the solution centrifuged for five minutes at 180g. The supernatant was discarded and any pellet re-suspended in complete medium 'A'. This was then transferred to vented cell culture dishes (Δ-surface range, Nunc) and incubated under standard conditions (see *section 2.1.3.1*).

### 2.1.2.2) Mechanical isolation

Vessels were slit longitudinally, opened and pinned, intimal side up, to the base of a Sylgard-lined Petri dish. In the case of rat vessels, tissues were covered with sterile HBSS. Pig vessels were first dissected free of connective tissue, then rinsed and covered with sterile Dulbecco's phosphate buffered saline (DPBS).

A sterile rounded scalpel blade was gently dragged longitudinally along the intimal surface of the vessel. Cells that had collected on the blade were dispersed into complete culture medium ('A' for rat vessels, 'C' or 'D' for pig vessels) and centrifuged for three minutes at 180g. Supernatant was discarded and the cell pellet

suspended in fresh culture media. The cell suspension was transferred to vented cell culture dishes (Δ-surface range, Nunc) and incubated under standard conditions (see *section 2.1.3.1*).

2.1.2.3) Explant culture

Collagen gel was prepared according to suppliers instructions. Briefly, 1ml of collagen gel contained: tissue culture water (0.45ml), collagen solution (0.44ml), PBS (0.1ml) and 1M sodium hydroxide (0.01ml). The mixture was held on ice before aliquoting 0.2ml into the bottom of individual 10mm diameter culture wells (Δ-surface range, Nunc). Well-plates were then left undisturbed for 40mins at room temperature, allowing the collagen gel to set.

Wells were then partially filled with complete medium 'B' and incubated for four hours under standard conditions (see *section 2.1.3.1*).

Vessels were sliced into rings or short segments, and laid at the bottom of gel-based wells. The majority of culture media was removed to ensure that tissues were in contact with the gel, to allow for adherence. Well-plates were incubated overnight under standard conditions.

Once tissues had adhered to the gel, wells were topped up with culture medium 'B'. Well-plates were returned to the incubator for a further 2-4 days to allow for outgrowth of cells.

Collagenase (type 1A) solution was prepared at a concentration of 0.25% in HBSS, and sterilised by 0.2$\mu$m filtration.

Culture medium was aspirated and tissue carefully removed using sterilised forceps. 0.2ml collagenase solution was then added to each well and plates returned to the incubator until the collagen gel had dissolved (~20mins). Enzyme activity was quenched by dilution with complete medium 'B', and solutions centrifuged at 180g for three minutes. Supernatant was discarded and the cell pellet re-suspended in complete medium 'B'. The cell suspension was transferred to a 25cm$^2$ culture flask (Δ-surface range, Nunc) and returned to the incubator.

This culture method is based on that described by McGuire & Orkin (1987).

## 2.1.3) Cell culture

### 2.1.3.1) General protocol

The principles of aseptic technique were observed to limit the risk of culture infection. Gloves were worn and, wherever practical, procedures carried out inside a class I or II biological safety cabinet. Culture solutions were purchased as sterile and single-use sterile plasticware used. Other equipment was sterilised by flaming or by spraying with 70% ethanol.

Cultures were maintained in a research $CO_2$ incubator. Standard conditions are defined as a temperature of 37°C with 5% atmospheric $CO_2$. A tray of copper sulphate solution was positioned inside the incubator cavity in order to maintain a high humidity whilst deterring infection.

For all cultures, medium was replaced twice weekly.

### 2.1.3.2) Lifting cells

In order to yield isolated cells from cultures, or to seed cells on to coverslips, the following protocol was observed:

Culture medium was removed and cells rinsed with sterile HBSS. Cells were then exposed to trypsin-EDTA solution and returned to the incubator for one minute. Trypsin activity was quenched by dilution in the appropriate complete culture medium and cells dispersed by gentle trituration using a wide-bore transfer pipette. The cell suspension was centrifuged for three minutes at 180g and supernatant discarded. Cells were re-suspended in fresh complete culture medium and re-plated as required.

### 2.1.3.3) Freezing / thawing cells

For freezing, cells were lifted (see *section 2.1.3.2*) and re-suspended in 90% complete culture medium, 10% dimethylsulphoxide. Suspensions were then aliquoted into cryovials (NUNC), sealed, and placed in a container insulated with isopropyl

alcohol. After overnight freezing at -70°C, cryovials were removed from the insulated container and stored in a liquid nitrogen freezer at -120°C.

For thawing, cryovials were removed from the nitrogen freezer and rapidly warmed to room temperature. Defrosted suspensions were diluted in complete culture medium and centrifuged for three minutes at 180g. Following discarding of the supernatant and re-suspension in fresh complete culture medium, cells were plated and cultured as normal.

2.1.3.4) Culture media

The following complete culture media were used in these studies:

**Complete medium 'A'** (enzyme digestion)**:**
89% Dulbecco's modified Eagle's medium (DMEM)
10% foetal bovine serum (FBS)
1% penicillin/streptomycin mix (P/S)

**Complete medium 'B'** (explant culture)**:**
90% RPMI-1640 medium
10% FBS
50$\mu$g/ml endothelial cell growth supplement (ECGS)

**Complete medium 'C'** (pig cell culture)**:**
89% Medium 199
10% FBS
1% P/S

**Complete medium 'D'** (supplemented pig cell culture):

85.4% Medium 199

10% FBS

1.3% 'modified Eagles medium' vitamin supplement

1.3% non-essential amino acids supplement

1% 200mM L-glutamine solution

1% P/S

# 2.2) Electrophysiology

## 2.2.1) Overview

### 2.2.1.1) General equipment arrangement

Experiments were performed on the moveable stage of an inverted microscope. This was mounted on an anti-vibration air table surrounded by an open-fronted Faraday cage. All metal within the Faraday cage was joined from a single point to a common earth.

A 35mm culture dish containing cells was placed into a custom-made Perspex holder, together constituting the 'bath'. Cells were viewed under phase contrast at 600x magnification. A digital video camera attached to the microscope enabled cells to be observed on a remote monitor. Since cells were very flat and difficult to see, this aided positioning and monitoring of the patch electrode.

Extracellular solutions (ES) were held in plastic syringe barrels above the microscope and continually delivered to the bath under gravity via silicone tubing. A series of taps allowed diversion of different solutions into the bath, and a gate-clamp enabled adjustment of flow rate to ~5ml/min. At the opposite side of the bath from the inflow, an outflow, connected to a remote vacuum pump, maintained a constant bath volume of ~1.5ml. Excess bath solution was removed to waste. The inflow was placed as close to the studied cell as possible to ensure efficient delivery of extracellular solutions.

Recordings were made using a patch clamp amplifier (EPC7, List Medical), the headstage of which was mounted on a water-filled hydraulic micromanipulator. This in turn was mounted on a coarse manipulator secured to the anti-vibration table.

A patch electrode (PE) (see *section 2.2.1.2*) was mounted in an electrode holder (Q-series, Harvard), in turn connected to the amplifier headstage. Electrical continuity between the headstage and the PE was achieved using a silver wire, coated at the PE-end with silver chloride.

An isolated bath electrode was formed from a silver chloride pellet connected to the signal ground input of the amplifier headstage. The pellet was housed in a small isolated ES-filled reservoir adjacent to the bath. A conducting agar bridge connected the isolated reservoir with the bath solution.

A side port in the electrode holder allowed application of negative pressure within the PE.

2.2.1.2) Patch electrodes

Micropipettes were formed from filamented glass capillaries (GC150TF-15, Harvard) using a 2-stage vertical pipette puller (L/M-3P-A, List Medical). Fluid Sylgard (Dow Corning) was carefully applied to the shank of each pipette under a dissection microscope, and then rapidly cured using a heating coil. Pipette tips were smoothed by 'fire polishing' on a micro-forge (MO-103R, Narashige).

Immediately prior to use, a micropipette was backfilled with 0.2μm-filtered intracellular solution (IS). This constituted a patch electrode (PE).

Adjustments were made to the pipette puller settings so that patch electrodes had a resistance of 2.5-6 MΩ when mounted as described in *section 2.2.1.1* and lowered into the bath ES.

## 2.2.2) Rat cell studies

### 2.2.2.1) Recording equipment setup

The current output of the patch amplifier was internally filtered at ten kHz, and connected, along with the unfiltered voltage output, to a digitising computer interface (Digidata 1200, Axon Instruments). Amplifier outputs were simultaneously monitored on a digital storage oscilloscope and a chart recorder.

Data was recorded on a Windows 3.1-based computer using acquisition software (Clampex 6, Axon Instruments) and sampling at a rate of 5kHz. A connection from the Digidata interface to the stimulus input of the amplifier allowed the software to control voltage-clamp potential.

Holding potential was set and capacitance transients balanced using controls on the front of the amplifier.

### 2.2.2.2) Protocol

Single cells or small clusters of 2-3 cells were selected for recording. After lowering a mounted PE onto a cell, a gigaseal was formed through application of negative pressure within the PE. Fast transients, owing to electrode capacitance, were balanced, and holding potential set to -20mV. Whole-cell mode was entered by further increasing negative pressure until the appearance of capacitance transients. Slow transients, owing to cell membrane capacitance and ruptured patch resistance, were balanced where possible, and the holding current allowed to stabilise.

In order to characterise whole cell currents, sequential 100ms voltage pulses (steps) were applied, clamping cells from -60 to +120mV in increments of 20mV.

Cells were exposed to ES containing a range of different pharmacological agents. Whole cell responses were assessed by comparing voltage steps applied prior to, during and following the washout of these agents. Following a change of solution, resting whole-cell currents were allowed to stabilise prior to application of voltage steps. For an individual voltage-step, the corresponding current trace was measured by averaging the current plateau.

All experiments were performed at room temperature (~23°C).

## 2.2.3) Pig cell studies

### 2.2.3.1) Recording equipment setup

The current (I) and voltage (V) outputs of the amplifier were connected to both a digitising computer interface (Digidata 1320A, Axon Instruments) and a laboratory digital audio tape (DAT) recorder (DTR 1204, Bio Logic). $I_{Digidata}$ and $I_{DAT}$ signals were filtered by the amplifier at ten and three kHz, respectively.

Data was recorded on a Windows 2000-based PC, using acquisition software (Clampex 8, Axon Instruments). Outputs from both the Digidata interface and a stimulator (Physiological Stimulator, Farnell) were connected to the stimulus input of the amplifier. These inputs were alternated by means of a manual two-way switchbox and allowed generation of voltage-clamp ramps and pulses by the computer and stimulator, respectively.

Holding potential was set and capacitance transients balanced using controls on the front of the amplifier.

Whole-cell currents were continually recorded in Clampex 'gap-free' mode.

In voltage clamp studies, a combination of voltage pulses and ramps were used to determine changes to whole-cell currents. Since the acquisition software does not allow for generation of voltage-ramps during gap-free recording, data was continually acquired to DAT at a sampling rate of 48kHz. The acquisition software was used to generate voltage ramps whilst simultaneously recording amplifier output at a sampling rate of 10kHz. Other events were simply 'viewed' via the acquisition software. At the end of each study, signals from relevant portions of gap free recordings were located on DAT, played into Digidata interface, and recorded at a sampling rate of 2kHz by the acquisition software. Raw data therefore consisted of files containing gap-free recordings and files containing data from single ramps.

In a small number of studies, the DAT recorder was substituted with a digitiser (VR-10, Instrutech Corporation) and a video cassette recorder. These were used in an identical manner to the DAT recorder and recorded at a sampling rate of 18.5kHz.

Current-clamp protocols were recorded directly by the acquisition software. In some experiments, current pulses were applied by the external stimulator via the stimulus input.

2.2.3.2) Voltage-clamp protocol

Single cells or small clusters of 2-3 cells were selected for voltage clamp experiments. Whole-cell recordings were obtained following the procedure outlined in *section 2.2.2.2*. Holding potential was set to -50mV.

In a few unsuccessful studies, attempts were made at the 'perforated-patch' modification of the voltage-clamp technique. Briefly, amphotericin-B was prepared and diluted in intracellular solution (IS) to a concentration of 125μg/ml. The tip of a micropipette was dipped into freshly-filtered amphotericin-free IS, and then the pipette back-filled with amphotericin-containing IS. In some cases, tip-dipping was omitted. The pipette was lowered on to the chosen cell within 45s of filling, and gigaseal formation attempted. Where seals were obtained, the electrode was left undisturbed to allow amphotericin to diffuse to the tip of the electrode.

Holding potential was set to -50mV and whole-cell current allowed to stabilise. Capacitance transients were balanced where possible for recordings using 30nM and 500nM free-calcium IS (see *section 2.4.2.2*). For recordings made using 1.5μM free-calcium IS, balancing of capacitance transients was not usually undertaken since this interrupted recording of current activation.

In order to characterise whole cell currents, regular +50mV voltage-pulses (~200mS, 0.5Hz) were applied using the external stimulator. For studies using 30nM and 500nM free-calcium IS, voltage ramps (-120 to +50mV over 200ms) were applied prior to and at the peak of cell responses to agonists.

For analysis, holding current was measured by averaging a stable portion of the recording across 1000ms. Pulses were measured by averaging a 100ms portion of the pulse plateau. Ramps were measured by applying a linear fit to the approximately linear portion (-70 to -40mV) of the current trace.

All experiments were performed at room temperature (~23°C).

2.2.3.3) Current-clamp protocol

Single cells or multi-cellular 'rafts' were selected for current clamp experiments. The whole-cell mode of the voltage-clamp technique was achieved as discussed in *section 2.2.2.2*. The patch amplifier was then switched to current-clamp mode.

In some recordings, current pulses of various dimensions were applied.

For analysis, membrane potentials prior to and at the peak of agonist responses were measured by averaging stable portions of the trace over 1000ms. Pulses were used only as a visual indicator of membrane resistance and therefore not measured.

All experiments were performed at room temperature (~23°C).

## 2.2.4) Data Analysis

Owing to the varied amplitude of ATP- and 1-EBIO- evoked currents, sensitivity to blockers is expressed as a percentage of the block of the activated current; where activated current is defined as the difference between the resting current and the current recorded at the response peak.

Current voltage relationships (CVR)s for ATP- or 1-EBIO-evoked currents are calculated as the difference between the CVR prior to addition of agonist and the CVR at the response peak. CVRs for blocker-sensitive currents are calculated as the difference between the CVR of the 'agonist-evoked current prior to blocker' and the CVR of the 'agonist-evoked current in the presence of blocker'.

Where currents were activated by dialysing cells with 1.5μM free-calcium, no value for resting current could be established because of the rapid onset of current activation. For these experiments, amplitude of the blocked current (the difference between net-outward current prior to blocker and net-outward current in the presence of blocker) is expressed as a percentage of the net-outward current prior to blocker.

Unless otherwise stated, data in the text and tables are given as 'mean ± standard error of the mean (SEM)', followed by the sample size.

One- or two-tailed unpaired or paired Student's t-tests were used to compare numerical data where appropriate. Significance is defined as $P<0.05$.

## 2.3) Imaging Studies

### 2.3.1) Immunohistochemistry

On the day prior to study cells were seeded onto glass coverslips, then placed in 35mm culture dishes and incubated overnight under standard conditions.

All solutions were made in phosphate-buffered saline (PBS) and the entire method performed at room temperature.

Culture medium was aspirated and cells rinsed once in PBS prior to fixing with 1% paraformaldehyde solution for 20mins. Cells were then rinsed three times in PBS and permeabilised in pure methanol for 10mins. Following a further three rinses with PBS, cells were exposed for one hour to an antigen blocking buffer (ABB) consisting of 3% bovine serum albumin and 2% horse serum.

Primary antibodies were diluted as appropriate in ABB (*table 2.1*) and applied to cells for four hours. Antibody solutions were aspirated and cells rinsed three times in 0.1% Tween-20 detergent, each rinse lasting for three minutes on an orbital shaker. Cells were rinsed a further three times in PBS to remove remaining detergent.

Secondary antibodies were also diluted in ABB (*table 2.2*) and applied to cells for one hour. Antibody solutions were aspirated and cells treated to the same rinsing protocol as with removal of primary antibodies.

Coverslips were inverted and mounted on microscope slides using Vectashield preservative mounting agent. Samples were immobilised by applying a continuous border of nail varnish around the perimeter of the coverslip.

Slides were stored in darkness at 4°C for up to a week prior to study by confocal microscopy.

| Name | Origin species | Target | Working dilution | Supplier |
|---|---|---|---|---|
| A0082 | rabbit | von Willebrand factor (human) | 1:200 | DakoCytomation[1] |
| ab6994 | rabbit | von Willebrand factor (human) | 1:200 – 1:800 | Abcam |
| M0581 | mouse | smooth muscle actin (1A4) (human) | 1:25 – 1:50 | DakoCytomation |
| M1 | rabbit | SK2 (human / rat) *for epitope see appendix i* | 1:20 – 1:200 | GlaxoSmithKline[2] |
| AB5350 | rabbit | SK3 (human / rat) *for epitope see appendix ii* | 1:20 – 1:200 | Chemicon |
| M4 | rabbit | IK1 (human) *for epitope see appendix iii* | 1:20 – 1:200 | GlaxoSmithKline[2] |
| R212 | rabbit | IK1 (rat) *for epitope see appendix iii* | 1:20 – 1:200 | GlaxoSmithKline[3] |

**Table 2.1)** Primary antibodies.

| Name | Origin species | Target | Fluorophore | Working dilution | Supplier |
|---|---|---|---|---|---|
| PA42004 | goat | rabbit IgG | Cy-2 | 1:200 | Amersham |
| PA43004 | goat | rabbit IgG | Cy-3 | 1:200 | Amersham |
| AQ300F | sheep | mouse IgG | FITC | 1:10 – 1:20 | Chemicon |

**Table 2.2)** Flurophore-conjugated secondary antibodies.



[1] Kindly provided by T Carter. National Institute for Medical Research, London, UK
[2] (Chen *et al.*, 2004) Kindly provided by DJ Trezise, MX Chen and AJ Jowett. GlaxoSmithKline, Stevenage, UK
[3] (Bahia *et al.*, 2005) Kindly provided by DJ Trezise, MX Chen and AJ Jowett. GlaxoSmithKline, Stevenage, UK

## 2.3.2) Acetylated-LDL labelling

In preparation, cells were seeded onto glass coverslips placed in 35mm culture dishes and incubated under standard conditions overnight.

DiI-conjugated acetylated low density lipoprotein (aLDL) was briefly centrifuged to clear the solution of aggregates, and diluted to 10$\mu$g/ml in complete medium 'C'.

Culture medium was aspirated from cells and replaced with medium containing aLDL. Cells were then returned to the incubator for four hours. aLDL medium was removed and cells rinsed three times in PBS before fixing with 1% paraformaldehyde in PBS for 20mins. Cells were rinsed a further three times and then mounted on microscope slides as described in *section 2.3.1.*

Slides were stored in darkness at 4°C for up to a week prior to study by confocal microscopy.

## 2.3.3) Silver staining

Arterial segments were cleaned of connective tissue, opened longitudinally and pinned, intimal-side up in a Sylgard-lined Petri dish containing PBS. Vessels were then fixed with 2.5% glutaraldehyde for five minutes and rinsed in PBS then water. Vessels were exposed to 1% silver nitrate for one minute, followed by a mixture of 1% ammonium bromide / 3% cobalt bromide for a further minute. Tissues were then rinsed and left in PBS and exposed to the light from an ordinary lamp for ten minutes.

Vessels staining was observed under an upright microscope.

## 2.3.4) Image capture

Immunostained and aLDL-labelled cells were studied under a laser-scanning confocal microscope (LSM 510-Meta, Carl Zeiss or TCS, Leica) and images captured using associated software.

Images of silver-stained vessels, explant cultures and isolated cells were captured using a digital camera attached to an upright microscope.

## 2.4) Physiological solutions

### 2.4.1) General

All solutions were formulated in purified, deionised water. Unless otherwise stated, all concentrations are given in millimolar.

For calcium-buffered solutions, free calcium concentrations are calculated assuming a working temperature of 25°C, using WinMAXC32 v2.5 software[4] (Patton *et al.*, 2004). Constants used in this program are those currently published by the US Federal National Institute for Standards and Technology.

### 2.4.2) Electrophysiology

#### 2.4.2.1) Extracellular solutions

Standard extracellular solution:

| | |
|---|---|
| NaCl | 126mM |
| KCl | 5mM |
| $CaCl_2$ | 1mM |
| $MgCl_2$ | 1.2mM |
| Glucose | 11mM |
| HEPES (free acid) | 10mM |
| NaOH | (to pH 7.4) |

[4] http://www.stanford.edu/~cpatton/maxc.html

'Sollini *et al.*' extracellular solution:

| | |
|---|---|
| NaCl | 130mM |
| KCl | 5.6mM |
| $CaCl_2$ | 2mM |
| $MgCl_2$ | 1mM |
| Glucose | 10mM |
| HEPES (free acid) | 8mM |
| NaOH | (to pH 7.5) |

Sodium-free extracellular solution:

| | |
|---|---|
| N-methyl-D-glucamine | 130mM |
| KCl | 5mM |
| $CaCl_2$ | 1mM |
| $MgCl_2$ | 1.2mM |
| Glucose | 11mM |
| HEPES (free acid) | 10mM |
| HCl | (to pH 7.4) |

Low-chloride extracellular solution:

| | |
|---|---|
| Sodium isethionate | 126mM |
| KCl | 5mM |
| $CaCl_2$ | 1mM |
| $MgCl_2$ | 1.2mM |
| Glucose | 11mM |
| HEPES (free acid) | 10mM |
| NaOH | (to pH 7.4) |

2.4.2.2) Intracellular solutions

'30nM free-calcium' intracellular solution:

| | |
|---|---|
| KCl | 130mM |
| $CaCl_2$ (added) | 0.08mM |
| *$Ca^{2+}$ (free)* | *~30nM* |
| $MgCl_2$ (added) | 1mM |
| *$Mg^{2+}$ (free)* | *~1mM* |
| EGTA | 0.5mM |
| HEPES (free acid) | 10mM |
| KOH | (to pH 7.2) |

'Sollini *et al.*' intracellular solution:

| | |
|---|---|
| KCl | 130mM |
| $MgCl_2$ | 1mM |
| Mg-ATP | 5mM |
| HEPES (free acid) | 10mM |
| NaOH | (to pH 7.3) |

'1.5μM free-calcium' intracellular solution:

| | |
|---|---|
| KCl | 130mM |
| $CaCl_2$ (added) | 1.19mM |
| *$Ca^{2+}$ (free)* | *~1.5μM* |
| HEDTA | 5mM |
| HEPES (free acid) | 10mM |
| KOH | (to pH 7.2) |

'500nM free-calcium' intracellular solution:

| | |
|---|---|
| KCl | 130mM |
| $CaCl_2$ (added) | 0.383mM |
| *$Ca^{2+}$ (free)* | *~500nM* |
| $MgCl_2$ (added) | 1mM |
| *$Mg^{2+}$ (free)* | *~1mM* |
| EGTA | 0.5mM |
| HEPES (free acid) | 10mM |
| KOH | (to pH 7.2) |

'30nM free-calcium, low chloride' intracellular solution:

| | |
|---|---|
| Potassium gluconate | 130mM |
| KCl | 3.98mM |
| $CaCl_2$ (added) | 0.08mM |
| *$Ca^{2+}$ (free)* | *~30nM* |
| $MgCl_2$ (added) | 1mM |
| *$Mg^{2+}$ (free)* | *~1mM* |
| EGTA | 0.5mM |
| HEPES (free acid) | 10mM |
| KOH | (to pH 7.2) |

## 2.4.3) Other solutions

Krebs solution:

| | |
|---|---|
| NaCl | 94mM |
| KCl | 4.7mM |
| $CaCl_2$ | 2.52mM |
| $MgSO_4$ | 0.45mM |
| $KH_2PO_4$ | 1.18mM |
| $NaHCO_3$ | 25mM |
| Glucose | 11mM |

(solution gassed with 95% $O_2$/5% $CO_2$)

Phosphate buffered saline (PBS):

| | |
|---|---|
| NaCl | 137.5mM |
| KCl | 2.7mM |
| $Na_2HPO_4$ | 9.2mM |
| $KH_2PO_4$ | 1.8mM |
| NaOH | (to pH 7.4) |

# 2.5) Reagents & Drugs

## 2.5.1) Cell culture

| Reagent | Notes | Supplier |
|---|---|---|
| collagen* | type I (from rat tail) | BD Biosciences |
| collagenase | type IA | Sigma |
| collagenase | type II | Worthington |
| DL-dithiothreitol | | Sigma |
| Dimethylsulphoxide* | | Sigma |
| Dulbecco's MEM* | + lg, py and 1000mg/l gl | Invitrogen |
| Dulbecco's PBS* | - $Ca^{2+}$ and $Mg^{2+}$ | Invitrogen |
| endothelial cell growth supp. | | Sigma |
| foetal bovine serum* | | Invitrogen |
| L-glutamine* | 200mM (100x) | Invitrogen |
| Hanks' balanced salt solution* | - $Ca^{2+}$ and $Mg^{2+}$ | Invitrogen |
| medium 199* | + Earle's salts and gx | Invitrogen |
| MEM non-essential amino acids* | 100x | Invitrogen |
| MEM vitamins* | 100x | Invitrogen |
| neuraminidase | type V | Sigma |
| papain | | Sigma |
| penicillin (P)/streptomycin (S)* | $10^4$ U/ml P and $10^4\mu$g/ml S | Invitrogen |
| protease | type XIV | Sigma |
| RPMI-1640* | + lg and py | Sigma |
| trypsin-EDTA* | in HBSS - $Ca^{2+}$ and $Mg^{2+}$ | Sigma |
| water* | | Sigma |

**Table 2.3)** Details of cell culture reagents. Abbreviations: glucose (gl), L-glutamine (lg), Glutamax™ stable L-glutamine substitute (gx), Hanks' balanced salt solution (HBSS) sodium pyruvate (py), modified Eagle medium (MEM), phosphate buffered saline (PBS), supplement (supp.). *Items marked with an asterisk were purchased as sterile solutions. The remainder were dissolved in Hanks' balanced salt solution and passed through a sterile 0.2μm-pore filter prior to use.

## 2.5.2) Other reagents and drugs

| Reagent | Notes | Supplier |
|---|---|---|
| acetylated LDL (DiI labelled)[2] | | Biogenesis |
| acetylcholine (ACh) | | Sigma |
| ammonium bromide | | Aldrich |
| amphotericin-B† | HPLC grade | Sigma |
| apamin | synthetic, HPLC grade | Sigma |
| ATP (magnesium salt) | | Sigma |
| ATP (sodium salt) | | Sigma |
| bovine serum albumin | fraction V | ICN Biomedicals |
| bradykinin | | Sigma |
| calcium chloride | AnalaR grade solution | BDH |
| carbachol | | BDH |
| charybdotoxin (ChTx)[5] | recombinant | Sigma |
| clotrimazole† (CTZ) | | Sigma |
| cobalt (II) bromide | | Aldrich |
| dimethylsulphoxide (DMSO) | AnalaR grade | BDH |
| EGTA[3] | | Sigma |
| 1-EBIO[4] | | Aldrich |
| ethanol | AnalaR grade | BDH |
| (D) glucose | AnalaR grade | BDH |
| glutaraldehyde (dialdehyde) | | Aldrich |
| HEDTA[5] | | Sigma |
| HEPES[6] | free acid | Calbiochem |
| histamine | | Sigma |

**Table 2.4)** General reagents and drugs. †These drugs are sparingly soluble in water and were dissolved in DMSO. Cells were not exposed to concentrations of DMSO exceeding 0.1%.

[2] Kindly provided by T Carter. National Institute for Medical Research, London, UK
[3] Ethylene glycol-bis(2-aminoethylether)-*N,N,N',N'*-tetraacetic acid
[4] 1-ethyl-2-benzimidazolinone
[5] *N*-(2-Hydroxyethyl)ethylenediamine-*N,N',N'*-triacetic acid
[6] 4-(2-hydroxyethyl)-1-piperazineethanesulfonic acid, 4-(2-hydroxyethyl)-1-piperazineethanesulphonic acid

(Continued)

| Reagent | Notes | Supplier |
|---|---|---|
| iberiotoxin (IbTx) | recombinant | Sigma |
| ketoconazole† | | Sigma |
| magnesium chloride | AnalaR grade | BDH |
| magnesium sulphate | AnalaR grade | BDH |
| methanol | AnalaR grade | BDH |
| N-methyl D-glucamine | | Sigma |
| paraformaldehyde | | Sigma |
| potassium chloride | AnalaR grade | BDH |
| potassium gluconate | | Sigma |
| potassium hydroxide | AnalaR grade | BDH |
| potassium phosphate monobasic | AnalaR grade | BDH |
| silver nitrate | | Hopkin & Williams |
| sodium chloride | AnalaR grade | BDH |
| sodium hydrogen carbonate | AnalaR grade | BDH |
| sodium hydroxide | AnalaR grade | BDH |
| sodium isethionate | | Sigma |
| sodium phosphate dibasic | AnalaR grade | BDH |
| substance P | | Sigma |
| Sylgard™ | type 184 | Dow Corning |
| tetraethyl ammonium chloride | | Sigma |
| Tween-20 | | Promega |
| UCL 1848[7†] | | Chemistry Dept., UCL |
| Vectashield™ | | Vector Laboratories |

**Table 2.4** ***continued)*** General reagents and drugs. †These drugs are sparingly soluble in water and were dissolved in DMSO. Cells were not exposed to concentrations of DMSO exceeding 0.1%.

[7] 8,14-diaza-1,7(1,4)-diquinolinacyclotetradecaphanedium ditrifluoroacetate

# Chapter 3: Endothelial cell culture

## 3.1) Isolation of cells

### 3.1.1) Rat cells

Since EDHF-mediated responses have been extensively studied in rat mesenteric arteries, initial attempts at endothelial cell isolation focussed on these vessels. EDHF contributes most to vasodilation in secondary and tertiary mesenteric artery branches (Shimokawa *et al.*, 1996), however these were considered impractical for endothelial cell isolation owing to their diminutive size. Instead, the superior mesenteric artery was used.

Attempts were also made to isolate endothelial cells from segments of thoracic aorta and carotid arteries.

Initial endothelial cell isolation protocols used proteolytic enzymes to digest structural proteins within the vessel wall. In some cases, vessels were pre-treated with neuraminidase, which has been shown to render endothelial cells more susceptible to protease activity (Gorog & Pearson, 1985). Despite many attempts, however, no endothelial cells could be isolated using these methods.

Alternatively, in some studies the endothelium was physically separated from the underlying smooth muscle by gentle scraping or teasing away of the intimal surface of the vessel (see *figure 3.1*). Cells derived in this manner did not survive in culture.

Subsequently, an explant culture was investigated since this method has been reported to produce a pure endothelial cell culture (McGuire & Orkin, 1987). Briefly, small segments of vessel were incubated in culture medium on a collagen gel matrix. As vascular cells proliferated over a number of days, these spread throughout the matrix surrounding the tissue (*figure 3.2*). Following three to five days in culture, vessel tissue was removed and the matrix digested with collagenase, allowing the release of proliferated cells. These were then plated in tissue culture dishes and cultured under standard conditions.

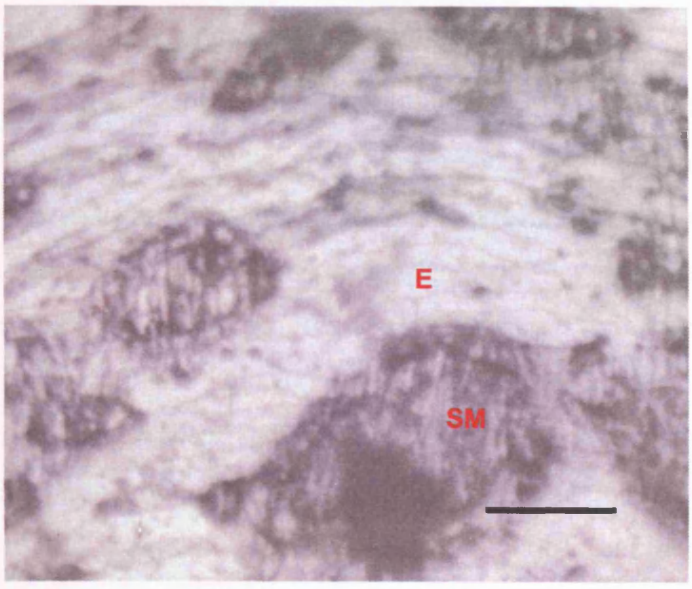


**Figure 3.1)** The silver stained intimal surface of a segment of rat thoracic aorta. Endothelial cell 'tiles' (E) can be seen in the foreground running from left to right (parallel to blood flow). Smooth muscle cells (SM) run from top to bottom and can be seen in patches where the endothelium has been damaged. Viewed under phase contrast using a water-immersion objective. Scale bar: ~50μm.

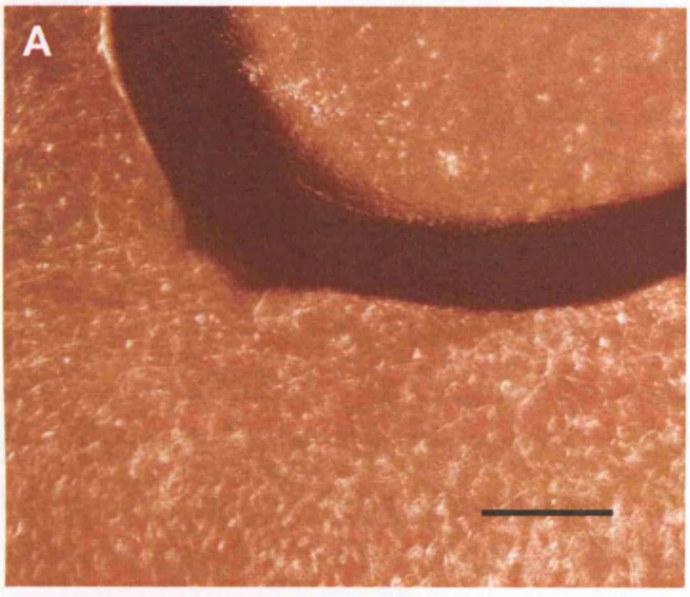


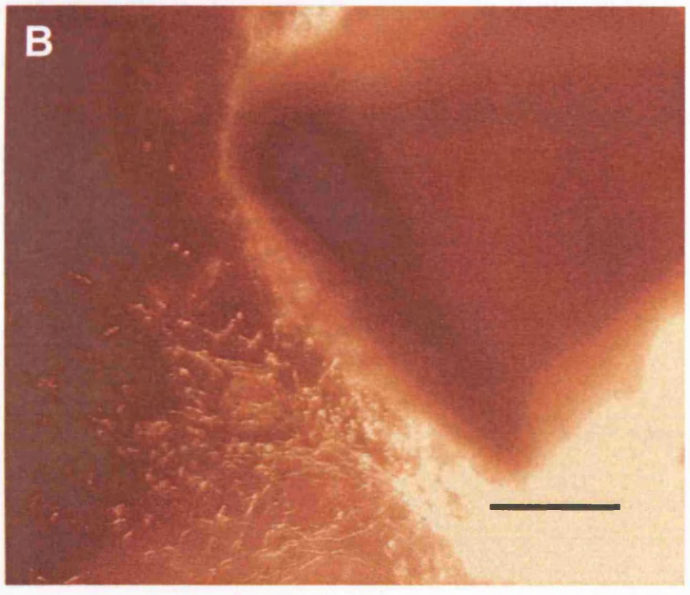


**Figure 3.2)** A ring of rat thoracic aorta (A) and segment of superior mesenteric artery (B) in explant culture. Cells can be seen in the otherwise clear matrix surrounding the tissue. Viewed under phase contrast. Scale bars: ~250μm.

## 3.1.2) Pig cells

Owing to difficulties in both the identification of (see *section 3.2.2*) and study of rat explant cells, an alternative was sought. Porcine coronary arteries were chosen, as a small number of studies had recently described EDHF-type responses in this vascular bed e.g. (Edwards *et al.*, 2001). Furthermore, endothelial cell isolation from these vessels is regarded as relatively straightforward.

Sections of right (R) or left anterior descending (LAD) coronary artery, 5-10cm in length, were used for harvesting endothelial cells. Scraping the vessel intima with a scalpel blade yielded endothelial tissue which could then be cultured (*figures 3.3* to *3.5*). Harvesting was most effective when the blade was lightly dragged, tilted in the direction of motion. Best results were achieved when the scrape was completed as a smooth, uninterrupted sweep. Endothelial tissue could be clearly seen as a smear on the underside of the blade, which was then dispersed into culture medium. A second scrape of the vessel using a clean blade yielded no smear, indicating that mainly endothelial cells are removed using this method.

Following overnight incubation, a proportion of tissue fragments would be adhered to the bottom of culture dishes. Culture medium was then replaced, removing non-adhered tissue. Cells proliferated at various rates, and cultures developed as small 'islands' of cells surrounding 'scraped' endothelial tissue (*figure 3.4*). Some cultures reached confluence within three to four days (*figure 3.5*). Cultures were more successful from R than LAD arteries. This may be because the convoluted nature of R arteries is likely to confer greater protection against drying following exsanguination.

Owing to the need for single or small clusters of cells for electrophysiology studies, cells were lifted and re-plated at a lower density on the evening prior to study.

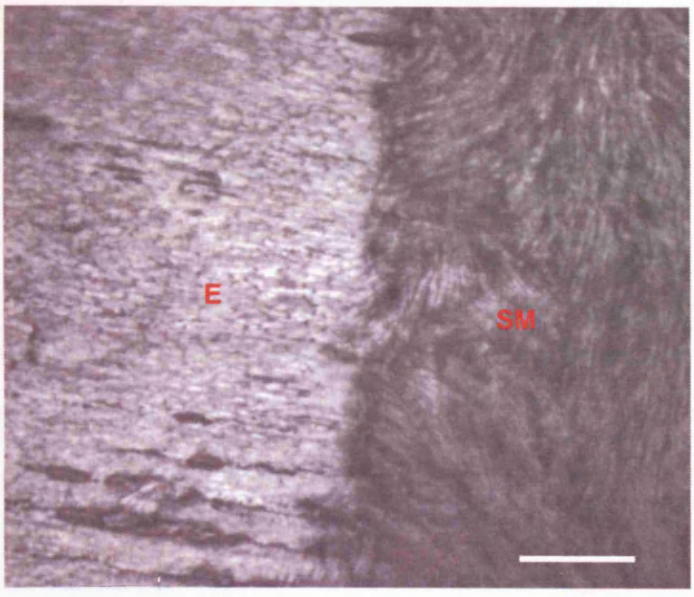


**Figure 3.3)** The silver stained intimal surface of a segment of pig right coronary artery. Endothelial cells (E) can be seen in the left half of the picture. Smooth muscle cells (SM) can be seen on the right side of the picture where the endothelium has been scraped away. Viewed under phase contrast using a water-immersion objective. Scale bar: ~100μm.

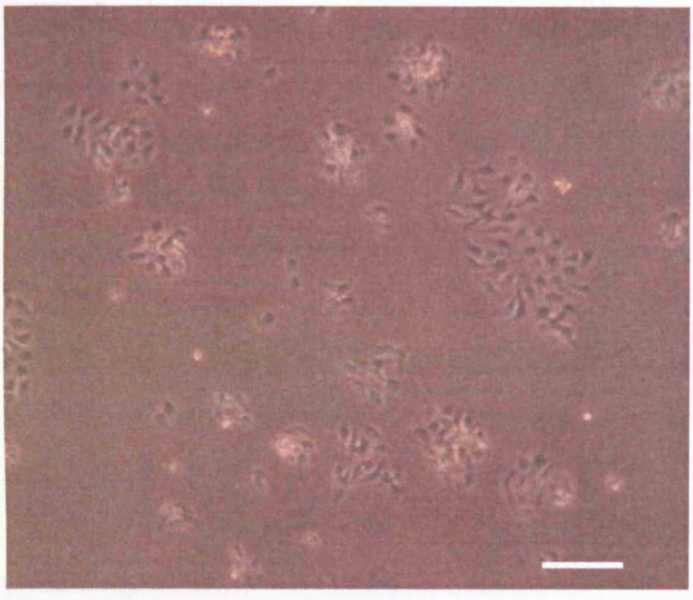

**Figure 3.4)** Isolated pig right coronary artery endothelial cells following one day in culture. Viewed under phase contrast. Scale bar: ~50μm.

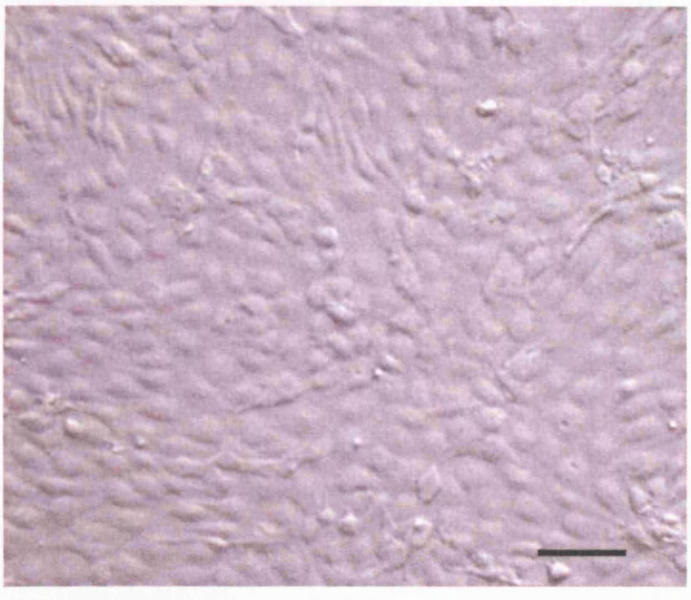

**Figure 3.5)** Pig right coronary artery endothelial cells following four days in culture. Viewed under phase contrast using a water-immersion objective. Scale bar: ~25μm.

## 3.2) Identification of cells

### 3.2.1) Introduction

As discussed in *section 1.2*, blood vessels contain two major cell types of functional significance; endothelial cells and vascular smooth muscle cells. When isolating cells from the vascular wall, it is important to determine identity because cultures will frequently contain a mixture of the two cell phenotypes. Although endothelial and smooth muscle cells have distinct classical morphologies, these can alter during culture.

Typically, cultured endothelial cells grow as tight clusters, eventually forming polygonal or 'cobblestone' monolayers (for example, see *figures 3.4 and 3.5*). The most common endogenous marker used to identify endothelial cells is the clotting mediator 'von Willebrand factor' (vWF) (Ulger *et al.*, 2002). vWF is not expressed in all endothelial cells, although where present, is mainly confined to Weibel Palade bodies (storage granules) located in the cytosol. A further distinguishing feature of endothelial cells is their expression of macrophage scavenger receptors which enable them to internalise acetylated low density lipoprotein (aLDL) (Dhaliwal & Steinbrecher, 1999).

Vascular smooth muscle cells usually grow as sharp spindles and can be identified by immunostaining for smooth muscle actin. Actin filaments become visible as thin strands crossing the cytosol (for example, see *figure 3.7*).

### 3.2.2) Rat explant cells

#### 3.2.2.1) Morphology

Rat aortic, mesenteric- and carotid artery explant cells were more similar to endothelial cells than smooth muscle cells in terms of morphology. Generally, cells were spread flat rather than spindle-shaped, however confluent monolayers were noticeably flatter than the cobblestone morphology associated with endothelial cells.

### 3.2.2.2) Expression of von Willebrand factor

vWF expression in explant cells was determined by immunostaining using one of two polyclonal antibodies. Primary antibody binding was then detected using a Cy2-conjugated secondary antibody.

No above-background fluorescence was identified in passaged cells or those studied immediately following isolation from the explant culture. The absence of vWF was confirmed by repeating the study in excess of five times, using varied antibody concentrations (see *table 2.1*). On the contrary, primary cultures of human umbilical vein endothelial cells (HUVEC)[8] exhibited a classical pattern of vWF staining when subjected to the same immunostaining protocol (*figure 3.6*). No above-background fluorescence was detected when the primary antibody was omitted from the procedure.

Both of the antibodies used in these studies have been reported to detect the rat isoform of vWF, and detection has previously been reported in the endothelium of rat mesenteric artery (Goto *et al.*, 2004).

### 3.2.2.3) Internalisation of acetylated LDL

Mesenteric and carotid artery explant cells, which had been frozen following three weeks in culture (passage four), were thawed and cultured for a further three days. Unlike HUVEC (see *figure 3.8*), explant cells did not internalise fluorescently labelled aLDL.

[8] Kindly provided by T Carter. National Institute for Medical Research, London

### 3.2.2.4) Expression of smooth muscle actin

Mesenteric and carotid artery explant cells, which had been frozen following three weeks in culture (passage four), were thawed and cultured for a further three days. Immunostaining was carried out using a monoclonal primary antibody raised against human smooth muscle actin (clone 1A4). Primary antibody binding was then detected using a FITC-conjugated secondary antibody.

In both cultures, filamentous actin staining could be clearly seen in the majority of cells (*figure 3.7*). Similar results were seen when cultured human pulmonary artery smooth muscle cells (HPASM)[9] were subjected to the same immunostaining protocol (*figure 3.7*). No above-background fluorescence occurred in either study when the primary antibody was omitted from the procedure.

### 3.2.2.5) Summary

Although it was initially considered that explant cultures bore a closer morphological resemblance to endothelial than smooth muscle cells, they did not express vWF. It was also noted that removing endothelial cell growth supplement (ECGS) from the complete culture medium did not affect cell growth or morphology (data not shown). The observation that passaged explant cells expressed smooth muscle actin, and failed to internalise aLDL, further suggests that they are not endothelial; though it is possible that these cells may have changed during several weeks in culture.

In published studies, similar explant cultures have been used with the purpose of culturing vascular smooth muscle cells e.g. (Leik *et al.*, 2004). The explant cells in the present study could alternatively be fibroblasts which are known to be flat when in culture, and can also express smooth muscle actin.

[9] Kindly provided by L Clapp. UCL Clinical Pharmacology

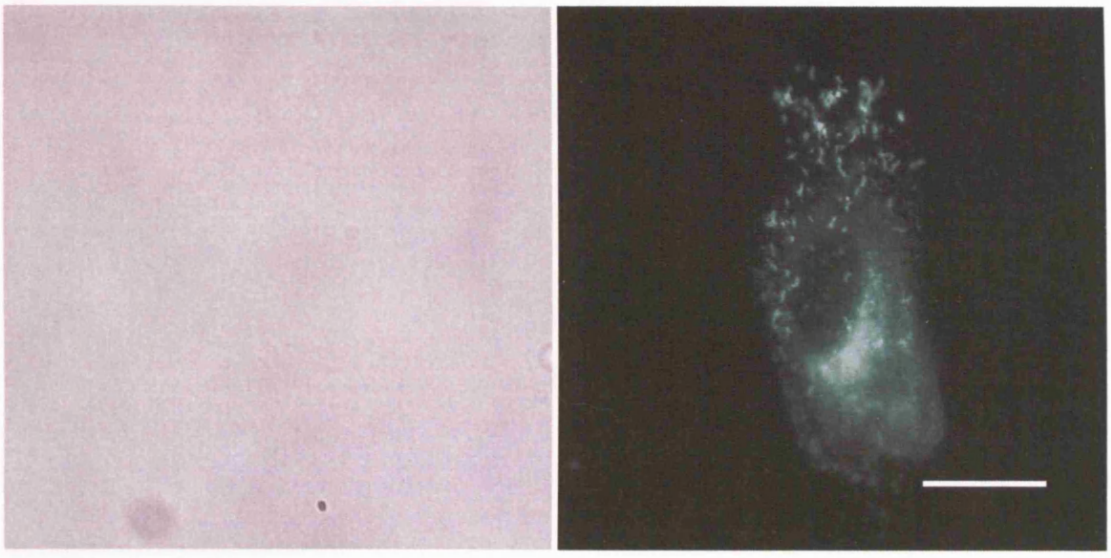

**Figure 3.6)** A single HUVEC immunostained with a primary antibody raised against von Willebrand factor (abcam). Primary antibody detected using a Cy2-conjugated secondary antibody. The flecks at the top half of the fluorescence image are likely to be Weibel Palade bodies; storage vesicles which contain vWF. Corresponding brightfield and green fluorescence images are displayed in the left and right panels, respectively. Scale bar: 10μm.

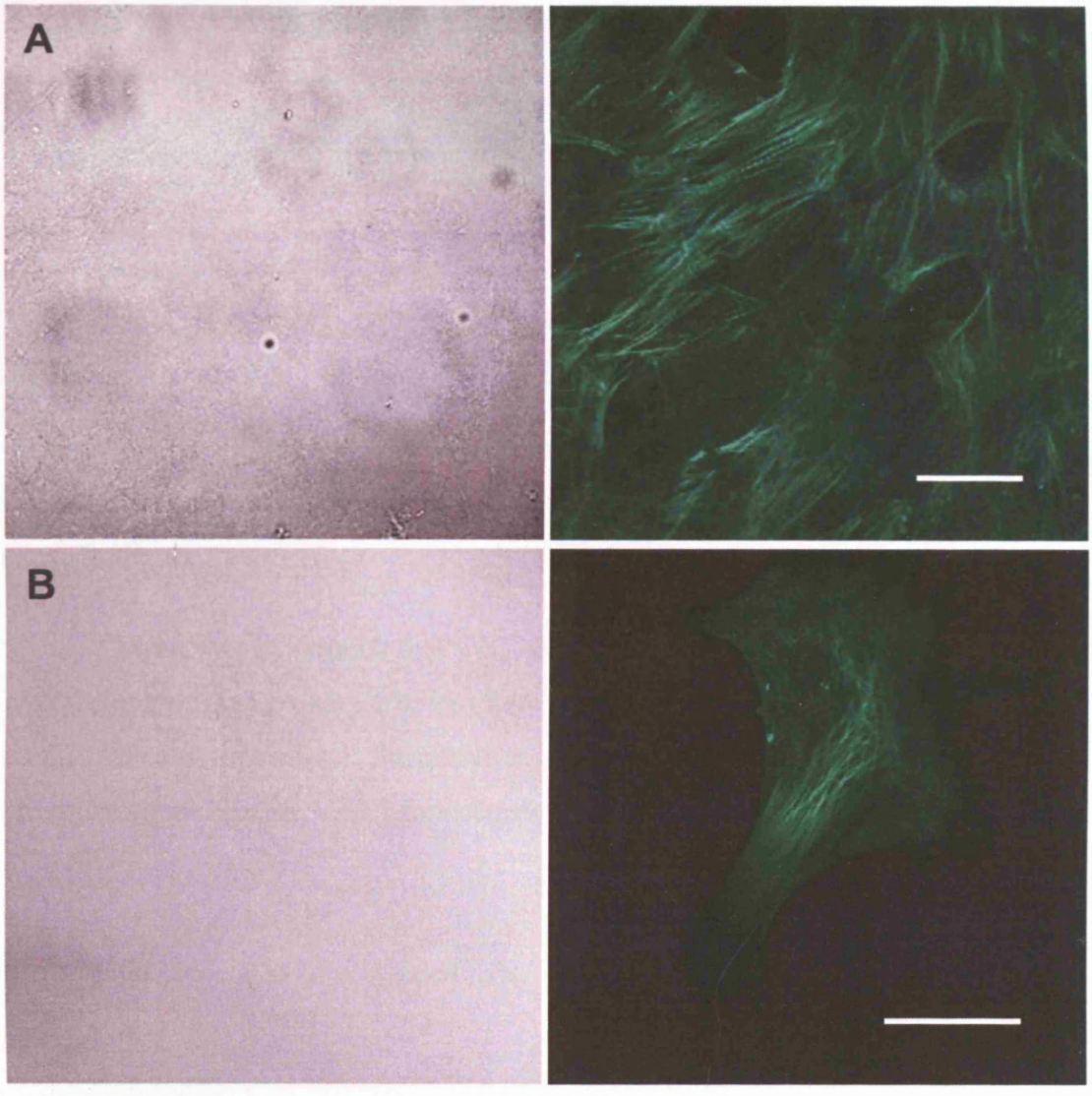


**Figure 3.7)** Rat carotid artery explant cells (passage 4) (A) and a human pulmonary artery smooth muscle cell (B) immunostained with a primary antibody raised against smooth muscle actin (DakoCytomation). Primary antibody detected using a FITC-conjugated secondary antibody. Corresponding brightfield and green fluorescence images are displayed in the left and right panels, respectively. Scale bars: 50μm (A) and 20μm (B).

## 3.2.3) Pig coronary artery cells

### 3.2.3.1) Morphology

Cells isolated from R or LAD pig coronary arteries grew to confluence in 'cobblestone' morphology, typical of endothelial cells. When plated at a low density, cells became quite flat.

### 3.2.3.2) Expression of von Willebrand factor

Consistent with reports that vWF is not significantly expressed in the endothelium of pig coronary arteries (Rand *et al.*, 1987), immuno-fluorescence studies failed to demonstrate the presence of this protein in pig R or LAD coronary artery cells (see *section 3.2.2.2* for procedure).

### 3.2.3.3) Internalisation of acetylated LDL

Pig R and LAD coronary artery cells, cultured for less than five days, internalised fluorescently labelled aLDL in a similar manner to HUVEC (*figure 3.8*).

In a further study, cells which had been frozen following 2-3 weeks in culture (passage 2), were thawed and cultured for a further three days. Although a proportion of cells retained the ability to internalise fluorescently labelled aLDL, many did not.

### 3.2.3.4) Expression of smooth muscle actin

Smooth muscle actin immunostaining (see *section 3.2.2.4* for procedure) was carried out on cells which had been frozen following 2-3 weeks in culture (passage 2) then cultured for a further three days. Although a small number of pig coronary artery cells (*figure 3.9*) exhibited similar staining to that seen in explant cells and HPASM (*figure 3.7*), many did not show above-background staining. Other cells appeared to express smooth muscle actin in the sub-plasmalemmal region, but this did not cross the cytosol. Above-background fluorescence did not occur in any cells when the primary antibody was omitted from the procedure.

### 3.2.3.5) Summary

Cells which had been in culture for less then one week grew to the same classical 'cobblestone' morphology associated with endothelial cells, and were also capable of internalising aLDL. Following one week in culture, however, monolayers became flattened and some cells lost the ability to internalise aLDL. Expression of actin was not studied in short-term cultures, however it is possible that actin became expressed as cells de-differentiated. In a process termed endothelial-mesenchymal trans-differentiation, cells from purified endothelial cultures have been demonstrated to gradually spontaneously down-regulate endothelial markers (Frid *et al.*, 2002). The same cells then begin to express smooth muscle proteins, including actin, fully transforming into smooth muscle cells within several weeks.

## 3.2.4) Conclusion of cell identification studies

A disappointing conclusion of these studies is that cells cultured from rat vessels using explant cultures are unlikely to be endothelial. However, those cultured from pig coronary arteries are of the expected morphology for endothelial cells and, for at least seven days retain the ability to internalise the specific endothelial cell marker, aLDL.

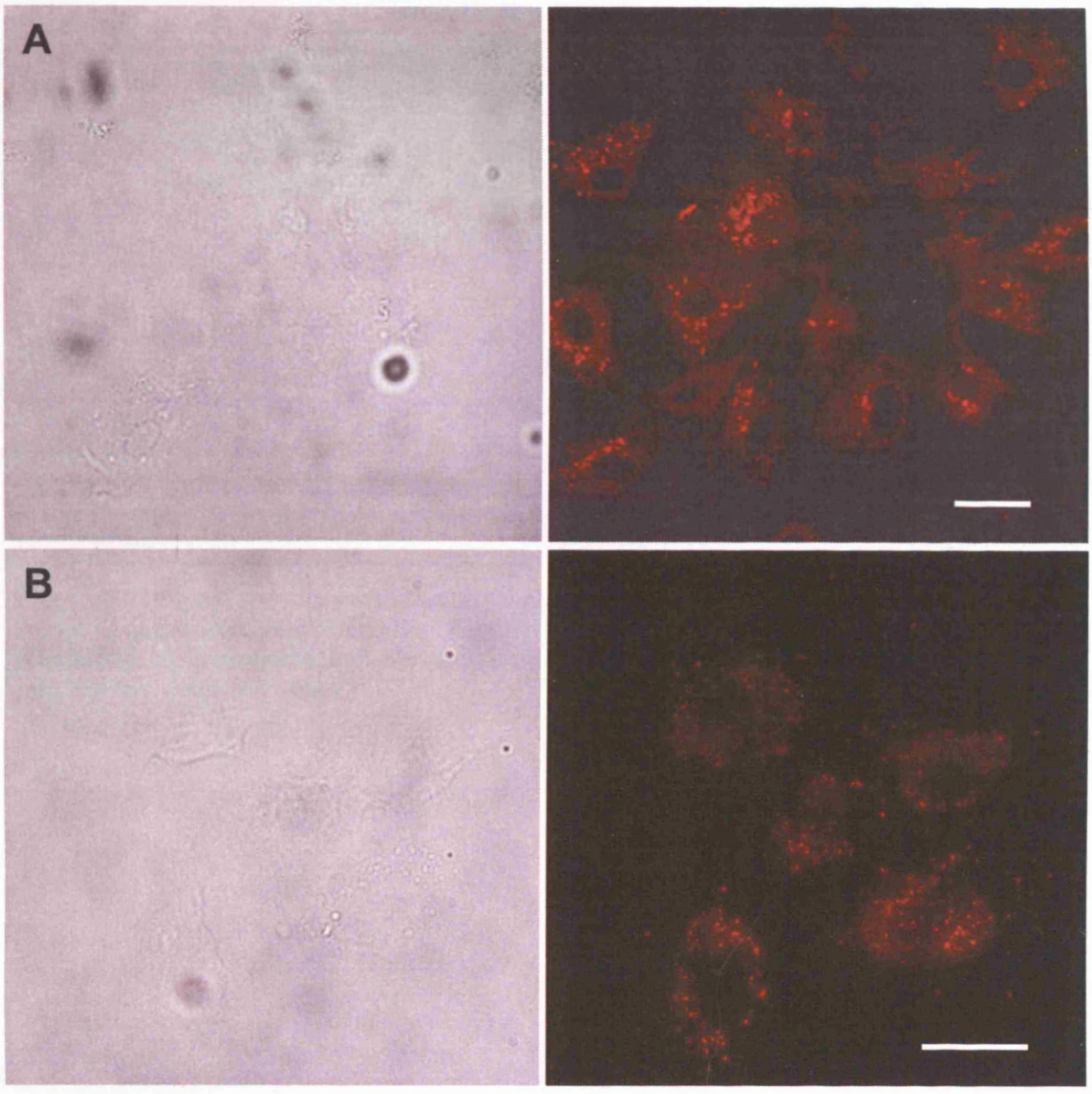


**Figure 3.8)** Pig right coronary endothelial cells (passage 0) (A) and HUVEC (B) cultured with DiI-labelled acetylated LDL. Corresponding brightfield and red fluorescence images are displayed in the left and right panels, respectively. Scale bars: 20$\mu$m.

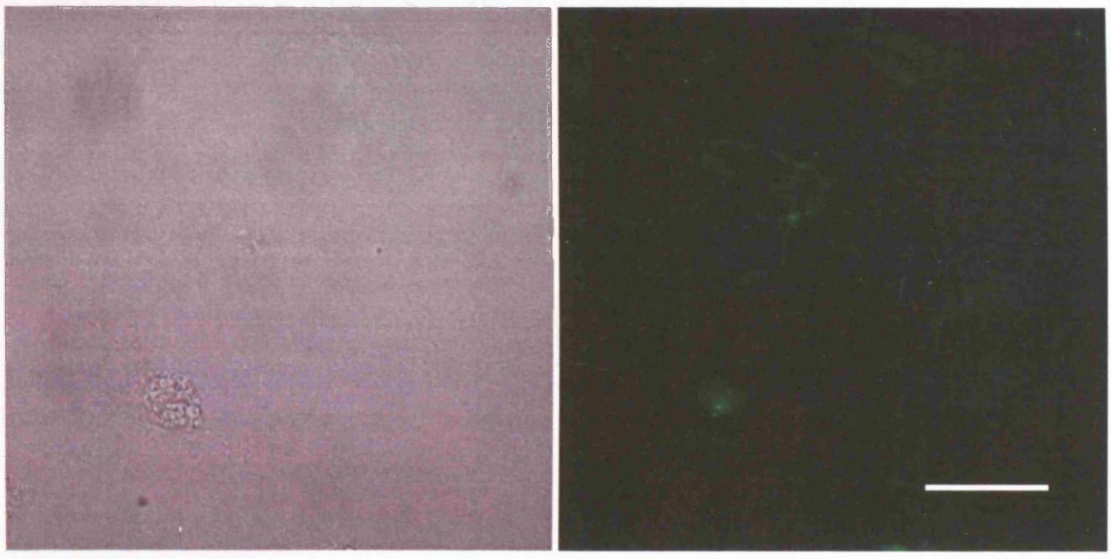

**Figure 3.9)** Pig right coronary artery cells (passage 2) immunostained with a primary antibody raised against smooth muscle actin, and detected using a FITC-conjugated secondary antibody. Corresponding brightfield and fluorescence images are displayed in the left and right panels, respectively. Scale bar: 50μm.

# Chapter 4: Rat explant cell electrophysiology

## 4.1) Foreword

As discussed in *chapter 3*, although similar in morphology to endothelial cells, rat explant cells did not express vWF or internalise aLDL. Preliminary studies were carried out to further clarify whether these cells might in fact exhibit electrophysiological characteristics of endothelial cells.

## 4.2) Introduction

Rat explant cells were particularly difficult to study using the patch clamp technique. This was principally due to the poor ability of patch electrodes to form seals with the cells. Gigaseals were possible with less than one cell in twenty, and altering pipette dimensions did little to improve this.

A further obstacle to successful recording was the very flat geometry of the cells. In early studies, it was difficult to place a patch electrode anywhere on a cell without it making contact with the bottom of the bath and thus puncturing the cell membrane. Attempts were made to round the cells by exposure to trypsin-EDTA or calcium/magnesium-free solutions, however, these procedures tended to result in cells lifting without rounding. The problem was partially relieved by lifting and re-plating cells between two and four hours prior to study. Using this method it was possible to place a patch electrode onto the nuclear region a cell when approached at a steep angle.

Cells used for patch clamp studies had been in culture for between two and four weeks (passage 1-3).

## 4.3) Studies with 30nM intracellular calcium

### 4.3.1) Control recordings

Explant cells were studied using patch electrodes filled with a 30nM free-calcium-containing intracellular (patch pipette) solution. The following data were recorded in cells cultured from mesenteric artery.

Resting membrane potentials were between -15 and -5mV, and whole-cell input resistances were between 1 and 8 GΩ at -20mV (n=5). Cells were held at -20mV, and current voltage relationships (CVR)s determined by a series of 100ms steps from -60 to +120mV, in increments of 20mV. CVRs were shallow and linear at potentials negative to +60mV, outwardly rectifying at more positive potentials (*figure 4.1A*). Currents reversed at between -50 and 0mV.

### 4.3.2) Application of pharmacological agents

0.1-3 μM histamine was without effect on the whole-cell currents of five cells. At these concentrations, histamine has been shown to evoke EDHF-mediated vasodilation in rat mesenteric arteries (Adeagbo & Triggle, 1993).

In order to determine whether $BK_{Ca}$ channel activity could account for voltage-dependence of control currents, ketoconazole, which has been demonstrated to activate (Rittenhouse *et al.*, 1997) or block (Wu *et al.*, 1999b) different populations of $BK_{Ca}$ channels, was applied to cells. Whole-cell currents of three cells remained unaltered in the presence of 20-30μM ketoconazole.

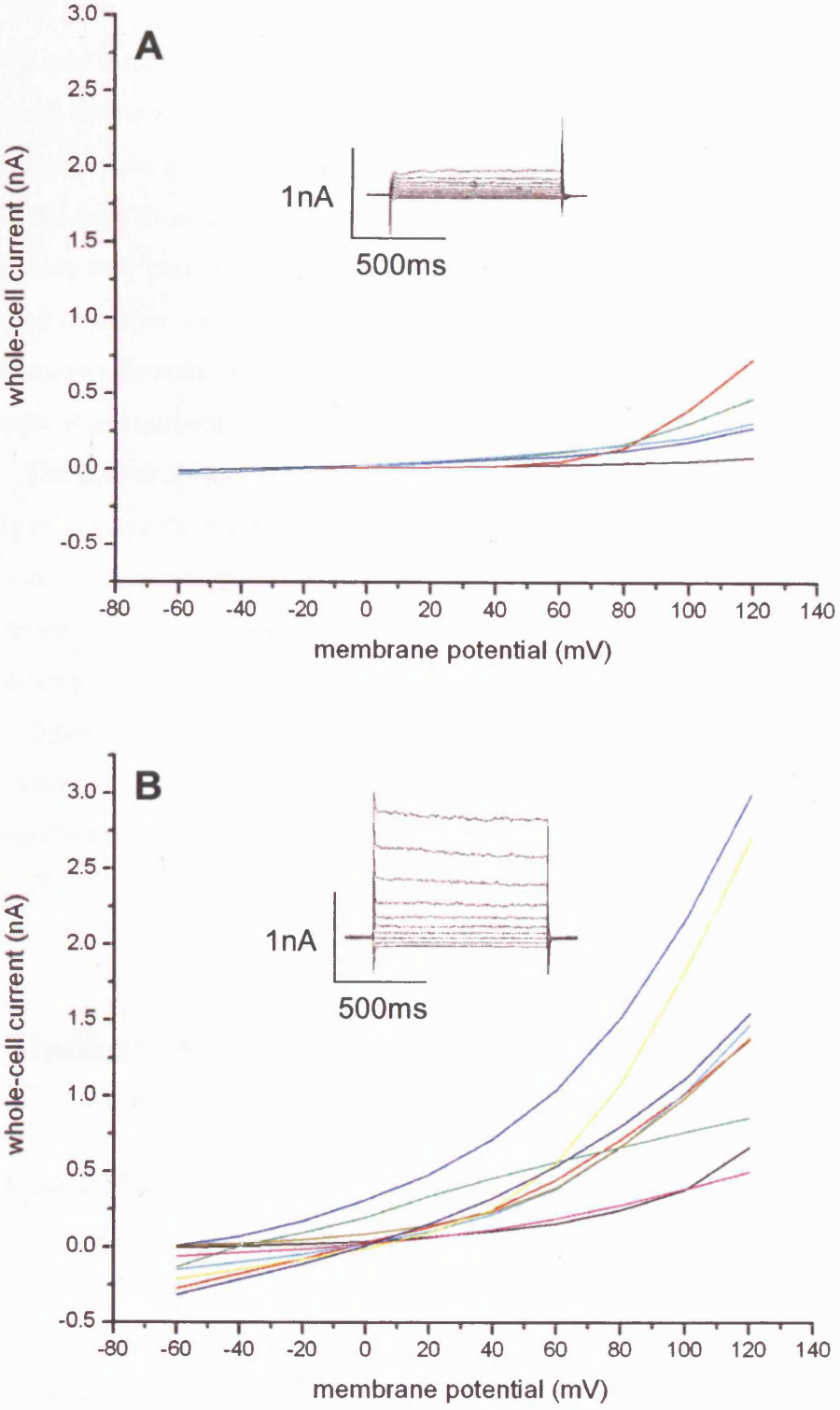


**Figure 4.1)** Whole-cell current voltage relationships recorded in explant cells dialysed with an intracellular (patch pipette) solution containing 30nM (A) or 1.5µM (B) free-calcium. Each line represents a different cell; colours bear no relevance other than to enable distinction of traces. *Inset* figures are example recordings.

### 4.3.3) Summary

Since histamine is able to trigger EDHF-attributed vasodilation in rat mesenteric arteries, it can be assumed that this occurs via hyperpolarisation of the endothelium (Adeagbo & Triggle, 1993). This has been demonstrated in isolated endothelial cells from other vascular beds. While the lack of a response to histamine in this study may cast doubt on the cells being endothelial, a down-regulation of histamine receptors, associated transduction pathways or ion channels, during culture, cannot be ruled out. Down-regulation of agonist and calcium-activated responses of pig coronary artery endothelial cells are reported in *chapter five.*

The outwardly rectifying component of whole-cell CVRs indicates an activity of voltage-dependent potassium channels. Of these, $BK_{Ca}$ channels are the most commonly expressed type in endothelial cells. The effects of ketoconazole on $BK_{Ca}$ channels have only been reported in a small number of studies, so it remains unclear whether all $BK_{Ca}$ channels are sensitive to this agent.

Other channels that could account for outwardly rectifying currents recorded in this study include members of the $K_V$ family, however these have only occasionally been reported in endothelial cells (Nilius & Droogmans, 2001; Adams & Hill, 2004).

## 4.4) Studies with 1.5μM intracellular calcium

### 4.4.1) Control recordings

Cells were further studied using patch electrodes filled with a 1.5μM free-calcium-containing intracellular (patch pipette) solution. Dialysing cells with this concentration of calcium should activate most $K_{Ca}$ channels. The following data are from cells cultured from rat aorta or mesenteric artery.

Following stabilisation of the whole-cell current, input resistances were typically 100-500MΩ at -20mV (n=9). At this potential, input resistances were significantly less than for cells dialysed with 30nM free-calcium (4.2±1.2GΩ n=5,

0.5±0.2GΩ n=9, for 30nM and 1.5μM, respectively; P=0.019, one-tailed unpaired Student's t-test). This is consistent with the activation of $K_{Ca}$ channels.

Cells were held at -20mV and voltage pulses applied as described previously (see *section 4.3.1*). Although reversal potentials for whole cell currents varied widely between -70 and 0mV, similar to cells dialysed with 30nM calcium, outward currents were significantly larger (0.4±0.1nA n=5, 1.5±0.3nA n=9, for 30nM and 1.5μM, respectively; currents recorded at +120mV; P=0.002, one-tailed unpaired Student's t-test). Most CVRs were linear at membrane potentials negative to +40mV, outwardly rectifying at more positive potentials (*figure 4.1B*). One exception was a cell with an approximately linear whole-cell CVR (*green trace, figure 4.1*), however there was no reason to suppose that this was not a valid recording.

## 4.4.2) Application of pharmacological agents

In three cells, 10-20μM clotrimazole reversibly blocked an approximately linear component of the whole-cell CVR, constituting ~4-20% of the control current at +120mV. Clotrimazole blocked a current with an expected reversal potential of ~-70mV in one cell (*figure 4.2*) whilst in the remaining two, blocked currents reversed at -50 and 0mV.

In two out of three cells, 2-50μM ketoconazole reversibly blocked an approximately linear component of the whole-cell CVR, constituting ~13-39% of the control current at +120mV. In the same cell as featured in *figure 4.2*, 20μM ketoconazole blocked a current with an expected reversal potential of ~-70mV (*figure 4.3*). In a second cell, 2μM ketoconazole blocked a current which reversed at approximately 0mV, whilst in a third, 30μM ketoconazole was without effect.

5mM TEA reversibly blocked an approximately linear component of the whole-cell CVR when applied to the cell featured in *figures 4.2 and 4.3* (*figure 4.4*). The blocked current had an expected reversal potential of ~-70mV and accounted for ~18% of the control whole-cell current at +120mV. 1mM TEA blocked a smaller, similar current in the same cell.

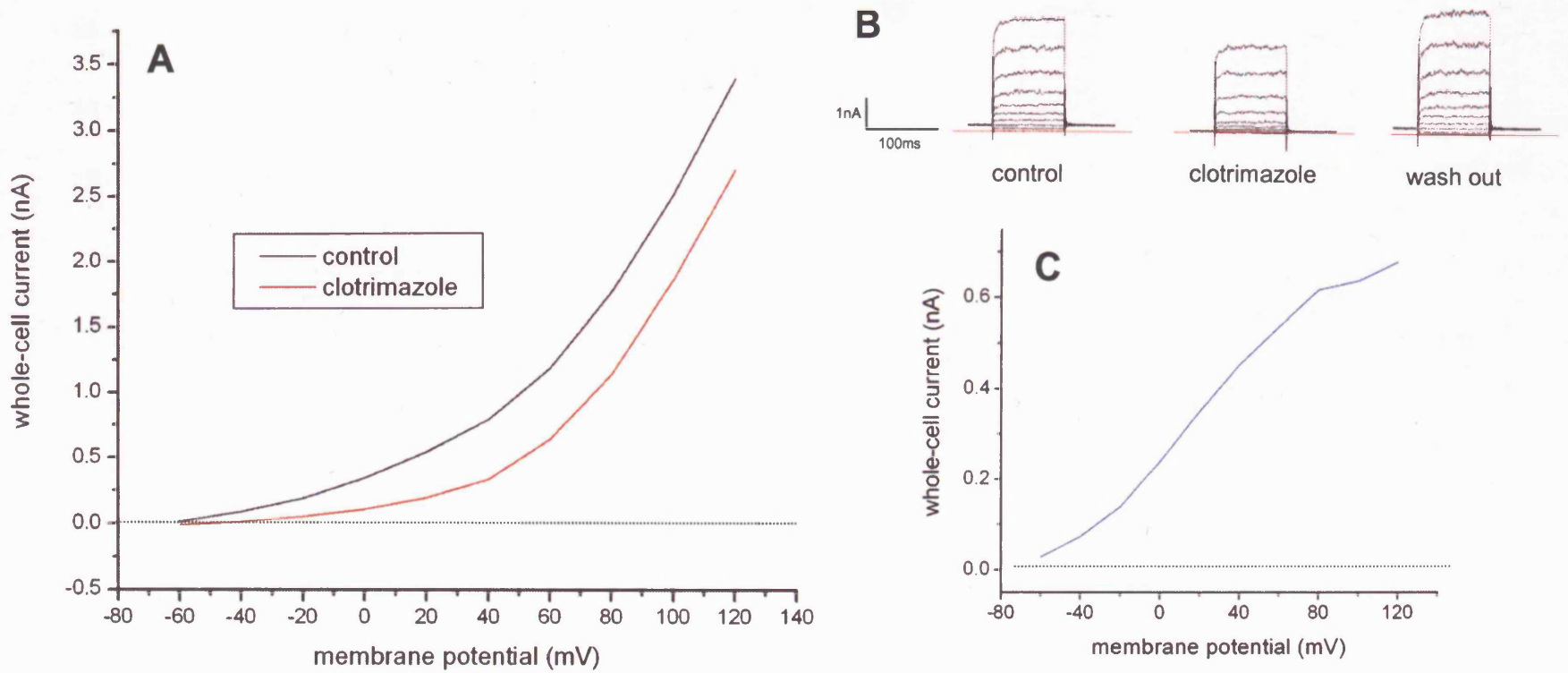


**Figure 4.2)** Effect of 10μM clotrimazole on the whole-cell current of a rat aortic explant cell dialysed with an intracellular (patch pipette) solution containing 1.5μM free-calcium. Panel A: Plots of the control current (black) and that recorded two minutes into application of clotrimazole (red). The difference current is plotted in panel C. Whole-cell current recordings in response to voltage steps are displayed in panel B, including that recorded 3mins following wash out. Zero current is highlighted by a dotted line on graphs and by a red line on each current plot.

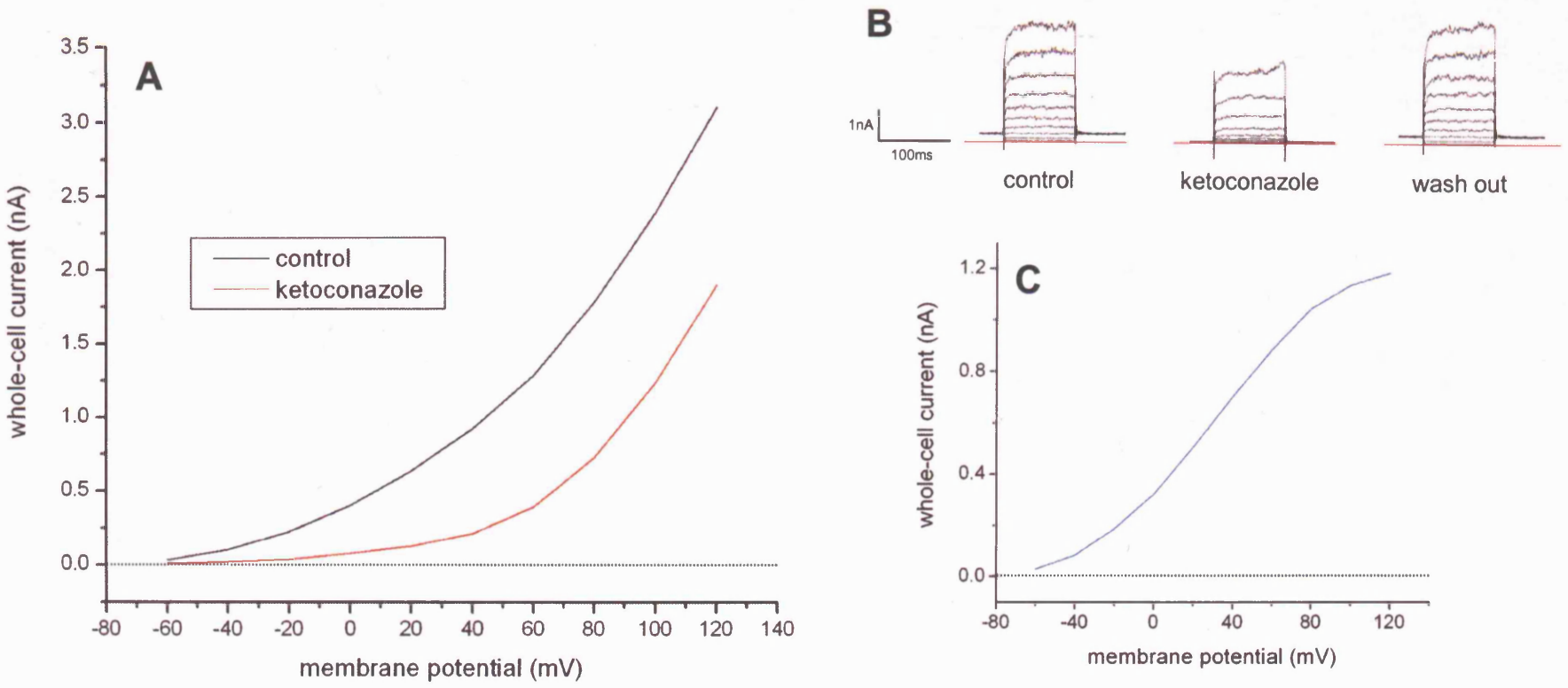


**Figure 4.3)** Effect of 50μM ketoconazole on the whole-cell current of a rat aortic explant cell dialysed with an intracellular (patch pipette) solution containing 1.5μM free-calcium. Panel A: Plots of the control current (black) and that recorded two minutes into application of ketoconazole (red). The difference current is plotted in panel C. Whole-cell current recordings in response to voltage steps are displayed in panel B, including that recorded 3mins following wash out. Zero current is highlighted by a dotted line on graphs and by a red line on each current plot.

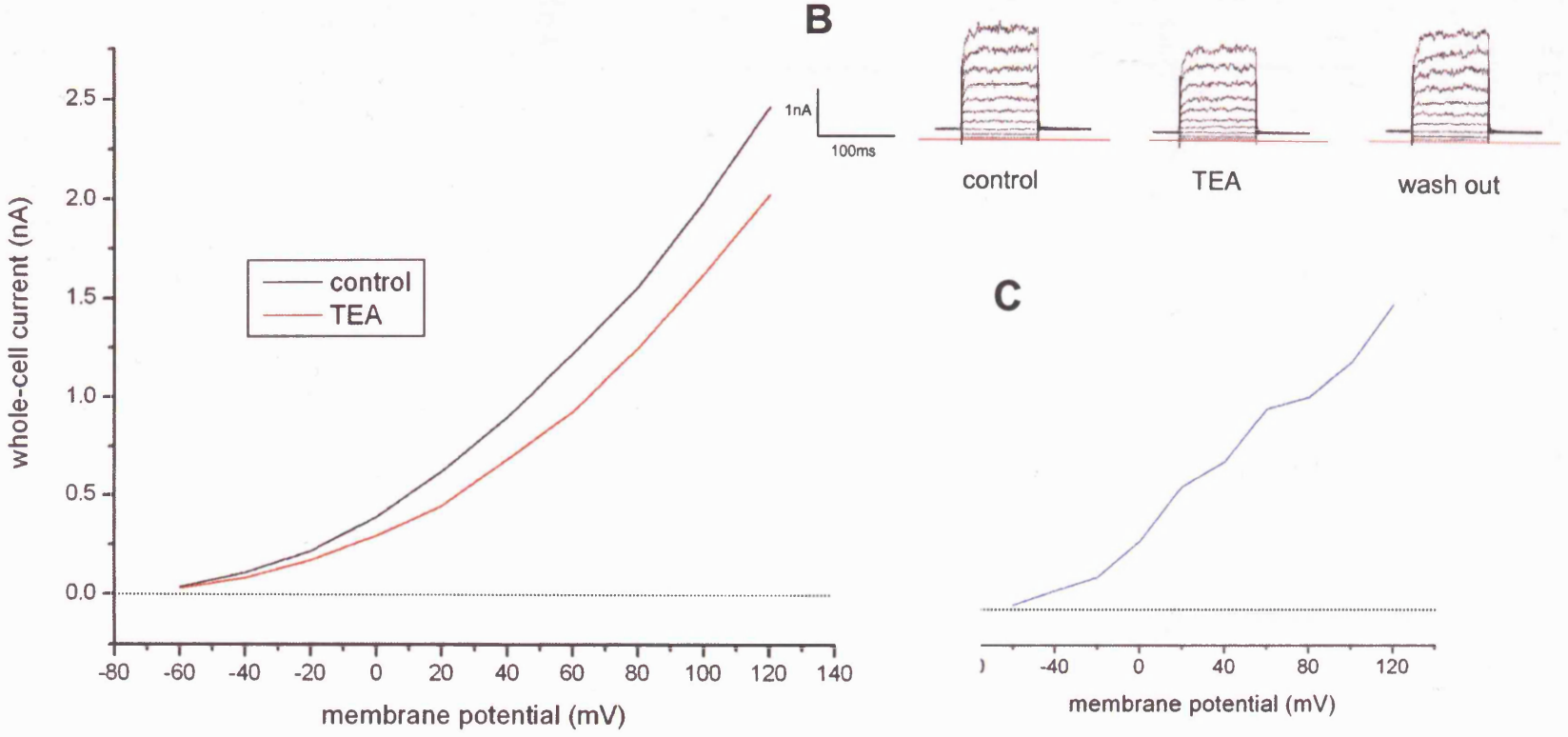


**Figure 4.4)** Effect of 5mM TEA on the whole-cell current of a rat aortic explant cell dialysed with an intracellular (patch pipette) solution containing 1.5μM free-calcium. Panel A: Plots of the control current (black) and that recorded two minutes into application of TEA (red). The difference current is plotted in panel C. Whole-cell current recordings in response to voltage steps are displayed in panel B, including that recorded 3mins following wash out. Zero current is highlighted by a dotted line on graphs and by a red line on each current plot.

Whole-cell currents were not affected by 30nM apamin (n=1) or 50nM UCL 1848 (n=1) (see *figure 4.5*).

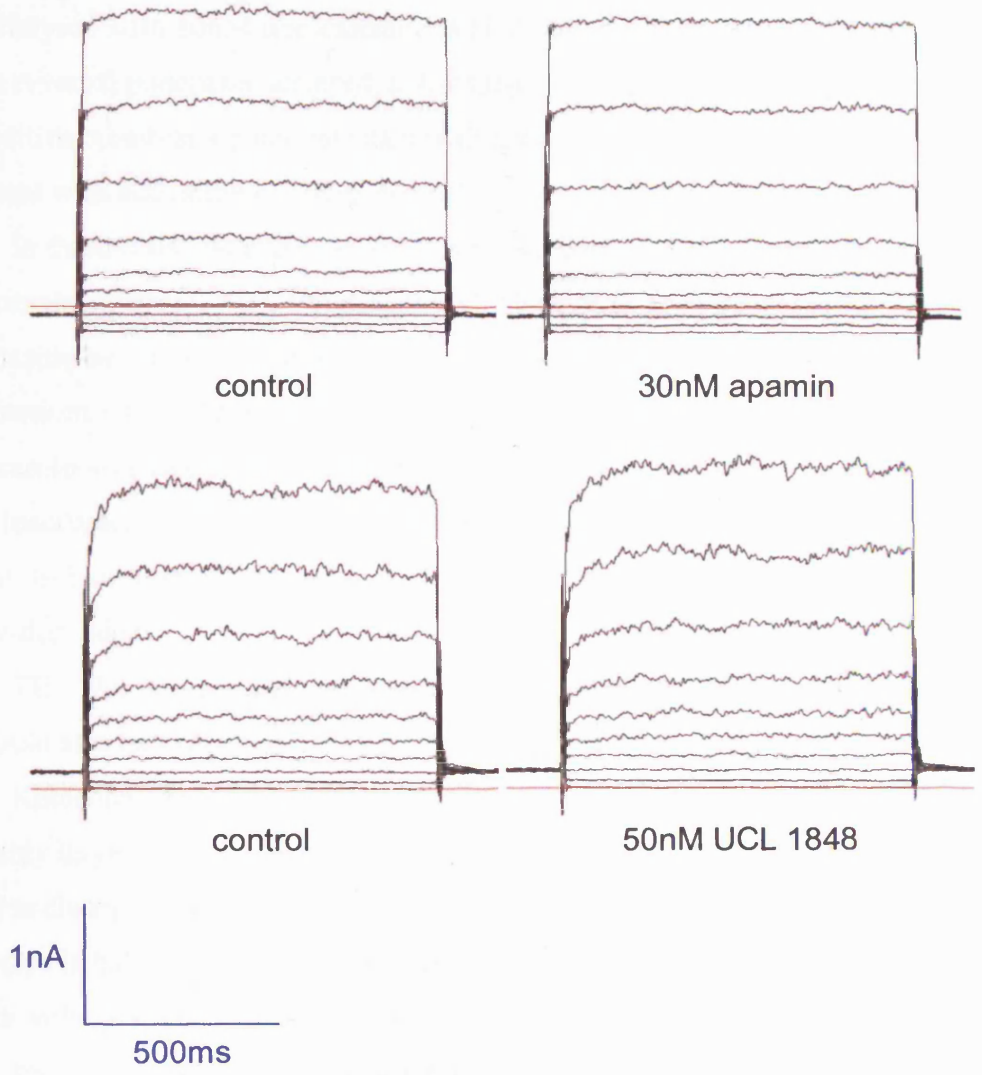


**Figure 4.5)** Example traces showing insensitivity of rat aortic explant cell whole-cell currents to apamin and UCL 1848. Both cells were dialysed with intracellular (patch pipette) solution containing 1.5μM free-calcium. Zero current is marked by the red line. Currents are in response to voltage steps from -60 to +120mV; the holding potential was -20mV.

### 4.4.3) Summary

Cells dialysed with an intracellular solution containing 1.5μM free-calcium had significantly lower input resistances, and larger outward currents, compared to those dialysed with 30nM free-calcium. Whilst no significant change in whole-cell current reversal potentials occurred, a voltage-dependent component became active at less positive membrane potentials than with lower cytosolic calcium. This is consistent with activation of $BK_{Ca}$ channels.

In three cells, clotrimazole-sensitive components of whole-cell currents had approximately linear CVRs. Consistent with block of $IK_{Ca}$ channels, in one cell the clotrimazole-sensitive current had a reversal potential within 15mV of that calculated for potassium ions (-85mV under these conditions). In the two other cells, clotrimazole-sensitive currents reversed at -50 and 0mV, suggesting possible voltage-clamp inaccuracies in some of these experiments. $BK_{Ca}$ channel block does not account for clotrimazole sensitivity of these cells since the inhibited currents were not voltage-dependent.

TEA also blocked a linear component of the whole-cell current of one cell. This could also be explained by block of $IK_{Ca}$ but not $BK_{Ca}$ or $K_V$ channels.

Ketoconazole blocked a linear component of the whole-cell CVR which was noticeably larger than that blocked by clotrimazole or TEA. Although structurally related to clotrimazole, ketoconazole is ineffective in blocking $IK_{Ca}$ channels. Whilst ketoconazole has been shown to block $BK_{Ca}$ and some $K_V$ channels, it is not reported to block voltage-independent channels that could account for its activity in this study.

Insensitivity of whole-cell currents to apamin and UCL 1848 suggest that these cells do not express functional $SK_{Ca}$ channels.

## 4.5) Conclusion of rat explant cell studies

Rat explant cultures were employed following other unsuccessful attempts at isolating rat arterial endothelial cells. Although it has been reported that this method produces a predominantly endothelial cell culture (McGuire & Orkin, 1987), similar protocols have also been used to culture smooth muscle cells. Whilst the cells cultured in this study appeared to be morphologically similar to endothelial cells, particularly when plated at low density, they did not internalise aLDL or express vWF. This was true of cells cultured for the shortest possible period of time using this culture method (5 days). Explant cells also expressed smooth muscle actin, usually found in smooth muscle and fibroblasts, but not endothelial cells.

Electrophysiological study of rat explant cells was particularly arduous since cells rarely sealed to electrodes. Over several weeks, only a small number of whole-cell recordings were achieved. Cells were unresponsive to histamine, and calcium-activated currents were insensitive to $SK_{Ca}$ channel blockers. As cells were studied only following two to three weeks in culture, a down-regulation of channel proteins involved in agonist-evoked hyperpolarisation cannot be ruled out.

On account of these various findings, further attempts to isolate and study endothelial cells from rat vessels were abandoned. Since it is unlikely that rat explant cells were endothelial, data described in this chapter will not be considered further in this thesis.

# Chapter 5: Pig endothelial cell electrophysiology

## 5.1) Introduction

As previously discussed, various approaches to isolating rat vascular endothelial cells were unsuccessful. Recent studies e.g. (Burnham *et al.*, 2002; Sollini *et al.*, 2002) suggested, however, that endothelium could be relatively easily isolated from pig coronary arteries. In keeping with this, endothelial cells were successfully isolated and cultured from pig coronary arteries, and used in all further studies.

Pig coronary artery endothelial cells, like rat explant cells, are very flat making them difficult to study. When plated at a low density, cells became flatter the longer they remained attached to tissue culture plastic, so were routinely lifted and re-plated on the evening prior to study.

By adopting a steep angle of approach, a patch electrode could be placed on the cell membrane overlying the nucleus. The small distance between the tip of the cell-attached patch electrode and the base of the perfusion bath remained a constant difficulty. Recordings were frequently lost through sub-micron drift of the hydraulic micromanipulators.

The ability of electrodes to seal with cell membranes, and ease of entry into whole-cell configuration varied greatly between culture batches. Cells were also prone to 'resealing' i.e. whole-cell configuration would revert back to cell attached configuration.

Initially cells were studied following one to two weeks in culture, however outward currents could not be evoked in these cells. This was true both in response to agonists and when cells were dialysed with an intracellular solution containing 1.5μM free-calcium. It was subsequently determined that outward currents could only be evoked in cells cultured for less than five days. After only one day in culture, cells were often sickly in appearance and did not easily seal to patch electrodes. As a result, all studies were carried out on cells cultured for between two and four days.

## 5.2) Current-clamp studies

### 5.2.1) Introduction

The initial studies were carried out on large rafts of pig right or left anterior descending coronary artery endothelial cells, using current-clamp. The size of such rafts varied considerably from small clumps containing approximately eight cells, to vast confluent monolayers comprising in excess of one hundred cells.

Membrane potential was monitored continuously (gap-free recording) in order to fully capture agonist-evoked responses. Patch electrodes were filled with intracellular solution containing 30nM free-calcium.

### 5.2.2) Cells at rest

As expected, the typical input resistances of large cell rafts (<200MΩ) were much lower than those of small clusters of cells used in voltage-clamp studies (>1GΩ) (see *section 5.3.2.2*).

The mean resting membrane potentials ($E_m$s) for right (R) and left-anterior descending (LAD) coronary artery cells are shown in *table 5.1*. $E_m$s were similar for cells cultured from both arteries, with a small but significant difference between cells cultured for three days. No significant differences were found between mean $E_m$s of cells cultured for different lengths of time. Pooling all data gives a mean $E_m$ of -5.9±0.5mV (n=102). Distributions of $E_m$s according to artery of origin and length of time in culture are shown in *figure 5.1*. In subsequent studies, no distinction is made between cells on the basis of originating artery or time in culture.

In some experiments, $E_m$ gradually depolarised towards zero mV over the first few minutes of recording (data not shown).

The $E_m$s reported in this study are substantially less negative than values given in published studies of isolated pig coronary artery endothelial cells. To determine whether this was due to the experimental conditions, both intracellular and extracellular recording solutions were replaced with those used by Sollini *et al.*

(2002). Additionally, some batches of cells were cultured in medium equivalent to that used by Sollini *et al.* Neither intervention had any noticeable effect on $E_m$ (data not shown) (see also *section 5.3.2.3*). The low membrane potentials reported in these studies are further discussed in *chapter seven.*

| Cells | (Days in culture) | | |
|---|---|---|---|
| | 2 | 3 | 4 |
| R | -8.3±2.0mV (14) | -7.2±0.7mV (23)† | -5.7±0.8mV (10) |
| LAD | -5.4±1.1mV (18) | -4.5±1.3mV (21)† | -4.9±2.6mV (15) |

**Table 5.1)** Resting membrane potentials recorded from rafts of cultured pig right (R) and left anterior descending (LAD) coronary artery endothelial cells. Data given as mean ± standard error (sample size). Using an unpaired two-tailed Student's t-test, statistical comparison was made between R and LAD groups (controlling for time in culture), and between different length of time in culture (controlling for artery of origin). All differences were non-significant (P>0.05), except between marked groups (†) ( P=0.041).

## 5.2.3) Responses to 'EDHF agonists'

### 5.2.3.1) Introduction

Endothelial cells from both LAD and R arteries hyperpolarised in the presence of extracellular ATP, substance-P or bradykinin (for example see *figures 5.2* to *5.4* and *5.6*). Histamine also hyperpolarised cells (for example see *figure 5.5*), but because desensitisation was apparent with repeat exposure, this agonist was not further studied. No change in membrane potential was evoked by the muscarinic receptor agonist, carbachol (10μM, n=3) (data not shown).

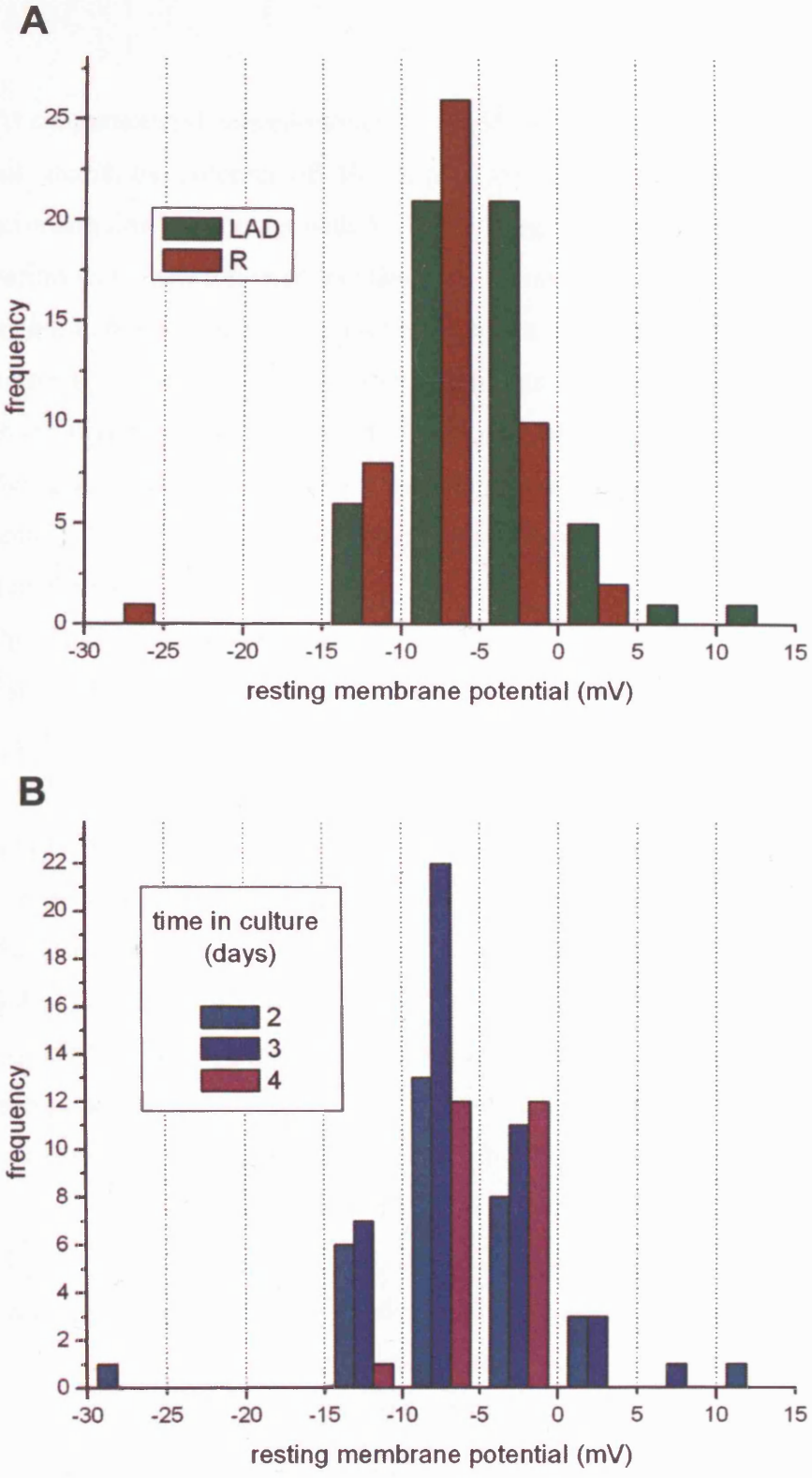


**Figure 5.1)** Resting membrane potentials recorded from rafts of endothelial cells cultured from pig left anterior descending (LAD) or right (R) coronary arteries. The same data are presented in two different ways: firstly according to artery of origin (irrespective of time in culture) (histogram A), secondly according to length of time in culture (irrespective of originating artery) (histogram B).

5.2.3.2) ATP

At supramaximal concentrations (1-10μM), ATP hyperpolarised cells to a mean peak membrane potential of -50.7±1.6mV (n=76) (for example see *figure 5.2*). Where cells remained in contact with ATP following the response peak, partial repolarisation was often followed by slow oscillations in membrane potential. With each oscillation, membrane potential returned closer to resting values until re-polarisation was complete, usually within 1-2 minutes (for example see *figure 5.3*).

In the majority of recordings, ATP was washed out of the bath once the hyperpolarisation had peaked. In many recordings, removal of ATP triggered a second smaller hyperpolarisation (for example see *figure 5.2*). The reasons for this were not explored.

Provided that a recovery interval of at least one minute was allowed between applications, repeated ATP exposure evoked reproducible hyperpolarisations in most recordings. However, stable recordings were usually only sustainable for a few minutes, making determination of a concentration-response relationship for ATP particularly difficult. Furthermore, concentration-response relationships were steep, and ATP-sensitivity varied considerably between cells; whereas some cells fully hyperpolarised to 30nM ATP, others failed to respond to 300nM, yet fully hyperpolarised to 1μM.

Concentration-response data has been compiled in two different ways; firstly using mean peak responses to a given ATP concentration (*table 5.2A*). The second comparison uses more stable recordings in which it was possible to express responses as a percentage of the hyperpolarisation to 1μM ATP evoked in the same cell raft (*table 5.2B*).

During some experiments, in order to monitor changing input resistance, current pulses were applied to cells at regular intervals (for example see *figure 5.2, lower trace*). In these records, voltage deflections in response to the current pulses diminish as the cells hyperpolarise, demonstrating that input resistance decreases during hyperpolarisation. This suggests that the change in membrane potential is largely due to the opening of potassium channels rather than the closure of chloride or non-selective cation channels.

**A**

| [ATP] (μM) | peak hyperpolarisation (mV) *including unresponsive cells* | number of unresponsive cells |
|---|---|---|
| 10 | -48.3±2.4 (44) | - |
| 3 | -48.4±3.6 (7) | 0 |
| 1 | -49.7±2.6 (37) | 2 |
| 0.3 | -21.0±4.9 (12) | 3 |
| 0.1 | -17.2±3.9 (19) | 6 |
| 0.03 | -9.1±5.1 (14) | 11 |

**B**

| [ATP] (μM) | peak hyperpolarisation (as % of paired 1μM ATP response) *including unresponsive cells* | number of unresponsive cells |
|---|---|---|
| 0.3 | 47.8±9.3 (11) | 2 |
| 0.1 | 31.4±7.3 (14) | 4 |
| 0.03 | 12.2±9.0 (11) | 9 |

**Table 5.2)** Mean peak hyperpolarisations to different concentrations of ATP (combined data for endothelial cells cultured from left anterior descending and right pig coronary arteries). Data in table A refer to absolute values from unpaired recordings. Data in table B refer to paired responses; peak hyperpolarisation calculated as a percentage of that to 1μM ATP. Data is given as mean ± standard error (sample size). Neither table contains data from cells which, at the end of the experiment, did not respond to ATP at the highest concentration applied (1 or 10μM). Data from two cells was omitted since in these, hyperpolarisations were greater in response to lower concentrations of ATP than for 1μM.

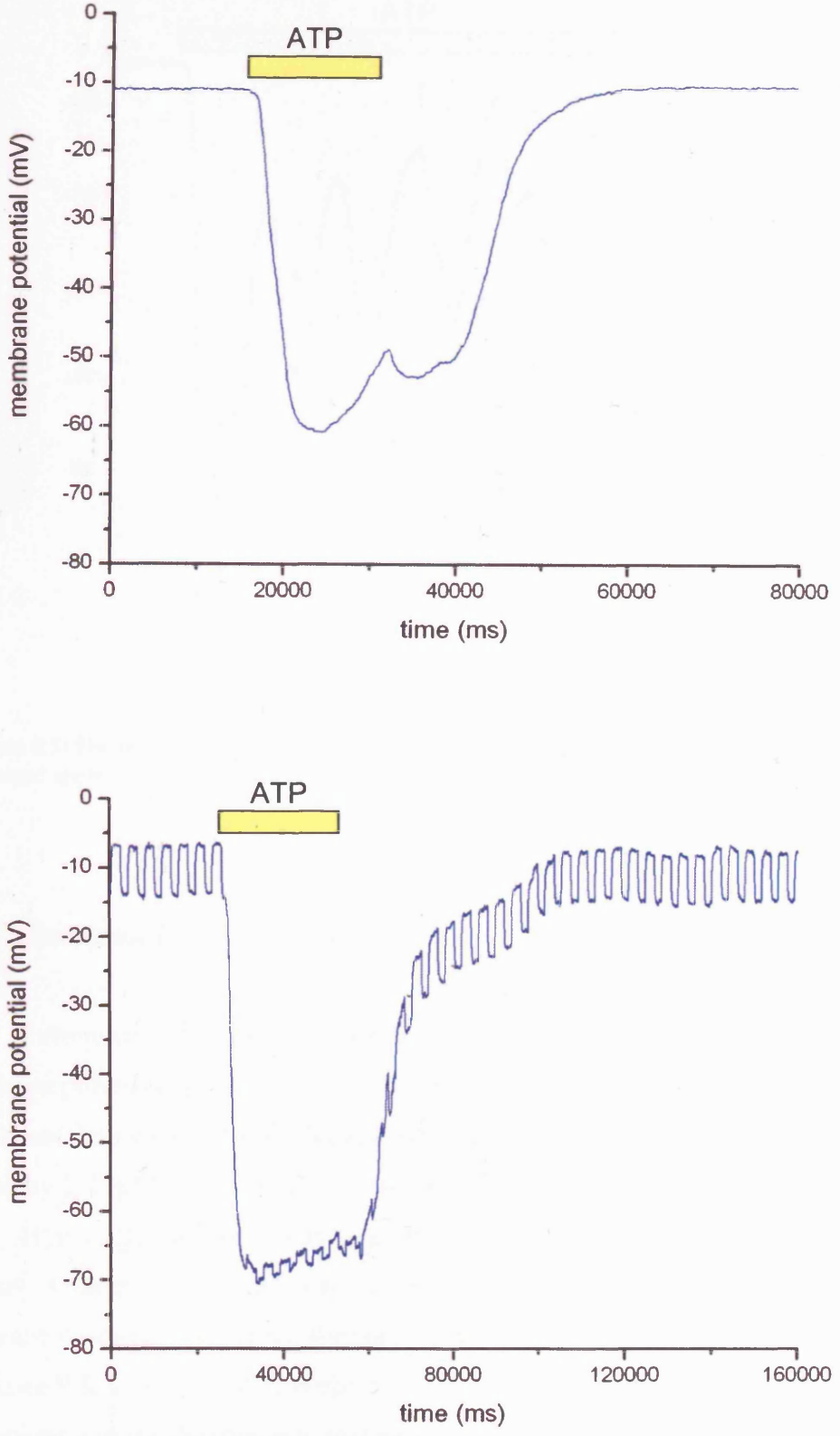


**Figure 5.2)** Hyperpolarisation evoked by transient application of 1μM ATP to two rafts of pig left anterior descending coronary artery endothelial cells. During the recording depicted in the *lower trace*, current pulses were applied in order to monitor changing input resistance (-50pA, duration: 0.5s, 0.25Hz).

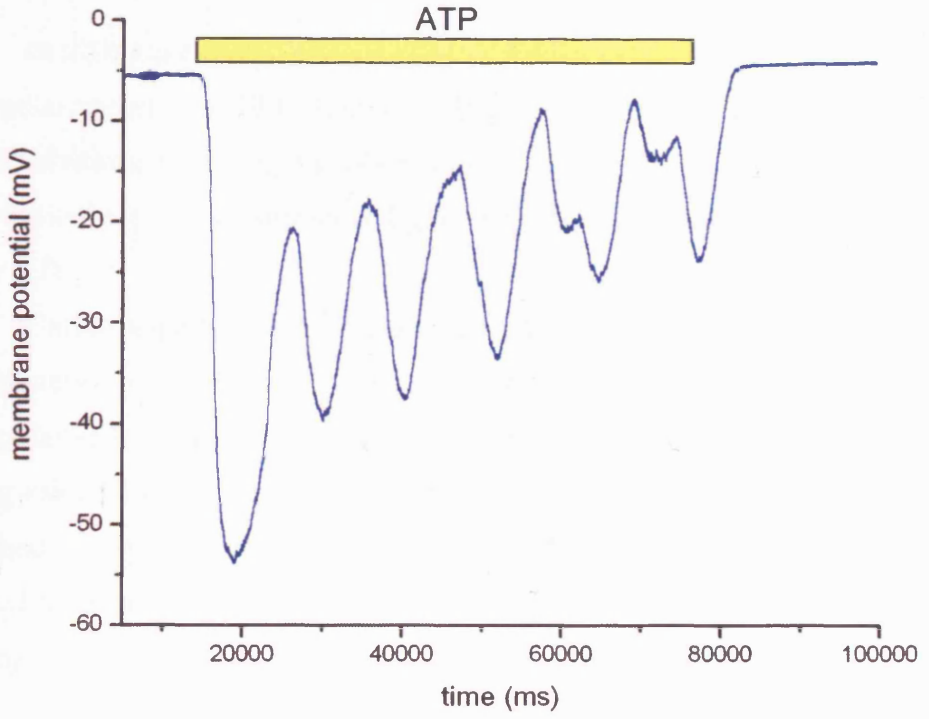


**Figure 5.3)** Hyperpolarisation and subsequent membrane potential oscillation evoked by sustained application of 10μM ATP in a raft of pig right coronary artery endothelial cells.

5.2.3.3) Substance P

Substance P hyperpolarised cells to a similar extent at 1 and 10nM, eliciting a peak hyperpolarisation of -45.7±4.7 (n=19) (pooled data) (for example see *figure 5.4*). These data were not significantly different from the peak hyperpolarisations evoked by 1-10μM ATP (*table 5.3 & figure 5.7*).

Hyperpolarisations to substance P were also similar to those of ATP in terms of onset, duration and decay. However, no second hyperpolarisation was seen when substance P was removed from the bath. As with ATP, continued presence of substance P following peak hyperpolarisation resulted in membrane potential oscillations and repolarisation to resting values within 1-2 minutes (data not shown).

5.2.3.4) Bradykinin

Bradykinin hyperpolarised cells to a similar extent at 1 to 100nM; the peak hyperpolarisation was -59.1±3.5mV (n=16) (pooled data) (for example see *figure 5.6*). Bradykinin-evoked hyperpolarisations were found to be significantly larger than those evoked by ATP or substance P (P=0.038 and 0.028. respectively) (*table 5.3 & figure 5.7*).

Unlike responses to ATP and substance P, cells did not repolarise immediately once bradykinin had been removed from the bath. Instead, the hyperpolarisation was sustained, with membrane potential steadily returning to the resting value within 2-5 minutes. The membrane potential did not oscillate during the sustained hyperpolarisation, and cells responded similarly when bradykinin was allowed to remain in the bath after cells had reached peak hyperpolarisation (data not shown).

| ATP (1-10μM) | substance P (1-10nM) | bradykinin (1-100nM) |
|---|---|---|
| -50.7±1.6mV (76)$^{\dagger}$ | -45.7±4.7mV (19)$^{*}$ | -59.1±3.5mV (16)$^{\dagger *}$ |

**Table 5.3)** Peak hyperpolarisations to supramaximal concentrations of ATP, substance P and bradykinin. Data given is mean ± standard error (sample size). Statistical comparisons were carried out using an unpaired two-tailed Student's t-test (†: P=0.038, *: P=0.028, no significant difference was found between ATP and substance P (P>0.05).

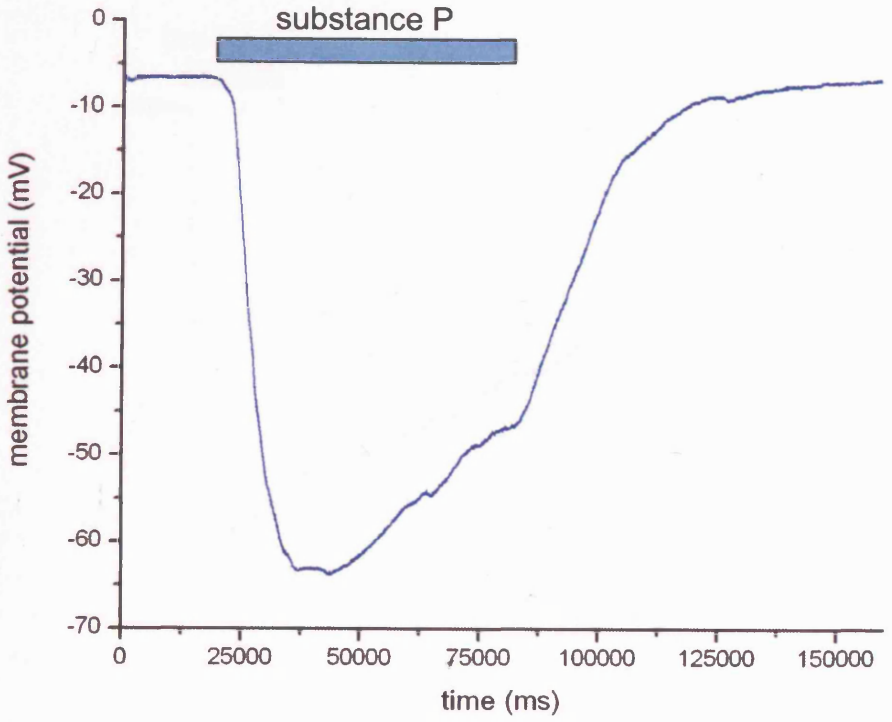


**Figure 5.4)** Hyperpolarisation evoked by transient application of 10nM substance P in a raft of pig left anterior descending coronary artery endothelial cells.

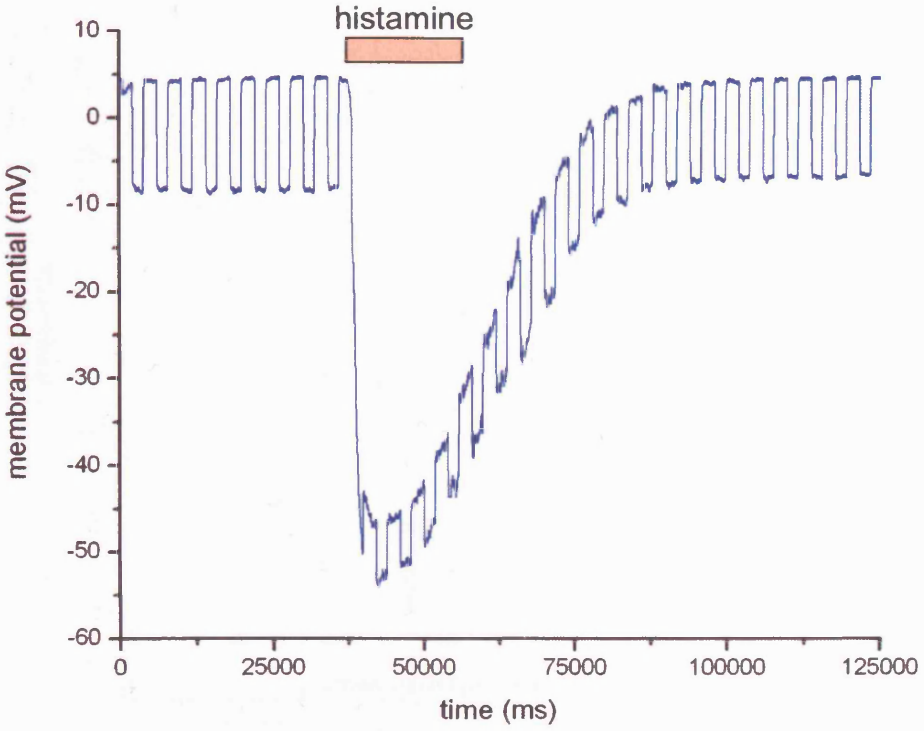


**Figure 5.5)** Hyperpolarisation evoked by transient application of 10μM histamine in a raft of pig left anterior descending coronary artery endothelial cells. In this recording current pulses were applied in order to monitor changes in input resistance (-5pA, duration: 1.5s, 0.25Hz).

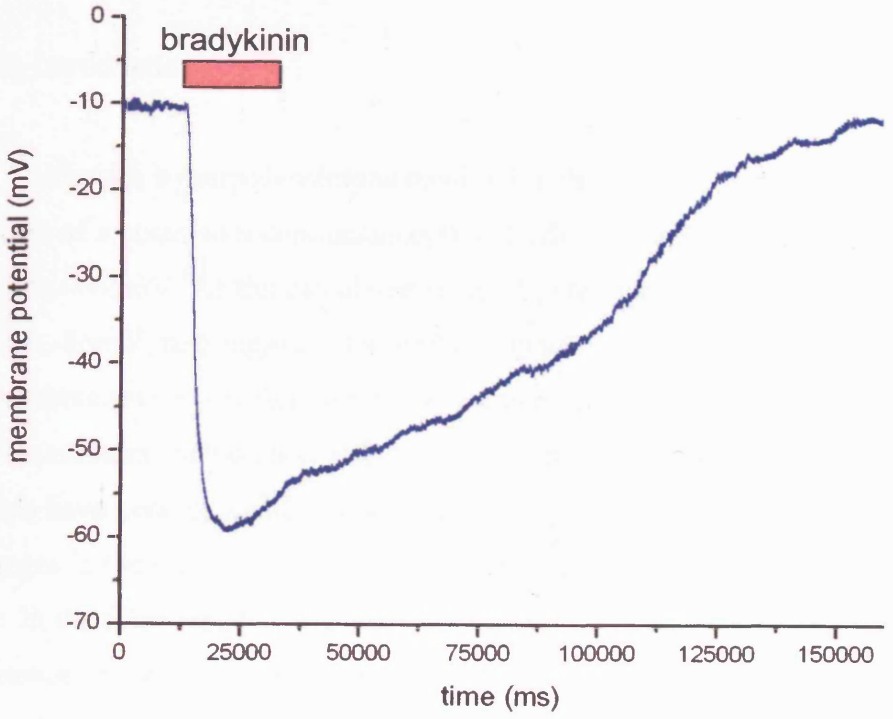


**Figure 5.6)** Hyperpolarisation evoked by transient application of 100nM bradykinin in a raft of pig right coronary artery endothelial cells.

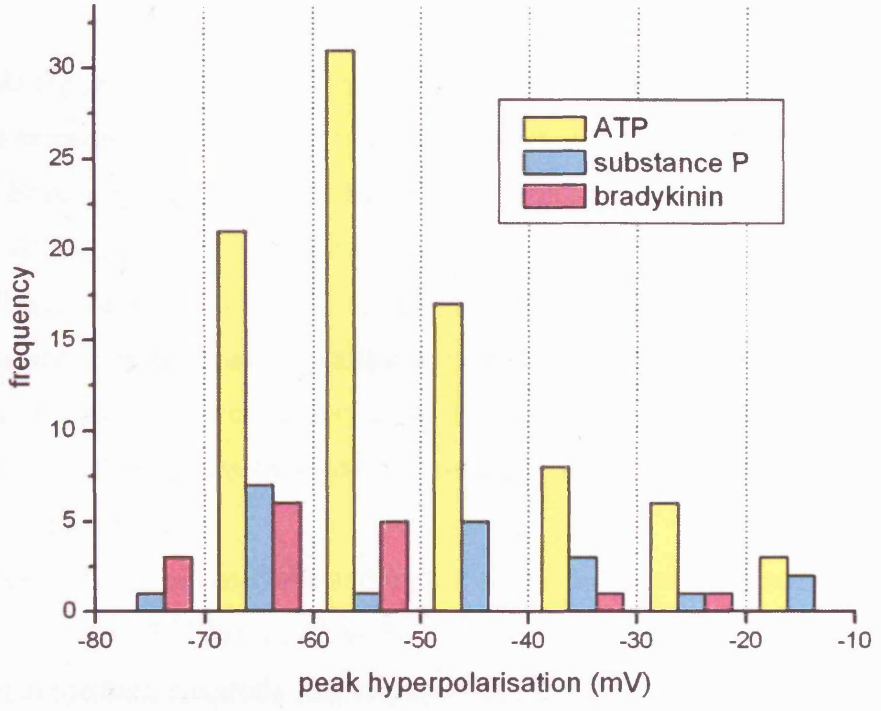


**Figure 5.7)** A histogram depicting the distribution of peak hyperpolarisations to supramaximal concentrations of ATP (1-10μM), substance P (1-10nM) and bradykinin (1-100nM).

## 5.2.4) Ion substitution studies

### 5.2.4.1) Introduction

Although hyperpolarisations recorded in these cells are consistent with activation of a potassium conductance(s), cells did not typically hyperpolarise to more than ~-65mV. As the calculated reversal potential for potassium ions in these studies is -86mV, this suggests that perhaps an additional conductance(s), with a more positive reversal potential than potassium, opposed hyperpolarisation to $E_K$. Likely candidates include non-selective cation channels, and chloride channels; both of which have been described in endothelial cells. To examine this further, the effects of changes in the ionic composition of the extracellular solution were explored.

In the following two studies, ATP-evoked hyperpolarisations were recorded in the absence of sodium or chloride ions. Throughout both studies, bath flow was increased to ~10ml/min to ensure rapid and efficient substitution of extracellular ions.

### 5.2.4.2) Sodium-free study

At the peak of a control hyperpolarisation, ATP was washed from the bath using an extracellular solution in which N-methyl D-glucamine was substituted for sodium. Following one minute of superfusion with sodium-free solution, ATP was re-applied. At the peak of the resulting hyperpolarisation, ATP was washed from the bath with standard (sodium-containing) extracellular solution. A third ATP response was evoked one minute later. To allow for the occurrence of the moderate degree of response rundown that was observed, 'average control' values were calculated as the mean of control responses recorded 'one minute pre'- and 'one minute post'-exposure to sodium-free solution.

Removal of extracellular sodium caused an apparent depolarisation in resting membrane potential (7.2±0.2mV, n=3), likely to reflect a change in the junction potential at the bath electrode (for example see *figure 5.8*). Hyperpolarisation amplitudes were not significantly different for sodium-free responses compared to

'average control' values (54.6±5.7mV: 57.0±3.8mV, respectively. Paired t-test, n=3; P>0.05).

5.2.4.3) Low-chloride study

Since chloride was the major anion in both the standard extracellular and intracellular (patch pipette) solutions, each required modification. Initially, potassium gluconate was entirely substituted for potassium chloride in a modified '30nM free-calcium' intracellular solution, however the resulting junction potential change placed recording signals beyond the range of the amplifier. To overcome this, the chloride concentration of the intracellular solution was raised to 5mM. For low-chloride extracellular solution, sodium isethionate was substituted for sodium chloride, leaving a chloride concentration of 7mM.

In the presence of standard (135mM chloride containing) extracellular solution, and assuming complete dialysis with low-chloride intracellular solution, $E_{Cl}$ is calculated as -84mV. This compares to 0mV when using the standard (132mM chloride containing) intracellular solution. Despite this difference, in the presence of standard extracellular solution, 10μM ATP hyperpolarised cells by 26.5 - 54.4mV (n=3), well within the range of responses recorded in the presence of standard intracellular solution (6.54 - 61.4mV, n=44). At the peak of hyperpolarisation to 10μM ATP in the presence of normal (chloride-containing) extracellular solution, ATP was washed from the bath with 7mM chloride-containing extracellular solution. Following one minute of superfusion with low chloride solution, ATP was re-applied. At the peak of the subsequent hyperpolarisation, ATP was washed from the bath with standard extracellular solution.

Lowering the extracellular chloride concentration caused an apparent depolarisation of the resting membrane potential (9.8±3.5mV, n=3), when compared with control (for example see *figure 5.9*). As with the sodium-free experiments, this is likely to be due to a change in junction potential. ATP evoked hyperpolarisations which were significantly larger in amplitude under low extracellular chloride conditions than control (55.1±5.7mV: 41.6±8.1mV, respectively. Paired one-tailed t-test, n=3; P=0.027).

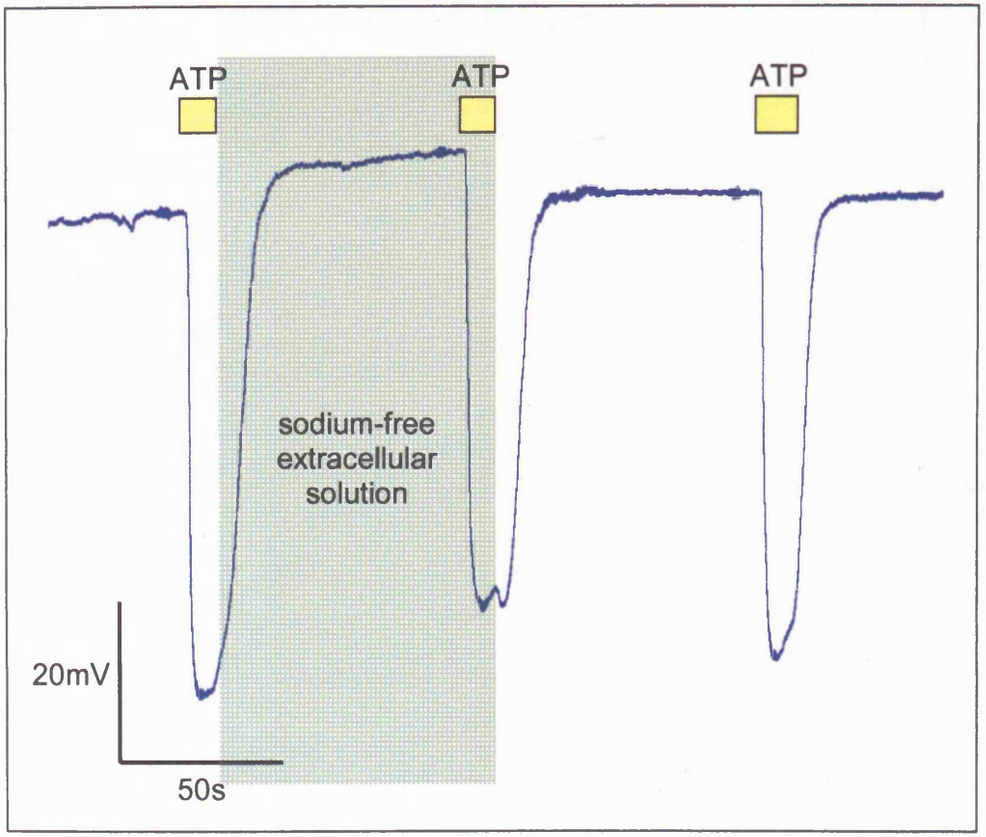


**Figure 5.8)** The effect of extracellular sodium substitution on hyperpolarisations evoked by transient exposure to 10μM ATP. Recording made in a raft of endothelial cells cultured from pig right coronary artery. Green shading indicates the period in which cells were exposed to extracellular solution wherein N-methyl D glucamine was substituted for sodium.

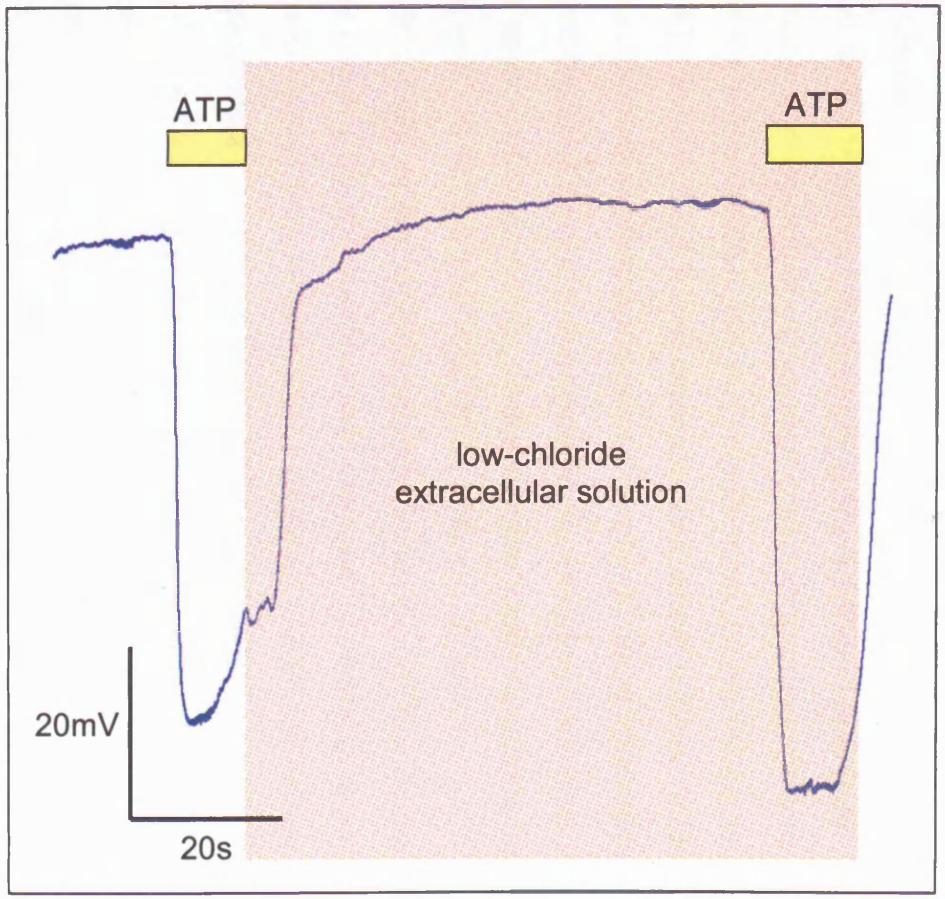


**Figure 5.9)** The effect of reduced extracellular chloride on hyperpolarisations evoked by transient exposure to 10μM ATP. Recording made in a raft of endothelial cells cultured from pig right coronary artery. Pink shading indicates the period in which cells were exposed to extracellular solution wherein sodium isethionate was substituted for sodium chloride. The recording was made using a patch electrode filled with an intracellular solution containing only 5mM chloride (most potassium chloride substituted with potassium gluconate).

## 5.2.5) Summary of current-clamp data

Typical of endothelial cells at rest and indicative of a high degree of electrical coupling (Nilius & Droogmans, 2001), large endothelial cell rafts had typical input resistances of <200MΩ; substantially lower than the GΩ values seen with small clusters of cells (see *section 5.3.2.2*). The mean resting membrane potential ($E_m$) was -5.9mV and, despite a small but significant difference following three days in culture, values were similar between cells cultured from right and left anterior descending coronary arteries (*table 5.1*). No significant difference was found between $E_m$s recorded from cells cultured for different lengths of time.

Although endothelial cell $E_m$ is reported to vary greatly between vascular beds (ranging from 0 to -80mV; Nilius & Droogmans (2001)), the mean value of -5.9mV obtained in the present study is low when compared with $E_m$s reported in published studies of isolated pig coronary artery endothelial cells (*table 7.1*). In the present study, altering neither culture conditions nor recording solutions influenced $E_m$s. The low $E_m$s recorded in this study are discussed further in *chapter seven.*

ATP and substance P both hyperpolarised cells to ~-50mV (*table 5.3*), and membrane potential oscillations frequently developed during longer exposure to these agonists. Input resistance decreased during the hyperpolarisation, consistent with the opening of $SK_{Ca}$ and $IK_{Ca}$ channels as previously reported in these cells (Frieden *et al.*, 1999; Bychkov *et al.*, 2002; Sollini *et al.*, 2002).

Bradykinin evoked larger hyperpolarisations than ATP or substance P (~-60mV) (*table 5.3*), and responses were sustained for several minutes after the agonist was washed from the bath. Unlike responses to ATP and substance P, no membrane potential oscillations followed the hyperpolarisation peak. In published studies of cultured pig coronary artery endothelial cells, it has been reported that bradykinin opens $IK_{Ca}$ and $BK_{Ca}$ but not $SK_{Ca}$ channels (Frieden *et al.*, 1999; Sollini *et al.*, 2002). This has, however been refuted in a study of freshly isolated endothelium which concluded that both substance P and bradykinin activated $SK_{Ca}$ and $IK_{Ca}$ but not $BK_{Ca}$ channels (Bychkov *et al.*, 2002).

Histamine also evoked hyperpolarisation of endothelial cell rafts, although cells rapidly desensitised to this agent. Carbachol, conversely, did not affect

endothelial cell membrane potential, consistent with a reported lack of $IP_3$-coupled muscarinic receptors in pig coronary endothelial cells (Ito *et al.*, 1979).

Ion substitution studies were carried out to determine why cells did not hyperpolarise to values closer to $E_K$. In the absence of extracellular sodium ions, amplitudes of ATP-evoked hyperpolarisations were comparable with controls, indicating that non-selective cation currents are unlikely to play a major role in these responses. Under conditions of reduced intracellular chloride, ATP-evoked hyperpolarisations were comparable with those occurring in the presence of standard ionic gradients. When *extracellular* chloride was also reduced, the amplitude of ATP-evoked hyperpolarisations became significantly larger. However, because of the junction potential changes which occurred in this study, the contribution of chloride ions to ATP-evoked hyperpolarisations cannot be readily quantified. Nevertheless, the larger hyperpolarisations seen in low chloride solutions suggest that chloride conductances may limit peak hyperpolarisation, in keeping with findings recently reported in a study of mouse aortic endothelial cells (Ahn *et al.*, 2004).

## 5.3) Voltage-clamp studies: ATP-evoked currents

### 5.3.1) Introduction

Single cells or clusters of 2-3 cells were used in all voltage-clamp experiments to ensure adequate voltage-clamping. For simplification, and in view of the apparent high degree of electrical coupling, the term 'cell' is applied to both single cells and clusters.

Unless otherwise stated, studies were performed using patch electrodes filled with the same intracellular solution used for current-clamp studies (30nM free-calcium). A holding potential of -50mV was used in all experiments, and currents were recorded continuously during agonist application. Voltage-pulses (+50mV, 200ms duration) were applied at a frequency of 0.5Hz, and voltage ramps (-120 to +50mV over 200ms) performed prior to and at the peak of all evoked currents.

Capacitance compensation was applied in all recordings, however this was often imperfect or incomplete in clusters of three cells. For recordings in which a good balance was achieved, an approximate value for cell capacitance was noted.

It was found that series-resistance constantly fluctuated throughout recordings. This resulted in transients, of continuously varying size, appearing at the start and end of each voltage pulse and ramp. The brevity of these artefacts was such that an impact on any measurement is unlikely. For clarity and to enable distinction of pulses at a low timebase gain, artefacts have been removed from all presented traces (see *appendix iv* for examples of unmodified traces and details of the procedure).

Data reported in this section were recorded entirely from right coronary artery (R) cells, since culture of these was more successful than of cells from the left anterior descending coronary artery (LAD) (see *section 3.1.2* for comment). In preliminary voltage-clamp experiments wherein cells from LAD were studied, no difference in electrophysiological properties was noted when compared with R cells (data not shown).

ATP was chosen to evoke all responses in these studies, since the sensitivity of cells to substance P or bradykinin was more variable (data not shown). Unless

otherwise stated, ATP was applied at 10μM and was washed from the bath immediately following the response peak.

Except for current-voltage relationships, all measurements were made at the holding potential (-50mV).

## 5.3.2) ATP-evoked currents

### 5.3.2.1) Selection of data

Mean data described in *sections 5.3.2.2* and *5.3.2.3* are from a randomly selected sample of recordings. To enable fair comparison of data relating to length of time in culture, ten culture batches were chosen at random. For each batch, up to five studied cells were randomly selected from each day of recording (2, 3 and 4 days following culture). Data relates to the first ATP-evoked response recorded from a selected cell.

Cells in which ATP evoked an 'early-inward' current component (see *section 5.3.2.4*), or no current at all, were excluded from selection.

### 5.3.2.2) Control recordings: characteristics of resting cells

As expected, the measured cell capacitance significantly increased approximately proportionally to the number of cells in the cluster studied. A significant increase was also recorded between cells cultured for two and three days (*table 5.4*).

On average, cells passed a small inward current at the holding potential (*table 5.5A*). Estimates of conductance were made by determining the gradient of a linear fit applied to an approximately linear portion of the current-voltage relationship (CVR) (-70 to -40mV). The fit was also used to estimate reversal potentials for resting cell currents. To control for cluster size, currents are expressed as a function of capacitance.

Disregarding cluster size, cells had a median input resistance of ~5GΩ, irrespective of time in culture (range: 0.4-140 GΩ, n=127). Because of the inability of the amplifier to accurately measure very high input resistances, the data is better described by the median value rather than the mean.

Resting cell CVRs were varied and could be described as one of four basic 'shapes'. Most CVRs exhibited a voltage-activated component at positive potentials, with approximately half of these also displaying an inwardly-rectifying component (for examples see *figures 5.10A&B*). A smaller proportion of CVRs showed inward-rectification with no voltage-activated component (*figure 5.10C*), or were approximately linear (*figure 5.10D*).

5.3.2.3) ATP-evoked outward currents

At the holding potential, 10μM ATP evoked an outward whole-cell current in the majority of cells to which it was applied (for example see *figure 5.11*). The amplitude of ATP-activated currents was proportional to cluster size, and inversely related to the length of time cells had been in culture (*table 5.5B*).

Unlike the heterogeneity between CVRs for resting cells, those for ATP-activated components were all of a similar shape to the example shown in *figure 5.12*. The lack of outward rectification between -50 and +50mV suggests that ATP does not activate voltage-dependent channels over this range of potentials.

Voltage-ramps applied prior to- and at the peak of- responses to ATP, enabled estimates to be made of conductance and reversal potential for the ATP-activated component (*table 5.5B*). Although reversal at ~-70mV is consistent with the activation of a potassium conductance(s), this is short of the $E_K$ calculated for these studies (-86mV). The reversal potentials did not greatly alter with culture age suggesting that age-related reduction in ATP-evoked outward currents are due to a reduction in the number of open potassium channels, rather than up-regulation of an opposing current.

On occasions, ATP-evoked outward current occurred in two or three 'steps' (for example see *figure 5.13*). Since this was seen only in clusters of 2-3 rather than single cells, this may have been due to a delay in response between compartments (cells) of the cluster.

| time in culture (days) | cluster size | | |
|---|---|---|---|
| | single cell | 2 | 3 |
| 2 | 28.3±1.2pF (21) | 45.9±2.1pF (20) | 68±2.9pF (3) |
| 3 | 37.1±3.4pF (10) | 53.7±1.7pF (33) | 89.3±4.5pF (4) |
| 4 | - | 61.2±3.3pF (23) | 83.6±4.5pF (10) |

**Table 5.4)** Capacitance measurements made from clusters of different sizes and ages. Data is mean ± standard error (sample size). Using an unpaired two-tailed Student's t-test, statistical comparison was made between time in culture (controlling for cluster size), and between different length of time in culture (controlling for artery of origin). *All* differences were significant ($P<0.05$), *except* those occurring between days 3 and 4.

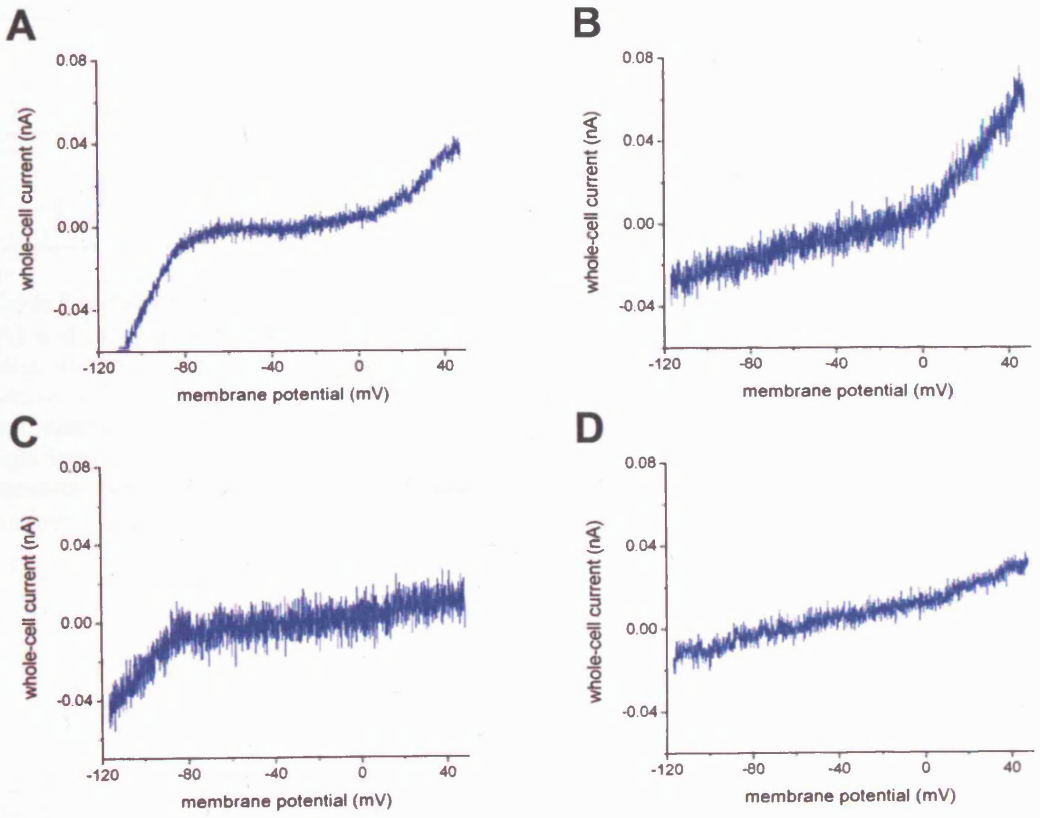


**Figure 5.10)** Typical examples of whole-cell CVRs recorded from pig right coronary artery endothelial cells. Currents were obtained by applying a voltage ramp from -120 to +50mV.

**A** *resting current*

| time in culture (days) | outward current at -50mV (pA/pF) | conductance* (pS/pF) | reversal potential* (mV) |
|---|---|---|---|
| 2 | -0.24±0.09 (45) | 10.6±1.9 (32) | -22.2±4.0 (32)† |
| 3 | -0.27±0.07 (43) | 8.0±1.9 (27) | -25.1±6.4 (27) |
| 4 | -0.25±0.06 (27) | 7.0±0.2 (20) | -12.7±2.4 (20)† |

**B** *ATP-activated current*

| time in culture (days) | outward current at -50mV (pA/pF) | conductance* (pS/pF) | reversal potential* (mV) |
|---|---|---|---|
| 2 | 6.19±0.62 (46) | 243.0±27.1 (40) | -72.9±0.8 (35)‡ |
| 3 | 2.27±0.26 (44) | 83.8±12.4 (37) | -72.6±1.1 (33) |
| 4 | 0.85±0.13 (27) | 30.7±6.4 (28) | -69.2±1.5 (19)‡ |

**Table 5.5)** Outward holding current, conductance and reversal potential of whole-cell resting currents (A), and currents activated by 10μM ATP (B), recorded from pig right coronary artery endothelial cells. Holding potential: -50mV. *data from a linear fit of an approximately linear portion of the CVR (-40 to -70mV). Data is mean ± standard error (sample size). Using an unpaired two-tailed Student's t-test, statistical comparison of each parameter was made according to time in culture. For table A, significance was only found between groups marked † (P=0.049). For table B, *all* differences in outward current and conductance were significant (P<0.05), however difference in reversal potential was *only* significant (P=0.40) between groups marked ‡.

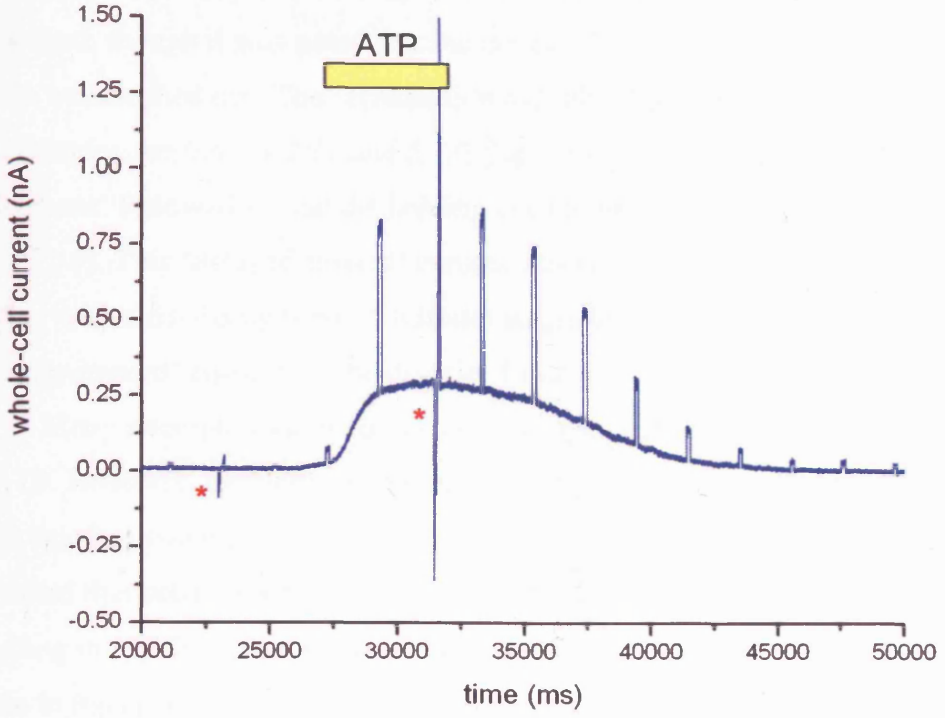


**Figure 5.11)** An outward current evoked by 10μM ATP recorded from a pig right coronary artery endothelial cell. Holding potential: -50mV, pulse amplitudes: +50mV. Asterisks denote application of voltage-ramps (-120 to +50mV).

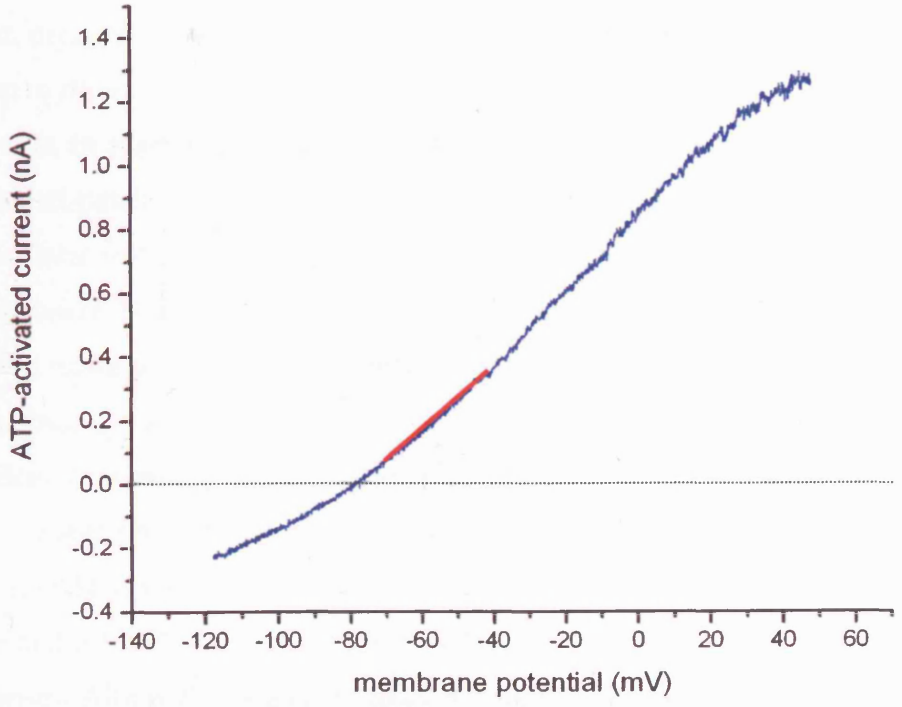


**Figure 5.12)** The current-voltage relationship of a current activated by 10μM ATP. Data are taken from the recording depicted in *figure 5.11* and are calculated as the difference between whole-cell CVRs at rest and in the presence of ATP. The red line is a representation of a linear fit applied to the recording at potentials between -70 and -40mV.

In all experiments ATP was removed from the bath soon after the response had peaked, though it was noted that the currents began to decrease before the agonist was washed out. The currents in most cells then returned to resting levels (for examples see *figures 5.11 and 5.13*). However, in some cells a small 'undershoot' followed so that the holding current became inward (for example see *figure 5.14*). This 'delayed-inward' current was not explored, but its late onset together with slow decay (up to 1 minute) suggests that it is unlikely to be related to the 'early-inward' currents, to be described in *section 5.3.2.4*.

Many attempts were made to study the concentration-response relationship for ATP. However, problems with longevity of recordings and response-rundown meant that this could not be satisfactorily achieved. As with current-clamp studies, it was noted that cells varied substantially in sensitivity to ATP. An example of a recording in which different concentrations of ATP were successfully applied is shown in *figure 5.15*.

Rundown of ATP-evoked responses was a particular concern during voltage-clamp studies. Some cells produced outward currents of consistent amplitude when ATP was repeatedly applied at intervals of several minutes. However, in other cells, the responses fell with each repeat agonist exposure, or increased with the first repeat, decreasing thereafter (*figure 5.16*). An example of progressive rundown is shown in *figure 5.17*.

In an attempt to prevent response rundown, the possibility of using the perforated-patch technique was explored. The inclusion of amphotericin-B in the intracellular solution made cell-electrode sealing much more difficult. Varying amphotericin-B concentration or filling patch electrodes tips with amphotericin-free solution made no appreciable difference. When seals were successful, cells failed to permeabilise, and the seal was usually lost within ten minutes. These attempts were abandoned following several weeks of perseverance.

Some preliminary studies were performed with the solutions used by Sollini *et al.* (2003) in voltage-clamp experiments. Since the 'Sollini' intracellular solution contained ATP, it was thought possible that this might have prevented rundown of responses. Although few experiments were attempted, rundown in response to repeated application of ATP was apparent in several of the studied cells. Cell capacitance values were not recorded in these studies and so it is not possible to make quantitative comparisons of current amplitudes. However, neither control nor

ATP-evoked whole-cell currents were noticeably different to those recorded when using the standard solutions (data not shown).

Several cultures were prepared and maintained in media similar to that used by Sollini *et al.* (2002); only the antibiotic was different. Cells cultured in 'Sollini' media responded to ATP in a manner indistinguishable from cells cultured in the standard culture medium. Response amplitudes and age-related down-regulation of currents were not noticeably different to those recorded from cells cultured under standard conditions (data not shown). Response-rundown was similarly observed.

5.3.2.4) ATP-evoked 'early-inward' currents

In the majority of cells tested, ATP evoked an uninterrupted outward holding current in response to ATP. However, in approximately 12% of cells, ATP activated an additional 'early'-inward current component at this potential. Incidences of early-inward currents were usually clustered, occurring in some culture batches, but not in others. Approximately three times the number of early-inward currents were observed in cells cultured for three days when compared with cells cultured for two days.

In most of the cells showing an early-inward current component, ATP-activated inward and outward components were 'entangled', but were noticeable either because the inward components had a more rapid onset (for example see *figure 5.18*), or because increases in pulse amplitude were disproportionate to increases in holding current (for example see *figure 5.19A*).

In some cells, ATP evoked only a net-inward holding current (for example see *figure 5.19B*). Voltage ramps conducted prior to at the peak of net-inward currents allowed CVRs to be determined in some cells (*figure 5.20*). Reversal potentials for net inward currents ranged between -45 and -8mV ($n=6$). The variation is likely to be due to differences in the contribution of potassium conductances.

Data from cells which appeared to contain an early-inward current component, such as those in *figures 5.18 and 5.19*, were excluded from analysis of potassium conductance changes.

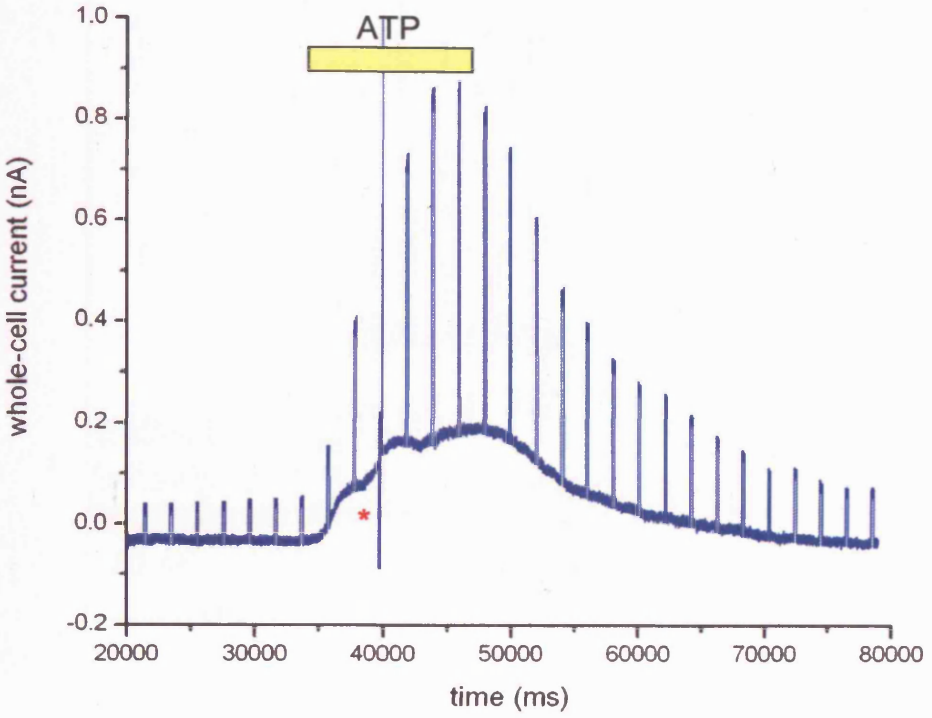


**Figure 5.13)** An outward current recorded from a cluster of pig right coronary artery endothelial cells, evoked by 10μM ATP. Holding potential: -50mV, pulse amplitudes: +50mV. Asterisk denotes application of a voltage-ramp (-120 to +50mV), pre-ATP ramp not shown.

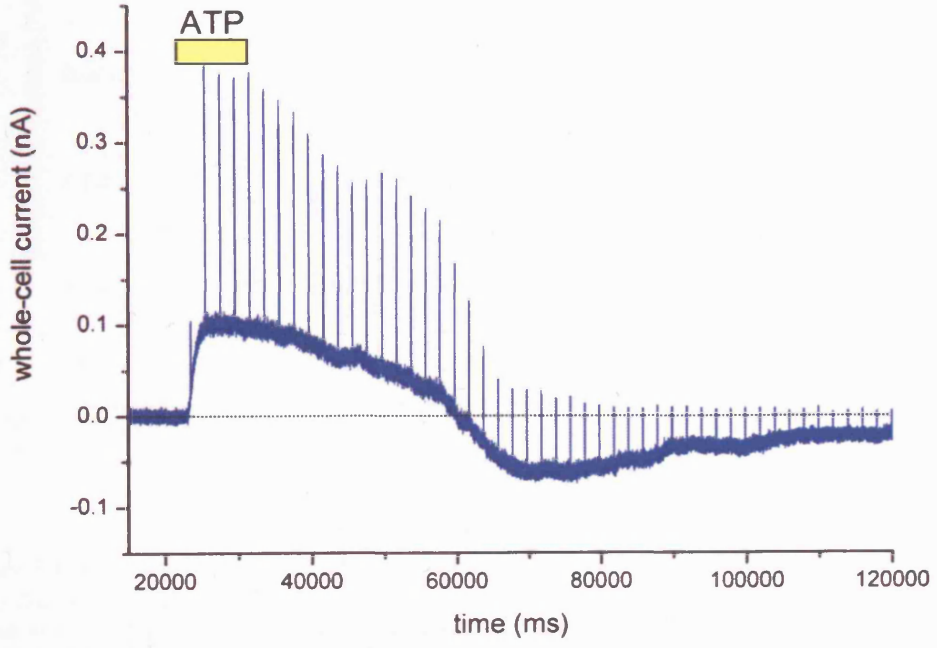


**Figure 5.14)** An outward current with following 'undershoot' (delayed-inward current) recorded from a pig right coronary artery endothelial cell, evoked by 10μM ATP. Holding potential: -50mV, pulse amplitudes: +50mV.

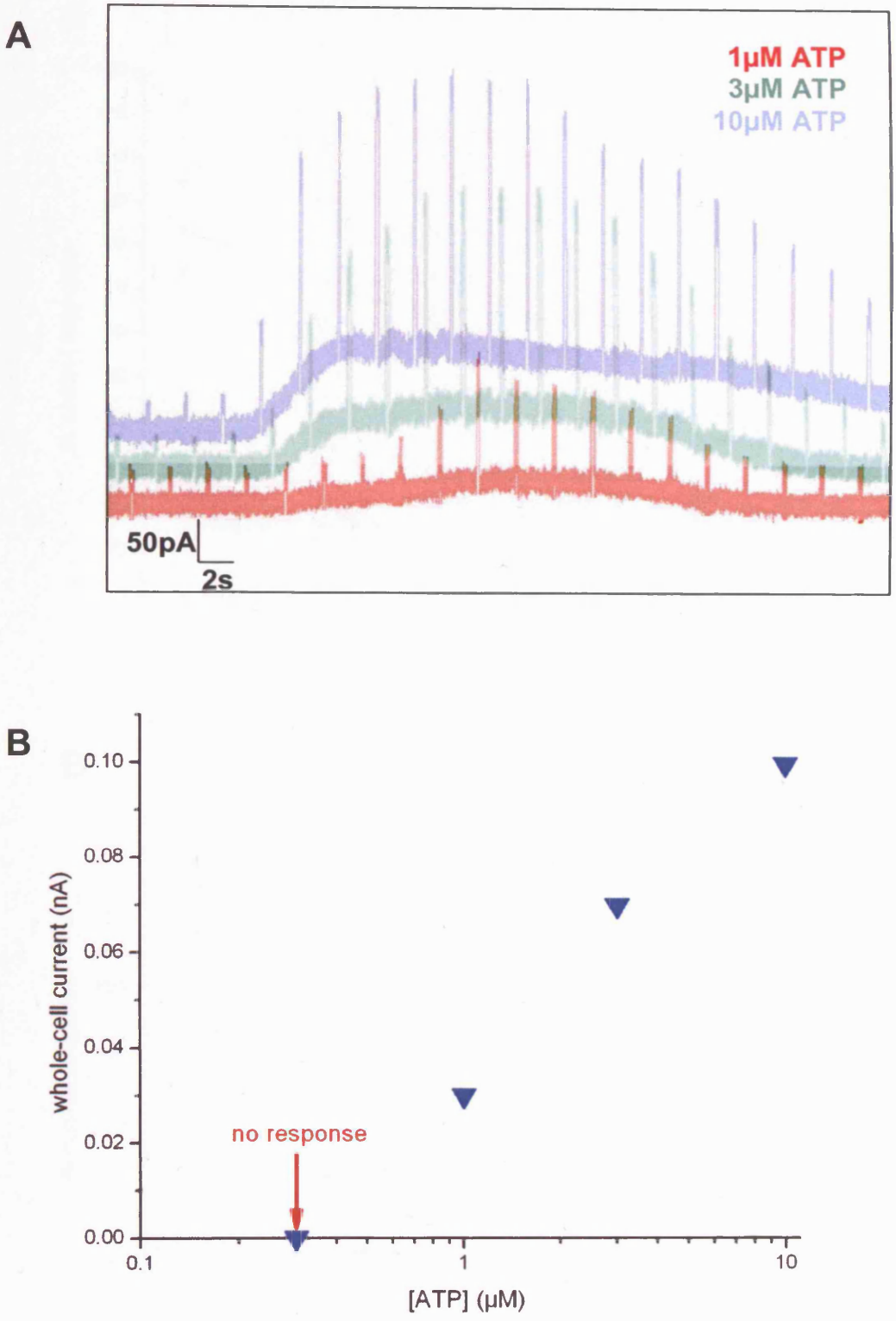


**Figure 5.15)** Current recordings and a concentration-response plot for ATP in a pig right coronary artery endothelial cell. Panel *A* contains superimposed current traces from the same recording. Traces have been staggered vertically and horizontally to enable distinction of pulses. Holding potential: -50mV, pulse amplitudes: +50mV. A plot of the measured ATP responses from the same recording is shown in panel *B*.

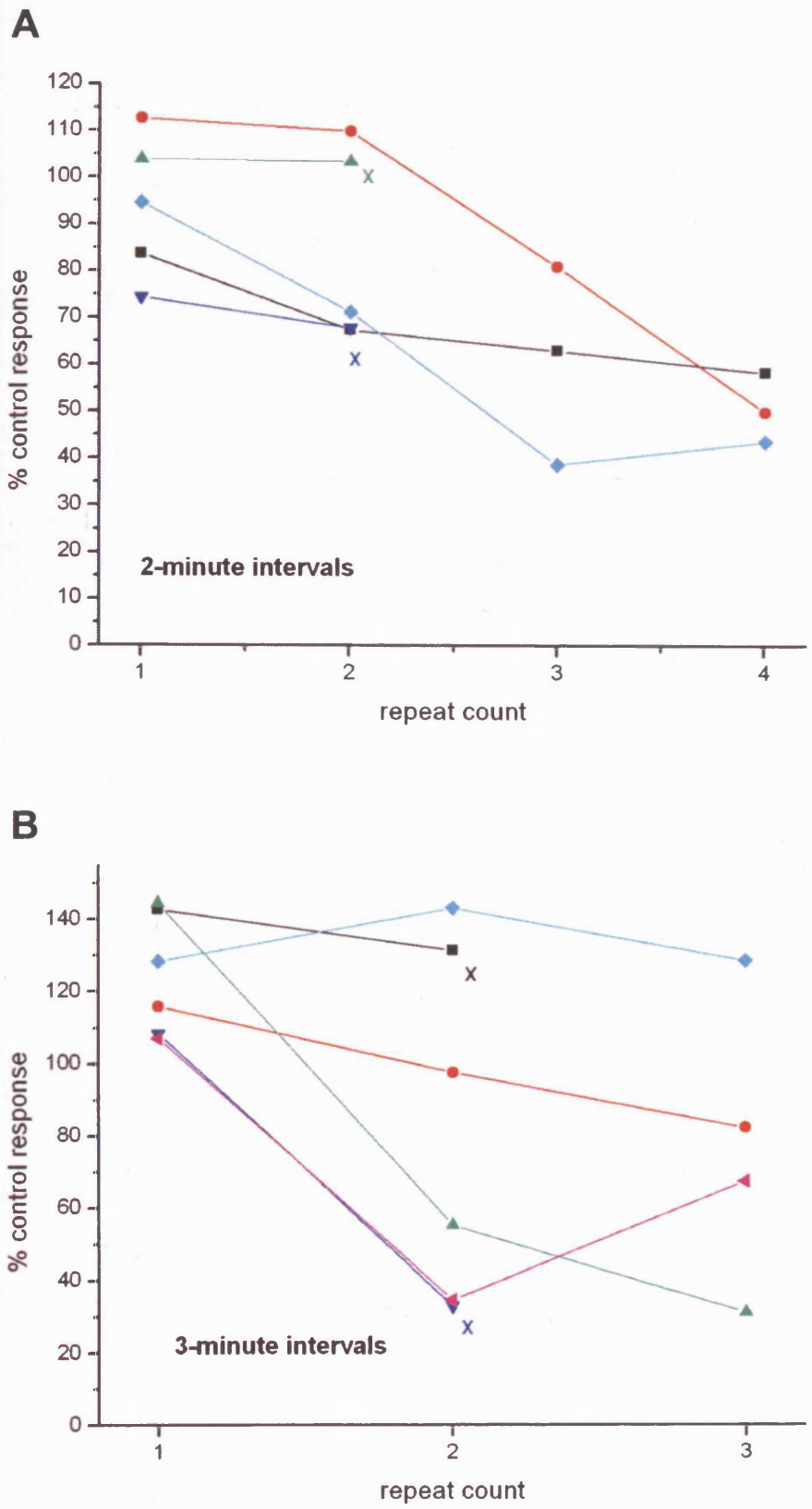


**Figure 5.16)** Effect of repeat application of 10μM ATP on pig right coronary endothelial cells. Applications were repeated at intervals of 2 (A) or 3 minutes (B), and in each case ATP was removed once currents had peaked. Each symbol represents a different cell. Data are expressed as % of an initial ATP-activated current, recorded at the holding potential (-50mV). Crosses indicate loss of recording.

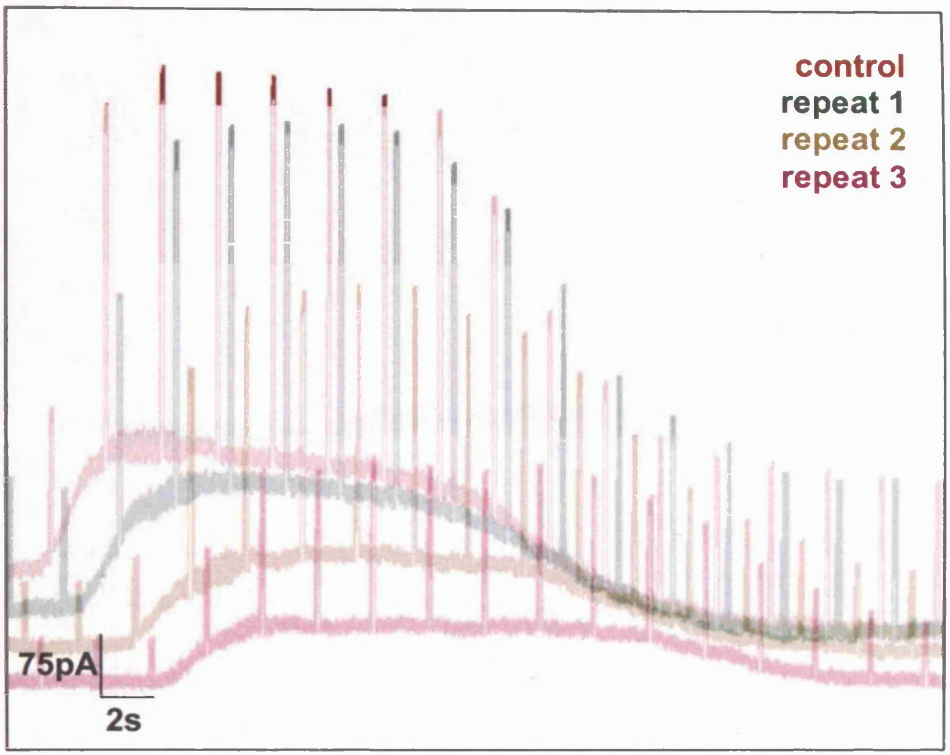


**Figure 5.17)** An example of decreasing amplitude of outward currents with repeated ATP application; recording from a pig right coronary artery endothelial cell. 10μM ATP was repeatedly applied at intervals of two minutes. Holding potential: -50mV, pulse amplitudes: +50mV. Traces have been staggered vertically and horizontally to enable distinction of pulses.

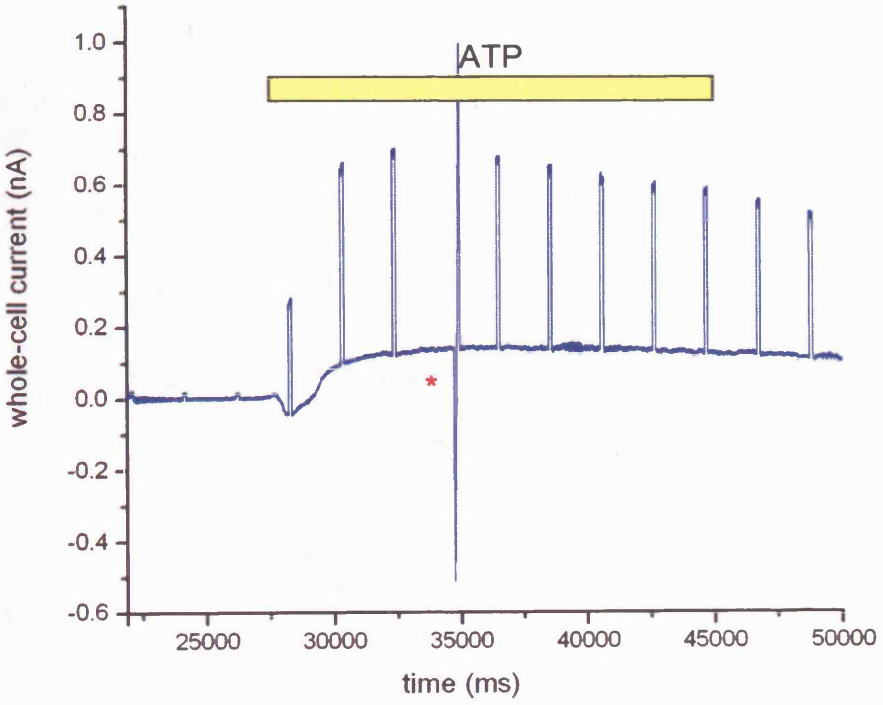


**Figure 5.18)** An example of a recording in which 10μM ATP evoked both early-inward and outward currents in pig right coronary artery endothelial cells. Holding potential: -50mV, pulse amplitudes: +50mV. Asterisk denotes application of a voltage-ramp (-120 to +50mV), pre-ATP ramp not shown.

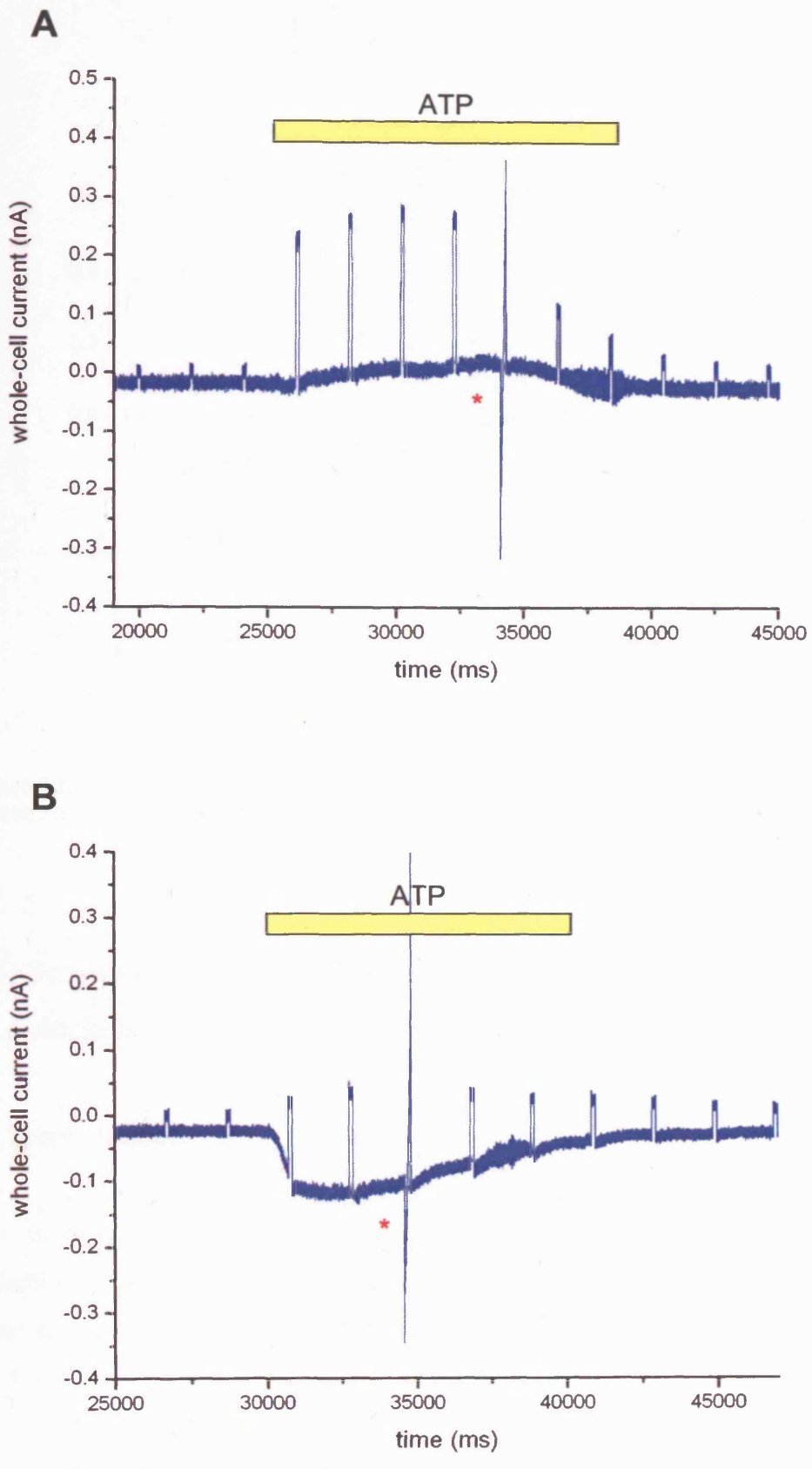


**Figure 5.19)** Further examples of recordings in which 10μM ATP evoked both early-inward and outward (A), or early-inward (B) currents in pig right coronary artery endothelial cells. Holding potential: -50mV, pulse amplitudes: +50mV. Asterisks denote application of a voltage-ramp (-120 to +50mV), pre-ATP ramps not shown.

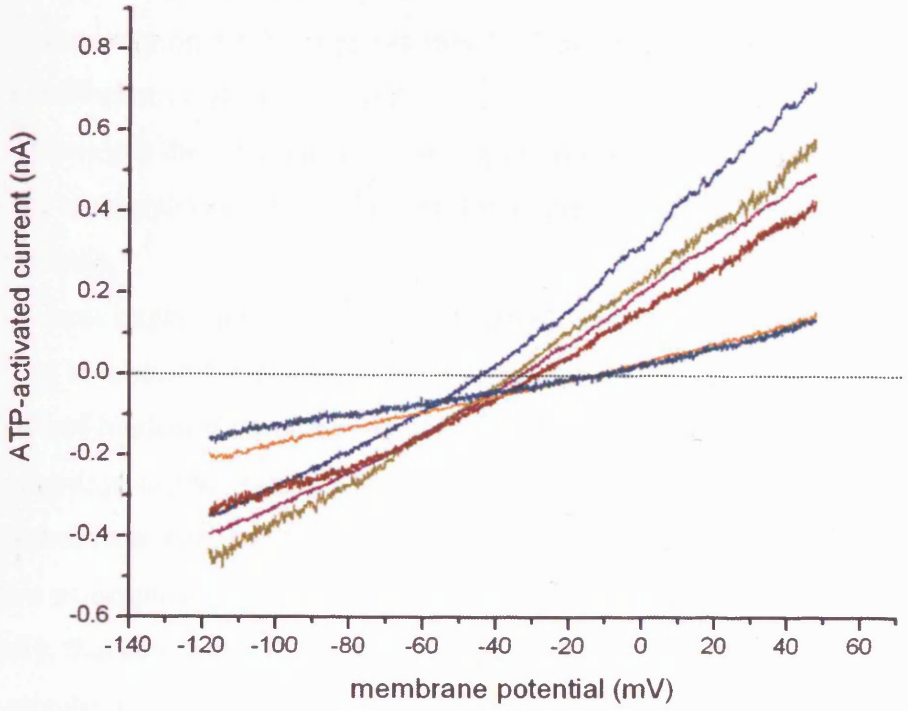


**Figure 5.20)** Current-voltage plots of 'net early-inward' currents activated by 10μM ATP. Data are calculated as the difference between whole-cell CVRs at rest and in the presence of ATP.

## 5.3.3) Sensitivity of ATP-evoked outward currents to $K_{Ca}$ channel blockers

### 5.3.3.1) Introduction

In the next part of the study, $K_{Ca}$ channel blockers were used to investigate the identity of potassium channels underlying ATP-evoked outward currents. A comparison of the $K_{Ca}$ channel subtype selectivity for each of these agents is given in *table 5.6.*

In each experiment, a control response to ATP was established, and a blocker then applied continuously for three minutes (see *figure 5.21*). ATP was re-applied in the presence of the blocker, after which cells were superfused with blocker-free solution for a further three minutes. ATP was then applied for a third time to

determine recovery from block (for example traces see *figure 5.22*). The rate of onset and offset of the agents used, as judged by their effects on calcium-dialysis activated currents (see section 5.5.3), suggests that three minutes is sufficient time for block to reach equilibrium, and for wash-out.

Owing to the difficulty in maintaining recordings, a large proportion were lost prior to completion of the block protocol. Incomplete recordings were excluded from analysis.

These experiments were complicated by response rundown, which, as discussed in *section 5.3.2.3*, was highly variable between recordings. To reduce the influence of rundown, current evoked in the presence of blocker has been expressed as a percentage of the 'average control'. Average control is defined as the mean of the 'control response' and the 'recovery response'. For data to be measured in this way two assumptions are made: firstly, that rundown occurred in a linear nature; and secondly, that blockers had completely dissociated from their binding sites following three minutes of wash-out. Neither premise will hold exactly. However, on account of the variability in run-down and difficulty of the experimental procedure, a more rigorous method of measurement was not feasible.

Data from recordings in which rundown between 'control' and 'recovery' responses was excessive (>75%), or where responses 'ran-up' by more than 5% across the same interval, were excluded from analysis.

A second 'recovery' response recorded three minutes after the first, was almost always smaller in amplitude, so was not used in analysis.

Owing to response rundown and the brevity of recordings, it was not possible to investigate more than one blocker concentration in a single recording.

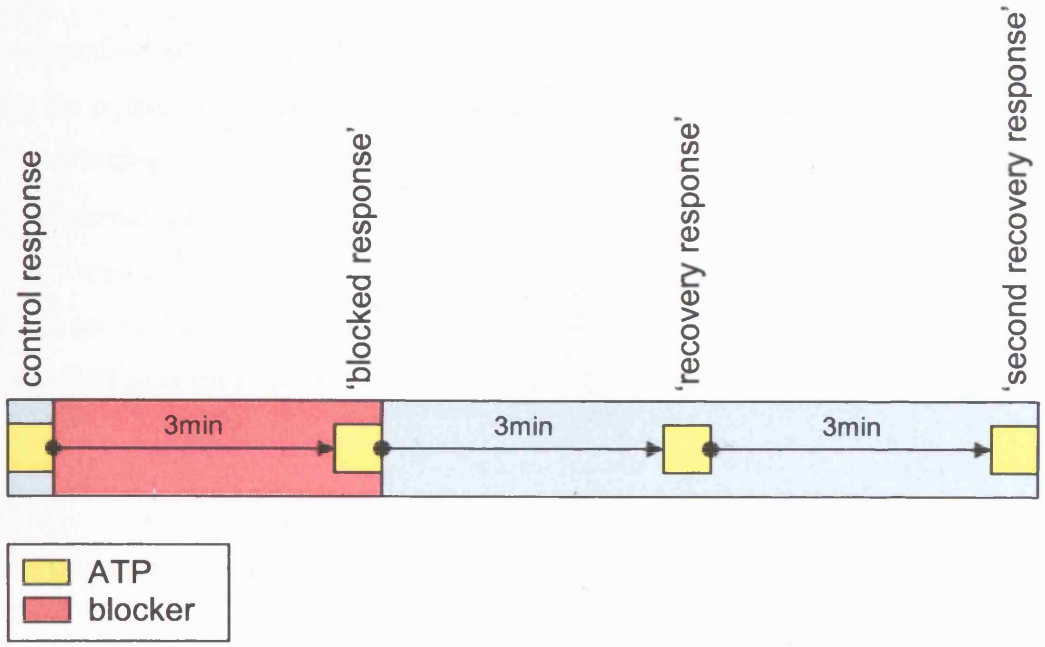


**Figure 5.21)** Protocol for determining the effects of $K_{Ca}$ channel blockers on 10μM ATP-evoked outward currents.

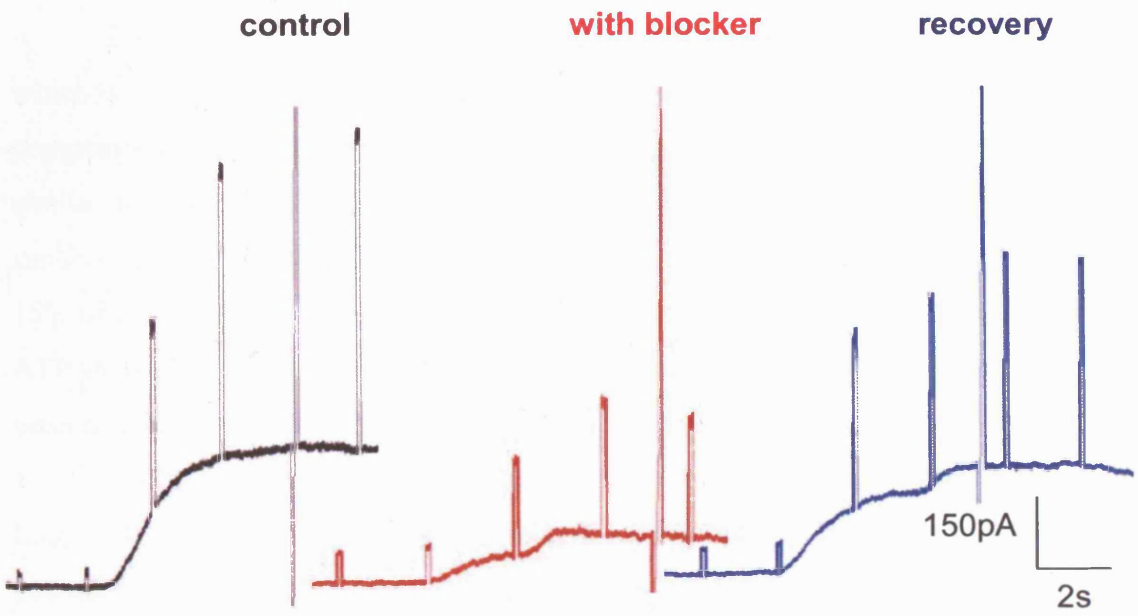


**Figure 5.22)** ATP-responses from the same recording; evoked prior to, during and following washout of a channel blocking agent. In this particular example, the blocker was 100nM UCL 1848.

5.3.3.2) UCL 1848

The contribution of $SK_{Ca}$ channels to ATP-evoked outward currents was determined using the potent and selective non-peptide blocker, UCL 1848 (*table 5.6*).

Plotting UCL 1848 concentration on a log scale against % block of the ATP-evoked current gives a sigmoidal relationship (*figure 5.23*). Least squares curve fitting[10] was applied to the data using the Hill equation (see below), although, for the reasons set out below, the low end of the curve was not constrained to zero. The resulting fit gave an $IC_{50}$ of 1.18±0.03nM and a Hill coefficient of 1.43±0.05.

Hill equation: $$\%\ \text{inhibition} = 100 \times \frac{[I]^n}{[I]^n + IC_{50}{}^n}$$

[ I ]= concentration of blocker

n= Hill coefficient

Low concentrations of UCL 1848 seemed to produce measurable inhibition, which is very possibly due to overestimation of block owing to inadequate compensation for response rundown. Consistent with this being a systematic error, a similar anomaly was noted when studying low concentrations of clotrimazole (see *section 5.3.3.3*). Considering both sets of data, this error accounts for approximately 15% of the ATP-evoked current. Taking this into account, the apparent block of the ATP-evoked current by supramaximal concentrations of UCL 1848 (~70%), has been re-calculated as 65% (calculation: 70-15 expressed as a percentage of 100-15).

CVRs for 10nM UCL 1848-sensitive currents are shown in *figure 5.24*. Linear fits applied to these traces between -70 and -30mV give a mean reversal potential of -74.0±1.6mV (n=7).

[10] Curve fitted using Origin v.7 (OriginLab) software

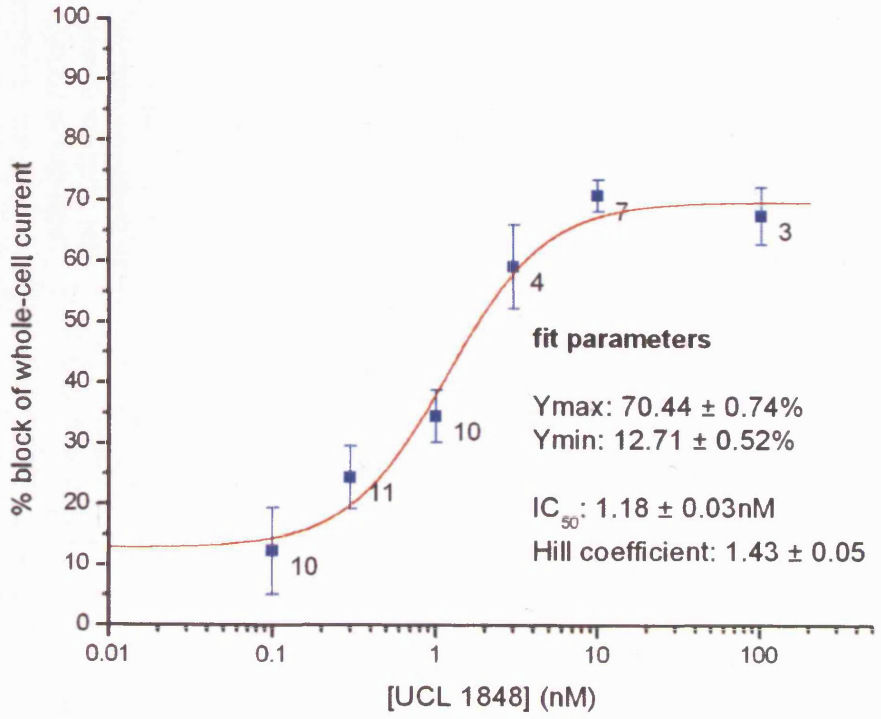


**Figure 5.23)** Concentration-inhibition relationship for UCL 1848 sensitivity of outward currents evoked from pig right coronary artery endothelial cells by 10μM ATP. Data are calculated as % block of 'average control' current, recorded at -50mV. Data are expressed as means, bars represent standard error and labels indicate sample size.

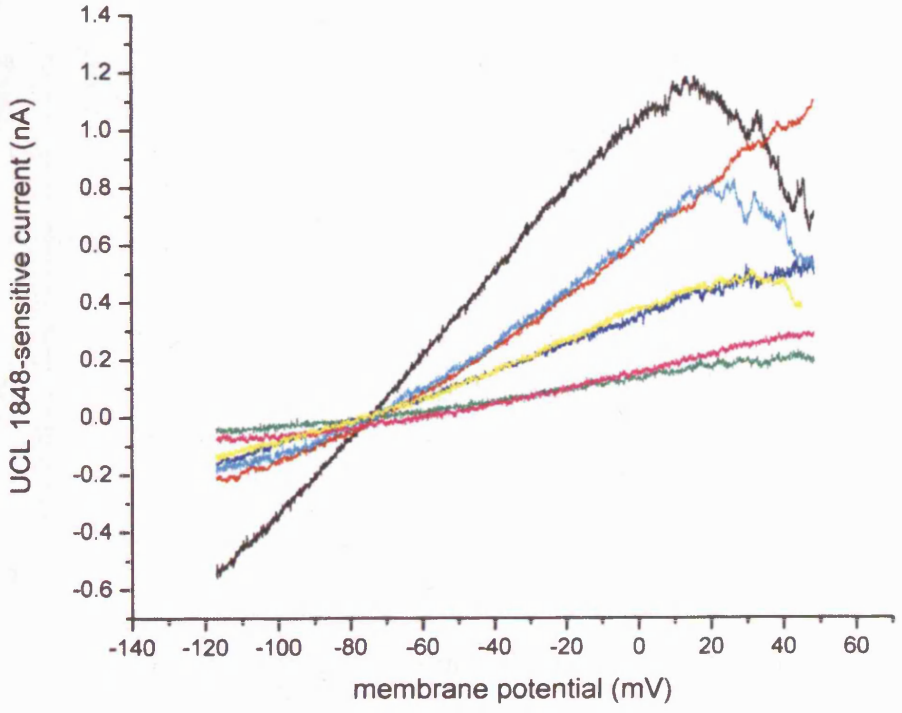


**Figure 5.24)** Current-voltage plots of 10nM UCL 1848 sensitive currents (evoked by 10μM ATP), recorded from pig right coronary artery endothelial cells.

| | SK1 | SK2 | SK3 | IK (SK4) | BK (Slo)(Slo1) |
|---|---|---|---|---|---|
| apamin | **7.7nM** (hSK1) (Shah & Haylett, 2000) | **0.08nM** (rSK2) (Strobaek *et al.*, 2000) | **1.4nM** (rSK3) (Hosseini *et al.*, 2001) | *ineffective at 100nM* (hSK4) (Joiner *et al.*, 1997) | *ineffective at 100nM* (rat SCG neurones) (unpublished obs. by DCH Benton) |
| charybdotoxin | *ineffective at 100nM* (hSK1) (Strobaek *et al.*, 2000) | *ineffective at 100nM* (rSK2) (Strobaek *et al.*, 2000) | *ineffective at 100nM* (unpublished obs. by DCH Benton) | **2.5nM** (hIK1) (Ishii *et al.*, 1997b) | **2.9nM** (bovine aortic SM) (Kaczorowski *et al.*, 1996) |
| clotrimazole | not determined | 21μM (hSK2) (Wulff *et al.*, 2000) | *Ineffective at 100nM*[1] 28μM[2] (hSK3) 1:(Carignani *et al.*, 2002) 2:(Wulff *et al.*, 2000) | **24.8nM[1] / 70nM[2]** (hIK1) 1:(Ishii *et al.*, 1997b) 2:(Wulff *et al.*, 2000) | 24μM (hSlo) (Wulff *et al.*, 2000) |
| iberiotoxin | not determined | not determined | *ineffective at 100nM* (rSK3) (Kohler *et al.*, 1996) | >1μM (hIK1)[1] 800nM (rat C6 cells)[2] 1:(Logsdon *et al.*, 1997) 2:(de Allie *et al.*, 1996) | **1.7nM** (bovine aortic SM) (Kaczorowski *et al.*, 1996) |
| UCL 1848 | **1.1nM** (hSK1) (Shah & Haylett, 2000) | **0.1nM** (rSK2) (Hosseini *et al.*, 2001) | **2.1nM** (rSK3) (Hosseini *et al.*, 2001) | not determined† | *ineffective at 100nM* (rat SCG neurones) (unpublished obs. by DCH Benton) |

**Table 5.6)** Relative sensitivities of different the $K_{Ca}$ channel subtypes to five different blocking agents. Values given are $IC_{50}$s from studies of cloned channel proteins expressed in mammalian cell lines, or from studies of native channels of superior cervical ganglion (SCG) neurones, or smooth muscle (SM). h and r, as in hSK1 or rSK2, denote the human and rat orthologues of the relevant channel proteins, respectively. 'inh.' denotes inhibition, 'obs.' denotes observations. Values highlighted in green are most relevant to these studies. †Although $IK_{Ca}$ channel sensitivity to UCL 1848 has not been determined, UCL 1684, a sister compound with near-identical pharmacology, failed to block $IK_{Ca}$ channel -mediated potassium efflux in rabbit erythrocytes when applied at 100nM (Malik-Hall *et al.*, 2000).

5.3.3.3) Clotrimazole

In the next experiments, clotrimazole was applied in order to evaluate the contribution of $IK_{Ca}$ channels to ATP-evoked currents (see *table 5.6*). Concentrations ranging from 10nM to 10μM were tested. The expected inhibition of $IK_{Ca}$ channels at these concentrations is estimated to be 16 and 99% respectively (based on an $IC_{50}$ of 50nM and a Hill coefficient of 1).

At low concentrations (10 to 30nM), clotrimazole appeared to block a similar minimum proportion of the whole-cell current as had been observed with low concentrations of UCL 1848 (see *figure 5.25*). Assuming that the same 15% systematic error applied, this suggested that little or no block occurred at these concentrations. On the same basis, 100nM and 1μM clotrimazole blocked ATP-evoked currents by ~20% and ~50%, respectively.

At 10μM, clotrimazole blocked ATP-evoked currents by ~95%, abolishing the response in three of the five cells to which it was applied. On account of ATP-evoked currents being partly mediated through $SK_{Ca}$ channel activity, this high degree of block was surprising as $SK_{Ca}$ channels are frequently reported as being insensitive to this concentration of clotrimazole (Carignani *et al.*, 2002). Even taking into account $IC_{50}$s from studies which show higher sensitivity (see *table 5.6*), 10μM clotrimazole would only be expected to block 33% of the $SK_{Ca}$ channel component (based on an $IC_{50}$ of 20μM and a Hill coefficient of 1).

As clotrimazole appears to block both $SK_{Ca}$ and $IK_{Ca}$ channels, block of each channel expected to have a distinct $IC_{50}$, the concentration-inhibition relationship would be likely to comprise two components. Consistent with this, fitting a single sigmoidal curve to the data gave a low Hill coefficient of 0.8, and an $IC_{50}$ much higher than expected for clotrimazole block of $IK_{Ca}$ channels (~800nM) (fit not shown). The data were not however sufficient to merit an attempt at a two-component fit.

CVRs for 1μM clotrimazole-sensitive currents are shown in *figure 5.26*. Linear fits applied to these traces between -70 and -30mV give a mean reversal potential of 72.3±1.6mV (n=6).

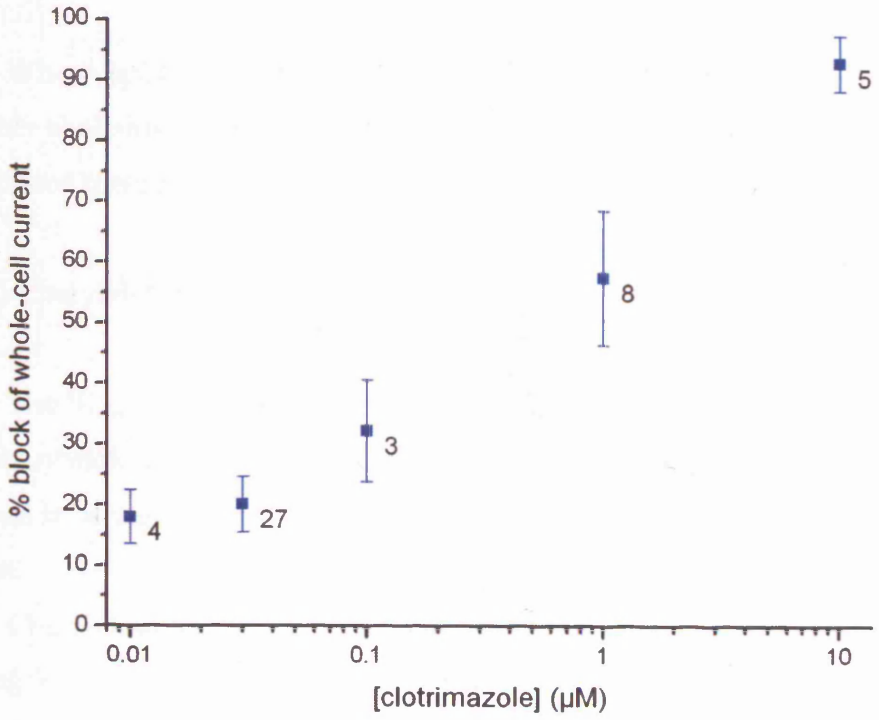


**Figure 5.25)** Concentration-inhibition relationship for clotrimazole sensitivity of outward currents evoked from pig right coronary artery endothelial cells by 10μM ATP. Data are calculated as % block of 'average control' current, recorded at -50mV. Data are expressed as means, bars represent standard error and labels indicate sample size.

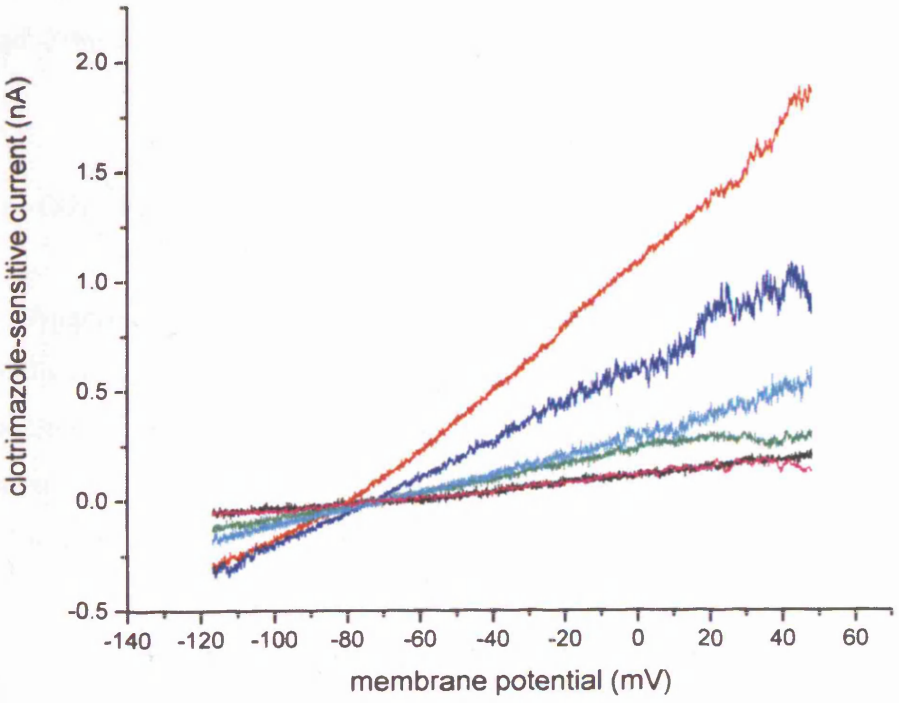


**Figure 5.26)** Current-voltage plots of 1μM clotrimazole-sensitive currents (evoked by 10μM ATP), recorded from pig right coronary artery endothelial cells.

5.3.3.4) Co-application of UCL 1848 and clotrimazole

When applied in combination, 100nM UCL 1848 and 10μM clotrimazole reversibly abolished ATP-evoked outward currents in all seven cells to which they were applied (data not shown).

5.3.3.5) Charybdotoxin

The $IK_{Ca}$ channel contribution to ATP-evoked currents was studied further using charybdotoxin. This peptide also blocks $BK_{Ca}$ channels, although, as will be discussed in *section 5.3.4*, these are thought unlikely to contribute to ATP-evoked currents.

Charybdotoxin was applied at concentrations between 1 and 100nM which, allowing for ~15% systematic rundown, blocked ATP-evoked currents by ~ 70-90% (*figure 5.27*). Block by the lowest concentrations was surprisingly high considering that the $IC_{50}$ for charybdotoxin block of $IK_{Ca}$ is reported to be 2.5nM (*table 5.6*). Pooling data for block by 30 and 100nM charybdotoxin gives an inhibition of ~85%.

Current-voltage plots for 10nM and 30nM charybdotoxin-sensitive currents are shown in *figure 5.28* (pooled data). Linear fits applied to these traces between -70 and -30mV give a mean reversal potential of 74.8±1.6mV (n=6).

5.3.3.6) Other blockers

Apamin (100nM) and iberiotoxin (100nM) were studied in a small number of cells, however, after exclusion of some data due to rundown, only a single example of block remained for each. In view of the high variability shown by individual cells in response to other blockers, it was decided that these data are insufficient for consideration.

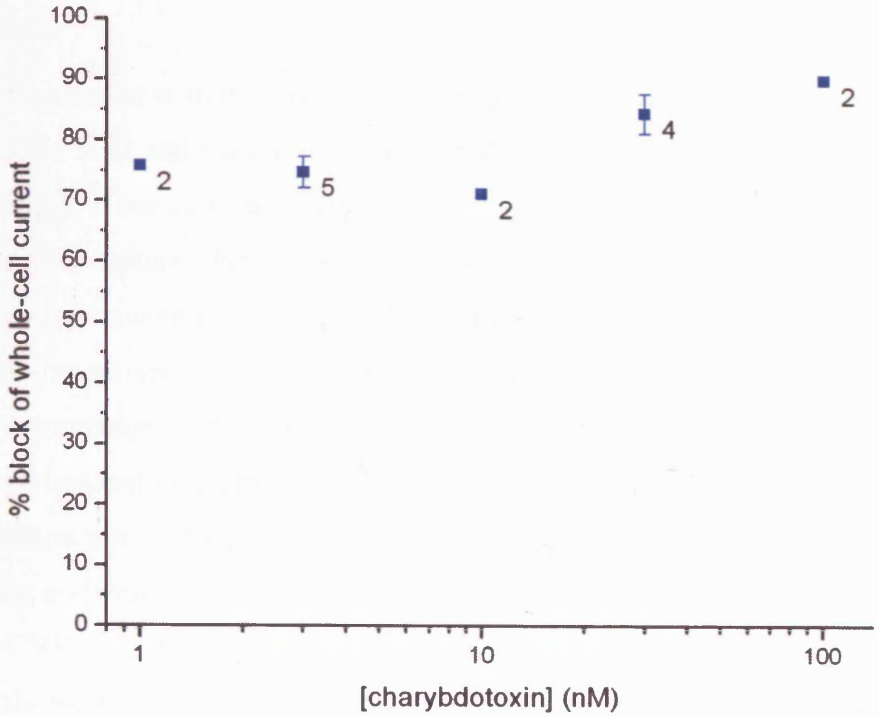


**Figure 5.27)** Concentration-inhibition relationship for charybdotoxin sensitivity of outward currents evoked from pig right coronary artery endothelial cells by 10μM ATP. Data are calculated as % block of 'average control' current, recorded at -50mV. Data are expressed as means. Bars represent standard error and labels indicate sample size.

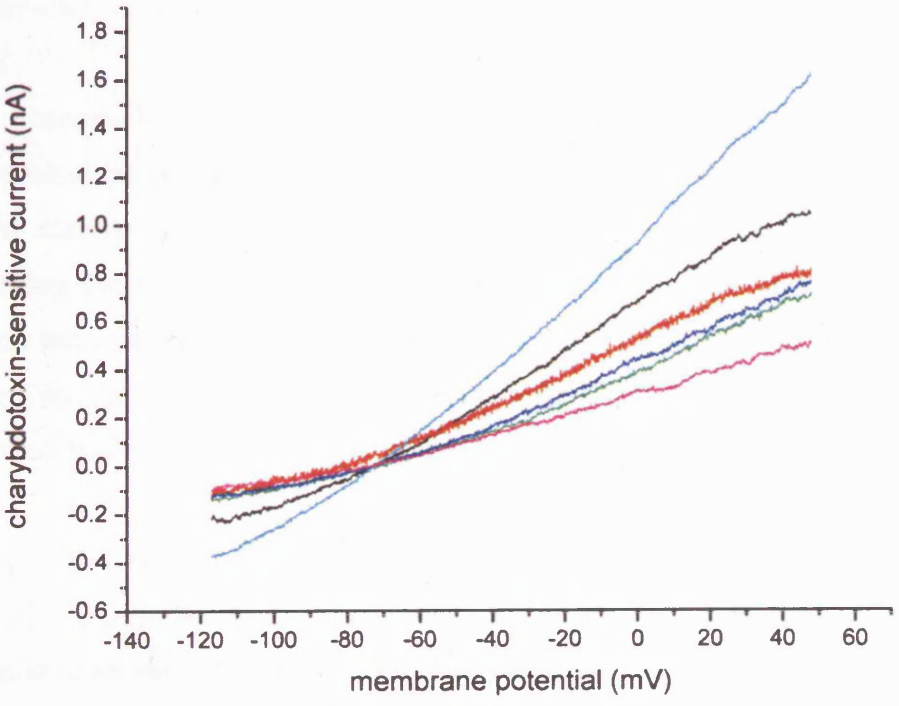


**Figure 5.28)** Current-voltage plots of 10nM or 30nM charybdotoxin-sensitive currents (evoked by 10μM ATP), recorded from pig right coronary artery endothelial cells (pooled data).

## 5.3.4) Summary of ATP-evoked current data

Consistent with published data, single endothelial cells had input resistances in excess of 1GΩ and capacitances of ~30-40pF (Nilius & Droogmans, 2001). Interestingly, mean cell capacitance for clusters of all sizes significantly increased between cells cultured for two and three days (*table 5.4*). Although not investigated, this could indicate an increase in cell volume, or perhaps an increased number of caveolae (membrane folds) which would also increase the cell surface area.

On average, resting cells held at -50mV passed small inward currents which had mean reversal potentials of -12 to -25mV (*table 5.5A*). Current-voltage relationships were heterogeneous, indicating different contributions of inwardly rectifying and voltage-dependent channels.

CVRs of ATP-evoked outward currents were approximately linear at potentials positive to -50mV, and reversed in the region of -73mV. As previously reported for cultured endothelial cells, agonist-evoked currents decreased with increasing time in culture, and had virtually disappeared five days following isolation (Frieden *et al.*, 1999; Ahn *et al.*, 2004). Down-regulation of channel expression is a more likely explanation than failure of receptor mechanisms since calcium-dialysis activated currents also diminished over this period (see *section 5.5.2*).

In some batches of cells, particularly following three or four days in culture, ATP evoked rapidly activating inward as well as outward currents. These 'early inward' currents were not observed in cells dialysed with 1.5μM free-calcium, suggesting that the underlying channels were not calcium-activated. Early inward currents were perhaps due to an up-regulation of P2X channels during culture. In keeping with this, ATP analogues have previously been demonstrated to activate P2X-mediated inward currents in bovine aortic endothelial cells (Ramirez & Kunze, 2002).

ATP-evoked outward currents were partially sensitive to UCL 1848 suggesting a contribution by $SK_{Ca}$ channels. The $IC_{50}$ of 1.2nM reported in this study is similar to values for cloned SK1 or SK3 homomultimers, but not of channels formed from SK2 which are approximately ten-fold more sensitive to this agent (see

*table 5.6*) (Shah & Haylett, 2000; Hosseini *et al.*, 2001). At supramaximal concentrations, UCL 1848 blocked ~65% of the ATP-evoked whole-cell current.

10nM UCL 1848-sensitive currents reversed at -74mV and CVRs were approximately linear between the reversal potential and +20mV. At potentials greater than this, a sharp reduction was seen in currents from some cells (see *figure 5.24*), which may have been due to divalent cation block as reported for $SK_{Ca}$ channels (Soh & Park, 2001). The reason that this did not occur in all recordings may relate to differences in peak intracellular calcium concentration. It should also be noted that the intracellular solution contained 1mM magnesium ions. CVRs similar in shape to those discussed have also been reported in studies of $IK_{Ca}$ currents (Logsdon *et al.*, 1997; Ahn *et al.*, 2004).

Charybdotoxin, which blocks both $IK_{Ca}$ and $BK_{Ca}$ channels, attenuated ATP-activated outward currents by a maximum of ~85%. Currents blocked by 10nM charybdotoxin reversed at -75mV and CVRs were approximately linear at potentials positive to the reversal potential.

An overlap of ~50% occurred between UCL 1848- and charybdotoxin-sensitive components of ATP-activated currents. This finding is similar to that reported for apamin- and charybdotoxin- sensitive components of substance P-evoked currents (Frieden *et al.*, 1999; Sollini *et al.*, 2002). Neither apamin nor charybdotoxin are believed to significantly block $IK_{Ca}$ and $SK_{Ca}$ channels, respectively, at the concentrations used in these studies. Although $IK_{Ca}$ channel sensitivity to UCL 1848 has not been studied, UCL 1684, a structurally-related compound with near identical pharmacology, is ineffective at blocking $IK_{Ca}$ channels at a concentration of 100nM (Malik-Hall *et al.*, 2000). Overlap of UCL 1848 and charybdotoxin sensitive current components is discussed in *chapter seven.*

Clotrimazole sensitivity of ATP-evoked currents was not as expected for two reasons. Firstly, currents were little sensitive to concentrations surrounding the published $IC_{50}$s for block of $IK_{Ca}$ channels. Secondly, at 10μM, clotrimazole blocked a substantial proportion of the UCL 1848-sensitive current. The unexpected sensitivity of $SK_{Ca}$ channels to clotrimazole is discussed in *chapter seven.*

Currents blocked by 1μM clotrimazole reversed at -72mV and CVRs were approximately linear at potentials positive to the reversal potential. (It is noted that despite apparent $SK_{Ca}$ block by clotrimazole, none of the featured CVRs for

clotrimazole-sensitive currents are inwardly rectifying as previously discussed; the reason for this is unclear).

As anticipated, when clotrimazole and UCL 1848 were applied in combination, ATP-evoked responses were completely abolished in all studied cells.

Iberiotoxin sensitivity of ATP-evoked currents was not determined in the present study, and thus a contribution by $BK_{Ca}$ channels cannot be ruled out. It has however been reported that substance P- and ATP-evoked potassium currents recorded from pig coronary artery- (Frieden *et al.*, 1999; Bychkov *et al.*, 2002) and mouse aortic- (Ahn *et al.*, 2004) endothelial cells, respectively, are insensitive to iberiotoxin.

# 5.4) Voltage-clamp studies: 1-EBIO-activated currents

## 5.4.1) Introduction

1-EBIO is reported to activate $SK_{Ca}$ and $IK_{Ca}$ channels at similar concentrations, in a manner dependent on intracellular calcium. When studied using 30nM free-calcium -containing intracellular (patch pipette) solution, cells in which currents were evoked by 10μM ATP, were insensitive to 300μM 1-EBIO (n=3).

Dialysing cells with an intracellular solution containing 500nM free-calcium did not itself activate maintained whole-cell currents. In these cells, however, 1-EBIO activated sustained outward currents (for example see *figure 5.29*).

That 500nM free-calcium did not itself activate sustained currents is perhaps surprising in view of the known calcium-sensitivity of $SK_{Ca}$ and $IK_{Ca}$ channels ($EC_{50}$ ~500nM). It was noticed in some recordings, however, that a transient outward current occurred following entry into whole-cell configuration. An example of this can be seen at the beginning of the trace shown in *figure 5.30*. Although cells initially behaved as if dialysed with the '30nM free-calcium' solution, in some of the longer recordings an outward current began to develop several minutes following entry into whole-cell configuration. In a few recordings, it was also noticed that, following exposure to ATP, outward currents persisted. These findings may suggest that cells were temporarily able to buffer cytosolic calcium to a concentration at which $K_{Ca}$ channels remained inactive.

## 5.4.2) Control recordings

The amplitude of 1-EBIO-activated currents varied widely between recordings. In some cells, responses to 1mM 1-EBIO were larger than those evoked by 300μM (for example see *figure 5.29*), although this was not always so. Where 1-EBIO activated currents were small, subsequent application of ATP evoked considerably larger responses (for example see *figure 5.30*).

In some recordings, voltage-ramps were applied prior to and at the peak of the response, providing CVRs for 1-EBIO-activated currents (for examples, see

*figure 5.31*). Linear fits applied to each of these traces at potentials between -70 and -40mV, gave a mean reversal potential of -75.1±0.7mV (n=5).

5.4.3) Sensitivity of 1-EBIO-evoked currents to UCL 1848 and clotrimazole

In three cells to which it was applied, 100nM UCL 1848 reversibly blocked 1-EBIO-activated currents by 36, 49 and 86% (for an example, see *figure 5.32*).

1μM clotrimazole reversibly blocked a more consistent proportion of 1-EBIO-activated currents (89.0±1.6% (n=4) (for an example see *figure 5.33*).

When applied in combination, UCL 1848 (100nM) and clotrimazole (1μM) almost abolished 1-EBIO-activated currents in three recordings (for an example, see *figure 5.34*). In each case, outward currents reappeared following a return to extracellular solution containing only 1-EBIO.

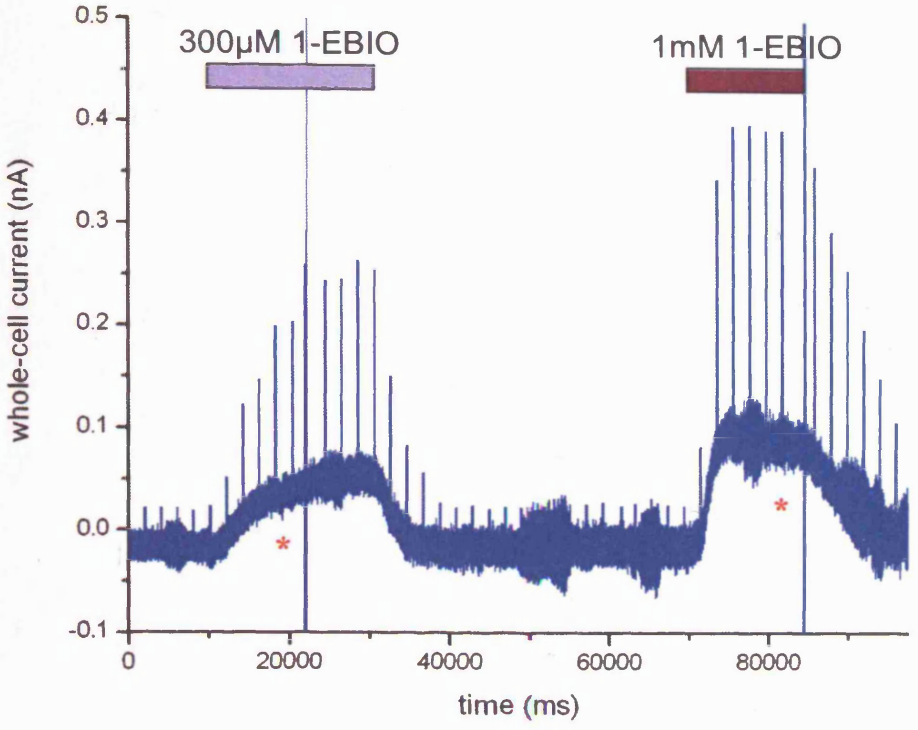


**Figure 5.29)** Currents evoked by 1-EBIO, recorded from pig right coronary artery endothelial cells dialysed with an intracellular solution containing 500nM free-calcium. Holding potential, -50mV; pulse amplitudes, +50mV. Asterisks denote application of voltage-ramps (-120 to +50mV).

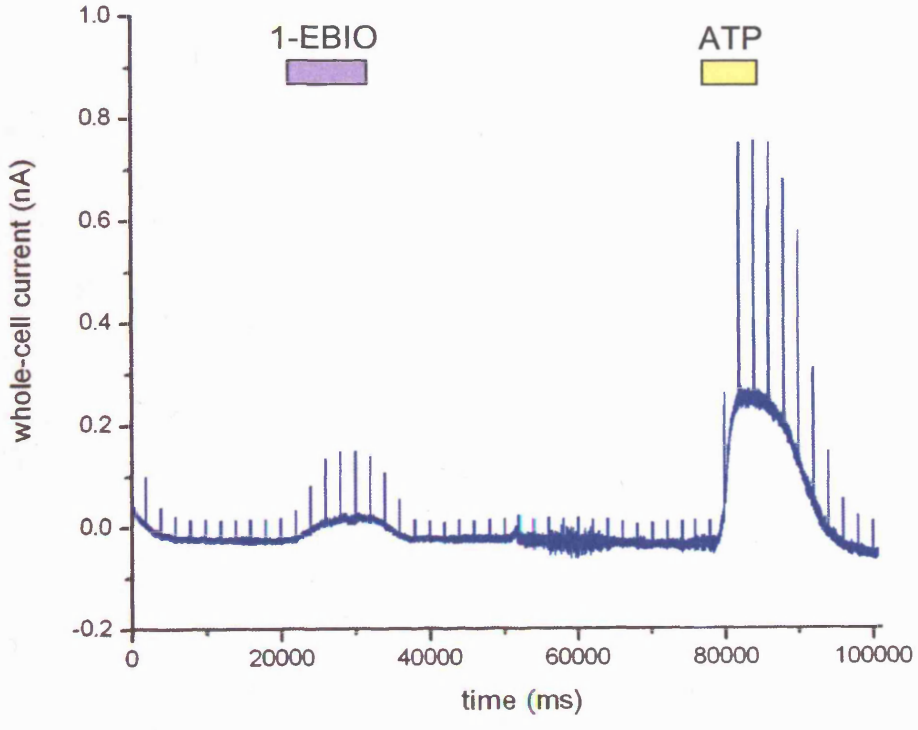


**Figure 5.30)** Currents evoked by 300μM 1-EBIO and 10μM ATP, recorded from pig right coronary artery endothelial cells dialysed with an intracellular solution containing 500nM free-calcium. Holding potential, -50mV; pulse amplitudes, +50mV.

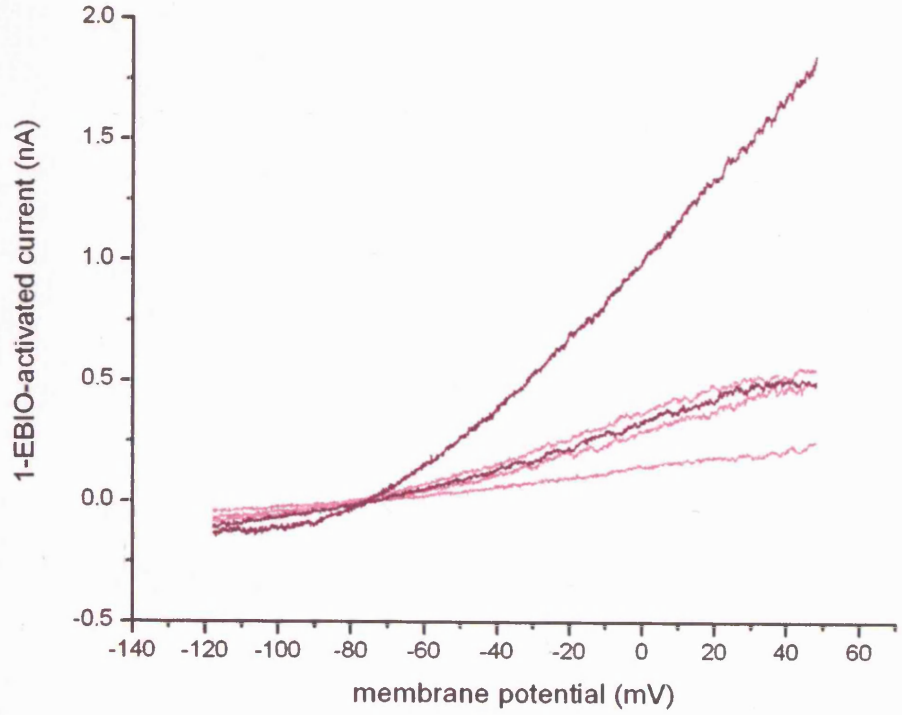


**Figure 5.31)** CVRs for 1-EBIO-activated currents recorded from pig right coronary artery endothelial cells dialysed with an intracellular solution containing 500nM free calcium. Pink and purple traces are from cells exposed to 300μM and 1mM 1-EBIO, respectively.

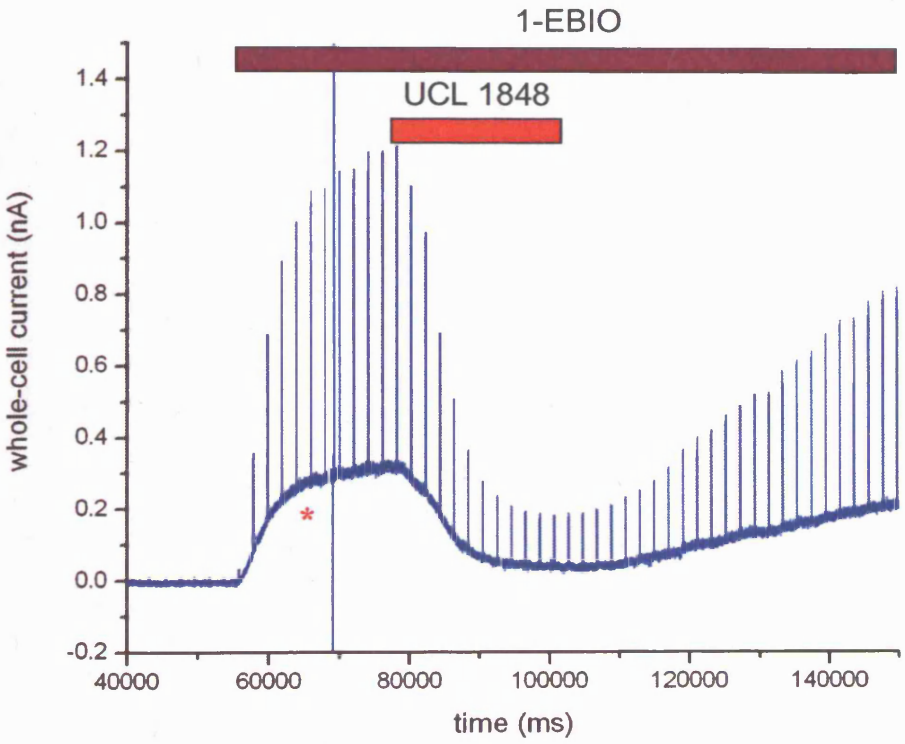


**Figure 5.32)** Block by 100nM UCL 1848 of a current evoked by 1mM 1-EBIO, recorded from pig right coronary artery endothelial cells dialysed with an intracellular solution containing 500nM free-calcium. Holding potential, -50mV; pulse amplitudes, +50mV. Asterisk denotes application of voltage-ramps (-120 to +50mV).

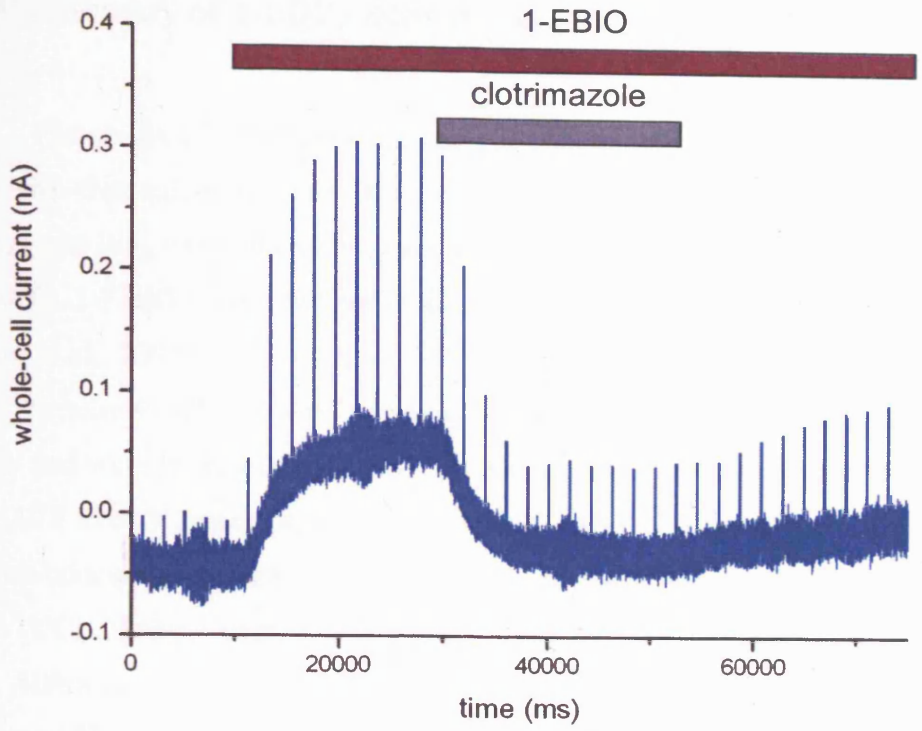


**Figure 5.33)** Block by 1μM clotrimazole of a current evoked by 1mM 1-EBIO, recorded from pig right coronary artery endothelial cells dialysed with an intracellular solution containing 500nM free-calcium. Holding potential, -50mV; pulse amplitudes, +50mV.

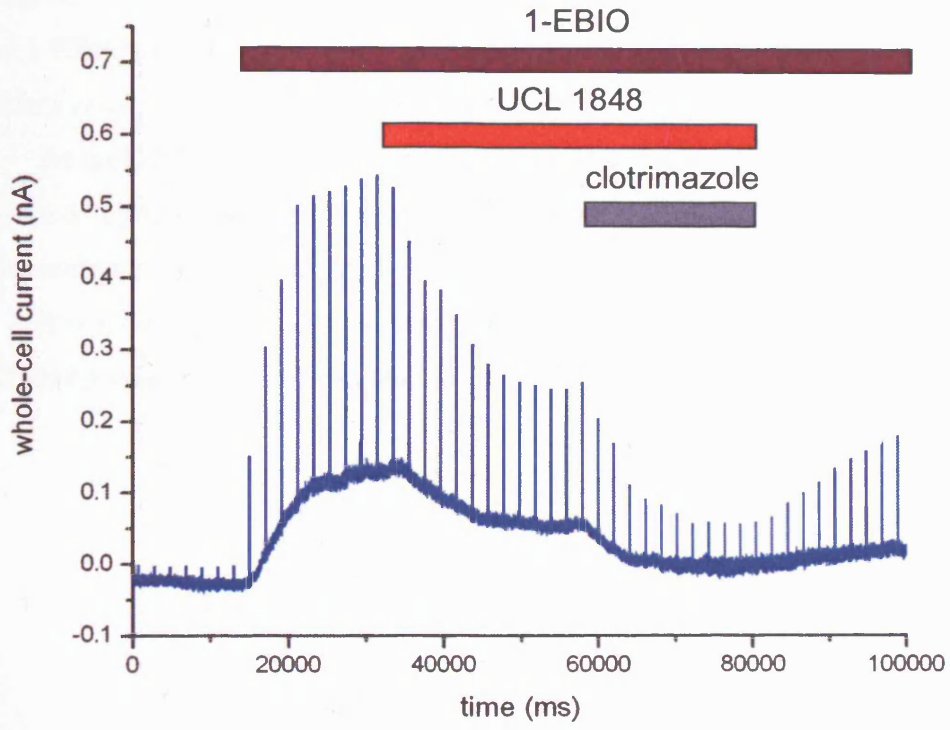


**Figure 5.34)** Block by 100nM UCL 1848 and 1μM clotrimazole, of a current evoked by 1mM 1-EBIO, recorded from pig right coronary artery endothelial cells dialysed with an intracellular solution containing 500nM free-calcium. Holding potential, -50mV; pulse amplitudes, +50mV.

## 5.4.4) Summary of 1-EBIO-activated current data

The ability of 1-EBIO to activate currents in cells dialysed with 500nM- but not 30nM- free-calcium, is consistent with this agent modifying calcium-sensitivity of $SK_{Ca}$ and $IK_{Ca}$ channels rather than acting by an independent mechanism (Syme *et al.*, 2000). 1-EBIO is reported not to activate $BK_{Ca}$ channels (Syme *et al.*, 2000; Walker *et al.*, 2001).

Similar to ATP-evoked currents, 1-EBIO -activated currents reversed at -74mV and were mostly linear positive to this potential. When applied to the same cells, ATP evoked larger currents than 1-EBIO indicating that at the given cytosolic calcium-concentration, 1mM 1-EBIO did not fully activate channels.

UCL 1848 reversed 1-EBIO current activation by a variable degree (36-86%, n=3). Although it is established that $SK_{Ca}$ channels are activated by 1-EBIO ($EC_{50}$ for cloned SK3 channels: 170μM (Wittekindt *et al.*, 2004b), a previous study of pig coronary artery endothelial cells found 1-EBIO-activated currents to be insensitive to apamin, indicating no contribution by $SK_{Ca}$ channels (Bychkov *et al.*, 2002).

Clotrimazole consistently blocked 1-EBIO activated currents by ~90%. This is in agreement with previous studies of pig coronary artery endothelial cells which found 1-EBIO activated currents to be charybdotoxin sensitive (Sollini *et al.*, 2002; Burnham *et al.*, 2002).

As with ATP-evoked currents, clotrimazole apparently blocked a UCL 1848-sensitive component of 1-EBIO -activated currents. Co-application of UCL 1848 and clotrimazole essentially abolished 1-EBIO-activated currents.

It is noted that in the present study, currents were sustained as long as 1-EBIO was present, unlike the transient activations reported by Sollini *et al.*, (2002)

## 5.5) Voltage-clamp studies: Calcium-activated currents

### 5.5.1) Introduction

The hypothesis that calcium-activated potassium channels underlay agonist-evoked currents was tested by dialysing cells with an intracellular solution containing 1.5μM free-calcium. As with previously described voltage-clamp studies, the holding potential was set at -50mV with +50mV 200ms pulses applied at 0.5Hz.

In these studies, unlike those where cells were dialysed with 30nM- or 500nM-free-calcium containing solutions, sustained outward currents began to activate immediately upon entry into the whole-cell configuration (see start of trace, *figure 5.37*). Outward currents reached stable plateaus within 30 seconds, at which point $K_{Ca}$ channel blockers were applied (refer back to *table 5.6* for a list of blockers and their $IC_{50}$ values). As with agonist studies, current amplitudes varied greatly between cells.

In many recordings, plateau holding currents began to decrease within one minute of activation. This was caused by development of an opposing current(s) which gradually resulted in a large net inward current. Pulse amplitude increased noticeably as inward currents developed, and thus served as a useful indicator to distinguish the development of inward currents from the effect of $K_{Ca}$ channel blockers. In order to maximise recording time prior to the development of delayed inward currents, no time was spent balancing capacitance transients or generating voltage ramps.

Owing to the immediate nature of current-activation following entry into whole-cell configuration, it was not possible to determine an accurate 'resting' current in these recordings. As a result, net outward currents could not be calculated. In order to compare the effects of $K_{Ca}$ channel blockers in cells where the calcium-activated currents varied widely in amplitude, blocked currents are expressed as a percentage of the *outward* portion of the plateau (control) holding current. This presented no problem with most recordings, however in some, an *inward* holding current was apparent immediately following entry into whole-cell configuration, which then became net-outward as the outward current developed. Block of outward current in these cells revealed net inward current, and so, owing to the method of

measurement used, some agents caused apparent block of more than 100%. To limit the skewing of data, which this inevitably caused, cells in which currents were blocked by >105%, were excluded from analysis.

Ideally, data would have been selected only from cells in which, following application of a $K_{Ca}$ channel blocker, outward currents recovered upon return to blocker-free extracellular solution. However, since in many cells, contaminating inward currents began to appear before recovery could be established, data were also selected from cells in which inward currents occurred only after block had reached a plateau.

## 5.5.2) Control currents

Dialysis-activated currents, as with those evoked by ATP, varied considerably in amplitude between different cells. Whilst in some, no outward-current was activated, in others, currents exceeded 0.5nA.

The currents recorded in these experiments were not expressed as a function of cell capacitance. However, some approximate comparisons relating to cell cluster size and length of time in culture are presented in *table 5.7.* As with the ATP-studies, dialysis-evoked outward currents appear to decrease with increasing time in culture. Unlike the findings with ATP (*section 5.3*), current amplitudes do not appear to increase with cluster size. This observation suggests that calcium from the patch electrode dialyses only into the cell to which it is attached, and does not activate channels in adjoining cells.

In a small number of recordings, including some where dialysis activated little or no outward current, 10μM ATP evoked a further outward current (*figure 5.35*). It was initially supposed that, in clusters containing two or three cells, this resulted from activation of adjoining cells, however ATP-evoked responses were also observed in single cells. This indicates that, in these cells at least, 1.5μM calcium in the patch pipette did not fully activate $K_{Ca}$ channels.

Though voltage-ramps were not performed routinely, two examples of ramps recorded at the peak of dialysis-activation are shown in *figure 5.36; blue traces.* Also plotted is a typical trace for an ATP-evoked current (red trace). Although gradients

are different, reflecting difference in current size, the similar shape of the three traces suggest that ATP and calcium activate a similar population of channels. The dialysis-activated currents reverse at ~-60 and ~-70mV.

In studies described earlier, ATP was shown to evoke transient 'early-inward' currents in approximately 12% of recordings (see *section 5.3.2.4*). In contrast, in over 300 stable recordings, these currents were never observed in cells dialysed with 1.5μM free-calcium containing intracellular solution.

| time in culture (days) | cluster size | | |
|---|---|---|---|
| | single cell | 2 | 3 |
| 2 | 93.2±22.5pA (15) | 117.6±30.3pA (15) | 99.6±25.7pA (7) |
| 3 | 55.8±36.7pA (15) | 55.1±18.1pA (15) | - |
| 4 | 29.0±12.7pA (3) | - | - |

**Table 5.7)** Peak outward currents recorded from pig right coronary artery endothelial cells dialysed with 1.5μM free-calcium containing intracellular solution. Data is mean ± standard error (sample size).

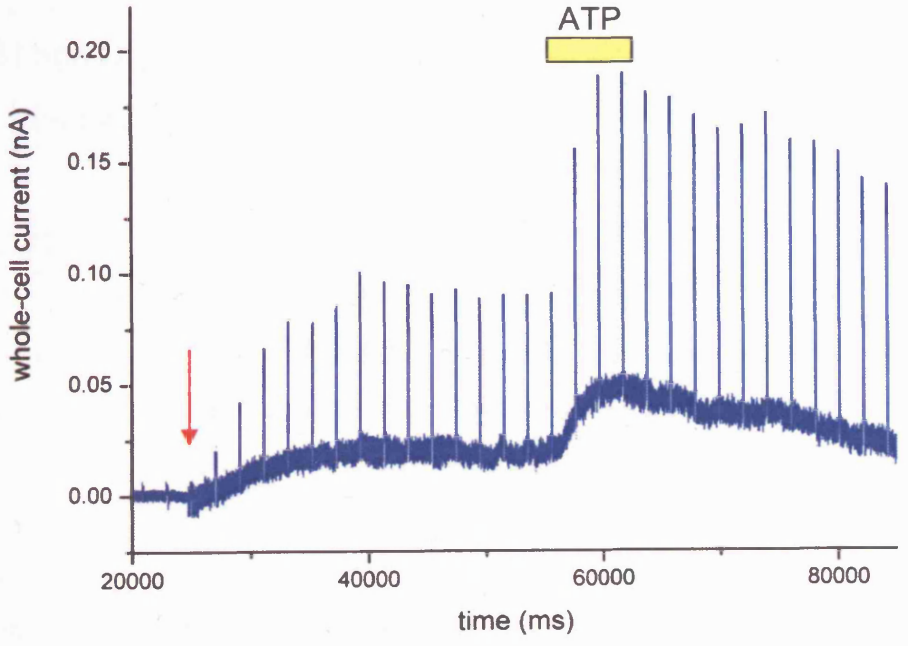


**Figure 5.35)** A 10μM ATP-evoked outward current recorded from a pig coronary artery endothelial cell dialysed with an intracellular solution containing 1.5μM free-calcium. Entry into whole-cell configuration, hence onset of dialysis, is indicated by the red arrow. Holding potential, -50mV; pulse amplitudes, +50mV.

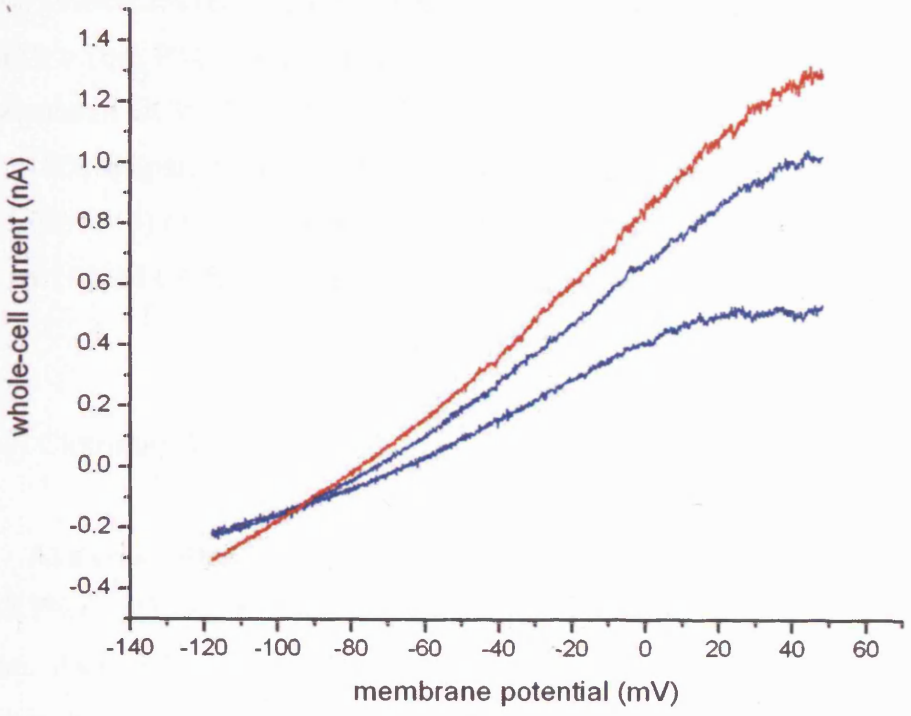


**Figure 5.36)** Blue traces: current-voltage relationships of currents determined following stabilisation of activated outward currents. Data recorded from pig right coronary artery endothelial cells dialysed with an intracellular solution containing 1.5$\mu$M free-calcium. For comparison, an equivalent ramp from the plateau of a cell response to 10µM ATP is shown (red trace); this cell was dialysed with an intracellular solution containing 30nM free-calcium.

## 5.5.3) Sensitivity of calcium dialysis-activated currents to $K_{Ca}$ channel blockers

### 5.5.3.1) UCL 1848 and apamin

At a concentration of 100nM, UCL 1848 blocked net-outward currents by 28.3±5.4% (n=27) when applied to cells immediately following stabilisation of currents. Where recordings were maintained without contamination by inward currents, this block fully reversed upon washout. Attempts at determining the concentration response relationship to UCL 1848 when applied at 1, 10 and 100nM sequentially, were hampered by the appearance of inward currents prior to completion. When applied immediately following stabilisation of dialysis-activated currents, block by 1nM UCL 1848 was found not to be significantly less than for

100nM; 19.0±6.2% (n=7) and 28.3±5.4% (n=27), respectively (unpaired one-tailed Student's t-Test, P>0.05). However, in some individual recordings concentration-dependence of UCL 1848 block was clear (see *figure 5.37*).

100nM apamin, which was applied to a small population of cells, blocked 20.6±5.0% (n=5) of the outward current. This is not significantly different from block by 100nM UCL 1848 (unpaired one-tailed Student's t-Test, P>0.05).

5.5.3.2) Clotrimazole

At a concentration of 1μM, clotrimazole blocked net-outward currents by 82.6±3.7% (n=22) when applied to cells immediately following stabilisation of currents. As with block by UCL 1848, where recordings were maintained without contamination by inward currents, clotrimazole block fully reversed upon washout.

In a number of cells, it was possible to sequentially apply rising concentrations of clotrimazole, and a concentration-response relationship was established for concentrations of 0.01, 0.1 and 1μM (see *figures 5.38* and *5.39*).

5.5.3.3) UCL 1848 and clotrimazole in combination

In order to study the effect of the blockers in combination, cells were first exposed to either UCL 1848 or clotrimazole, and then to a combination of the two.

For two recordings in which cells were exposed first to 100nM UCL 1848 and then a combination of 100nM UCL 1848 and 1μM clotrimazole, mean block of net-outward current was 18.9 and 94.6%, respectively. For an example trace, see *figure 5.40*. For a further two recordings in which cells were firstly exposed to 1μM clotrimazole and then a combination of 1μM clotrimazole and 100nM UCL 1848, mean block of net-outward current was 79.2 and 91.0%, respectively. For an example trace, see *figure 5.41*.

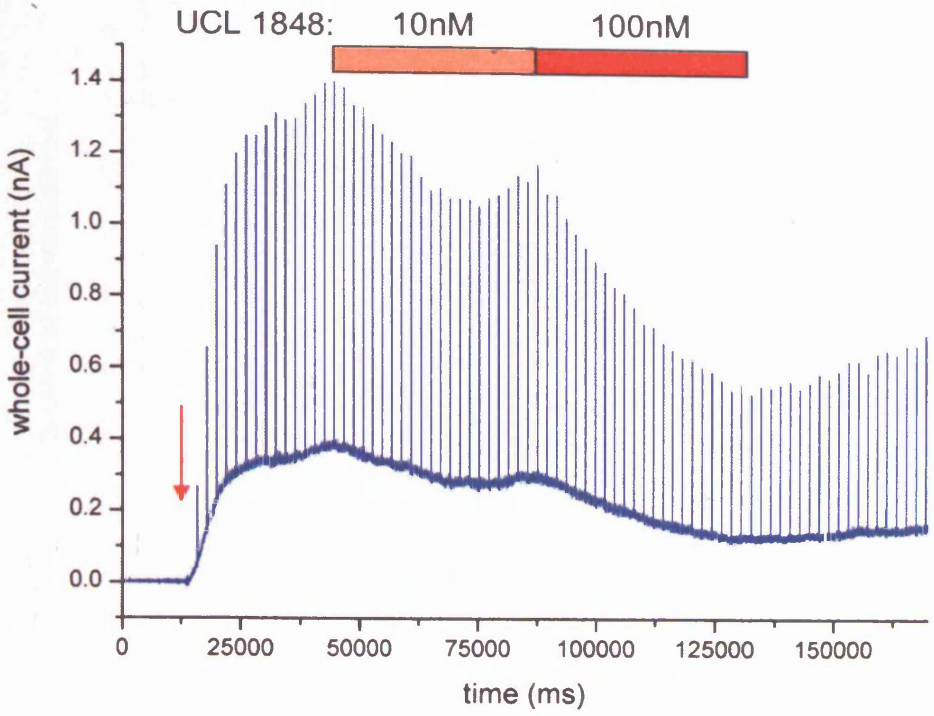


**Figure 5.37)** Block by 10 and 100nM UCL 1848 of an outward current recorded from a pig right coronary artery endothelial cell dialysed with 1.5μM free-calcium containing intracellular solution. Entry into whole-cell configuration, hence onset of dialysis, is indicated by the red arrow. Holding potential, -50mV; pulse amplitudes, +50mV.

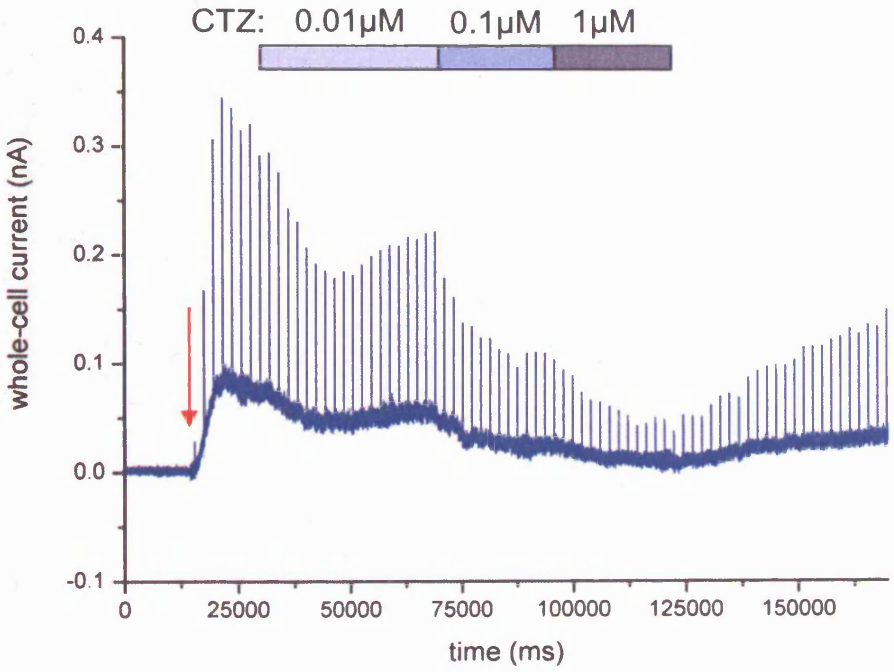


**Figure 5.38)** Block by 0.01, 0.1 and 1μM clotrimazole (CTZ) of an outward current recorded from a pig right coronary artery endothelial cell dialysed with 1.5μM free-calcium containing intracellular solution. Entry into whole-cell configuration, hence onset of dialysis, is indicated by the red arrow. Holding potential, -50mV; pulse amplitudes, +50mV.

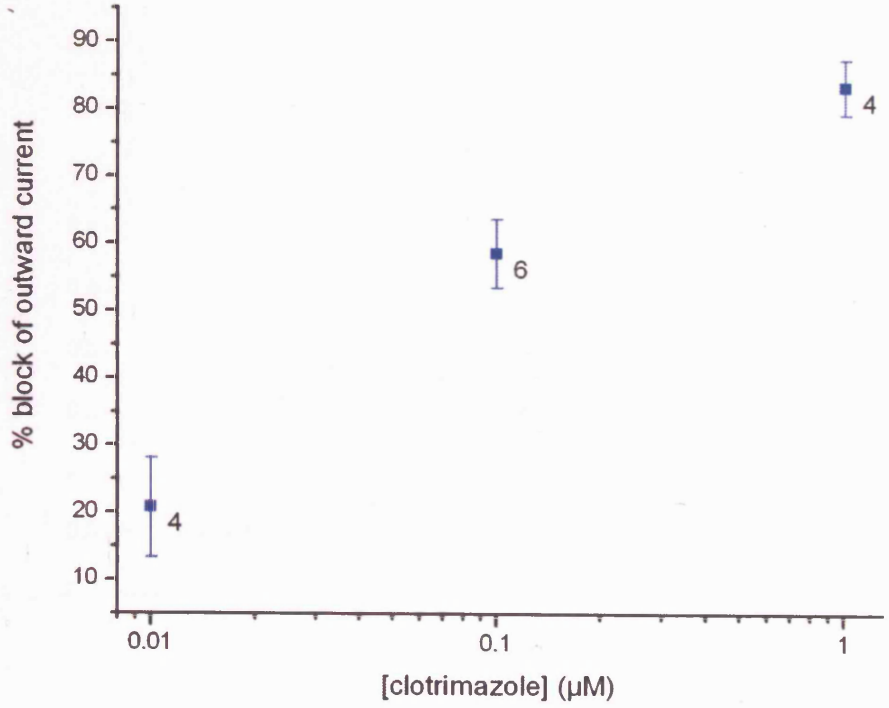


**Figure 5.39:** Clotrimazole sensitivity of net-outward currents recorded from pig right coronary artery endothelial cells dialysed with an intracellular solution containing 1.5μM free-calcium. Block is expressed as % dialysis activated net-outward control current. All measurements were taken at a holding potential of -50mV. Data are expressed as means. Bars represent standard error and labels indicate sample size.

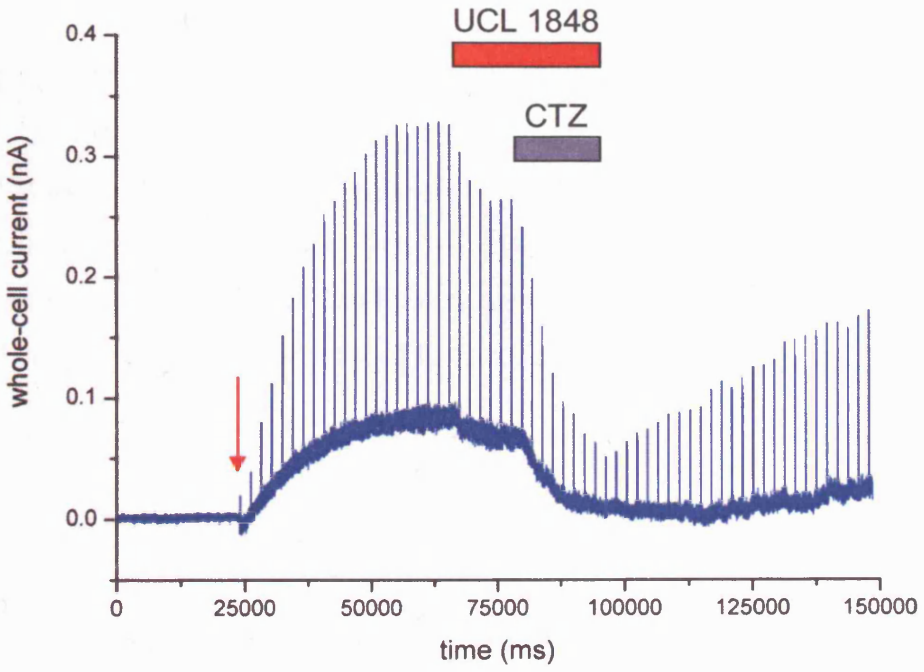


**Figure 5.40)** Block by 100nM UCL 1848, then a combination of UCL 1848 and 1μM clotrimazole (CTZ), of an outward current recorded from a pig right coronary artery endothelial cell dialysed with 1.5μM free-calcium containing intracellular solution. Entry into whole-cell configuration, hence onset of dialysis, is indicated by the red arrow. Holding potential, -50mV; pulse amplitudes, +50mV.

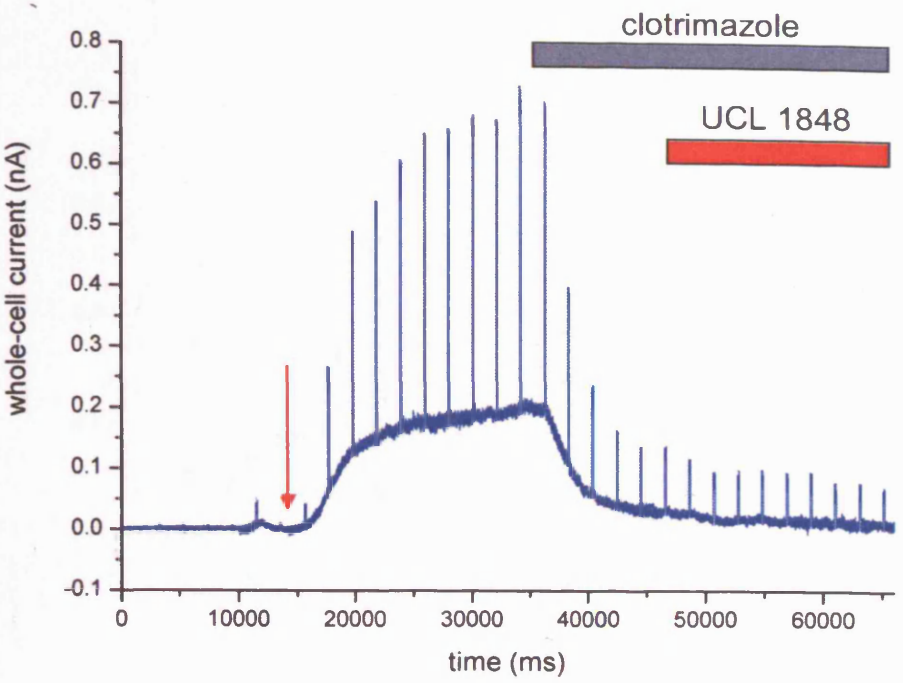


**Figure 5.41)** Block by 1μM clotrimazole, then a combination of clotrimazole and 100nM UCL 1848, of an outward current recorded from a pig right coronary artery endothelial cell dialysed with 1.5μM free-calcium containing intracellular solution. Entry into whole-cell configuration, hence onset of dialysis, is indicated by the red arrow. Holding potential, -50mV; pulse amplitudes, +50mV.

5.5.3.4) Charybdotoxin

When applied at a concentration of 100nM, charybdotoxin blocked dialysis-activated net-outward currents by 101.2±0.5% (n=3). An example of current block is shown in *figure 5.42*. Where recordings were maintained without contamination by inward currents, charybdotoxin block fully reversed upon washout.

5.5.3.5) Iberiotoxin

In two recordings, 100nM iberiotoxin blocked net-outward currents by 26.4 and 30.9%. After iberiotoxin, cells were immediately exposed to 1μM clotrimazole which blocked net-outward current by >105% in one cell, and 90.8% in the other, similar to data reported in *section 5.5.3.2*. An example trace is shown in *figure 5.43*.

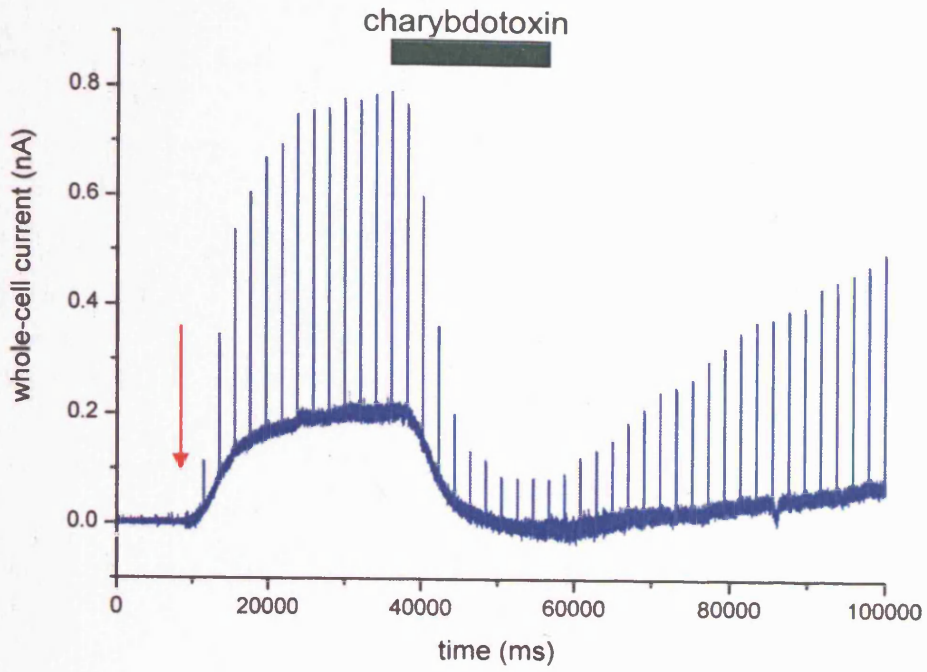


**Figure 5.42)** Block by 100nM charybdotoxin of an outward current recorded from a pig right coronary artery endothelial cell dialysed with 1.5μM free-calcium containing intracellular solution. Entry into whole-cell configuration, hence onset of dialysis, is indicated by the red arrow. Holding potential, -50mV; pulse amplitudes, +50mV.

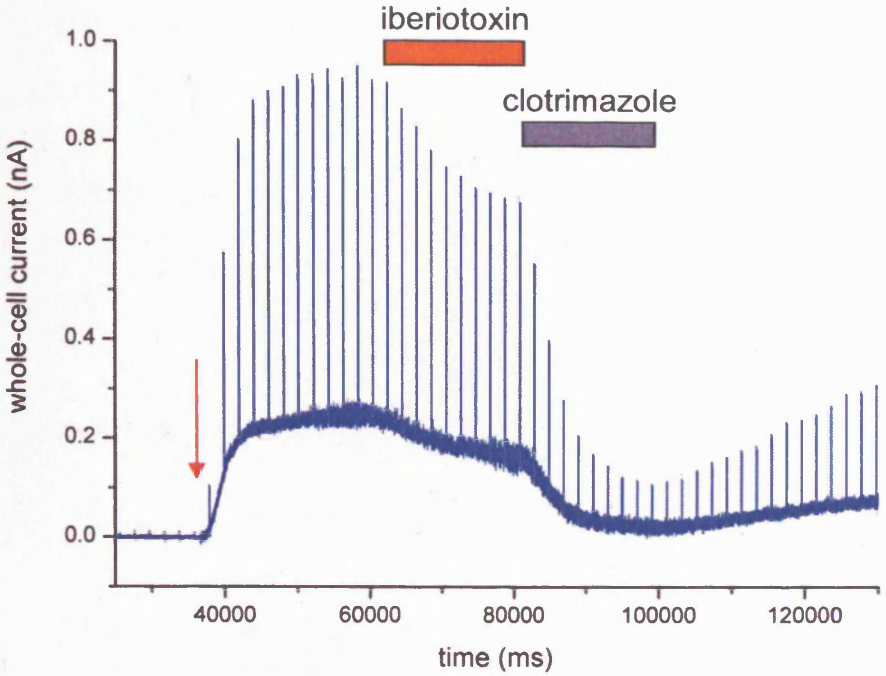


**Figure 5.43)** Block by 100nM iberiotoxin of an outward current recorded from a pig right coronary artery endothelial cell dialysed with 1.5μM free-calcium containing intracellular solution. Following iberiotoxin block, 1μM clotrimazole was applied to cells. Entry into whole-cell configuration, hence onset of dialysis, is indicated by the red arrow. Holding potential, -50mV; pulse amplitudes, +50mV.

## 5.5.4) Summary of calcium-activated current data

When whole-cell recordings were made with patch electrodes containing 1.5μM free-calcium, an outward holding current began to activate immediately upon entry into whole-cell configuration. Unlike ATP-evoked currents, current amplitudes were similar in clusters of one, two and three cells suggesting that dialysis raised calcium sufficiently to activate $K_{Ca}$ channels only in the cell directly attached to the patch electrode.

For two cells in which voltage ramps were applied, CVRs were similar in shape to those for ATP-activated currents, reversing at -73 and -64mV. The latter value suggests that non- potassium-selective channels may also be activated by calcium. These may include calcium-activated non-selective cation currents which have been described in cultured pig coronary artery (Baron *et al.*, 1996), rat carotid artery (Kohler *et al.*, 2001) and mouse aortic (Suh *et al.*, 1999) endothelial cells, and perhaps calcium-activated chloride channels; also present in many endothelial cells (Nilius & Droogmans, 2001).

The sensitivity of net-outward currents to $SK_{Ca}$ channel blockers varied greatly between recordings, the degree of block ranging from negligible to complete. The mean block was 28 and 21% with UCL 1848 and apamin, respectively. 1μM clotrimazole blocked a more consistent component of net-outward currents (mean block 83%), however 100nM charybdotoxin abolished net-outward currents when studied in three cells (mean block 101%). Iberiotoxin, a selective $BK_{Ca}$ channel blocker, inhibited net-outward current by a mean of 29% when applied at 100nM.

That UCL 1848 and apamin blocked a relatively small and variable component of calcium-activated net-outward currents was surprising. Currents evoked by ATP and 1-EBIO had larger UCL 1848-sensitive components, so it seems likely that not all $SK_{Ca}$ channels were activated by calcium-dialysis. Consistent with this, ATP further increased outward holding currents when applied to a number of cells dialysed with 1.5μM free-calcium. Although at this calcium concentration, $SK_{Ca}$ and $IK_{Ca}$ channels would both be expected to be maximally activated, incomplete dialysis at the time of ATP application, or unequal distribution of calcium throughout the cell coupled with an uneven expression pattern of $SK_{Ca}$ and $IK_{Ca}$ channels may explain this discrepancy. Furthermore, $SK_{Ca}$ channels are

reported to be a little less sensitive to calcium compared with $IK_{Ca}$ channels ($EC_{50}$s: 300-700nM (Kohler *et al.*, 1996) and 100-300nM (Joiner *et al.*, 1997; Ishii *et al.*, 1997b), respectively).

The sensitivity of calcium-activated net-outward currents to iberiotoxin indicates a contribution by $BK_{Ca}$ channels. This was also suggested by sensitivity to charybdotoxin, which was significantly more effective at abolishing net-outward currents than clotrimazole; widely reported to have little $BK_{Ca}$ blocking activity at the concentration used ($IC_{50}$ 24μM (Wulff *et al.*, 2000)). Previous studies of cultured pig coronary artery endothelial cells have suggested that $BK_{Ca}$ channels are present, and, at potentials negative to +50mV, are gated only by intracellular calcium (Baron *et al.*, 1997; Frieden *et al.*, 1999). The single channel studies by Baron *et al.* suggested that when the inner face of the channel is exposed to 1μM calcium, the open probability of the channel is ~0.05 at -50mV (Baron *et al.*, 1997). Activation of $BK_{Ca}$ channels at potentials exceeding +50mV has also been described in freshly isolated pig coronary artery endothelial cells (Bychkov *et al.*, 2002). As CVRs performed in the present study were not continued to potentials beyond +50mV, this could explain the apparent absence of a $BK_{Ca}$-attributable voltage-dependent component.

Although iberiotoxin may cause a small amount of $IK_{Ca}$ channel block at the concentration studied ($IC_{50}$s 800nM (de Allie *et al.*, 1996), >1μM (Logsdon *et al.*, 1997)), this is unlikely to account for the 29% block of net-outward currents reported in the present study.

The large component of net-outward currents which was insensitive to UCL 1848 and iberiotoxin, yet sensitive to clotrimazole and charybdotoxin is likely to be due to $IK_{Ca}$ channel activity.

# Chapter 6: $K_{Ca}$ channel protein expression in pig endothelial cells

## 6.1) Introduction

Further to the electrophysiology studies which demonstrated the presence of $K_{Ca}$ channels in pig coronary artery endothelial cells, fluorescence immunohistochemistry experiments were carried out to determine which channel proteins are expressed in these cultures.

Cells were immunostained using primary antibodies raised against the SK2, SK3 and IK1(SK4) channel proteins (refer back to *table 2.1*). Each of these have been designed to target an N- or C- terminal epitope unique to a specific SK or IK protein isoform (see *appendices i, ii & iii*). For some of the antibodies used, the target epitopes are highly conserved between species. For others, only specific orthologues are bound.

## 6.2) Protocol

All studies were performed using pig right coronary artery endothelial cells cultured for 2-3 days. In each experiment, primary antibodies were detected using a Cy3-conjugated secondary antibody.

Positive controls were carried out in HEK 293 cells transfected to over-express the relevant channel protein[11]. To enable identification of $K_{Ca}$ protein-expressing HEK cells, cultures were co-transfected with green fluorescent protein (GFP). Negative controls, whereby the primary antibody was omitted from the immunostaining procedure, were carried out in both pig coronary artery endothelial and HEK cells.

[11] Kindly provided by DCH Benton

All immunostained cells were viewed using a scanning laser confocal microscope. This allowed capture of 'optical slice' images, enabling resolution of membrane-delimited staining. Using negative control samples, the confocal detector gain was calibrated to minimise detection of non-specific (background) fluorescence in each experiment.

## 6.3) SK protein expression

### 6.3.1) SK2

SK2 expression was determined using the M1 primary antibody (see *appendix i* for epitope).

Though experiments were repeated on five occasions using M1 at dilutions between 1:20 and 1:200, no above-background fluorescence was detected in pig coronary artery endothelial cells.

In positive controls, however, primary antibody specific fluorescence was detected in the sub-plasmalemmal region of all SK2-transfected HEK cells (*figure 6.1*) (M1 dilution 1:200).

Pig SK2 has yet to be cloned and sequenced, however the epitope to which M1 has been designed is present in all currently cloned SK2 orthologues (bovine variants 1&2, chicken, human variants 1&2, mouse and rat).

Using a commercial antibody (Chemicon SK2) ~~see *appendix i* for epitope)~~, peri-nuclear SK2 immunostaining has previously been reported in the endothelium of pig coronary artery sections (Burnham *et al.*, 2002).

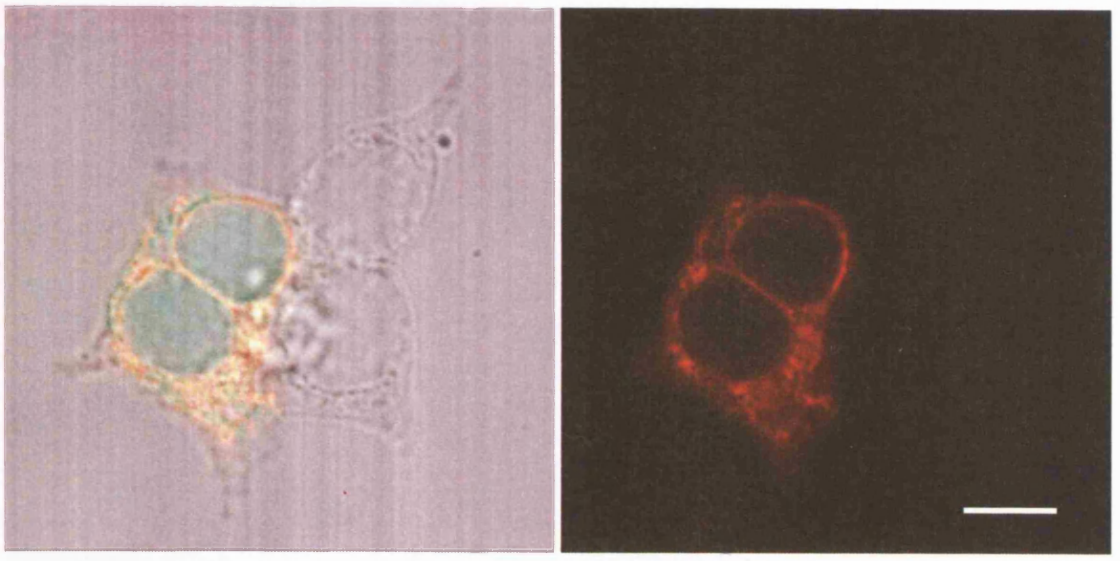

**Figure 6.1)** Immunostaining of rSK2/GFP co-transfected HEK cells using the M1 primary antibody. The primary antibody has been detected using a Cy3-conjugated secondary antibody. Corresponding bright-field/fluorescence overlay and red fluorescence images are displayed in the left and right panels, respectively. Scale bar: 10μm.

## 6.3.2) SK3

SK3 expression was determined using the 'Chemicon SK3' primary antibody (see *appendix ii* for epitope).

In the majority of pig coronary artery endothelial cells, little could be seen in the way of above-background staining. However, in plaques in which some cells had become rounded during the immunostaining process, primary antibody specific membrane-delimited staining was apparent in the round, but not the flat cells (*figure* 6.2A&B) ~~6.2~~) ('Chemicon SK3' dilution 1:200).

In positive controls, primary antibody specific membrane-delimited fluorescence also was detected in all SK3-transfected HEK cells (*figure* ~~6.2~~ 6.2C) ('Chemicon SK3' dilution 1:200).

The apparent absence of the SK3 protein in flat as opposed to rounded endothelial cells may simply reflect a difficulty in detecting membrane-delimited fluorescence signals in flat cells. Dense bands of staining are unlikely to be captured when viewing very flat cells since most of the membrane lies perpendicular to the optical path of the microscope. Conversely, an optical slice of a round cell is likely to contain membrane running more parallel to the light path, thus resulting in a greater density of the fluorescence signal.

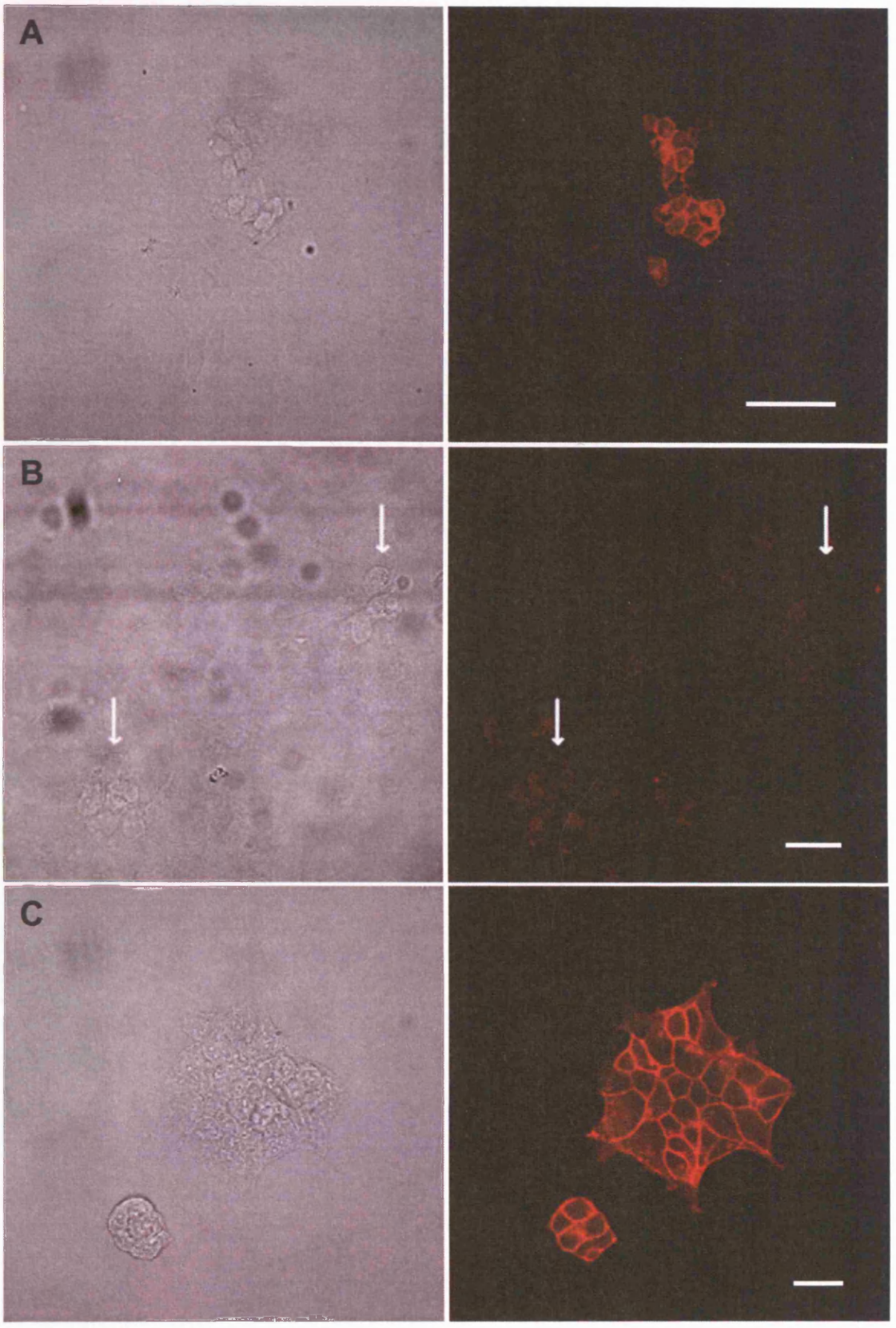


**Figure 6.2)** Immunostaining of pig right coronary artery endothelial cells using the Chemicon-SK3 primary antibody (A) (panel B shows negative control, where primary antibody was omitted). Panel C shows a positive control carried out in rSK3-transfected HEK cells. In each case the primary antibody has been detected using a Cy3-conjugated secondary antibody (also present in the negative control). Corresponding bright-field and red fluorescence images are displayed in the left and right panels, respectively. Scale bars: 50μm (A) and 20μm (B&C). Arrows in panel B indicate rounded cells similar to those stained in panel A.

## 6.4) IK protein expression

IK1 expression was determined using both the M4 (anti hIK1) and R212 (anti rIK1) primary antibodies (see *appendix iii* for epitopes).

Though experiments were repeated on five occasions using each antibody at dilutions between 1:20 and 1:200, no above-background fluorescence was detected in pig coronary artery endothelial cells.

In positive controls, primary antibody specific membrane-delimited fluorescence was detected only in HEK cells transfected with the corresponding IK1 orthologue (*figures 6.3 & 6.4*) (1:200 dilution used for both antibodies).

Since the target epitope of neither antibody is an exact match for the corresponding pig IK1 amino acid sequence, the lack of above-background staining may be due to poor binding of the primary antibodies.

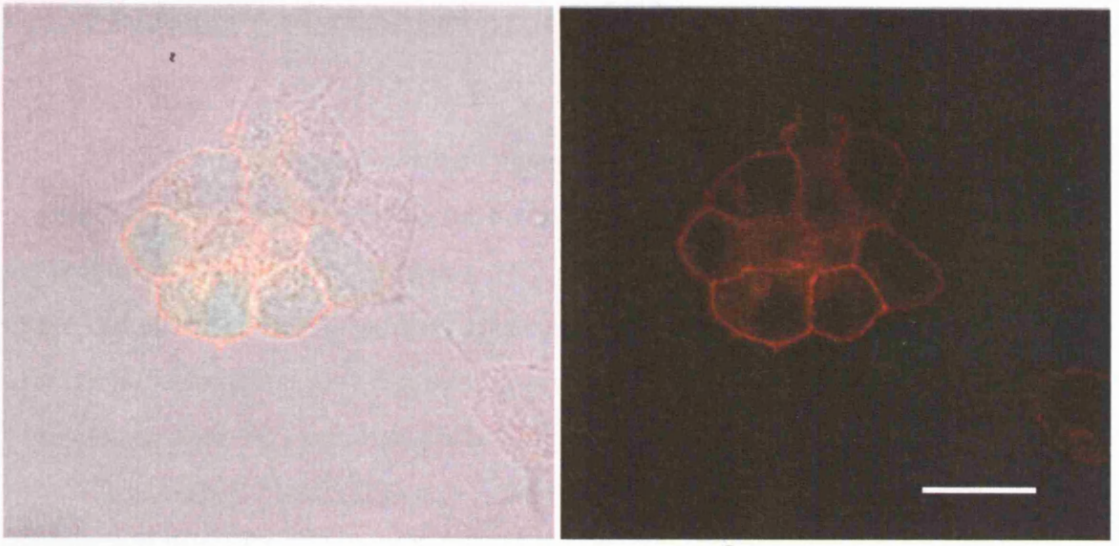

**Figure 6.3)** Immunostaining of hIK1/GFP co-transfected HEK cells using the M4 primary antibody. The primary antibody has been detected using a Cy3-conjugated secondary antibody. Corresponding bright-field/fluorescence overlay and red fluorescence images are displayed in the left and right panels, respectively. Scale bar: 20μm.

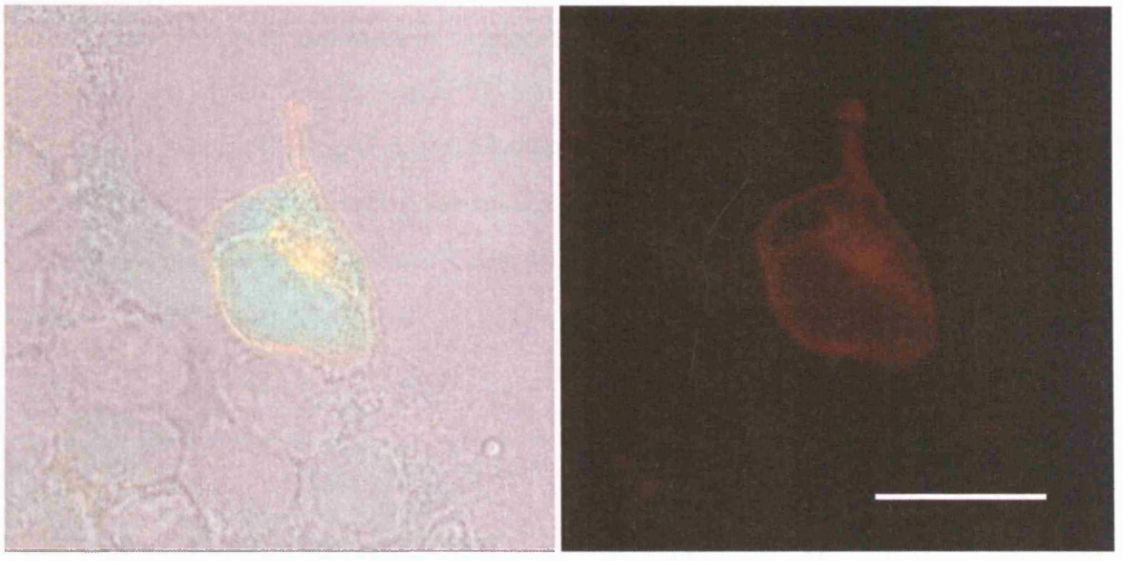

**Figure 6.4)** Immunostaining of an rIK1/GFP co-transfected HEK cell using the R212 primary antibody. The primary antibody has been detected using a Cy3-conjugated secondary antibody. Corresponding bright-field/fluorescence overlay and red fluorescence images are displayed in the left and right panels, respectively. Scale bar: 20μm.

## 6.5) Summary of channel protein expression data

These studies have provided evidence of SK3 channel protein expression in pig coronary artery endothelial cells, however antibody staining did not demonstrate the presence of SK2 or IK1 proteins. SK2 and SK3 have previously been identified in the endothelium of pig coronary artery sections, using fluorescence immunohistochemistry and Western blotting (Burnham *et al.*, 2002). IK1 has also been cloned from the same preparation (Bychkov *et al.*, 2002).

The reasons that SK2 and IK1 were not detected in the present study are unclear, but the antibodies used have previously been shown to selectively label the respective channel proteins (Chen *et al.*, 2004; Bahia *et al.*, 2005). Although the porcine SK2 amino acid sequence has not been published, the epitope to which the anti-SK2 antibody is raised (see *appendix i*) is completely conserved between human, rat, mouse, bovine, and chicken orthologues. It is likely therefore that porcine SK2 will also contain this sequence. The epitopes to which the IK1 antibodies are raised (see *appendix iii*) are only partially conserved in the porcine IK1 orthologue, indicating that these antibodies may not bind well. Failure to detect fluorescence in cells exposed to the SK2 and IK1 antibodies may also have resulted from a low channel density exacerbated by the narrow cross-section of the cultured cells.

# Chapter 7: Discussion

## 7.1 Foreword

For the past twenty-five years, our laboratory has had an interest in calcium-activated potassium channels, in particular the $SK_{Ca}$ and $IK_{Ca}$ subtypes.

In the mid-1990's, pharmacological evidence began to emerge of the involvement of $SK_{Ca}$ and $IK_{Ca}$ channels in EDHF-mediated vasodilation. At this time, the relevant channels were believed to be located on vascular smooth muscle cells. However, their location was later reconsidered and is now thought to be the endothelium, consistent with earlier studies of endothelial cell electrophysiology.

Of particular interest was the frequent observation that neither apamin nor charybdotoxin affected EDHF responses when applied alone, yet abolished when administered in combination. This led to speculation in the literature that these toxins may target a single novel channel with highly unusual pharmacology.

At the outset of this project in 2001, there were few published studies of the $SK_{Ca}$ and $IK_{Ca}$ currents which underlay EDHF. Up to this time, the majority of conclusions regarding $SK_{Ca}$ and $IK_{Ca}$ contribution to the EDHF pathway stemmed from the high selectivity of the peptide blockers apamin, charybdotoxin and (to distinguish $IK_{Ca}$ from $BK_{Ca}$) iberiotoxin.

It was therefore intended that this study should shed light on the relative contribution of $SK_{Ca}$, $IK_{Ca}$ and any novel $K_{Ca}$ channel to agonist-evoked endothelial cell hyperpolarisation. It was also our intention to identify which of the three $SK_{Ca}$ channel proteins are expressed in vascular endothelial cells.

## 7.2) Choice of tissue preparation

At the outset of the study it was undecided whether endothelial cells should be investigated immediately following isolation, or established as primary cultures. Acute study ensures that the cell phenotype is preserved, but dispersal of cells using proteolytic enzymes risks modifying or even destroying cell-surface receptors. The advantage of primary culture is that it can provide a convenient source of cells over a period of days. However protein expression may alter during culture. $BK_{Ca}$ channels for example are not expressed in endothelium freshly isolated from bovine coronary arteries, yet appear following several days of primary culture (Gauthier *et al.*, 2002b). Conversely, in some endothelial cells, agonist-evoked potassium currents begin to disappear after a few days in culture (Frieden *et al.*, 1999; Ahn *et al.*, 2004).

Endothelial cells were sourced from vascular beds in which EDHF-mediated vasodilation had been established. Initial efforts were focussed on isolating cells from rat superior mesenteric artery and to a lesser extent rat aorta and carotid artery. Numerous unsuccessful attempts were made at enzymatic dispersal of endothelial cells from these vessels. Protocols were followed or adapted from the few published accounts of endothelial cell isolation from small mammal vessels. Subsequent attempts at mechanical isolation were similarly without success.

An alternative method of producing isolated rat vascular endothelial cells is by way of explant culture (McGuire & Orkin, 1987). In the present study, explant cultures gave rise to large yields of cells morphologically similar to those pictured in the McGuire & Orkin paper. These cells did not, however, give rise to the electrophysiological responses expected from endothelial cells, and moreover did not internalise aLDL or express von Willebrand factor. Based on these findings, it was concluded that the explant cells were not of an endothelial phenotype and more likely to be fibroblasts or smooth muscle cells. It is noted that similar methods are commonly used for the purpose of culturing smooth muscle cells.

In light of continued difficulties with isolating rat endothelial cells, an alternative vascular bed was considered. Published work suggested that porcine or bovine arteries may be a suitable source of endothelium, and that vessels of large mammals are particularly suited to endothelial cell isolation.

Pig coronary arteries were selected because endothelial $SK_{Ca}$ and $IK_{Ca}$ channels had recently been reported in this vascular bed (Frieden *et al.*, 1999; Burnham *et al.*, 2002; Sollini *et al.*, 2002; Bychkov *et al.*, 2002). Owing to the time consuming process of collecting the tissue, it was considered more economical to establish primary cultures rather than to attempt studies on acutely isolated cells. Concurrent with the literature, pig coronary artery endothelial cells proved straightforward to culture, and their identity was subsequently confirmed through their ability to internalise aLDL.

## 7.3) Contribution of $SK_{Ca}$ and $IK_{Ca}$ channels to calcium mediated changes in endothelial cell membrane potential

Initially, large rafts of cells were exposed to various 'EDHF-activating' agonists which each evoked substantial hyperpolarisations.

Interestingly, it was noted that bradykinin evoked significantly larger hyperpolarisations than either ATP or substance P, consistent with a previous study in which bradykinin caused a larger rise in cytosolic calcium than substance P (Frieden *et al.*, 1999). During current-clamp studies it was also determined that hyperpolarisations to each of the agonists were predominantly due an increase in potassium ion conductance. However, the peak hyperpolarisation was less negative than $E_K$. Replacing chloride by a less permeant anion increased the amplitude of responses suggesting that the peak hyperpolarisation may have been limited by chloride conductances.

In voltage-clamp studies of small cell clusters, ATP, 1-EBIO and 1.5μM intracellular calcium each evoked outward whole-cell currents. Current-voltage relationships of these were consistent with a predominant activation of potassium conductances.

The potent novel $SK_{Ca}$ channel blocker, UCL 1848 maximally blocked ~65% of ATP-evoked outward currents and 36-86% of 1-EBIO-activated currents (range given as only three cells were studied). In cells dialysed with 1.5μM free-calcium, UCL 1848 blocked net-outward currents by a variable degree with a mean block of only 28%. The difference in % current block according to the method of activation is

possibly due to 1.5μM calcium failing to activate the entire $SK_{Ca}$ channel population (see *section 5.5.4* for comment).

The $IK_{Ca}/BK_{Ca}$ channel blocker charybdotoxin maximally blocked ~85% of ATP-evoked currents but abolished net-outward currents in cells dialysed with 1.5μM free-calcium. That charybdotoxin blocked the entire net-outward current was unexpected. However it is possible that in these cells, as with others, there was little or no UCL 1848-sensitive component present. Alternatively, any small UCL 1848-sensitive component may have been masked by an inward component of the activated current, and was not therefore observed.

Although there have been no detailed pharmacological studies of $BK_{Ca}$ channel contribution to ATP-evoked currents in pig coronary artery endothelial cells, currents evoked by substance P are known to be insensitive to iberiotoxin (Frieden *et al.*, 1999; Bychkov *et al.*, 2002). ATP-evoked currents recorded from cultured mouse aortic endothelial cells are also insensitive to iberiotoxin (Ahn *et al.*, 2004). On the other hand, bradykinin, which in this study evoked hyperpolarisations distinct from those of ATP and substance P, has been shown to evoke iberiotoxin-sensitive currents in cultured pig coronary artery endothelial cells (Frieden *et al.*, 1999). This finding has since been challenged, however, in a study of freshly isolated pig coronary artery endothelium (Bychkov *et al.*, 2002). Based on the available evidence, it would seem unlikely that $BK_{Ca}$ channels contributed to ATP-evoked currents in the present work. As $BK_{Ca}$ channels have nevertheless been reported in pig coronary artery endothelial cells, their contribution to calcium-dialysis -activated currents was investigated. 100nM iberiotoxin blocked ~30% of the current indicating that $BK_{Ca}$ channels were active under these conditions.

Clotrimazole was applied to cells on account of its $IK_{Ca}$ blocking activity, but appeared to inhibit both charybdotoxin- and UCL 1848-sensitive currents. This was true of currents evoked by ATP, 1-EBIO and calcium-dialysis. The finding was unexpected and is not easily explained (see *section 7.4.5* for discussion). Further work would be needed to determine whether this finding relates to a genuine novel effect of clotrimazole on porcine $SK_{Ca}$ channels, or is an experimental anomaly.

Rundown of ATP-evoked currents made the measurement of block particularly difficult. Both UCL 1848 and charybdotoxin inhibition were, however, measured and analysed using the same criteria. The calculated block of 65% and 85% by UCL 1848 and charybdotoxin, respectively, is therefore a likely reflection of

relative contribution of $SK_{Ca}$ and $IK_{Ca}$ channels to ATP-evoked currents, though some uncertainty remains. The overlap of block in response to UCL 1848 and charybdotoxin is further considered in *section 7.4.4.*

In relation to the subtype of $SK_{Ca}$ channels expressed in pig coronary artery endothelial cells, the $IC_{50}$ for UCL 1848-sensitivity of the ATP-evoked outward current (1.2nM) is close to that for block of cloned rSK3 (2.1nM) (Hosseini *et al.*, 2001) and hSK1 (1.1nM) (Shah & Haylett, 2000) channels. The published $IC_{50}$ for UCL 1848 block of rSK2 channels is 0.1nM (Hosseini *et al.*, 2001).

Additionally, using fluorescence immunohistochemistry, it was possible to identify expression of SK3 proteins in cells cultured for this study. This is in agreement with the recent cloning of SK3 from the endothelium of pig coronary arteries (Burnham *et al.*, 2002).

## 7.4) Issues raised during the present studies

### 7.4.1) Low resting membrane potentials

The resting membrane potential ($E_m$) of endothelial cells is reported to vary considerably according to originating species and vascular bed (ranging from 0 to -80mV) (Nilius & Droogmans, 2001). $E_m$s recorded in the present study (mean -5.9mV), however, were considerably lower than those reported in published studies of isolated pig coronary artery endothelial cells (*table 7.1*). Values recorded in the present study were consistent in all ~100 batches of cells cultured; standard deviation of mean $E_m$ was low, and no outliers were excluded. Furthermore, no significant difference was found between $E_m$ of cells cultured for two and four days (refer to *figure 5.1*).

To establish the cause of low membrane potentials, culture media and experimental salt solutions were in turn substituted for those used in a published study of cultured pig coronary artery endothelial cells (reported mean $E_m$ -29.7mV) (Sollini *et al.*, 2002). Neither substitution made a difference to $E_m$ values recorded in the present study. When a small number of cells were impaled with KCl-filled

intracellular electrodes, $E_m$s were similar to those recorded under current-clamp conditions (data not shown).

The high input resistance of single endothelial cells is indicative of a low resting conductance. Accordingly, a small change in the number and/or type of open channels will have a large impact on resting membrane potential. Inwardly rectifying potassium channels are generally considered to underlie the negative resting membrane potential of endothelial cells (Nilius & Droogmans, 2001). However when studied under voltage-clamp, small inwardly-rectifying components of whole-cell currents were observed in only ~⅓ of cells (refer to *figure 5.10*).

Whilst it was not established that culture conditions were the reason for low membrane potentials, it seems unlikely that an undetermined difference in animal strain would account for such a change. In the absence of an obvious cause, it is tentatively suggested that a culture-related down-regulation of inwardly rectifying potassium channels may underlie this discrepancy.

| Vessel | Preparation | Method | Mean $E_m$ | Reference |
|---|---|---|---|---|
| LAD/R | 2-5 day culture | IC / CC | -29.7mV | (Sollini *et al.*, 2002) |
| LAD/epi | culture *duration not given* | IC | -32.3mV | (Olanrewaju *et al.*, 2002) |
| LAD/cir | 24hr culture | CC | -42mV | (Sharma & Davis, 1994) |

**Table 7.1)** Mean resting membrane potentials reported in studies of isolated pig coronary artery endothelial cells. Abbreviations: left anterior descending coronary artery (LAD), right coronary artery (R), epicardial coronary artery (epi), circumflex coronary artery (cir), intracellular electrode recording (IC), current-clamp recording (CC), resting membrane potential ($E_m$).

## 7.4.2) Comment on the relationship between potassium permeability and membrane potential

It is frequently reported in studies of EDHF-mediated vasodilation that applying either an $SK_{Ca}$- or an $IK_{Ca}$-channel blocker makes little difference to smooth muscle hyperpolarisation and vasodilation, yet when the same blockers are applied in combination, EDHF responses are abolished. Though it has been suggested that this may imply the presence of a novel channel with highly unusual pharmacology, this phenomenon may simply be due to the non-linear relationship between potassium permeability and membrane potential.

To illustrate this, arbitrary values of potassium permeability ($P_K$) can be substituted into the Goldman-Hodgkin-Katz voltage equation, and the relationship between $P_K$ and membrane potential predicted (*figure 7.1*). Because in the present study, ion substitution experiments suggested a contribution by chloride channels to endothelial cell membrane potential, the effect of a constant chloride conductance has been factored into the calculation. Conversely, since sodium substitution made no measurable difference to ATP-evoked hyperpolarisations, a contribution by sodium ions will be disregarded for the sake of simplicity. Values relating to ionic gradients and temperature are based on the standard conditions used in the present study.

Assuming the black trace in *figure 7.1* to be representative of the $P_K$/membrane potential relationship for a given cell, we see that increasing $P_K$ from 0 to 20 results in a hyperpolarisation of 62mV. Further increasing $P_K$ by the same amount again, however, only hyperpolarises the cell by an additional 8mV.

We can apply this relationship to a theoretical cell in which full activation of $IK_{Ca}$ and $SK_{Ca}$ equally contribute to a $P_K$ of 80 (refer to *figure 7.1*). Blocking either the $SK_{Ca}$ or the $IK_{Ca}$ component, hence reducing $P_K$ to 40, only reduces the membrane potential from -78mV to -73mV; a reduction of 6%. Under experimental conditions, this small difference may not even be detectable. Consistent with this, it was noted in the present study that despite a large reduction in ATP-evoked conductance when cells were cultured for more than two days, ATP still evoked large hyperpolarisations in cells cultured for three days.

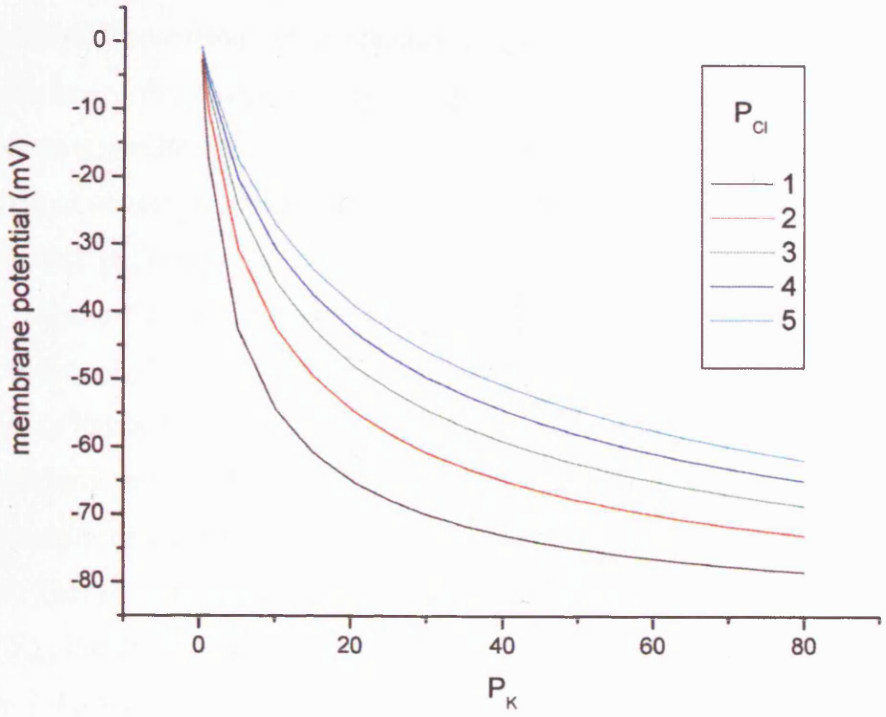


**Figure 7.1)** The relationship between $P_K$ and membrane potential, accounting for different values of $P_{Cl}$. Each curve is plotted using the modified GHK equation given below. Values used were: thermodynamic gas constant (R) 8.31 J/K/mol, temperature (T) 298°K, Faraday's constant (F) 96500 C/mol, external potassium ion concentration ($[K^+]_o$) 5mM, internal potassium ion concentration ($[K^+]_i$) 140mM, external chloride ion concentration ($[Cl^-]_o$) 135mM, internal chloride ion concentration ($[Cl^-]_i$) 134mM. Other abbreviations: reversal potential ($E_{rev}$), potassium ion permeability ($P_K$), chloride ion permeability ($P_{Cl}$).

Goldman-Hodgkin-Katz voltage equation: $$E_{rev} = \frac{RT}{F} \ln \frac{P_K[K^+]_o + P_{Na}[Na^+]_o + P_{Cl}[Cl^-]_i}{P_K[K^+]_i + P_{Na}[Na^+]_i + P_{Cl}[Cl^-]_o}$$

Equation used to construct graphs in *figure 7.1*: $$E_{rev} = \frac{RT}{F} \ln \frac{P_K[K^+]_o + P_{Cl}[Cl^-]_i}{P_K[K^+]_i + P_{Cl}[Cl^-]_o}$$

The relevance of the above modelling on the EDHF response as a whole will depend largely on the events which constitute the remainder of the EDHF response. If endothelial cell membrane potential *per se* is critical, for example in maintaining a driving force for calcium-entry, then this may be a valid explanation of how currents can be partially blocked without affecting smooth muscle relaxation. If however,

EDHF is due to release of potassium ions or the activity of myoendothelial gap junctions, then membrane potential of the endothelium is of less significance than the underlying potassium ion conductance. If this is true then it is more difficult to reconcile how a drop in endothelial cell potassium conductance does not directly translate to a similar reduction in smooth muscle hyperpolarisation and relaxation. This may of course be explained by yet unidentified redundancy further downstream in the EDHF pathway.

*Figure 7.1* also serves to illustrate the effect of a small, constant chloride permeability ($P_{Cl}$) on the $P_K$/membrane potential relationship. Increasing $P_{Cl}$ effectively limits the membrane potential that can be obtained by increasing $P_K$. This is particularly relevant because, in a cell, $P_K$ will be finite. In the present study, in which a chloride conductance was identified, cells rarely hyperpolarised beyond -65mV. This is short of both the calculated $E_K$ (-86mV) and the reversal potential of $SK_{Ca}/IK_{Ca}$ currents (-73 to -75mV; measured in voltage-clamp experiments, see *section 7.4.3* for comment).

## 7.4.3) Possible changes in $E_K$ consequent on potassium channel activation

The calculated $E_K$ for experiments in which ATP-evoked currents were studied was -86mV, however the *measured* mean reversal potential for ATP-evoked currents was -72mV. It was initially supposed that this discrepancy could for example be due to the chloride conductance identified in current-clamp studies, however currents blocked by UCL 1848, charybdotoxin and clotrimazole, or activated by 1-EBIO also reversed in the region of -72 to -75mV. Interestingly, similar discrepancies in $E_K$ are apparent in comparable published studies, but often receive little comment. A recent study of mouse aortic endothelial cells has, however, questioned the selectivity of identified $IK_{Ca}$ channels (Ahn *et al.*, 2004).

In the present study CVRs were determined at the plateau of each ATP response, hence several seconds into the outward current. $E_K$ may therefore have changed as a consequence of the sustained outflow of potassium ions.

This can be considered as follows:

Based on the volume of a disc 20μm in diameter and 1μm in depth, an endothelial cell would have an approximate volume of 300fl. During the plateau of a 200pA outward holding current (typical for a single cell), it is calculated that a cell would lose intracellular potassium at an initial rate of ~5%/s. Whilst potassium from the patch electrode would counteract this loss, constant flux of potassium ions may also raise the external potassium concentration in a localised region immediately outside the cell perimeter.

Although it would be difficult to calculate accurately the diffusion of potassium from the patch electrode into the cell and the localised external potassium concentration in a flowing bath, the effect of small potassium concentration adjustments on $E_K$ can be considered.

The values in *table 7.2* demonstrate that relatively small changes in intracellular and/or localised extracellular potassium concentration could shift $E_K$ by +10mV.

One expectation of this phenomenon is that any shift in $E_K$ will be proportional to the potassium conductance of a given cell. In the present study, however, no such correlation was identified. It is unclear therefore whether potassium flux accounts for the discrepancies in potassium reversal potential reported in the present study.

Nernst equation for calculating reversal potential of a given ion (X): $E_X = \frac{RT}{zF} \ln \frac{[X^+]_o}{[X^+]_i}$

Equation used to derive values in table 7.2: $E_K = \frac{RT}{F} \ln \frac{[K^+]_o}{[K^+]_i}$

| $[K^+]_o$ (mM) *localised* | $[K^+]_i$ (mM) | $E_K$ (mV) |
|---|---|---|
| 8 | 140 | -73 |
| 7 | 130 | -75 |
| 6 | 110 | -75 |
| 5 | 90 | -74 |

**Table 7.2)** The effect of altering localised potassium gradient on values of $E_K$. Values were calculated using the Nernst equation for potassium ions given on the previous page. Values used were: thermodynamic gas constant (R) 8.31 J/K/mol, temperature (T) 298°K, Faraday's constant (F) 96500 C/mol. Other abbreviations: reversal potential for potassium (or ion X) ($E_{K\,(or\,X)}$), valency (V), external concentration of potassium (or ion X) ($[K^+$ (or X)$]_o$), internal concentration of potassium (or ion X) ($[K^+$ (or X)$]_i$).

## 7.4.4) Overlap of UCL 1848- and charybdotoxin-sensitive current components

In the present study, UCL 1848 and charybdotoxin maximally blocked ATP-evoked whole cell currents by 65 and 85%, respectively. As previously discussed, these agents are believed to be reasonably selective for $SK_{Ca}$ and $IK_{Ca}$ channels, respectively, at the concentrations used (*table 5.6*). As blockers were always studied in different cells, the apparent overlap in block between the two agents may simply be due to intercellular variability of the relative proportion of $SK_{Ca}$ and $IK_{Ca}$ channels. However, this overlap is worthy of consideration, not least because similar findings have been reported in another study. In two separate publications on cultured pig coronary artery endothelial cells, Bény and colleagues have reported that 1μM apamin and 50nM charybdotoxin block substance P-evoked currents by 65% and 80%, respectively (Frieden *et al.*, 1999; Sollini *et al.*, 2002).

In light of these findings, it is tempting to speculate on the existence of heteromeric $K_{Ca}$ channels which comprise both $SK_{Ca}$ and $IK_{Ca}$ subunits, and are sensitive to both $SK_{Ca}$ and $IK_{Ca}$ channel blockers. At present, however, there is no

published evidence that such channels exist; indeed preliminary data from our laboratory suggest that when co-transfected into HEK cells, cloned hIK1 subunits do not co-assemble with hSK1 (Monaghan *et al.*, 2004) or hSK2 (unpublished observations by YA Shah).

### 7.4.5) Sensitivity of $SK_{Ca}$ channels to clotrimazole

In the present study, clotrimazole was applied to cells with the intention of selectively blocking $IK_{Ca}$ channels. The resulting data, however, suggests that at 1 and 10μM, clotrimazole also substantially blocked the UCL 1848-sensitive component. This was surprising because, compared to $IK_{Ca}$ channels, $SK_{Ca}$ channels are regarded as relatively insensitive to clotrimazole ($IC_{50}$s: 21μM (hSK2), 28μM (hSK3) (Wulff *et al.*, 2000), insensitive to 10μM (hSK3) (Carignani *et al.*, 2002)).

As the clotrimazole-sensitivity of pig $SK_{Ca}$ channels has not been studied elsewhere, it was considered whether porcine SK3 (cloned from pig coronary artery endothelium) may contain a binding site for clotrimazole. Two amino acid residues located in the pore-forming region (threonine$^{250}$) and the S6 transmembrane domain (valine$^{275}$) of the IK1 protein have recently been identified as necessary for clotrimazole sensitivity of $IK_{Ca}$ channels (Wulff *et al.*, 2001). These residues are not, however, present in the porcine SK3 orthologue (Burnham *et al.*, 2002). In fact, so conserved is the SK3 sequence between species that the amino acid sequence is identical between porcine, human and rat orthologues in all but the N and C termini. In total, porcine SK3 is 93% identical to the human orthologue. On the basis of sequence therefore, there is little reason to suppose that porcine SK3 would be any more susceptible to clotrimazole block than the human or rat orthologues.

On account of its cP450 blocking activity, a number of studies have investigated the clotrimazole sensitivity of EDHF-mediated vasodilation. In pig coronary arteries, 3μM clotrimazole reportedly abolished bradykinin-evoked EDHF-mediated dilation in one study (Popp *et al.*, 1996), yet in others concentrations of 10-100μM caused only partial inhibition (Hecker *et al.*, 1994; Weintraub *et al.*, 1994; Ishizaka & Kuo, 1997). This is inconsistent with the present findings because the

activity of endothelial $SK_{Ca}$ and $IK_{Ca}$ channels appears to be essential for EDHF-mediated vasodilation.

It has been reported in voltage-clamped mouse aortic endothelial cells that both clotrimazole and charybdotoxin unexpectedly inhibit ATP-evoked rises in cytosolic calcium (Ahn *et al.*, 2004). If this occurred in the present study, it could account for the absence of an $SK_{Ca}$ channel component of ATP-evoked currents. However, clotrimazole also blocked a substantial portion of the UCL 1848-sensitive current in cells stimulated with 1-EBIO or dialysed with 1.5μM free-calcium.

One further consideration is that clotrimazole was dissolved in DMSO, so when applied at 10μM, cells would have been exposed to 0.1% solvent. Although no vehicle controls were performed in the present studies, this concentration of DMSO has no noticeable effect on cloned human or rat $SK_{Ca}$ channel subunits expressed in HEK cells (unpublished observations by DCH Benton).

The reason for clotrimazole-inhibition of UCL 1848-sensitive currents therefore remains unresolved.

## 7.5) Difficulties encountered

Though pig coronary artery endothelial cells were cultured with a high success rate, electrophysiological studies were challenging in the extreme. In terms of obtaining recordings, the ability of electrodes to form gigaseals with cells varied considerably, as did the ease of conversion into whole-cell configuration. Cells from many apparently healthy cultures were simply 'un-patchable'.

In all electrophysiology studies, electrodes were mounted on water- or oil-filled micromanipulators. The sub-micron drift associated with this equipment is barely noticeable when studying large cells such as neurones or cell lines, however, this movement proved destructive when recording from endothelial cells with a depth of ~1μm. A countless number of recordings were lost due to this problem.

Rundown of agonist-evoked responses was perhaps the most frustrating of issues since this affected recordings in which whole-cell configuration had been achieved *and* maintained for several minutes. In preliminary studies, it was ascertained that rundown still occurred when ATP was included in the intracellular

solution. The perforated patch technique often allows more stable recordings and was also attempted; but despite many attempts, successful recordings were not achieved.

Electrophysiological studies remained demanding throughout, particularly where recording stability was required for more than a couple of minutes. In particular, it took several months to record data sufficient to construct concentration-inhibition relationships for block of ATP-evoked currents. The slow rate of progress meant that I was regrettably unable to pursue investigation of novel channel-blocking compounds and carry out further biochemical studies.

## 7.6) Future studies

To more satisfactorily answer questions raised in this study, a number of further experiments would be necessary.

In order to carry out further electrophysiological work, it would be economical to improve conditions related to recording stability and response rundown. This would include the use of low-drift micromanipulators, and further attempts at using the perforated patch technique. Altering culture conditions with the aim of reducing channel down-regulation would also be beneficial.

It would be a valuable exercise to study the effects of UCL 1848 and charybdotoxin on ATP-evoked hyperpolarisation. It is likely that activation of only a portion of channels is necessary for maximal hyperpolarisation; therefore it would be interesting to determine whether a full response is possible when either $SK_{Ca}$ or $IK_{Ca}$ channels are fully blocked.

The apparent sensitivity of $SK_{Ca}$ channels to clotrimazole suggested in the present study requires further investigation. It would be useful therefore to establish more precisely the concentration-inhibition curve for clotrimazole block of ATP-evoked currents. This would include studying clotrimazole at concentrations of 0.3 and 3μM to enable curve fitting of the concentration-inhibition relationship. Direct application of clotrimazole to isolated pig coronary artery endothelial cell membrane patches containing $SK_{Ca}$ channels, could further help in the explanation of this finding.

Although it is not believed that ATP-evoked currents comprise a $BK_{Ca}$ channel component, this could be simply verified using iberiotoxin. Additionally, charybdotoxin block of ATP-evoked currents should be further studied at sub-maximal concentrations to fully determine the concentration-inhibition relationship.

In addition to $SK_{Ca}$ channel blocking agents such as UCL 1848 and UCL 1684, our laboratory has contributed to the design of potential $IK_{Ca}$ channel blockers (Roxburgh *et al.*, 2001). A number of these compounds have yet to be fully characterised, so it would be interesting to investigate the pharmacology of these agents on pig coronary artery endothelial cells and EDHF-mediated vasodilation.

Despite only partial success with fluorescence immunohistochemistry studies, using the same primary antibodies for Western blot experiments would be likely to overcome potential detection problems caused by low expression of protein. If, as determined by Burnham *et al.*, the SK2 as well as the SK3 channel protein is found to be present, it would be useful to clone and sequence this channel.

## 7.7) Concluding remarks

At the outset of this study, the majority of published electrophysiological data regarding EDHF-mediated vasodilation were limited to measurements of smooth muscle cell hyperpolarisation. Over the past few years however, single channel electrophysiology and protein expression studies have confirmed the presence of $SK_{Ca}$ and/or $IK_{Ca}$ channels in the endothelium of rat aorta (Marchenko & Sage, 1996), human mesenteric artery (Kohler *et al.*, 2000) rat carotid artery (Kohler *et al.*, 2001), pig coronary artery (Burnham *et al.*, 2002; Bychkov *et al.*, 2002), mouse mesenteric artery (Taylor *et al.*, 2003) and mouse aorta (Ahn *et al.*, 2004). In vessels where $SK_{Ca}$ channels are present, SK3 but not SK1 protein has been detected. SK2 expression, however, appears to be varied, being absent in rat carotid artery endothelium (Kohler *et al.*, 2001), present only in the nuclear region of pig coronary artery endothelium (Burnham *et al.*, 2002), and becomes up-regulated in human saphenous vein endothelial cells exposed to shear stress (Sultan *et al.*, 2004).

The lack of endothelial $SK_{Ca}$ channels in some vascular beds is consistent with EDHF-mediated vasodilation being completely inhibited by charybdotoxin in these vessels.

It still remains the case that few studies have investigated the contribution of $SK_{Ca}$ and $IK_{Ca}$ channels to endothelial whole-cell currents. Unlike single-channel studies which can be performed on isolated membrane patches, whole-cell voltage-clamp experiments require separation of individual endothelial cells. As discussed in this thesis, this can be technically difficult and culturing endothelial cells is not without drawbacks. Just as important, the geometry of endothelial cells makes their study a daunting prospect for electrophysiologists.

# Appendix i

Amino acid sequence alignment for the human (h) and rat (r) orthologues of SK2 (pig SK2 has yet to be identified)

```
hSK2 MSSCRYNGGVMRPLSNLSASRRNLHEMDSEAQPLQPPAS-VGGGGGASSPSAAAAAAAAV 59
rSK2 MSSCRYNGGVMRPLSNLSSSRRNLHEMDSEAQPLQPPASVVGGGGGASSP----SAAAAA 56
     ******************:******************** **********     :****.

hSK2 SSSAPEIVVSKPEHNNSNNLALYGTGGGGSTGGGGGGGG----SGHGSSSGTKSSKKKNQ 115
rSK2 SSSAPEIVVSKPEHNNSNNLALYGTGGGGSTGGGGGGGGGGGSGHGSSSGTKSSKKKNQ 116
     ************************************    ****************

                                  TMD 1
hSK2 NIGYKLGHRRALFEKRKRLSDYALIFGMFGIVVMVIETELSWGAYDKASLYSLALKCLIS 175
rSK2 NIGYKLGHRRALFEKRKRLSDYALIFGMFGIVVMVIETELSWGAYDKASLYSLALKCLIS 176
     ************************************************************
          TMD 2                                        TMD 3
hSK2 LSTIILLGLIIVYHAREIQLFMVDNGADDWRIAMTYERIFFICLEILVCAIHPIPGNYTF 235
rSK2 LSTIILLGLIIVYHAREIQLFMVDNGADDWRIAMTYERIFFICLEILVCAIHPIPGNYTF 236
     ***************************************************************
                                  TMD 4
hSK2 TWTARLAFSYAPSTTTADVDIILSIPMFLRLYLIARVMLLHSKLFTDASSRSIGALNKIN 295
rSK2 TWTARLAFSYAPSTTTADVDIILSIPMFLRLYLIARVMLLHSKLFTDASSRSIGALNKIN 296
     **************************************************************
                                  TMD 5
hSK2 FNTRFVMKTLMTICPGTVLLVFSISLWIIAAWTVRACERYHDQQDVTSNFLGAMWLISIT 355
rSK2 FNTRFVMKTLMTICPGTVLLVFSISLWIIAAWTVRACERYHDQQDVTSNFLGAMWLISIT 356
     ******************************************************************
            P-loop                        TMD 6
hSK2 FLSIGYGDMVPNTYCGKGVCLLTGIMGAGCTALVVAVVARKLELTKAEKHVHNFMMDTQL 415
rSK2 FLSIGYGDMVPNTYCGKGVCLLTGIMGAGCTALVVAVVARKLELTKAEKHVHNFMMDTQL 416
     ****************************************************************

hSK2 TKRVKNAAANVLRETWLIYKNTKLVKKIDHAKVRKHQRKFLQAIHQLRSVKMEQRKLNDQ 475
rSK2 TKRVKNAAANVLRETWLIYKNTKLVKKIDHAKVRKHQRKFLQAIHQLRSVKMEQRKLNDQ 476
     ************************************************************

hSK2 ANTLVDLAKTQNIMYDMISDLNERSEDFEKRIVTLETKLETLIGSIHALPGLISQTIRQQ 535
rSK2 ANTLVDLAKTQNIMYDMISDLNERSEDFEKRIVTLETKLETLIGSIHALPGLISQTIRQQ 536
     ************************************************************

hSK2 QRDFIEAQMESYDKHVTYNAERSRSSSRRRRSSSTAPPTSSESS 579
rSK2 QRDFIETQMENYDKHVTYNAERSRSSSRRRRSSSTAPPTSSESS 580
     ******:***.*********************************
```

Red highlighted region: 'M1' primary antibody designed to recognise this epitope

Green boxes highlight regions encoding trans-membrane domains (TMD) and P-loop

Genbank accession codes for sequences: NP_067627.2 (human) (Jager *et al.*, 2000), U69882 (rat) (Kohler *et al.*, 1996)

Alignment made using ClustalW v.1.82 freeware[12]

[12] www.ebi.ac.uk/clustalw

# Appendix ii

Amino acid sequence alignment for the human (h), pig (p) and rat (r) orthologues of SK3

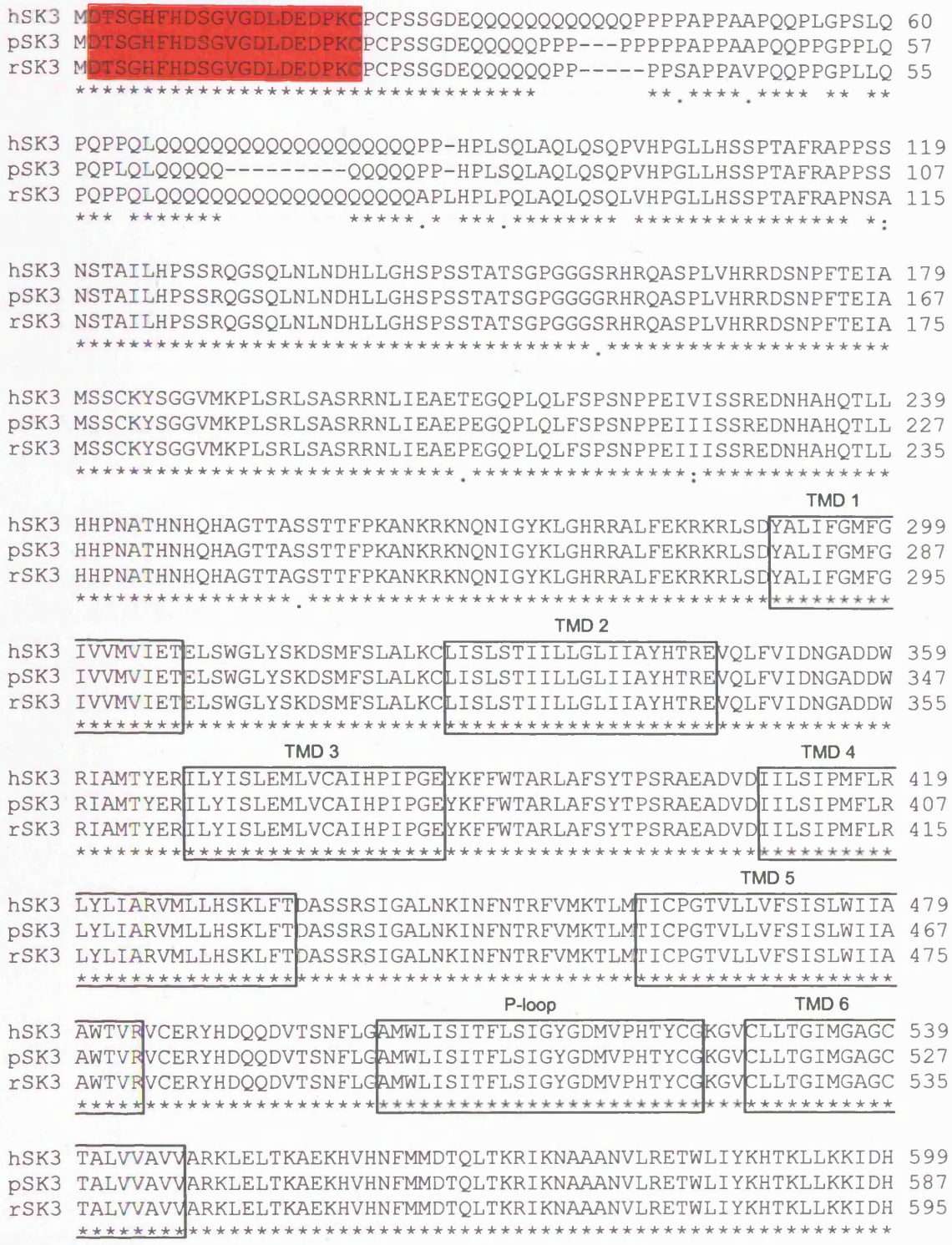


*continued on the following page*

```
hSK3 AKVRKHQRKFLQAIHQLRSVKMEQRKLSDQANTLVDLSKMQNVMYDLITELNDRSEDLEK 659
pSK3 AKVRKHQRKFLQAIHQLRSVKMEQRKLSDQANTLVDLSKMQNVMYDLITELNDRSEDLEK 647
rSK3 AKVRKHQRKFLQAIHQLRGVKMEQRKLSDQANTLVDLSKMQNVMYDLITELNDRSEDLEK 655
     ******************.****************************************

hSK3 QIGSLESKLEHLTASFNSLPLLIADTLRQQQQQLLSAIIEARGVSVAVGTTHTPISDSPI 719
pSK3 QIGSLESKLEHLTASFNSLPLLIADTLRQQQQQLLSALMEARGVSVAVGTTHTPLSDSPI 707
rSK3 QIGSLESKLEHLTASFNSLPLLIADTLRQQQQQLLTAFVEARGISVAVGTSHAPPSDSPI 715
     ************************************:*::****:******:*:* *****

hSK3 GVSSTSFPTPYTSSSSC 736
pSK3 GVSSTSFPTPYTSSSSC 724
rSK3 GISSTSFPTPYTSSSSC 732
     *:***************
```

Red highlighted region: 'Chemicon' primary antibody designed to recognise this epitope

Green boxes highlight regions encoding trans-membrane domains (TMD) and P-loop

Genbank accession codes for sequences: CAB61331 (human) (Terstappen *et al.*, 2001), AY038049 (pig) (Burnham *et al.*, 2002), AF292389 (rat) (Hosseini *et al.*, 2001)

Alignment made using ClustalW v.1.82 freeware[13]

[13] www.ebi.ac.uk/clustalw

# Appendix iii

Amino acid sequence alignment for the human (h), pig (p) and rat (r) orthologues of IK1

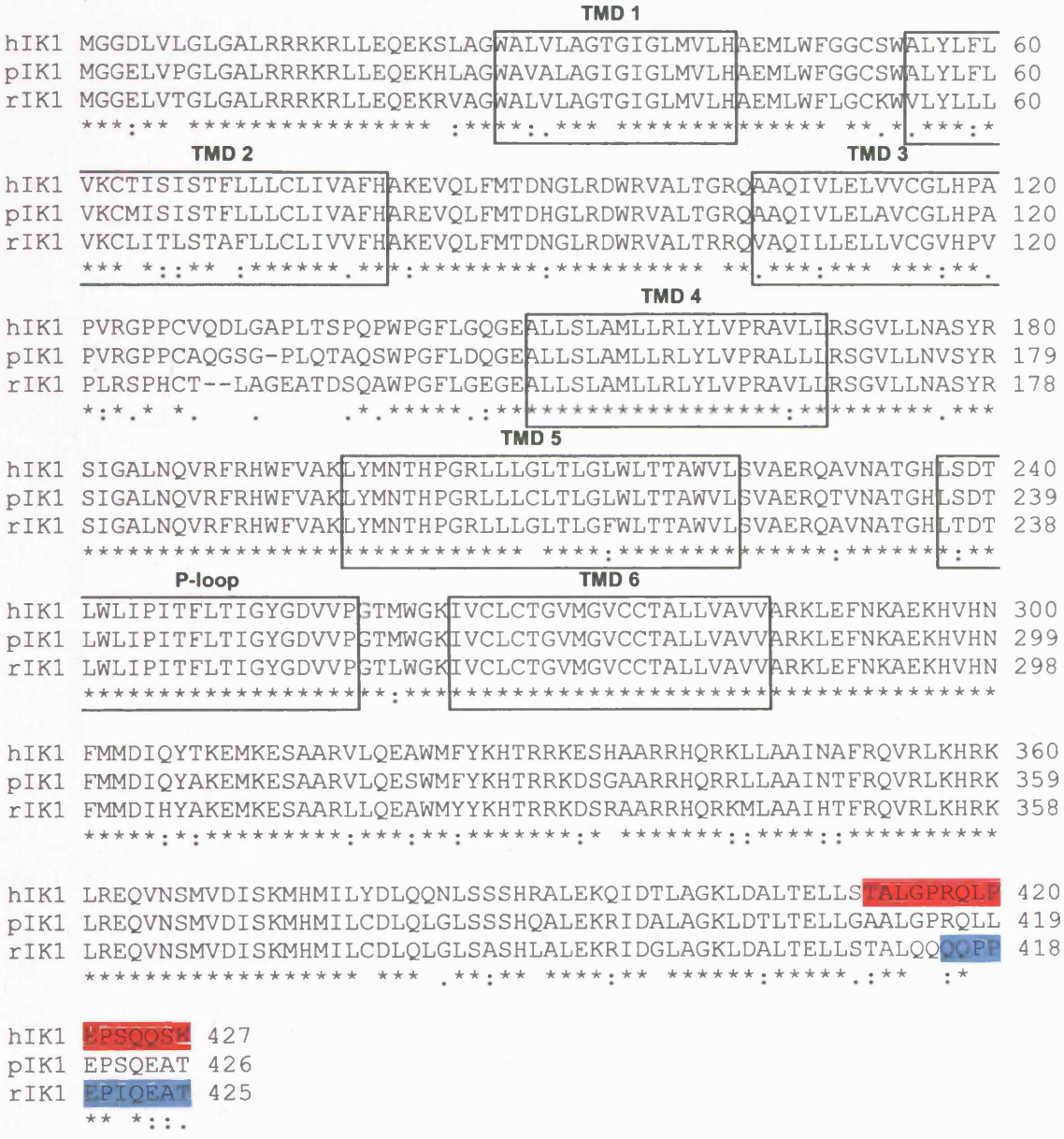


Highlighted regions: 'M4' (red) and 'R212' (turquoise) primary antibodies designed to recognise these epitopes

Green boxes highlight regions encoding trans-membrane domains (TMD) and P-loop

Genbank accession codes for sequences: NP_002241.1 (human) (Joiner *et al.*, 1997), AY062036 (pig) (Bychkov *et al.*, 2002), Q9QYW1 (rat) (Warth *et al.*, 1999)

Alignment made using ClustalW v.1.82 freeware[14]

[14] www.ebi.ac.uk/clustalw

# Appendix iv

As discussed in *section 5.3.1*, transients (see *example 1*), which resulted from a continuously fluctuating series resistance, were removed from all presented voltage-clamp records to aid clarity (see *example 2*). This was achieved by converting traces into graphics files and then manually erasing artefacts using Corel Photopaint software. This was particularly necessary to enable distinction of pulses in traces with a low timebase gain (see *example 3*).

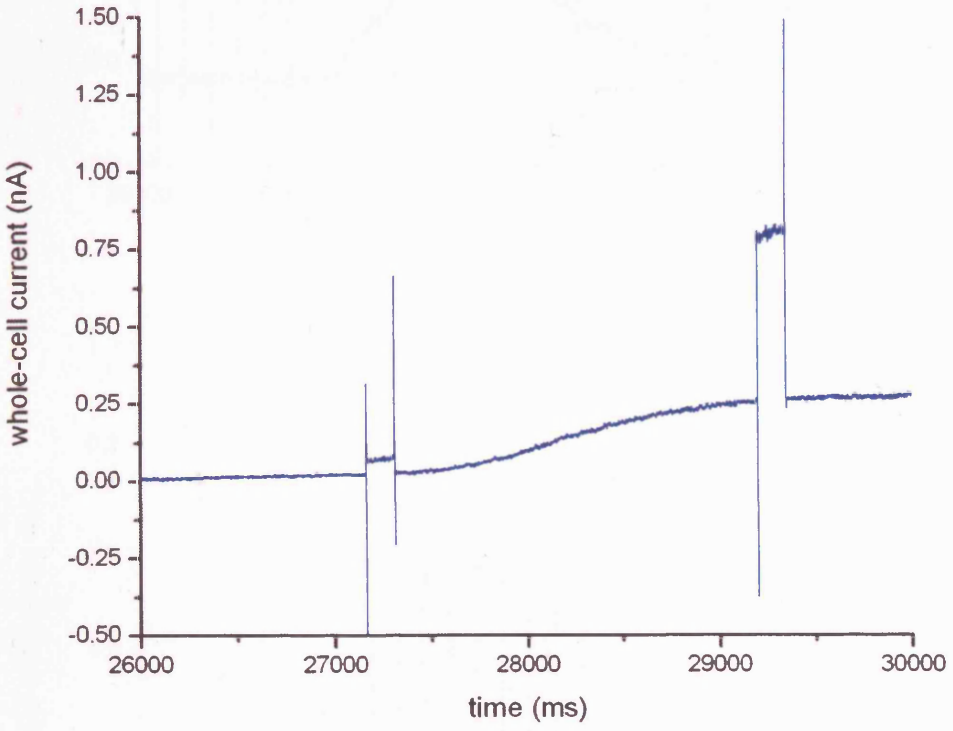


**Example 1)** Series resistance transients displayed at a high timebase gain.

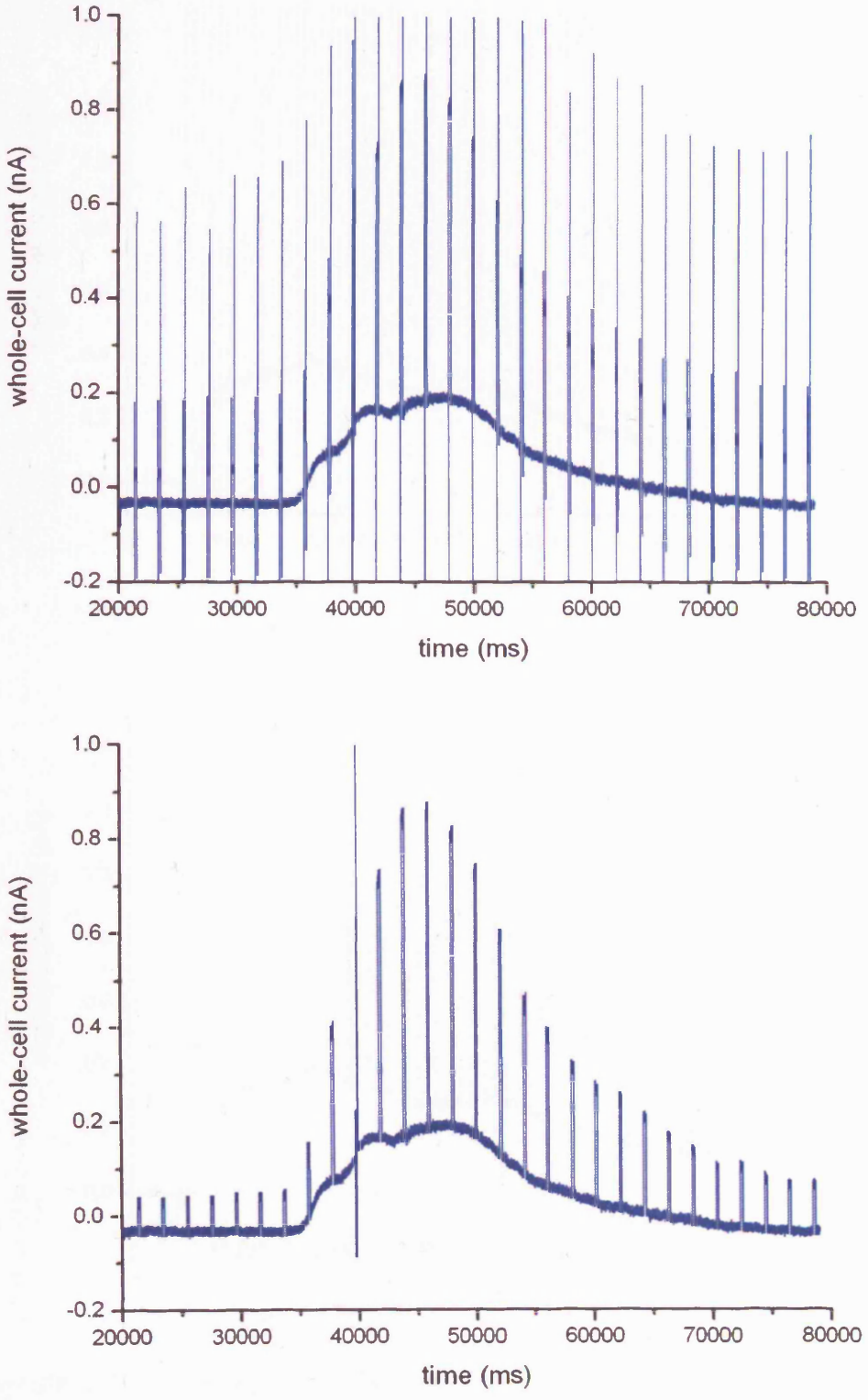


**Example 2)** The trace from *figure 5.13* prior to (upper) and following (lower) removal of transients.

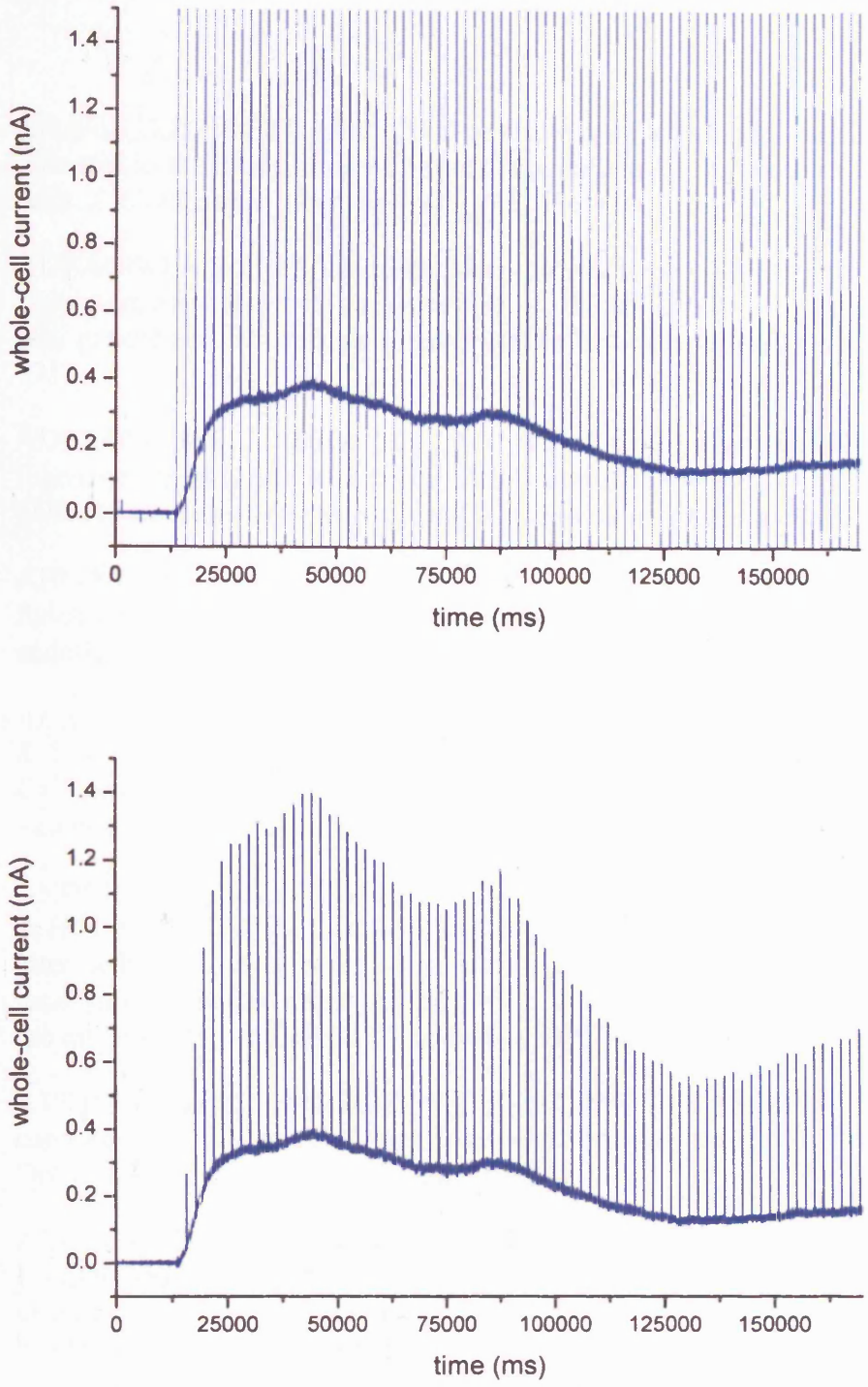


**Example 3)** The trace from *figure 5.37* prior to (upper) and following (lower) removal of transients.

# References


1. ADAMS,D.J. & HILL,M.A. (2004). Potassium channels and membrane potential in the modulation of intracellular calcium in vascular endothelial cells. *J. Cardiovasc. Electrophysiol.*, **15**, 598-610.

2. ADEAGBO,A.S. (1997). Endothelium-derived hyperpolarizing factor: characterization as a cytochrome P450 1A-linked metabolite of arachidonic acid in perfused rat mesenteric prearteriolar bed. *Am. J. Hypertens.*, **10**, 763-771.

3. ADEAGBO,A.S. & TRIGGLE,C.R. (1993). Varying extracellular $K^+$: a functional approach to separating EDHF- and EDNO-related mechanisms in perfused rat mesenteric arterial bed. *J. Cardiovasc. Pharmacol.*, **21**, 423-429.

4. AHN,S.C., SEOL,G.H., KIM,J.A. & SUH,S.H. (2004). Characteristics and a functional implication of $Ca^{2+}$-activated $K^+$ current in mouse aortic endothelial cells. *Pflugers Arch.*, **447**, 426-435.

5. ALIOUA,A., MAHAJAN,A., NISHIMARU,K., ZAREI,M.M., STEFANI,E. & TORO,L. (2002). Coupling of c-Src to large conductance voltage- and $Ca^{2+}$-activated $K^+$ channels as a new mechanism of agonist-induced vasoconstriction. *Proc. Natl. Acad. Sci. U. S. A*, **99**, 14560-14565.

6. ANDERSSON,D.A., ZYGMUNT,P.M., MOVAHED,P., ANDERSSON,T.L. & HÖGESTÄTT,E.D. (2000). Effects of inhibitors of small- and intermediate-conductance calcium-activated potassium channels, inwardly-rectifying potassium channels and $Na^+/K^+$ ATPase on EDHF relaxations in the rat hepatic artery. *Br. J. Pharmacol.*, **129**, 1490-1496.

7. ATKINSON,N.S., ROBERTSON,G.A. & GANETZKY,B. (1991). A component of calcium-activated potassium channels encoded by the Drosophila slo locus. *Science*, **253**, 551-555.

8. AUGUSTE,P., HUGUES,M., MOURRE,C., MOINIER,D., TARTAR,A. & LAZDUNSKI,M. (1992). Scyllatoxin, a blocker of $Ca^{2+}$-activated $K^+$ channels: structure-function relationships and brain localization of the binding sites. *Biochemistry*, **31**, 648-654.

9. BAHIA,P.K., SUZUKI,R., BENTON,D.C., JOWETT,A.J., CHEN,M.X., TREZISE,D.J., DICKENSON,A.H. & MOSS,G.W. (2005). A functional role for small-conductance calcium-activated potassium channels in sensory pathways including nociceptive processes. *J. Neurosci.*, **25**, 3489-3498.

10. BANKS,B.E.C., BROWN,C., BURGESS,G.M., BURNSTOCK,G., CLARET,M., COCKS,T.M. & JENKINSON,D.H. (1979). Apamin blocks certain neurotransmitter-induced increases in potassium permeability. *Nature*, **282**, 415-417.

11. BARON,A., FRIEDEN,M. & BENY,J.L. (1997). Epoxyeicosatrienoic acids activate a high-conductance, $Ca^{2+}$-dependent $K^+$ channel on pig coronary artery endothelial cells. *J. Physiol*, **504** ( Pt 3), 537-543.

12. BARON,A., FRIEDEN,M., CHABAUD,F. & BENY,J.L. (1996). $Ca^{2+}$-dependent non-selective cation and potassium channels activated by bradykinin in pig coronary artery endothelial cells. *J. Physiol*, **493** ( Pt 3), 691-706.

13. BEECH,D.J. & BOLTON,T.B. (1987). The effects of tetraethylammonium ions, 4-aminopyridine or quinidine on $K^+$-currents in single smooth muscle cells of the rabbit portal vein. *Biomed. Biochim. Acta*, **46**, S673-S676.

14. BEGG,M., MO,F.M., OFFERTALER,L., BATKAI,S., PACHER,P., RAZDAN,R.K., LOVINGER,D.M. & KUNOS,G. (2003). G protein-coupled endothelial receptor for atypical cannabinoid ligands modulates a $Ca^{2+}$-dependent $K^+$ current. *J. Biol. Chem.*, **278**, 46188-46194.

15. BENTON,D.C., MONAGHAN,A.S., HOSSEINI,R., BAHIA,P.K., HAYLETT,D.G. & MOSS,G.W. (2003). Small conductance $Ca^{2+}$-activated $K^+$ channels formed by the expression of rat SK1 and SK2 genes in HEK 293 cells. *J. Physiol*, **553**, 13-19.

16. BENY,J.L. & SCHAAD,O. (2000). An evaluation of potassium ions as endothelium-derived hyperpolarizing factor in porcine coronary arteries. *Br. J. Pharmacol.*, **131**, 965-973.

17. BLATZ,A.L. & MAGLEBY,K.L. (1986). Single apamin-blocked Ca-activated $K^+$ channels of small conductance in cultured rat skeletal muscle. *Nature*, **323**, 718-720.

18. BOLTON,T.B., LANG,R.J. & TAKEWAKI,T. (1984). Mechanisms of action of noradrenaline and carbachol on smooth muscle of guinea-pig anterior mesenteric artery. *J. Physiol*, **351**, 549-572.

19. BONDARENKO,A. (2004). Sodium-calcium exchanger contributes to membrane hyperpolarization of intact endothelial cells from rat aorta during acetylcholine stimulation. *Br. J. Pharmacol.*, **143**, 9-18.

20. BRAKEMEIER,S., EICHLER,I., KNORR,A., FASSHEBER,T., KOHLER,R. & HOYER,J. (2003a). Modulation of $Ca^{2+}$-activated $K^+$ channel in renal artery endothelium in situ by nitric oxide and reactive oxygen species. *Kidney Int.*, **64**, 199-207.

21. BRAKEMEIER,S., KERSTEN,A., EICHLER,I., GRGIC,I., ZAKRZEWICZ,A., HOPP,H., KOHLER,R. & HOYER,J. (2003b). Shear stress-induced up-regulation of the intermediate-conductance $Ca^{2+}$-activated $K^+$ channel in human endothelium. *Cardiovasc. Res.*, **60**, 488-496.

22. BRANDES,R.P., POPP,R., OTT,G., BREDENKOTTER,D., WALLNER,C., BUSSE,R. & FLEMING,I. (2002). The extracellular regulated kinases (ERK) 1/2 mediate cannabinoid-induced inhibition of gap junctional communication in endothelial cells. *Br. J. Pharmacol.*, **136**, 709-716.

23. BRAY,K. & QUAST,U. (1991). Differences in the $K^+$-channels opened by cromakalim, acetylcholine and substance P in rat aorta and porcine coronary artery. *Br. J. Pharmacol.*, **102**, 585-594.

24. BRENNER,R., PEREZ,G.J., BONEV,A.D., ECKMAN,D.M., KOSEK,J.C., WILER,S.W., PATTERSON,A.J., NELSON,M.T. & ALDRICH,R.W. (2000). Vasoregulation by the beta1 subunit of the calcium-activated potassium channel. *Nature*, **407**, 870-876.

25. BURNHAM,M.P., BYCHKOV,R., FELETOU,M., RICHARDS,G.R., VANHOUTTE,P.M., WESTON,A.H. & EDWARDS,G. (2002). Characterization of an apamin-sensitive small-conductance $Ca^{2+}$-activated $K^+$ channel in porcine coronary artery endothelium: relevance to EDHF. *Br. J. Pharmacol.*, **135**, 1133-1143.

26. BUSSE,R., EDWARDS,G., FELETOU,M., FLEMING,I., VANHOUTTE,P.M. & WESTON,A.H. (2002). EDHF: bringing the concepts together. *Trends Pharmacol. Sci.*, **23**, 374-380.

27. BUSSEMAKER,E., WALLNER,C., FISSLTHALER,B. & FLEMING,I. (2002). The Na-K-ATPase is a target for an EDHF displaying characteristics similar to potassium ions in the porcine renal interlobar artery. *Br. J. Pharmacol.*, **137**, 647-654.

28. BUUS,N.H., SIMONSEN,U., PILEGAARD,H.K. & MULVANY,M.J. (2000). Nitric oxide, prostanoid and non-NO, non-prostanoid involvement in acetylcholine relaxation of isolated human small arteries. *Br. J. Pharmacol.*, **129**, 184-192.

29. BYCHKOV,R., BURNHAM,M.P., RICHARDS,G.R., EDWARDS,G., WESTON,A.H., FELETOU,M. & VANHOUTTE,P.M. (2002). Characterization of a charybdotoxin-sensitive intermediate conductance $Ca^{2+}$-activated $K^+$ channel in porcine coronary endothelium: relevance to EDHF. *Br. J. Pharmacol.*, **137**, 1346-1354.

30. CAI,S., GARNEAU,L. & SAUVE,R. (1998). Single-channel characterization of the pharmacological properties of the $K_{Ca}$ channel of intermediate conductance in bovine aortic endothelial cells. *J. Membr. Biol.*, **163**, 147-158.

31. CALDERONE,V. (2002). Large-conductance, $Ca^{2+}$-activated $K^+$ channels: function, pharmacology and drugs. *Curr. Med. Chem.*, **9**, 1385-1395.

32. CAMPBELL,W.B., GEBREMEDHIN,D., PRATT,P.F. & HARDER,D.R. (1996). Identification of epoxyeicosatrienoic acids as endothelium-derived hyperpolarizing factors. *Circ. Res.*, **78**, 415-423.

33. CARIGNANI,C., RONCARATI,R., RIMINI,R. & TERSTAPPEN,G.C. (2002). Pharmacological and molecular characterisation of SK3 channels in the TE671 human medulloblastoma cell line. *Brain Res.*, **939**, 11-18.

34. CASTLE,N.A., LONDON,D.O., CREECH,C., FAJLOUN,Z., STOCKER,J.W. & SABATIER,J.M. (2003). Maurotoxin: a potent inhibitor of intermediate conductance $Ca^{2+}$-activated potassium channels. *Mol. Pharmacol.*, **63**, 409-418.

35. CASTLE,N.A. & STRONG,P.N. (1986). Identification of two toxins from scorpion (Leiurus quinquestriatus) venom which block distinct classes of calcium-activated potassium channel. *FEBS Lett.*, **209**, 117-121.

36. CHATAIGNEAU,T., FELETOU,M., DUHAULT,J. & VANHOUTTE,P.M. (1998). Epoxyeicosatrienoic acids, potassium channel blockers and endothelium-dependent hyperpolarization in the guinea-pig carotid artery. *Br. J. Pharmacol.*, **123**, 574-580.

37. CHAUHAN,S., RAHMAN,A., NILSSON,H., CLAPP,L., MACALLISTER,R. & AHLUWALIA,A. (2003a). NO contributes to EDHF-like responses in rat small arteries: a role for NO stores. *Cardiovasc. Res.*, **57**, 207-216.

38. CHAUHAN,S.D., HOBBS,A.J. & AHLUWALIA,A. (2004). C-type natriuretic peptide: new candidate for endothelium-derived hyperpolarising factor. *Int. J. Biochem. Cell Biol.*, **36**, 1878-1881.

39. CHAUHAN,S.D., NILSSON,H., AHLUWALIA,A. & HOBBS,A.J. (2003b). Release of C-type natriuretic peptide accounts for the biological activity of endothelium-derived hyperpolarizing factor. *Proc. Natl. Acad. Sci. U. S. A*, **100**, 1426-1431.

40. CHAYTOR,A.T., MARSH,W.L., HUTCHESON,I.R. & GRIFFITH,T.M. (2000). Comparison of glycyrrhetinic acid isoforms and carbenoxolone as inhibitors of EDHF-type relaxations mediated via gap junctions. *Endothelium*, **7**, 265-278.

41. CHAYTOR,A.T., MARTIN,P.E., EDWARDS,D.H. & GRIFFITH,T.M. (2001). Gap junctional communication underpins EDHF-type relaxations evoked by ACh in the rat hepatic artery. *Am. J. Physiol Heart Circ. Physiol*, **280**, H2441-H2450.

42. CHEN,G., SUZUKI,H. & WESTON,A.H. (1988). Acetylcholine releases endothelium-derived hyperpolarizing factor and EDRF from rat blood vessels. *Br. J. Pharmacol.*, **95**, 1165-1174.

43. CHEN,J.Q., GALANAKIS,D., GANELLIN,C.R., DUNN,P.M. & JENKINSON,D.H. (2000). bis-Quinolinium cyclophanes: 8,14-diaza-1,7(1, 4)-diquinolinacyclotetradecaphane (UCL 1848), a highly potent and selective, nonpeptidic blocker of the apamin-sensitive $Ca^{2+}$-activated $K^+$ channel. *J. Med. Chem.*, **43**, 3478-3481.

44. CHEN,M.X., GORMAN,S.A., BENSON,B., SINGH,K., HIEBLE,J.P., MICHEL,M.C., TATE,S.N. & TREZISE,D.J. (2004). Small and intermediate conductance $Ca^{2+}$-activated K+ channels confer distinctive patterns of distribution in human tissues and differential cellular localisation in the colon and corpus cavernosum. *Naunyn Schmiedebergs Arch. Pharmacol.*, **369**, 602-615.

45. CHEN,W.T., BRACE,R.A., SCOTT,J.B., ANDERSON,D.K. & HADDY,F.J. (1972). The mechanism of the vasodilator action of potassium. *Proc Soc. Exp. Biol. Med.*, **140**, 820-824.

46. COATS,P., JOHNSTON,F., MACDONALD,J., MCMURRAY,J.J. & HILLIER,C. (2001). Endothelium-derived hyperpolarizing factor : identification and mechanisms of action in human subcutaneous resistance arteries. *Circulation*, **103**, 1702-1708.

47. COLEMAN,H.A., TARE,M. & PARKINGTON,H.C. (2001a). EDHF is not $K^+$ but may be due to spread of current from the endothelium in guinea pig arterioles. *Am. J. Physiol Heart Circ. Physiol*, **280**, H2478-H2483.

48. COLEMAN,H.A., TARE,M. & PARKINGTON,H.C. (2001b). $K^+$ currents underlying the action of endothelium-derived hyperpolarizing factor in guinea-pig, rat and human blood vessels. *J. Physiol*, **531**, 359-373.

49. COLEMAN,H.A., TARE,M. & PARKINGTON,H.C. (2004). Endothelial potassium channels, endothelium-dependent hyperpolarization and the regulation of vascular tone in health and disease. *Clin. Exp. Pharmacol. Physiol*, **31**, 641-649.

50. CORTES,S.F., REZENDE,B.A., CORRIU,C., MEDEIROS,I.A., TEIXEIRA,M.M., LOPES,M.J. & LEMOS,V.S. (2001). Pharmacological evidence for the activation of potassium channels as the mechanism involved in the hypotensive and vasorelaxant effect of dioclein in rat small resistance arteries. *Br. J. Pharmacol.*, **133**, 849-858.

51. COWAN,C.L., PALACINO,J.J., NAJIBI,S. & COHEN,R.A. (1993). Potassium channel-mediated relaxation to acetylcholine in rabbit arteries. *J. Pharmacol. Exp. Ther.*, **266**, 1482-1489.

52. DE ALLIE,F.A., BOLSOVER,S.R., NOWICKY,A.V. & STRONG,P.N. (1996). Characterization of $Ca^{2+}$-activated $^{86}Rb^+$ fluxes in rat C6 glioma cells: a system for identifying novel IKCa-channel toxins. *Br. J. Pharmacol.*, **117**, 479-487.

53. DE VRIESE,A.S., VAN,D., V & LAMEIRE,N.H. (2002). Effects of connexin-mimetic peptides on nitric oxide synthase- and cyclooxygenase-independent renal vasodilation. *Kidney Int.*, **61**, 177-185.

54. DHALIWAL,B.S. & STEINBRECHER,U.P. (1999). Scavenger receptors and oxidized low density lipoproteins. *Clin. Chim. Acta*, **286**, 191-205.

55. DONG,H., JIANG,Y., COLE,W.C. & TRIGGLE,C.R. (2000). Comparison of the pharmacological properties of EDHF-mediated vasorelaxation in guinea-pig cerebral and mesenteric resistance vessels. *Br. J. Pharmacol.*, **130**, 1983-1991.

56. DORA,K.A. & GARLAND,C.J. (2001). Properties of smooth muscle hyperpolarization and relaxation to $K^+$ in the rat isolated mesenteric artery. *Am. J. Physiol Heart Circ. Physiol*, **280**, H2424-H2429.

57. DORA,K.A., INGS,N.T. & GARLAND,C.J. (2002). $K_{Ca}$ channel blockers reveal hyperpolarization and relaxation to $K^+$ in rat isolated mesenteric artery. *Am. J. Physiol Heart Circ. Physiol*, **283**, H606-H614.

58. DOUGHTY,J.M., BOYLE,J.P. & LANGTON,P.D. (2000). Potassium does not mimic EDHF in rat mesenteric arteries. *Br. J. Pharmacol.*, **130**, 1174-1182.

59. DOUGHTY,J.M., PLANE,F. & LANGTON,P.D. (1999). Charybdotoxin and apamin block EDHF in rat mesenteric artery if selectively applied to the endothelium. *Am. J. Physiol*, **276**, H1107-H1112.

60. EA KIM,L., JAVELLAUD,J. & OUDART,N. (1992). Endothelium-dependent relaxation of rabbit middle cerebral artery to a histamine H3-agonist is reduced by inhibitors of nitric oxide and prostacyclin synthesis. *Br. J. Pharmacol.*, **105**, 103-106.

61. ECKMAN,D.M., HOPKINS,N., MCBRIDE,C. & KEEF,K.D. (1998). Endothelium-dependent relaxation and hyperpolarization in guinea-pig coronary artery: role of epoxyeicosatrienoic acid. *Br. J. Pharmacol.*, **124**, 181-189.

62. EDWARDS,G., DORA,K.A., GARDENER,M.J., GARLAND,C.J. & WESTON,A.H. (1998). $K^+$ is an endothelium-derived hyperpolarizing factor in rat arteries. *Nature*, **396**, 269-272.

63. EDWARDS,G., FELETOU,M., GARDENER,M.J., GLEN,C.D., RICHARDS,G.R., VANHOUTTE,P.M. & WESTON,A.H. (2001). Further investigations into the endothelium-dependent hyperpolarizing effects of bradykinin and substance P in porcine coronary artery. *Br. J. Pharmacol.*, **133**, 1145-1153.

64. EDWARDS,G., FELETOU,M., GARDENER,M.J., THOLLON,C., VANHOUTTE,P.M. & WESTON,A.H. (1999a). Role of gap junctions in the responses to EDHF in rat and guinea-pig small arteries. *Br. J. Pharmacol.*, **128**, 1788-1794.

65. EDWARDS,G., GARDENER,M.J., FELETOU,M., BRADY,G., VANHOUTTE,P.M. & WESTON,A.H. (1999b). Further investigation of endothelium-derived hyperpolarizing factor (EDHF) in rat hepatic artery: studies using 1-EBIO and ouabain. *Br. J. Pharmacol.*, **128**, 1064-1070.

66. EDWARDS,G. & WESTON,A.H. (1998). Endothelium-derived hyperpolarizing factor - a critical appraisal. *Prog. Drug Res.*, **50**, 107-133.

67. EDWARDS,G. & WESTON,A.H. (2004). Potassium and potassium clouds in endothelium-dependent hyperpolarizations. *Pharmacol. Res.*, **49**, 535-541.

68. EICHLER,I., WIBAWA,J., GRGIC,I., KNORR,A., BRAKEMEIER,S., PRIES,A.R., HOYER,J. & KOHLER,R. (2003). Selective blockade of endothelial $Ca^{2+}$-activated small- and intermediate-conductance $K^+$-channels suppresses EDHF-mediated vasodilation. *Br. J. Pharmacol.*, **138**, 594-601.

69. EMERSON,G.G. & SEGAL,S.S. (2000). Electrical coupling between endothelial cells and smooth muscle cells in hamster feed arteries: role in vasomotor control. *Circ. Res.*, **87**, 474-479.

70. FANG,Y., SCHRAM,G., ROMANENKO,V., SHI,C., CONTI,L., VANDENBERG,C.A., DAVIES,P.F., NATTEL,S. & LEVITAN,I. (2005). Functional expression of Kir2.x in human aortic endothelial cells: the dominant role of Kir2.2. *Am. J. Physiol Cell Physiol*, **(in print)**.

71. FELETOU,M. & VANHOUTTE,P.M. (1988). Endothelium-dependent hyperpolarization of canine coronary smooth muscle. *Br. J. Pharmacol.*, **93**, 515-524.

72. FERNANDEZ-FERNANDEZ,J.M., NOBLES,M., CURRID,A., VAZQUEZ,E. & VALVERDE,M.A. (2002). Maxi $K^+$ channel mediates regulatory volume decrease response in a human bronchial epithelial cell line. *Am. J. Physiol Cell Physiol*, **283**, C1705-C1714.

73. FICHTNER,H., FROBE,U., BUSSE,R. & KOHLHARDT,M. (1987). Single nonselective cation channels and $Ca^{2+}$-activated $K^+$ channels in aortic endothelial cells. *J. Membr. Biol.*, **98**, 125-133.

74. FISSLTHALER,B., FLEMING,I. & BUSSE,R. (2000). EDHF: a cytochrome P450 metabolite in coronary arteries. *Semin. Perinatol.*, **24**, 15-19.

75. FISSLTHALER,B., POPP,R., KISS,L., POTENTE,M., HARDER,D.R., FLEMING,I. & BUSSE,R. (1999). Cytochrome P450 2C is an EDHF synthase in coronary arteries. *Nature*, **401**, 493-497.

76. FLEMING,I. (2004). Cytochrome P450 epoxygenases as EDHF synthase(s). *Pharmacol. Res.*, **49**, 525-533.

77. FLEMING,I., SCHERMER,B., POPP,R. & BUSSE,R. (1999). Inhibition of the production of endothelium-derived hyperpolarizing factor by cannabinoid receptor agonists. *Br. J. Pharmacol.*, **126**, 949-960.

78. FORSYTH,S.E., HOGER,A. & HOGER,J.H. (1997). Molecular cloning and expression of a bovine endothelial inward rectifier potassium channel. *FEBS Lett.*, **409**, 277-282.

79. FRID,M.G., KALE,V.A. & STENMARK,K.R. (2002). Mature vascular endothelium can give rise to smooth muscle cells via endothelial-mesenchymal transdifferentiation: in vitro analysis. *Circ. Res.*, **90**, 1189-1196.

80. FRIEDEN,M., SOLLINI,M. & BENY,J. (1999). Substance P and bradykinin activate different types of $K_{Ca}$ currents to hyperpolarize cultured porcine coronary artery endothelial cells. *J. Physiol*, **519** Pt 2, 361-371.

81. FUJIKI,T., SHIMOKAWA,H., MORIKAWA,K., KUBOTA,H., HATANAKA,M., TALUKDER,M.A., MATOBA,T., TAKESHITA,A. & SUNAGAWA,K. (2005). Endothelium-derived hydrogen peroxide accounts for the enhancing effect of an angiotensin-converting enzyme inhibitor on endothelium-derived hyperpolarizing factor-mediated responses in mice. *Arterioscler. Thromb. Vasc. Biol.*, **25**, 766-771.

82. FUKAO,M., HATTORI,Y., KANNO,M., SAKUMA,I. & KITABATAKE,A. (1997). Evidence against a role of cytochrome P450-derived arachidonic acid metabolites in endothelium-dependent hyperpolarization by acetylcholine in rat isolated mesenteric artery. *Br. J. Pharmacol.*, **120**, 439-446.

83. FURCHGOTT,R.F. & ZAWADZKI,J.V. (1980). The obligatory role of endothelial cells in the relaxation of arterial smooth muscle by acetylcholine. *Nature*, **288**, 373-376.

84. FURNESS,J.B., KEARNEY,K., ROBBINS,H.L., HUNNE,B., SELMER,I.S., NEYLON,C.B., CHEN,M.X. & TJANDRA,J.J. (2004). Intermediate conductance potassium (IK) channels occur in human enteric neurons. *Auton. Neurosci.*, **112**, 93-97.

85. FURNESS,J.B., ROBBINS,H.L., SELMER,I.S., HUNNE,B., CHEN,M.X., HICKS,G.A., MOORE,S. & NEYLON,C.B. (2003). Expression of intermediate conductance potassium channel immunoreactivity in neurons and epithelial cells of the rat gastrointestinal tract. *Cell Tissue Res.*, **314**, 179-189.

86. GAO,Y.J., HIROTA,S., ZHANG,D.W., JANSSEN,L.J. & LEE,R.M. (2003). Mechanisms of hydrogen-peroxide-induced biphasic response in rat mesenteric artery. *Br. J. Pharmacol.*, **138**, 1085-1092.

87. GARDOS,G. (1958). The function of calcium in the potassium permeability of human erythrocytes. *Biochim. Biophys. Acta*, **30**, 653-654.

88. GAUTHIER,K.M., DEETER,C., KRISHNA,U.M., REDDY,Y.K., BONDLELA,M., FALCK,J.R. & CAMPBELL,W.B. (2002a). 14,15-Epoxyeicosa-5(Z)-enoic acid: a selective epoxyeicosatrienoic acid antagonist that inhibits endothelium-dependent hyperpolarization and relaxation in coronary arteries. *Circ. Res.*, **90**, 1028-1036.

89. GAUTHIER,K.M., LIU,C., POPOVIC,A., ALBARWANI,S. & RUSCH,N.J. (2002b). Freshly isolated bovine coronary endothelial cells do not express the $BK_{Ca}$ channel gene. *J. Physiol*, **545**, 829-836.

90. GAUTHIER,K.M., SPITZBARTH,N., EDWARDS,E.M. & CAMPBELL,W.B. (2004). Apamin-sensitive $K^+$ currents mediate arachidonic acid-induced relaxations of rabbit aorta. *Hypertension*, **43**, 413-419.

91. GERLACH,A.C., GANGOPADHYAY,N.N. & DEVOR,D.C. (2000). Kinase-dependent regulation of the intermediate conductance, calcium-dependent potassium channel, hIK1. *J. Biol. Chem.*, **275**, 585-598.

92. GILLHAM,J.C., KENNY,L.C. & BAKER,P.N. (2003). An overview of endothelium-derived hyperpolarising factor (EDHF) in normal and compromised pregnancies. *Eur. J. Obstet. Gynecol. Reprod. Biol.*, **109**, 2-7.

93. GOROG,P. & PEARSON,J.D. (1985). Sialic acid moieties on surface glycoproteins protect endothelial cells from proteolytic damage. *J. Pathol.*, **146**, 205-212.

94. GOTO,K., RUMMERY,N.M., GRAYSON,T.H. & HILL,C.E. (2004). Attenuation of conducted vasodilatation in rat mesenteric arteries during hypertension: role of inwardly rectifying potassium channels. *J. Physiol*, **561**, 215-231.

95. GRAIER,W.F., KUKOVETZ,W.R. & GROSCHNER,K. (1993). Cyclic AMP enhances agonist-induced $Ca^{2+}$ entry into endothelial cells by activation of potassium channels and membrane hyperpolarization. *Biochem. J.*, **291** ( Pt 1), 263-267.

96. GRAIER,W.F., SIMECEK,S. & STUREK,M. (1995). Cytochrome P450 mono-oxygenase-regulated signalling of $Ca^{2+}$ entry in human and bovine endothelial cells. *J. Physiol*, **482** ( Pt 2), 259-274.

97. GRIFFITH,T.M. (2004). Endothelium-dependent smooth muscle hyperpolarization: do gap junctions provide a unifying hypothesis? *Br. J. Pharmacol.*, **141**, 881-903.

98. GRIFFITH,T.M., CHAYTOR,A.T. & EDWARDS,D.H. (2004). The obligatory link: role of gap junctional communication in endothelium-dependent smooth muscle hyperpolarization. *Pharmacol. Res.*, **49**, 551-564.

99. GRIFFITH,T.M., CHAYTOR,A.T., TAYLOR,H.J., GIDDINGS,B.D. & EDWARDS,D.H. (2002). cAMP facilitates EDHF-type relaxations in conduit arteries by enhancing electrotonic conduction via gap junctions. *Proc Natl. Acad. Sci. U. S. A*, **99**, 6392-6397.

100. GRIFFITH,T.M. & TAYLOR,H.J. (1999). Cyclic AMP mediates EDHF-type relaxations of rabbit jugular vein. *Biochem. Biophys. Res. Commun.*, **263**, 52-57.

101. GROSCHNER,K., GRAIER,W.F. & KUKOVETZ,W.R. (1992). Activation of a small-conductance $Ca^{2+}$-dependent $K^+$ channel contributes to bradykinin-induced stimulation of nitric oxide synthesis in pig aortic endothelial cells. *Biochim. Biophys. Acta*, **1137**, 162-170.

102. GUNS,P.J., KORDA,A., CRAUWELS,H.M., VAN ASSCHE,T., ROBAYE,B., BOEYNAEMS,J.M. & BULT,H. (2005). Pharmacological characterization of nucleotide P2Y receptors on endothelial cells of the mouse aorta. *Br. J. Pharmacol.*, **146**, 288-295.

103. HABURCAK,M., WEI,L., VIANA,F., PRENEN,J., DROOGMANS,G. & NILIUS,B. (1997). Calcium-activated potassium channels in cultured human endothelial cells are not directly modulated by nitric oxide. *Cell Calcium*, **21**, 291-300.

104. HAMILL,O.P. (1981). Potassium channel currents in human red blood cells. *J. Physiol.*, **319**, 97p-98p.

105. HARRIS,D., KENDALL,D.A. & RANDALL,M.D. (1999). Characterization of cannabinoid receptors coupled to vasorelaxation by endothelium-derived hyperpolarizing factor. *Naunyn Schmiedebergs Arch. Pharmacol.*, **359**, 48-52.

106. HASUNUMA,K., YAMAGUCHI,T., RODMAN,D.M., O'BRIEN,R.F. & MCMURTRY,I.F. (1991). Effects of inhibitors of EDRF and EDHF on vasoreactivity of perfused rat lungs. *Am. J. Physiol*, **260**, L97-104.

107. HATOUM,O.A., BINION,D.G., MIURA,H., TELFORD,G., OTTERSON,M.F. & GUTTERMAN,D.D. (2005). Role of hydrogen peroxide in ACh-induced dilation of human submucosal intestinal microvessels. *Am. J. Physiol Heart Circ. Physiol*, **288**, H48-H54.

108. HECKER,M., BARA,A.T., BAUERSACHS,J. & BUSSE,R. (1994). Characterization of endothelium-derived hyperpolarizing factor as a cytochrome P450-derived arachidonic acid metabolite in mammals. *J. Physiol*, **481 ( Pt 2)**, 407-414.

109. HILL,C.E., HICKEY,H. & SANDOW,S.L. (2000). Role of gap junctions in acetylcholine-induced vasodilation of proximal and distal arteries of the rat mesentery. *J. Auton. Nerv. Syst.*, **81**, 122-127.

110. HIMMEL,H.M., WHORTON,A.R. & STRAUSS,H.C. (1993). Intracellular calcium, currents, and stimulus-response coupling in endothelial cells. *Hypertension*, **21**, 112-127.

111. HINTON,J.M. & LANGTON,P.D. (2003). Inhibition of EDHF by two new combinations of $K^+$-channel inhibitors in rat isolated mesenteric arteries. *Br. J. Pharmacol.*, **138**, 1031-1035.

112. HOBBS,A., FOSTER,P., PRESCOTT,C., SCOTLAND,R. & AHLUWALIA,A. (2004). Natriuretic peptide receptor-C regulates coronary blood flow and prevents myocardial ischemia/reperfusion injury: novel cardioprotective role for endothelium-derived C-type natriuretic peptide. *Circulation*, **110**, 1231-1235.

113. HÖGESTÄTT,E.D., JOHANSSON,R., ANDERSSON,D.A. & ZYGMUNT,P.M. (2000). Involvement of sensory nerves in vasodilator responses to acetylcholine and potassium ions in rat hepatic artery. *Br. J. Pharmacol.*, **130**, 27-32.

114. HONING,M.L., SMITS,P., MORRISON,P.J., BURNETT,J.C., JR. & RABELINK,T.J. (2001). C-type natriuretic peptide-induced vasodilation is dependent on hyperpolarization in human forearm resistance vessels. *Hypertension*, **37**, 1179-1183.

115. HOSSEINI,R., BENTON,D.C., DUNN,P.M., JENKINSON,D.H. & MOSS,G.W. (2001). SK3 is an important component of $K^+$ channels mediating the afterhyperpolarization in cultured rat SCG neurones. *J. Physiol*, **535**, 323-334.

116. HOYER,J., KOHLER,R., HAASE,W. & DISTLER,A. (1996). Up-regulation of pressure-activated $Ca^{2+}$-permeable cation channel in intact vascular endothelium of hypertensive rats. *Proc. Natl. Acad. Sci. U. S. A*, **93**, 11253-11258.

117. ISHII,T.M., MAYLIE,J. & ADELMAN,J.P. (1997a). Determinants of apamin and d-tubocurarine block in SK potassium channels. *J. Biol. Chem.*, **272**, 23195-23200.

118. ISHII,T.M., SILVIA,C., HIRSCHBERG,B., BOND,C.T., ADELMAN,J.P. & MAYLIE,J. (1997b). A human intermediate conductance calcium-activated potassium channel. *Proc. Natl. Acad. Sci. U. S. A*, **94**, 11651-11656.

119. ISHIZAKA,H. & KUO,L. (1997). Endothelial ATP-sensitive potassium channels mediate coronary microvascular dilation to hyperosmolarity. *Am. J. Physiol*, **273**, H104-H112.

120. ITO,Y., KITAMURA,K. & KURIYAMA,H. (1979). Effects of acetylcholine and catecholamines on the smooth muscle cell of the porcine coronary artery. *J. Physiol*, **294**, 595-611.

121. JAGER,H., ADELMAN,J.P. & GRISSMER,S. (2000). SK2 encodes the apamin-sensitive $Ca^{2+}$-activated $K^+$ channels in the human leukemic T cell line, Jurkat. *FEBS Lett.*, **469**, 196-202.

122. JAGER,H., DREKER,T., BUCK,A., GIEHL,K., GRESS,T. & GRISSMER,S. (2004). Blockage of intermediate-conductance $Ca^{2+}$-activated $K^+$ channels inhibit human pancreatic cancer cell growth in vitro. *Mol. Pharmacol.*, **65**, 630-638.

123. JAGER,H. & GRISSMER,S. (2004). Characterization of the outer pore region of the apamin-sensitive $Ca^{2+}$-activated $K^+$ channel rSK2. *Toxicon*, **43**, 951-960.

124. JENSEN,B.S., STROBAEK,D., OLESEN,S.P. & CHRISTOPHERSEN,P. (2001). The $Ca^{2+}$-activated $K^+$ channel of intermediate conductance: a molecular target for novel treatments? *Curr. Drug Targets.*, **2**, 401-422.

125. JOINER,W.J., WANG,L.Y., TANG,M.D. & KACZMAREK,L.K. (1997). hSK4, a member of a novel subfamily of calcium-activated potassium channels. *Proc. Natl. Acad. Sci. U. S. A*, **94**, 11013-11018.

126. JOW,F., SULLIVAN,K., SOKOL,P. & NUMANN,R. (1999). Induction of $Ca^{2+}$-activated $K^+$ current and transient outward currents in human capillary endothelial cells. *J. Membr. Biol.*, **167**, 53-64.

127. KACZOROWSKI,G.J., KNAUS,H.G., LEONARD,R.J., MCMANUS,O.B. & GARCIA,M.L. (1996). High-conductance calcium-activated potassium channels; structure, pharmacology, and function. *J. Bioenerg. Biomembr.*, **28**, 255-267.

128. KAGOTA,S., YAMAGUCHI,Y., NAKAMURA,K. & KUNITOMO,M. (1999). Characterization of nitric oxide- and prostaglandin-independent relaxation in response to acetylcholine in rabbit renal artery. *Clin. Exp. Pharmacol. Physiol*, **26**, 790-796.

129. KESTLER,H.A., JANKO,S., HAUSSLER,U., MUCHE,R., HOMBACH,V., HOHER,M. & WIECHA,J. (1998). A remark on the high-conductance calcium-activated potassium channel in human endothelial cells. *Res. Exp. Med. (Berl)*, **198**, 133-143.

130. KITAGAWA,S., YAMAGUCHI,Y., KUNITOMO,M., SAMESHIMA,E. & FUJIWARA,M. (1994). NG-nitro-L-arginine-resistant endothelium-dependent relaxation induced by acetylcholine in the rabbit renal artery. *Life Sci.*, **55**, 491-498.

131. KOHLER,M., HIRSCHBERG,B., BOND,C.T., KINZIE,J.M., MARRION,N.V., MAYLIE,J. & ADELMAN,J.P. (1996). Small-conductance, calcium-activated potassium channels from mammalian brain. *Science*, **273**, 1709-1714.

132. KOHLER,R., BRAKEMEIER,S., KUHN,M., BEHRENS,C., REAL,R., DEGENHARDT,C., ORZECHOWSKI,H.D., PRIES,A.R., PAUL,M. & HOYER,J. (2001). Impaired hyperpolarization in regenerated endothelium after balloon catheter injury. *Circ. Res.*, **89**, 174-179.

133. KOHLER,R., DEGENHARDT,C., KUHN,M., RUNKEL,N., PAUL,M. & HOYER,J. (2000). Expression and function of endothelial $Ca^{2+}$-activated $K^+$ channels in human mesenteric artery: A single-cell reverse transcriptase-polymerase chain reaction and electrophysiological study in situ. *Circ. Res.*, **87**, 496-503.

134. KOHLER,R., WULFF,H., EICHLER,I., KNEIFEL,M., NEUMANN,D., KNORR,A., GRGIC,I., KAMPFE,D., SI,H., WIBAWA,J., REAL,R., BORNER,K., BRAKEMEIER,S., ORZECHOWSKI,H.D., REUSCH,H.P., PAUL,M., CHANDY,K.G. & HOYER,J. (2003). Blockade of the intermediate-conductance calcium-activated potassium channel as a new therapeutic strategy for restenosis. *Circulation*, **108**, 1119-1125.

135. KOLSKI-ANDREACO,A., TOMITA,H., SHAKKOTTAI,V.G., GUTMAN,G.A., CAHALAN,M.D., GARGUS,J.J. & CHANDY,K.G. (2004). SK3-1C, a dominant-negative suppressor of $SK_{Ca}$ and $IK_{Ca}$ channels. *J. Biol. Chem.*, **279**, 6893-6904.

136. KWON,S.C. (2001). Mechanisms of NO-resistant relaxation induced by acetylcholine in rabbit renal arteries. *J. Vet. Med. Sci.*, **63**, 37-40.

137. LACY,P.S., PILKINGTON,G., HANVESAKUL,R., FISH,H.J., BOYLE,J.P. & THURSTON,H. (2000). Evidence against potassium as an endothelium-derived hyperpolarizing factor in rat mesenteric small arteries. *Br. J. Pharmacol.*, **129**, 605-611.

138. LEIK,C.E., WILLEY,A., GRAHAM,M.F. & WALSH,S.W. (2004). Isolation and culture of arterial smooth muscle cells from human placenta. *Hypertension*, **43**, 837-840.

139. LIU,M.Y., HATTORI,Y., SATO,A., ICHIKAWA,R., ZHANG,X.H. & SAKUMA,I. (2002). Ovariectomy attenuates hyperpolarization and relaxation mediated by endothelium-derived hyperpolarizing factor in female rat mesenteric artery: a concomitant decrease in connexin-43 expression. *J. Cardiovasc. Pharmacol.*, **40**, 938-948.

140. LIU,Y.C., LO,Y.C., HUANG,C.W. & WU,S.N. (2003a). Inhibitory action of ICI-182,780, an estrogen receptor antagonist, on $BK_{Ca}$ channel activity in cultured endothelial cells of human coronary artery. *Biochem. Pharmacol.*, **66**, 2053-2063.

141. LIU,Y.C., LO,Y.K. & WU,S.N. (2003b). Stimulatory effects of chlorzoxazone, a centrally acting muscle relaxant, on large conductance calcium-activated potassium channels in pituitary GH3 cells. *Brain Res.*, **959**, 86-97.

142. LOGSDON,N.J., KANG,J., TOGO,J.A., CHRISTIAN,E.P. & AIYAR,J. (1997). A novel gene, hKCa4, encodes the calcium-activated potassium channel in human T lymphocytes. *J. Biol. Chem.*, **272**, 32723-32726.

143. LUKSHA,L., NISELL,H. & KUBLICKIENE,K. (2004). The mechanism of EDHF-mediated responses in subcutaneous small arteries from healthy pregnant women. *Am. J. Physiol Regul. Integr. Comp Physiol*, **286**, R1102-R1109.

144. MAGLEBY,K.L. (2003). Gating mechanism of BK (Slo1) channels: so near, yet so far. *J. Gen. Physiol*, **121**, 81-96.

145. MALIK-HALL,M., GANELLIN,C.R., GALANAKIS,D. & JENKINSON,D.H. (2000). Compounds that block both intermediate-conductance ($IK_{Ca}$) and small-conductance ($SK_{Ca}$) calcium-activated potassium channels. *Br. J. Pharmacol.*, **129**, 1431-1438.

146. MARCHENKO,S.M. & SAGE,S.O. (1996). Calcium-activated potassium channels in the endothelium of intact rat aorta. *J. Physiol*, **492** ( Pt 1), 53-60.

147. MARTY,A. (1981). Ca-dependent K channels with large unitary conductance in chromaffin cell membranes. *Nature*, **291**, 497-500.

148. MATOBA,T., SHIMOKAWA,H., KUBOTA,H., MORIKAWA,K., FUJIKI,T., KUNIHIRO,I., MUKAI,Y., HIRAKAWA,Y. & TAKESHITA,A. (2002). Hydrogen peroxide is an endothelium-derived hyperpolarizing factor in human mesenteric arteries. *Biochem. Biophys. Res. Commun.*, **290**, 909-913.

149. MATOBA,T., SHIMOKAWA,H., MORIKAWA,K., KUBOTA,H., KUNIHIRO,I., URAKAMI-HARASAWA,L., MUKAI,Y., HIRAKAWA,Y., AKAIKE,T. & TAKESHITA,A. (2003). Electron spin resonance detection of hydrogen peroxide as an endothelium-derived hyperpolarizing factor in porcine coronary microvessels. *Arterioscler. Thromb. Vasc. Biol.*, **23**, 1224-1230.

150. MATOBA,T., SHIMOKAWA,H., NAKASHIMA,M., HIRAKAWA,Y., MUKAI,Y., HIRANO,K., KANAIDE,H. & TAKESHITA,A. (2000). Hydrogen peroxide is an endothelium-derived hyperpolarizing factor in mice. *J. Clin. Invest*, **106**, 1521-1530.

151. MATSUMOTO,T., KOBAYASHI,T. & KAMATA,K. (2003). Alterations in EDHF-type relaxation and phosphodiesterase activity in mesenteric arteries from diabetic rats. *Am. J. Physiol Heart Circ. Physiol*, **285**, H283-H291.

152. MAYLIE,J., BOND,C.T., HERSON,P.S., LEE,W.S. & ADELMAN,J.P. (2004). Small conductance $Ca^{2+}$-activated $K^{+}$ channels and calmodulin. *J. Physiol*, **554**, 255-261.

153. MCCARRON,J.G. & HALPERN,W. (1990). Potassium dilates rat cerebral arteries by two independent mechanisms. *Am. J. Physiol*, **259**, H902-H908.

154. MCGUIRE,J.J., DING,H. & TRIGGLE,C.R. (2001). Endothelium-derived relaxing factors: a focus on endothelium-derived hyperpolarizing factor(s). *Can. J. Physiol Pharmacol.*, **79**, 443-470.

155. MCGUIRE,P.G. & ORKIN,R.W. (1987). Isolation of rat aortic endothelial cells by primary explant techniques and their phenotypic modulation by defined substrata. *Lab Invest*, **57**, 94-105.

156. MCINTYRE,C.A., BUCKLEY,C.H., JONES,G.C., SANDEEP,T.C., ANDREWS,R.C., ELLIOTT,A.I., GRAY,G.A., WILLIAMS,B.C., MCKNIGHT,J.A., WALKER,B.R. & HADOKE,P.W. (2001). Endothelium-derived hyperpolarizing factor and potassium use different mechanisms to induce relaxation of human subcutaneous resistance arteries. *Br. J. Pharmacol.*, **133**, 902-908.

157. MCLEAN,P.G., PERRETTI,M. & AHLUWALIA,A. (2000). Kinin B(1) receptors and the cardiovascular system: regulation of expression and function. *Cardiovasc. Res.*, **48**, 194-210.

158. MCNEISH,A.J., NELLI,S., WILSON,W.S., DOWELL,F.J. & MARTIN,W. (2003). Differential effects of ascorbate on endothelium-derived hyperpolarizing factor (EDHF)-mediated vasodilatation in the bovine ciliary vascular bed and coronary artery. *Br. J. Pharmacol.*, **138**, 1172-1180.

159. MICHIELS,C. (2003). Endothelial cell functions. *J. Cell Physiol*, **196**, 430-443.

160. MISTRY,D.K. & GARLAND,C.J. (1998). Nitric oxide (NO)-induced activation of large conductance $Ca^{2+}$-dependent $K^+$ channels ($BK_{Ca}$) in smooth muscle cells isolated from the rat mesenteric artery. *Br. J. Pharmacol.*, **124**, 1131-1140.

161. MIURA,H., BOSNJAK,J.J., NING,G., SAITO,T., MIURA,M. & GUTTERMAN,D.D. (2003). Role for hydrogen peroxide in flow-induced dilation of human coronary arterioles. *Circ. Res.*, **92**, e31-e40.

162. MOMBOULI,J.V., ILLIANO,S., NAGAO,T., SCOTT-BURDEN,T. & VANHOUTTE,P.M. (1992). Potentiation of endothelium-dependent relaxations to bradykinin by angiotensin I converting enzyme inhibitors in canine coronary artery involves both endothelium-derived relaxing and hyperpolarizing factors. *Circ. Res.*, **71**, 137-144.

163. MONAGHAN,A.S., BENTON,D.C., BAHIA,P.K., HOSSEINI,R., SHAH,Y.A., HAYLETT,D.G. & MOSS,G.W. (2004). The SK3 subunit of small conductance $Ca^{2+}$-activated $K^+$ channels interacts with both SK1 and SK2 subunits in a heterologous expression system. *J. Biol. Chem.*, **279**, 1003-1009.

164. MONGAN,L.C., HILL,M.J., CHEN,M.X., TATE,S.N., COLLINS,S.D., BUCKBY,L. & GRUBB,B.D. (2005). The distribution of small and intermediate conductance calcium-activated potassium channels in the rat sensory nervous system. *Neuroscience*, **131**, 161-175.

165. MORENO,A.P. (2004). Biophysical properties of homomeric and heteromultimeric channels formed by cardiac connexins. *Cardiovasc. Res.*, **62**, 276-286.

166. MURAKI,K., IMAIZUMI,Y., OHYA,S., SATO,K., TAKII,T., ONOZAKI,K. & WATANABE,M. (1997). Apamin-sensitive $Ca^{2+}$-dependent $K^+$ current and hyperpolarization in human endothelial cells. *Biochem. Biophys. Res. Commun.*, **236**, 340-343.

167. NELLI,S., WILSON,W.S., LAIDLAW,H., LLANO,A., MIDDLETON,S., PRICE,A.G. & MARTIN,W. (2003). Evaluation of potassium ion as the endothelium-derived hyperpolarizing factor (EDHF) in the bovine coronary artery. *Br. J. Pharmacol.*, **139**, 982-988.

168. NELSON,M.T. (1993). $Ca^{2+}$ -activated potassium channels and ATP-sensitive potassium channels as modulators of vascular tone. *Trends Cardiovasc. Med.*, **3**, 54-60.

169. NELSON,M.T., CHENG,H., RUBART,M., SANTANA,L.F., BONEV,A.D., KNOT,H.J. & LEDERER,W.J. (1995). Relaxation of arterial smooth muscle by calcium sparks. *Science*, **270**, 633-637.

170. NELSON,M.T. & QUAYLE,J.M. (1995). Physiological roles and properties of potassium channels in arterial smooth muscle. *Am. J. Physiol*, **268**, C799-C822.

171. NEYLON,C.B., D'SOUZA,T. & REINHART,P.H. (2004a). Protein kinase A inhibits intermediate conductance $Ca^{2+}$-activated $K^+$ channels expressed in Xenopus oocytes. *Pflugers Arch.*, **448**, 613-620.

172. NEYLON,C.B., LANG,R.J., FU,Y., BOBIK,A. & REINHART,P.H. (1999). Molecular cloning and characterization of the intermediate-conductance $Ca^{2+}$-activated $K^+$ channel in vascular smooth muscle: relationship between $K_{Ca}$ channel diversity and smooth muscle cell function. *Circ. Res.*, **85**, e33-e43.

173. NEYLON,C.B., NURGALI,K., HUNNE,B., ROBBINS,H.L., MOORE,S., CHEN,M.X. & FURNESS,J.B. (2004b). Intermediate-conductance calcium-activated potassium channels in enteric neurones of the mouse: pharmacological, molecular and immunochemical evidence for their role in mediating the slow afterhyperpolarization. *J. Neurochem.*, **90**, 1414-1422.

174. NILIUS,B. & DROOGMANS,G. (2001). Ion channels and their functional role in vascular endothelium. *Physiol Rev.*, **81**, 1415-1459.

175. NILIUS,B., DROOGMANS,G. & WONDERGEM,R. (2003). Transient receptor potential channels in endothelium: solving the calcium entry puzzle? *Endothelium*, **10**, 5-15.

176. NISHIKAWA,Y., STEPP,D.W. & CHILIAN,W.M. (1999). In vivo location and mechanism of EDHF-mediated vasodilation in canine coronary microcirculation. *Am. J. Physiol*, **277**, H1252-H1259.

177. O'SULLIVAN,S.E., KENDALL,D.A. & RANDALL,M.D. (2004). Heterogeneity in the mechanisms of vasorelaxation to anandamide in resistance and conduit rat mesenteric arteries. *Br. J. Pharmacol.*, **142**, 435-442.

178. OLANREWAJU,H.A., GAFUROV,B.S. & LIEBERMAN,E.M. (2002). Involvement of $K^+$ channels in adenosine A2A and A2B receptor-mediated hyperpolarization of porcine coronary artery endothelial cells. *J. Cardiovasc. Pharmacol.*, **40**, 43-49.

179. ORIO,P., ROJAS,P., FERREIRA,G. & LATORRE,R. (2002). New disguises for an old channel: MaxiK channel beta-subunits. *News Physiol Sci.*, **17**, 156-161.

180. OUADID-AHIDOUCH,H., ROUDBARAKI,M., DELCOURT,P., AHIDOUCH,A., JOURY,N. & PREVARSKAYA,N. (2004). Functional and molecular identification of intermediate-conductance $Ca^{2+}$-activated $K^+$ channels in breast cancer cells: association with cell cycle progression. *Am. J. Physiol Cell Physiol*, **287**, C125-C134.

181. PAPASSOTIRIOU,J., KOHLER,R., PRENEN,J., KRAUSE,H., AKBAR,M., EGGERMONT,J., PAUL,M., DISTLER,A., NILIUS,B. & HOYER,J. (2000). Endothelial $K^+$ channel lacks the $Ca^{2+}$ sensitivity-regulating beta subunit. *FASEB J.*, **14**, 885-894.

182. PARIHAR,A.S., COGHLAN,M.J., GOPALAKRISHNAN,M. & SHIEH,C.C. (2003). Effects of intermediate-conductance $Ca^{2+}$-activated $K^+$ channel modulators on human prostate cancer cell proliferation. *Eur. J. Pharmacol.*, **471**, 157-164.

183. PATTON,C., THOMPSON,S. & EPEL,D. (2004). Some precautions in using chelators to buffer metals in biological solutions. *Cell Calcium*, **35**, 427-431.

184. PETERSSON,J., ZYGMUNT,P.M. & HÖGESTÄTT,E.D. (1997). Characterization of the potassium channels involved in EDHF-mediated relaxation in cerebral arteries. *Br. J. Pharmacol.*, **120**, 1344-1350.

185. PLANE,F., HOLLAND,M., WALDRON,G.J., GARLAND,C.J. & BOYLE,J.P. (1997). Evidence that anandamide and EDHF act via different mechanisms in rat isolated mesenteric arteries. *Br. J. Pharmacol.*, **121**, 1509-1511.

186. PLATOSHYN,O., REMILLARD,C.V., FANTOZZI,I., MANDEGAR,M., SISON,T.T., ZHANG,S., BURG,E. & YUAN,J.X. (2004). Diversity of voltage-dependent $K^+$ channels in human pulmonary artery smooth muscle cells. *Am. J. Physiol Lung Cell Mol. Physiol*, **287**, L226-L238.

187. POMPOSIELLO,S., RHALEB,N.E., ALVA,M. & CARRETERO,O.A. (1999). Reactive oxygen species: role in the relaxation induced by bradykinin or arachidonic acid via EDHF in isolated porcine coronary arteries. *J. Cardiovasc. Pharmacol.*, **34**, 567-574.

188. POPP,R., BAUERSACHS,J., HECKER,M., FLEMING,I. & BUSSE,R. (1996). A transferable, beta-naphthoflavone-inducible, hyperpolarizing factor is synthesized by native and cultured porcine coronary endothelial cells. *J. Physiol*, **497** ( Pt 3), 699-709.

189. POPP,R., BRANDES,R.P., OTT,G., BUSSE,R. & FLEMING,I. (2002). Dynamic modulation of interendothelial gap junctional communication by 11,12-epoxyeicosatrienoic acid. *Circ. Res.*, **90**, 800-806.

190. PRATT,P.F., LI,P., HILLARD,C.J., KURIAN,J. & CAMPBELL,W.B. (2001). Endothelium-independent, ouabain-sensitive relaxation of bovine coronary arteries by EETs. *Am. J. Physiol Heart Circ. Physiol*, **280**, H1113-H1121.

191. PULVIRENTI,T.J., YIN,J.L., CHAUFOUR,X., MCLACHLAN,C., HAMBLY,B.D., BENNETT,M.R. & BARDEN,J.A. (2000). P2X (purinergic) receptor redistribution in rabbit aorta following injury to endothelial cells and cholesterol feeding. *J. Neurocytol.*, **29**, 623-631.

192. QUARTARA,L. & MAGGI,C.A. (1998). The tachykinin NK1 receptor. Part II: Distribution and pathophysiological roles. *Neuropeptides*, **32**, 1-49.

193. QUIGNARD,J.F., FELETOU,M., EDWARDS,G., DUHAULT,J., WESTON,A.H. & VANHOUTTE,P.M. (2000). Role of endothelial cell hyperpolarization in EDHF-mediated responses in the guinea-pig carotid artery. *Br. J. Pharmacol.*, **129**, 1103-1112.

194. QUIGNARD,J.F., FELETOU,M., THOLLON,C., VILAINE,J.P., DUHAULT,J. & VANHOUTTE,P.M. (1999). Potassium ions and endothelium-derived hyperpolarizing factor in guinea-pig carotid and porcine coronary arteries. *Br. J. Pharmacol.*, **127**, 27-34.

195. RAMIREZ,A.N. & KUNZE,D.L. (2002). P2X purinergic receptor channel expression and function in bovine aortic endothelium. *Am. J. Physiol Heart Circ. Physiol*, **282**, H2106-H2116.

196. RAND,J.H., BADIMON,L., GORDON,R.E., USON,R.R. & FUSTER,V. (1987). Distribution of von Willebrand factor in porcine intima varies with blood vessel type and location. *Arteriosclerosis*, **7**, 287-291.

197. RANDALL,M.D., ALEXANDER,S.P., BENNETT,T., BOYD,E.A., FRY,J.R., GARDINER,S.M., KEMP,P.A., MCCULLOCH,A.I. & KENDALL,D.A. (1996). An endogenous cannabinoid as an endothelium-derived vasorelaxant. *Biochem. Biophys. Res. Commun.*, **229**, 114-120.

198. RANDALL,M.D. & KENDALL,D.A. (1997). Involvement of a cannabinoid in endothelium-derived hyperpolarizing factor-mediated coronary vasorelaxation. *Eur. J. Pharmacol.*, **335**, 205-209.

199. RANDALL,M.D., KENDALL,D.A. & O'SULLIVAN,S. (2004). The complexities of the cardiovascular actions of cannabinoids. *Br. J. Pharmacol.*, **142**, 20-26.

200. RANDALL,M.D., MCCULLOCH,A.I. & KENDALL,D.A. (1997). Comparative pharmacology of endothelium-derived hyperpolarizing factor and anandamide in rat isolated mesentery. *Eur. J. Pharmacol.*, **333**, 191-197.

201. RICHARDS,G.R., WESTON,A.H., BURNHAM,M.P., FELETOU,M., VANHOUTTE,P.M. & EDWARDS,G. (2001). Suppression of $K^+$-induced hyperpolarization by phenylephrine in rat mesenteric artery: relevance to studies of endothelium-derived hyperpolarizing factor. *Br. J. Pharmacol.*, **134**, 1-5.

202. RITTENHOUSE,A.R., PARKER,C., BRUGNARA,C., MORGAN,K.G. & ALPER,S.L. (1997). Inhibition of maxi-K currents in ferret portal vein smooth muscle cells by the antifungal clotrimazole. *Am. J. Physiol*, **273**, C45-C56.

203. ROXBURGH,C.J., GANELLIN,C.R., ATHMANI,S., BISI,A., QUAGLIA,W., BENTON,D.C., SHINER,M.A., MALIK-HALL,M., HAYLETT,D.G. & JENKINSON,D.H. (2001). Synthesis and structure-activity relationships of cetiedil analogues as blockers of the $Ca^{2+}$-activated $K^+$ permeability of erythrocytes. *J. Med. Chem.*, **44**, 3244-3253.

204. RUSKO,J., TANZI,F., VAN BREEMEN,C. & ADAMS,D.J. (1992). Calcium-activated potassium channels in native endothelial cells from rabbit aorta: conductance, $Ca^{2+}$ sensitivity and block. *J. Physiol*, **455**, 601-621.

205. SAH,P. & FABER,E.S. (2002). Channels underlying neuronal calcium-activated potassium currents. *Prog. Neurobiol.*, **66**, 345-353.

206. SAITO,T., FUJIWARA,Y., FUJIWARA,R., HASEGAWA,H., KIBIRA,S., MIURA,H. & MIURA,M. (2002). Role of augmented expression of intermediate-conductance $Ca^{2+}$-activated $K^+$ channels in postischaemic heart. *Clin. Exp. Pharmacol. Physiol*, **29**, 324-329.

207. SAKAI,T. (1990). Acetylcholine induces Ca-dependent K currents in rabbit endothelial cells. *Jpn. J. Pharmacol.*, **53**, 235-246.

208. SANDOW,S.L. (2004). Factors, fiction and endothelium-derived hyperpolarizing factor. *Clin. Exp. Pharmacol. Physiol*, **31**, 563-570.

209. SANDOW,S.L., BRAMICH,N.J., BANDI,H.P., RUMMERY,N.M. & HILL,C.E. (2003). Structure, function, and endothelium-derived hyperpolarizing factor in the caudal artery of the SHR and WKY rat. *Arterioscler. Thromb. Vasc. Biol.*, **23**, 822-828.

210. SANDOW,S.L., GOTO,K., RUMMERY,N.M. & HILL,C.E. (2004). Developmental changes in myoendothelial gap junction mediated vasodilator activity in the rat saphenous artery. *J. Physiol*, **556**, 875-886.

211. SANDOW,S.L. & HILL,C.E. (2000). Incidence of myoendothelial gap junctions in the proximal and distal mesenteric arteries of the rat is suggestive of a role in endothelium-derived hyperpolarizing factor-mediated responses. *Circ. Res.*, **86**, 341-346.

212. SATHISHKUMAR,K., ROSS,R.G., BAWANKULE,D.U., SARDAR,K.K., PRAKASH,V.R. & MISHRA,S.K. (2005). Segmental heterogeneity in the mechanism of sodium nitroprusside-induced relaxation in ovine pulmonary artery. *J. Cardiovasc. Pharmacol.*, **45**, 491-498.

213. SAUVE,R., PARENT,L., SIMONEAU,C. & ROY,G. (1988). External ATP triggers a biphasic activation process of a calcium-dependent $K^+$ channel in cultured bovine aortic endothelial cells. *Pflugers Arch.*, **412**, 469-481.

214. SCHAEFER,U., SCHNEIDER,A., RUDROFF,C. & NEUGEBAUER,E. (2003). Nitric oxide mediates histamine induced down-regulation of H2 receptor mRNA and internalization of the receptor protein (R1). *Cell Mol. Life Sci.*, **60**, 1968-1981.

215. SCHILLING,W.P. (1989). Effect of membrane potential on cytosolic calcium of bovine aortic endothelial cells. *Am. J. Physiol*, **257**, H778-H784.

216. SCHUMACHER,M.A., RIVARD,A.F., BACHINGER,H.P. & ADELMAN,J.P. (2001). Structure of the gating domain of a $Ca^{2+}$-activated $K^+$ channel complexed with $Ca^{2+}$/calmodulin. *Nature*, **410**, 1120-1124.

217. SHAH,M. & HAYLETT,D.G. (2000). The pharmacology of hSK1 $Ca^{2+}$-activated $K^+$ channels expressed in mammalian cell lines. *Br. J. Pharmacol.*, **129**, 627-630.

218. SHARMA,G. & VIJAYARAGHAVAN,S. (2002). Nicotinic receptor signaling in nonexcitable cells. *J. Neurobiol.*, **53**, 524-534.

219. SHARMA,N.R. & DAVIS,M.J. (1994). Mechanism of substance P-induced hyperpolarization of porcine coronary artery endothelial cells. *Am. J. Physiol*, **266**, H156-H164.

220. SHIMOKAWA,H. & MATOBA,T. (2004). Hydrogen peroxide as an endothelium-derived hyperpolarizing factor. *Pharmacol. Res.*, **49**, 543-549.

221. SHIMOKAWA,H., YASUTAKE,H., FUJII,K., OWADA,M.K., NAKAIKE,R., FUKUMOTO,Y., TAKAYANAGI,T., NAGAO,T., EGASHIRA,K., FUJISHIMA,M. & TAKESHITA,A. (1996). The importance of the hyperpolarizing mechanism increases as the vessel size decreases in endothelium-dependent relaxations in rat mesenteric circulation. *J. Cardiovasc. Pharmacol.*, **28**, 703-711.

222. SINGER,H.A., SAYE,J.A. & PEACH,M.J. (1984). Effects of cytochrome P-450 inhibitors on endothelium-dependent relaxation in rabbit aorta. *Blood Vessels*, **21**, 223-230.

223. SINGH,S., SYME,C.A., SINGH,A.K., DEVOR,D.C. & BRIDGES,R.J. (2001). Benzimidazolone activators of chloride secretion: potential therapeutics for cystic fibrosis and chronic obstructive pulmonary disease. *J. Pharmacol. Exp. Ther.*, **296**, 600-611.

224. SOBEY,C.G., HEISTAD,D.D. & FARACI,F.M. (1998). Potassium channels mediate dilatation of cerebral arterioles in response to arachidonate. *Am. J. Physiol*, **275**, H1606-H1612.

225. SOH,H. & PARK,C.S. (2001). Inwardly rectifying current-voltage relationship of small-conductance $Ca^{2+}$-activated $K^+$ channels rendered by intracellular divalent cation blockade. *Biophys. J.*, **80**, 2207-2215.

226. SOLLINI,M., FRIEDEN,M. & BENY,J.L. (2002). Charybdotoxin-sensitive small conductance $K_{Ca}$ channel activated by bradykinin and substance P in endothelial cells. *Br. J. Pharmacol.*, **136**, 1201-1209.

227. STOCKER,M. (2004). $Ca^{2+}$-activated $K^+$ channels: molecular determinants and function of the SK family. *Nat. Rev. Neurosci.*, **5**, 758-770.

228. STOEN,R., LOSSIUS,K. & KARLSSON,J.O. (2003). Acetylcholine-induced vasodilation may depend entirely upon NO in the femoral artery of young piglets. *Br. J. Pharmacol.*, **138**, 39-46.

229. STRASSMAIER,T., BOND,C.T., SAILER,C.A., KNAUS,H.G., MAYLIE,J. & ADELMAN,J.P. (2005). A novel isoform of SK2 assembles with other SK subunits in mouse brain. *J. Biol. Chem.*, **280**, 21231-21236.

230. STROBAEK,D., JORGENSEN,T.D., CHRISTOPHERSEN,P., AHRING,P.K. & OLESEN,S.P. (2000). Pharmacological characterization of small-conductance $Ca^{2+}$-activated $K^+$ channels stably expressed in HEK 293 cells. *Br. J. Pharmacol.*, **129**, 991-999.

231. STROBAEK,D., TEUBER,L., JORGENSEN,T.D., AHRING,P.K., KAER,K., HANSEN,R.S., OLESEN,S.P., CHRISTOPHERSEN,P. & SKAANING-JENSEN,B. (2004). Activation of human IK and SK $Ca^{2+}$ - activated $K^+$ channels by NS309 (6,7-dichloro-1H-indole-2,3-dione 3-oxime). *Biochim. Biophys. Acta*, **1665**, 1-5.

232. STROES,E., HIJMERING,M., VAN ZANDVOORT,M., WEVER,R., RABELINK,T.J. & VAN FAASSEN,E.E. (1998). Origin of superoxide production by endothelial nitric oxide synthase. *FEBS Lett.*, **438**, 161-164.

233. SUH,S.H., VENNEKENS,R., MANOLOPOULOS,V.G., FREICHEL,M., SCHWEIG,U., PRENEN,J., FLOCKERZI,V., DROOGMANS,G. & NILIUS,B. (1999). Characterisation of explanted endothelial cells from mouse aorta: electrophysiology and $Ca^{2+}$ signalling. *Pflugers Arch.*, **438**, 612-620.

234. SUH,S.H., WATANABE,H., DROOGMANS,G. & NILIUS,B. (2002). ATP and nitric oxide modulate a $Ca^{2+}$-activated non-selective cation current in macrovascular endothelial cells. *Pflugers Arch.*, **444**, 438-445.

235. SULTAN,S., GOSLING,M., ABU-HAYYEH,S., CAREY,N. & POWELL,J.T. (2004). Flow-dependent increase of ICAM-1 on saphenous vein endothelium is sensitive to apamin. *Am. J. Physiol Heart Circ. Physiol*, **287**, H22-H28.

236. SYME,C.A., GERLACH,A.C., SINGH,A.K. & DEVOR,D.C. (2000). Pharmacological activation of cloned intermediate- and small-conductance $Ca^{2+}$-activated $K^+$ channels. *Am. J. Physiol Cell Physiol*, **278**, C570-C581.

237. TANAKA,Y., KOIKE,K., ALIOUA,A., SHIGENOBU,K., STEFANI,E. & TORO,L. (2004). Beta1-subunit of MaxiK channel in smooth muscle: a key molecule which tunes muscle mechanical activity. *J. Pharmacol. Sci.*, **94**, 339-347.

238. TANAKA,Y., MEERA,P., SONG,M., KNAUS,H.G. & TORO,L. (1997). Molecular constituents of maxi $K_{Ca}$ channels in human coronary smooth muscle: predominant alpha + beta subunit complexes. *J. Physiol*, **502** ( Pt 3), 545-557.

239. TARE,M., COLEMAN,H.A. & PARKINGTON,H.C. (2002). Glycyrrhetinic derivatives inhibit hyperpolarization in endothelial cells of guinea pig and rat arteries. *Am. J. Physiol Heart Circ. Physiol*, **282**, H335-H341.

240. TAYLOR,H.J., CHAYTOR,A.T., EDWARDS,D.H. & GRIFFITH,T.M. (2001). Gap junction-dependent increases in smooth muscle cAMP underpin the EDHF phenomenon in rabbit arteries. *Biochem. Biophys. Res. Commun.*, **283**, 583-589.

241. TAYLOR,H.J., CHAYTOR,A.T., EVANS,W.H. & GRIFFITH,T.M. (1998). Inhibition of the gap junctional component of endothelium-dependent relaxations in rabbit iliac artery by 18-alpha glycyrrhetinic acid. *Br. J. Pharmacol.*, **125**, 1-3.

242. TAYLOR,M.S., BONEV,A.D., GROSS,T.P., ECKMAN,D.M., BRAYDEN,J.E., BOND,C.T., ADELMAN,J.P. & NELSON,M.T. (2003). Altered expression of small-conductance $Ca^{2+}$-activated $K^+$ (SK3) channels modulates arterial tone and blood pressure. *Circ. Res.*, **93**, 124-131.

243. TERSTAPPEN,G.C., PULA,G., CARIGNANI,C., CHEN,M.X. & RONCARATI,R. (2001). Pharmacological characterisation of the human small conductance calcium-activated potassium channel hSK3 reveals sensitivity to tricyclic antidepressants and antipsychotic phenothiazines. *Neuropharmacology*, **40**, 772-783.

244. TORO,L., VACA,L. & STEFANI,E. (1991). Calcium-activated potassium channels from coronary smooth muscle reconstituted in lipid bilayers. *Am. J. Physiol*, **260**, H1779-H1789.

245. TRIGGLE,C.R., DING,H., ANDERSON,T.J. & PANNIRSELVAM,M. (2004). The endothelium in health and disease: a discussion of the contribution of non-nitric oxide endothelium-derived vasoactive mediators to vascular homeostasis in normal vessels and in type II diabetes. *Mol. Cell Biochem.*, **263**, 21-27.

246. TSANG,S.Y., YAO,X., WONG,C.M., CHAN,F.L., CHEN,Z.Y. & HUANG,Y. (2004). Differential regulation of $K^+$ and $Ca^{2+}$ channel gene expression by chronic treatment with estrogen and tamoxifen in rat aorta. *Eur. J. Pharmacol.*, **483**, 155-162.

247. ULGER,H., KARABULUT,A.K. & PRATTEN,M.K. (2002). Labelling of rat endothelial cells with antibodies to vWF, RECA-1, PECAM-1, ICAM-1, OX-43 and ZO-1. *Anat. Histol. Embryol.*, **31**, 31-35.

248. VAN RENTERGHEM,C. & LAZDUNSKI,M. (1992). A small-conductance charybdotoxin-sensitive, apamin-resistant $Ca^{2+}$-activated $K^+$ channel in aortic smooth muscle cells (A7r5 line and primary culture). *Pflugers Arch.*, **420**, 417-423.

249. VAN RENTERGHEM,C., VIGNE,P. & FRELIN,C. (1995). A charybdotoxin-sensitive, $Ca^{2+}$-activated $K^+$ channel with inward rectifying properties in brain microvascular endothelial cells: properties and activation by endothelins. *J. Neurochem.*, **65**, 1274-1281.

250. VANHEEL,B. & VAN DE VOORDE,J. (1999). Barium decreases endothelium-dependent smooth muscle responses to transient but not to more prolonged acetylcholine applications. *Pflugers Arch.*, **439**, 123-129.

251. VANHEEL,B. & VAN DE VOORDE,J. (2001). Regional differences in anandamide- and methanandamide-induced membrane potential changes in rat mesenteric arteries. *J. Pharmacol. Exp. Ther.*, **296**, 322-328.

252. VERGARA,C., LATORRE,R., MARRION,N.V. & ADELMAN,J.P. (1998). Calcium-activated potassium channels. *Curr. Opin. Neurobiol.*, **8**, 321-329.

253. VOGALIS,F., HARVEY,J.R. & FURNESS,J.B. (2003). PKA-mediated inhibition of a novel $K^+$ channel underlies the slow after-hyperpolarization in enteric AH neurons. *J. Physiol*, **548**, 801-814.

254. VOGALIS,F., HARVEY,J.R., NEYLON,C.B. & FURNESS,J.B. (2002). Regulation of $K^+$ channels underlying the slow afterhyperpolarization in enteric afterhyperpolarization-generating myenteric neurons: role of calcium and phosphorylation. *Clin. Exp. Pharmacol. Physiol*, **29**, 935-943.

255. VON DER WEID,P.Y. & BENY,J.L. (1993). Simultaneous oscillations in the membrane potential of pig coronary artery endothelial and smooth muscle cells. *J. Physiol*, **471**, 13-24.

256. WALCH,L., BRINK,C. & NOREL,X. (2001). The muscarinic receptor subtypes in human blood vessels. *Therapie*, **56**, 223-226.

257. WALDRON,G.J. & GARLAND,C.J. (1994). Effect of potassium channel blockers on the L-NAME insensitive relaxations in rat small mesenteric artery. *Can. J. Physiol. Pharmacol.*, **72**, (S1) 115.

258. WALKER,S.D., DORA,K.A., INGS,N.T., CRANE,G.J. & GARLAND,C.J. (2001). Activation of endothelial cell $IK_{Ca}$ with 1-ethyl-2-benzimidazolinone evokes smooth muscle hyperpolarization in rat isolated mesenteric artery. *Br. J. Pharmacol.*, **134**, 1548-1554.

259. WANG,D., BORREGO-CONDE,L.J., FALCK,J.R., SHARMA,K.K., WILCOX,C.S. & UMANS,J.G. (2003). Contributions of nitric oxide, EDHF, and EETs to endothelium-dependent relaxation in renal afferent arterioles. *Kidney Int.*, **63**, 2187-2193.

260. WANG,X.L., YE,D., PETERSON,T.E., CAO,S., SHAH,V.H., KATUSIC,Z.S., SIECK,G.C. & LEE,H.C. (2005). Caveolae targeting and regulation of large conductance $Ca^{2+}$-activated $K^+$ channels in vascular endothelial cells. *J. Biol. Chem.*, **280**, 11656-11664.

261. WARTH,R., HAMM,K., BLEICH,M., KUNZELMANN,K., VON HAHN,T., SCHREIBER,R., ULLRICH,E., MENGEL,M., TRAUTMANN,N., KINDLE,P., SCHWAB,A. & GREGER,R. (1999). Molecular and functional characterization of the small $Ca^{2+}$-regulated $K^+$ channel (rSK4) of colonic crypts. *Pflugers Arch.*, **438**, 437-444.

262. WEINGART,R. (1977). The actions of ouabain on intercellular coupling and conduction velocity in mammalian ventricular muscle. *J. Physiol*, **264**, 341-365.

263. WEINTRAUB,N.L., JOSHI,S.N., BRANCH,C.A., STEPHENSON,A.H., SPRAGUE,R.S. & LONIGRO,A.J. (1994). Relaxation of porcine coronary artery to bradykinin. Role of arachidonic acid. *Hypertension*, **23**, 976-981.

264. WESTON,A.H., FELETOU,M., VANHOUTTE,P.M., FALCK,J.R., CAMPBELL,W.B. & EDWARDS,G. (2005). Bradykinin-induced, endothelium-dependent responses in porcine coronary arteries: involvement of potassium channel activation and epoxyeicosatrienoic acids. *Br. J. Pharmacol.*, **145**, 775-784.

265. WESTON,A.H., RICHARDS,G.R., BURNHAM,M.P., FELETOU,M., VANHOUTTE,P.M. & EDWARDS,G. (2002). $K^+$-induced hyperpolarization in rat mesenteric artery: identification, localization and role of $Na^+/K^+$-ATPases. *Br. J. Pharmacol.*, **136**, 918-926.

266. WHITE,R. & HILEY,C.R. (1997). A comparison of EDHF-mediated and anandamide-induced relaxations in the rat isolated mesenteric artery. *Br. J. Pharmacol.*, **122**, 1573-1584.

267. WITTEKINDT,O.H., DREKER,T., MORRIS-ROSENDAHL,D.J., LEHMANN-HORN,F. & GRISSMER,S. (2004a). A novel non-neuronal hSK3 isoform with a dominant-negative effect on hSK3 currents. *Cell Physiol Biochem.*, **14**, 23-30.

268. WITTEKINDT,O.H., VISAN,V., TOMITA,H., IMTIAZ,F., GARGUS,J.J., LEHMANN-HORN,F., GRISSMER,S. & MORRIS-ROSENDAHL,D.J. (2004b). An apamin- and scyllatoxin-insensitive isoform of the human SK3 channel. *Mol. Pharmacol.*, **65**, 788-801.

269. WU,S.N., JAN,C.R., LI,H.F. & CHEN,S.A. (1999a). Stimulation of large-conductance $Ca^{2+}$-activated $K^+$ channels by Evans blue in cultured endothelial cells of human umbilical veins. *Biochem. Biophys. Res. Commun.*, **254**, 666-674.

270. WU,S.N., LI,H.F., JAN,C.R. & SHEN,A.Y. (1999b). Inhibition of $Ca^{2+}$-activated $K^+$ current by clotrimazole in rat anterior pituitary GH3 cells. *Neuropharmacology*, **38**, 979-989.

271. WULFF,H., GUTMAN,G.A., CAHALAN,M.D. & CHANDY,K.G. (2001). Delineation of the clotrimazole/TRAM-34 binding site on the intermediate conductance calcium-activated potassium channel, IKCa1. *J. Biol. Chem.*, **276**, 32040-32045.

272. WULFF,H., MILLER,M.J., HANSEL,W., GRISSMER,S., CAHALAN,M.D. & CHANDY,K.G. (2000). Design of a potent and selective inhibitor of the intermediate-conductance $Ca^{2+}$-activated $K^+$ channel, IKCa1: a potential immunosuppressant. *Proc. Natl. Acad. Sci. U. S. A*, **97**, 8151-8156.

273. YAMAMOTO,Y., IMAEDA,K. & SUZUKI,H. (1999). Endothelium-dependent hyperpolarization and intercellular electrical coupling in guinea-pig mesenteric arterioles. *J. Physiol*, **514 ( Pt 2)**, 505-513.

274. ZHANG,B.M., KOHLI,V., ADACHI,R., LOPEZ,J.A., UDDEN,M.M. & SULLIVAN,R. (2001). Calmodulin binding to the C-terminus of the small-conductance $Ca^{2+}$-activated $K^+$ channel hSK1 is affected by alternative splicing. *Biochemistry*, **40**, 3189-3195.

275. ZUNKLER,B.J., HENNING,B., GRAFE,M., BASS,R., HILDEBRANDT,A.G. & FLECK,E. (1995). Electrophysiological properties of human coronary endothelial cells. *Basic Res. Cardiol.*, **90**, 435-442.

276. ZYGMUNT,P.M., EDWARDS,G., WESTON,A.H., LARSSON,B. & HÖGESTÄTT,E.D. (1997a). Involvement of voltage-dependent potassium channels in the EDHF-mediated relaxation of rat hepatic artery. *Br. J. Pharmacol.*, **121**, 141-149.

277. ZYGMUNT,P.M. & HÖGESTÄTT,E.D. (1996). Role of potassium channels in endothelium-dependent relaxation resistant to nitroarginine in the rat hepatic artery. *Br. J. Pharmacol.*, **117**, 1600-1606.

278. ZYGMUNT,P.M., HÖGESTÄTT,E.D., WALDECK,K., EDWARDS,G., KIRKUP,A.J. & WESTON,A.H. (1997b). Studies on the effects of anandamide in rat hepatic artery. *Br. J. Pharmacol.*, **122**, 1679-1686.

279. ZYGMUNT,P.M., PETERSSON,J., ANDERSSON,D.A., CHUANG,H., SORGARD,M., DI,M., V, JULIUS,D. & HÖGESTÄTT,E.D. (1999). Vanilloid receptors on sensory nerves mediate the vasodilator action of anandamide. *Nature*, **400**, 452-457.

280. ZYGMUNT,P.M., SORGARD,M., PETERSSON,J., JOHANSSON,R. & HÖGESTÄTT,E.D. (2000). Differential actions of anandamide, potassium ions and endothelium-derived hyperpolarizing factor in guinea-pig basilar artery. *Naunyn Schmiedebergs Arch. Pharmacol.*, **361**, 535-542.